Rimicaris exoculata, un modèle de symbiose en milieu hydrothermal

Magali Zbinden

Université Pierre et Marie Curie

Mémoire en vue de l'obtention de l'Habilitation à Diriger des Recherches

Rimicaris exoculata, un modèle de symbiose en milieu hydrothermal

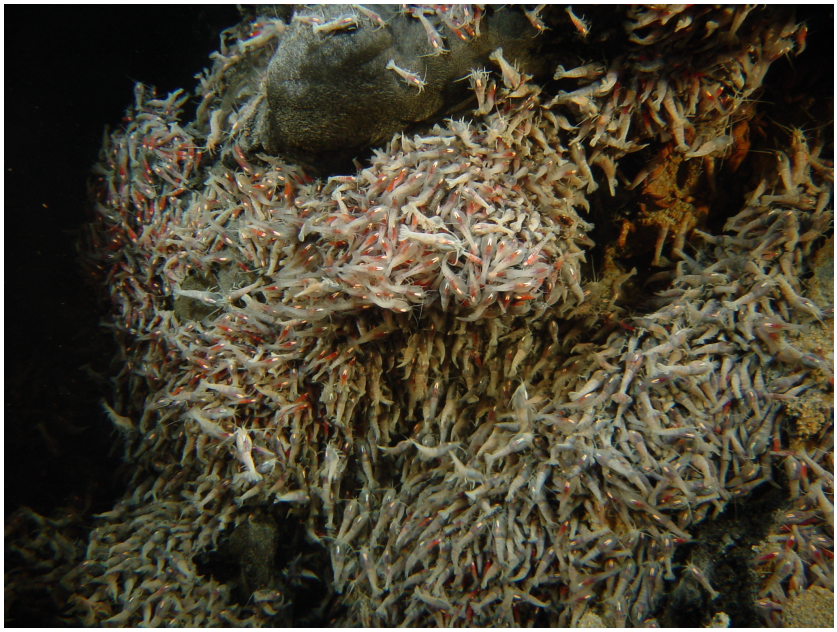

Magali Zbinden
Maître de Conférences - Université Pierre et Marie Curie,
UMR 7208 Biologie des Organismes et Ecosystèmes Aquatiques
Equipe « Adaptations aux Milieux Extrêmes »

13 Novembre 2017

Rapporteurs :
Dr. Ana Colaço, Institute of Marine Research - University of the Azores
Pr. Bénédicte Ménez, Institut de Physique du Globe de Paris
Dr. Pierre Chevaldonné, Institut Méditerranéen de Biodiversité et d'Ecologie Marine et Continentale

Membres du jury : Bénédicte Menez, IPGP – Jozée Sarrazin, Ifremer – Pierre Chevaldonné, IMBE – François Lallier, UPMC Roscoff – Marc-André Selosse, MNHN

Photo de couverture : © Exomar/Ifremer

Remerciements

Je voudrais remercier chaleureusement Ana Colaço, Bénédicte Menez et Pierre Chevaldonné d'avoir accepté de rapporter ce document et d'avoir su patienter que mes différentes occupations me laissent le temps de le terminer! Je remercie également vivement Jozée Sarrazin, François Lallier (président fidèle de toutes les HDR de l'équipe AMEX!) et Marc-André Selosse d'avoir accepté de faire partie du jury de soutenance.

Je voudrais exprimer toute ma gratitude à Françoise Gaill, qui m'a intégrée dans son équipe, m'a aidé à développer ma réflexion et ma curiosité scientifique et m'a transmis sa passion pour le milieu profond et son enthousiasme sans faille.

J'ai une pensée particulière pour Bruce et Juliette, aux côtés de qui j'ai fait mes premiers pas dans la recherche et qui sont devenus beaucoup plus que des collègues au cours de toutes ces années passées ensemble. Merci pour tous ces moments partagés au labo et en dehors. Et puis la vie de labo ne serait pas aussi stimulante sans tous les membres de l'équipe AMEX: Sébastien, Nelly, notre nouvel arrivant Louis, et tous les étudiants actuels et passés (Julia, Bérénice, Alison, Vincent, Kamil, Sven, Marie, Delphine, Caroline, Louise, SébH.....)

Je n'en serai sans doute là aujourd'hui sans Sylvie, qui m'a donné la chance de financer ma thèse, en travaillant à ses côtés au Laboratoire de Biologie Végétale Yves Rocher. Merci pour cette opportunité que tu m'as offerte et pour ton amitié depuis toutes ces années.

Je te remercie Marie-Anne, pour notre fructueuse collaboration depuis 15 ans à essayer de percer les mystères de cette sacrée crevette, ainsi que Philippe Compère pour m'avoir mis le pied à l'étrier dans le monde des crustacés.

Je voudrais aussi remercier toute l'équipe d'Océanopolis Dominique, Jean-Marie, Yann, Anne toute l'équipe d'aquariophilie pour avoir rendu le projet AbyssBox possible, pour leur collaboration fructueuse et leur accueil toujours chaleureux.

Je voudrais également remercier du fond du coeur tous les collègues qui sont aussi et surtout des amis : Juliette, Bruce, Fab, Céline, Lolo, Jean-Phi, Clara, Karen, Laure, Florence, Marie-Anne, Philou, Gégé, Eric; tous les amis qui ne sont pas des collègues : Anne-so, Kéké, la noelb (Sof, Sylvia, Didier, Marion, Marie-Sophie, Manu, que de chemin parcouru depuis notre 1ère année de deug à Jussieu!), Tic & Tac, CamCam & GuiGui, SebH, Yves. Tous et chacun à votre façon vous ensoleillez ma vie!

Je voudrais enfin remercier ma famille : mes parents, mes frères et ma soeur, qui sont toujours là, suivent mes aventures et me soutiennent depuis toujours.

Sommaire

Introduction

Je n'ai pas "toujours" voulu faire de l'océanographie. En arrivant à l'Université, mes goûts m'ont porté vers la biologie de façon générale, et ce n'est qu'en en 3ème année avec une option marine (L3, Licence de Biologie des Organismes) et vraiment en Maitrise (M1, Maitrise des Biologie des Organismes et des Populations, Mention Ecologie Marine) que je me suis orientée vers l'océanographie. Au cours de cette année, j'ai fait un stage de maitrise passionnant sur les grands dauphins de l'Île de Sein, à la suite duquel, on m'a fait comprendre que cette thématique n'offrait pas vraiment de débouchés! Mais j'avais mis les pieds dans la biologie marine et j'ai donc postulé pour un stage de DEA (M2) dans le laboratoire de Biologie Marine de l'UPMC, dirigé par Françoise Gaill.

N'ayant pas été prise en DEA cette année-là (1995-1996), j'ai fait un an de stage au laboratoire pendant lequel j'ai découvert les écosystèmes hydrothermaux, par des approches de laboratoire, mais aussi de mes propres yeux puisque j'ai eu la chance de partir sur ma première mission océanographique (Larva 95 avec Lauren Mullineaux et Chick Fischer) sur la Dorsale Est Pacifique, et de réaliser ma première plongée dans l'Alvin! Mise dans le bain passionnante quoique un peu abrupte car je parlais assez mal anglais à l'époque et ne connaissais quasiment rien à l'environnement hydrothermal! Au cours de cette année, puis de mon année de DEA (Adaptations et Survie en Environnements Extrêmes, à l'Université d'Aix-Marseille), j'ai été formée à la microscopie photonique et électronique et j'ai travaillé sur les caractéristiques morpho-fontionnelles du tube de *Lamellibrachia* sp., annélide siboglinidé inféodée aux suintements froids. Mes travaux ont apporté des données sur l'ultrastructure du tube et ont été intégré à une publication sur la perméabilité du tube de cet organisme (Julian et al. 1999), montrant un prélèvements des sulfures, non pas par le panache branchial, comme chez *Riftia pachyptila*, mais à travers la partie de son tube enfouie dans le sédiment, où la concentration en sulfures est nettement plus élevée qu'autour des branchies.

Ayant été happée par ces environnements fascinants, j'ai souhaité poursuivre en thèse au sein de cette équipe. N'ayant pas eu de bourse de thèse, j'ai eu la chance, grâce à Sylvie Tufeu-Marull, de pouvoir être financée pendant ma thèse en travaillant à mi-temps, comme technicienne en microscopie, pour les laboratoires Yves Rocher. Quatre ans de thèse, où j'ai beaucoup appris sur différentes techniques de microscopie, les cheveux, la peau, et en même temps sur les interactions biogéochimiques de l'annélide *Avinella pompejana* avec son environnement!

Activités de recherche

1. Travaux de thèse: *Alvinella pompejana*

Au cours de ma thèse (1997-2001), je me suis intéressée aux interactions biogéochimiques en milieu hydrothermal, avec pour modèle d'étude l'annélide *Alvinella pompejana*. L'objectif de ce travail était, via l'étude des minéralisations internes et externes associées au tube sécrété par l'animal, d'approcher les conditions du micro-habitat de cette espèce. *A. pompejana* colonise la paroi des cheminées hydrothermales actives, environnement hypervariable, chaud et soumis en permanence à une pluie de particules minérales qui précipitent lors du mélange entre le fluide hydrothermal chaud et l'eau de mer froide. L'utilisation de modules de colonisation a permis de montrer que ces animaux, bien que

sessiles, ont des capacités de sécrétion de tube et donc de migration le long de la paroi des cheminées extrêmement élevées (croissance du tube de 1 cm/jour). La mise au point de méthodes pour l'observation et l'analyse à l'échelle microscopique de matériaux biologiques fortement minéralisés m'a permis de montrer l'existence de nanocristaux de sulfures de zinc dans l'épaisseur du tube, très différents (en taille et en composition) des minéralisations retrouvées sur la surface externe de celui-ci. Ces résultats témoignent d'un micro-environnement à l'intérieur du tube très différent du milieu environnant, ce qui suggère que le tube agirait comme une barrière efficace entre l'animal et son environnement externe et pourrait expliquer la capacité exceptionnelle de ces animaux à coloniser ce biotope hostile (Zbinden et al. 2001, 2003; Le Bris et al. 2005).

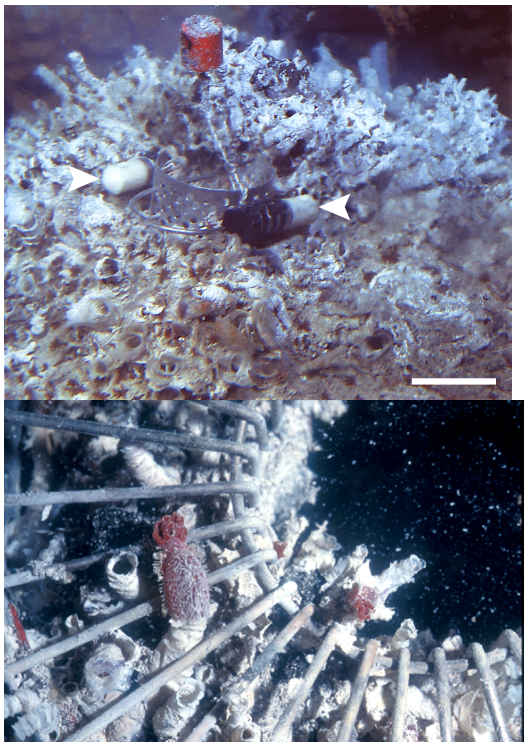

TRAC sur le site Pulsar (13°N/EPR) (de Pradillon et al. 2005), et colonisation par des *Alvinella* sp. sur le site Mvent (9°N/EPR).

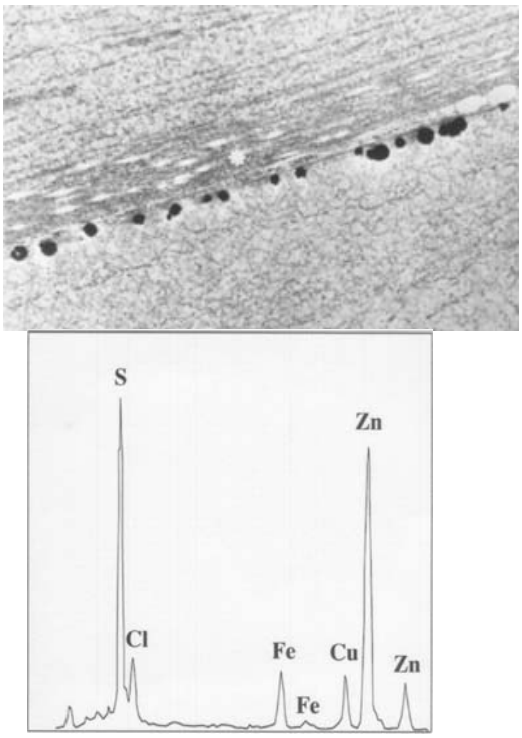

Nanocristaux de sulfure de zinc entre les couches de tube et analyse EDX (de Zbinden et al. 2001).

L'utilisation des modules de colonisation a également permis l'étude des processus de colonisation de substrat vierge par les micro-organismes (en collaboration avec les microbiologistes de l'Ifremer, Alain et al. 2004) et par la macrofaune (Pradillon et al. 2005, 2009).

2. Post-doctorat et suite: *Rimicaris exoculata* et ses symbiontes chimioautotrophes.

C'est lors de mon post-doctorat, au Laboratoire de Morphologie Fonctionnelle et Evolutive de l'Université de Liège, que j'ai commencé à travailler sur la symbiose de *Rimicaris exoculata,* sous la direction de Philippe Compère. Travail que j'ai continué depuis lors, dans l'équipe de Françoise Gaill au sein de l'UMR SAE 7138 Systématique, Adaptation et Evolution, puis dans l'équipe de Bruce Shillito au sein de l'UMR BOREA 7208 Biologie des ORganismes et Ecosystèmes Aquatiques, et cela en collaboration étroite avec Marie-Anne Cambon-Bonavita de Laboratoire de Microbiologie des Environnements Extrêmes de l'Ifremer de Brest.

Ce modèle a constitué le cœur de mes recherches depuis 14 ans et je présenterai l'ensemble de ces travaux sous la forme d'une revue (rédigée en anglais à des fins de publication) sur ce

modèle, incluant aussi bien mes travaux et collaborations que les travaux des différents auteurs ayant fait avancé nos connaissances sur cette crevette si étonnante!

3. L'axe Bois Coulés et les autres symbioses chimiosynthétiques

Lors de la création de l'UMR Systématique, Adaptation, Evolution (direction H. Leguyader / F. Gaill) en 2002, des axes transversaux ont été développés pour fédérer les équipes autour de thèmes communs. Un de ces axes concernait l'étude de bois coulés et de leur faune associée.

L'existence de débris végétaux et d'une faune associée originale et abondante a été documentée jusque dans les grands fonds marins dès les premières grandes expéditions de circumnavigation (Expédition Challenger 1873-1876, Expédition Galathea 1950-1952). Mais en dehors des inventaires faunistiques liés aux expéditions, peu d'études se sont penchées sur ces organismes, longtemps considérés comme de simples curiosités. Ces écosystèmes ont connu un fort regain d'intérêt en 2000, quand Distel et collaborateurs ont souligné les affinités évolutives de moules hydrothermales avec celles trouvées sur les bois coulés et les os de baleines.

Le co-encadrement de la thèse de Marie Pailleret avec des collègues de paléobotanique (J. Broutin et C. Privé-Gil, UMR5143) nous a permis de nous intéresser à la fois à la colonisation faunistique des bois coulés, mais également à la structure même du bois et sa dégradation sous l'action des bactéries, des champignons et des animaux (Pailleret et al. 2007a, b; Palacios et al. 2006, 2009; Dupont et al. 2009; Fagervold et al. 2012).

En collaboration avec d'autres collègues, je me suis intéressée à un certain nombre d'organismes associés à ces bois coulés et présentant des symbioses cellulolytiques et/ou chimioautotrophes: oursin (Becker et al. 2009), galathées (Hoyoux et al. 2009, 2012), patelle (Zbinden et al. 2010) ou encore chitons (Duperron et al. 2013).

Colonisation d'un bois coulé par *Pectinodonta* sp. (Zbinden et al. 2010).

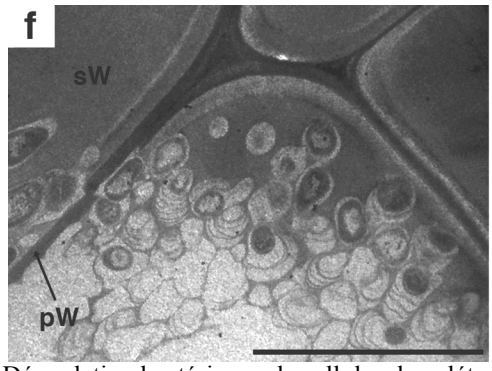

Dégradation bactérienne de cellules de palétuvier immergé expérimentalement pendant 20 mois (cliché MET Palacios et al. 2009)

***Rimicaris exoculata*, a symbiotic shrimp from hydrothermal vents : Review of its biology, ecology, physiology**

Rimicaris exoculata, a symbiotic shrimp from hydrothermal vents : Review of its biology, ecology, physiology.

1. Presentation

1.1. Distribution

The discovery of hydrothermal vents on ocean ridge crests in 1977, off the Galapagos Islands, was quickly followed by vent discoveries along the East Pacific Rise (EPR) (Lonsdale 1977; Corliss et al. 1979). But the exploration of the Mid-Atlantic Ridge (MAR) only started in 1985. Faunal assemblages were there very different from those found a few years earlier on the EPR. They were characterized by the absence of alvinellids and vestimentiferan tubeworms, and the presence of important motile swarms of shrimp (Fig. 1a) of the family Alvinocarididae, in particular *Rimicaris exoculata*, which dominates by far populations of the deep MAR vent fields (Van Dover et al. 1988; Segonzac 1992; Gebruk et al. 1997a; Desbruyères et al. 2001).

Rimicaris exoculata (Williams & Rona, 1986) is reported on most of the north MAR sites, except the shallowest ones (Fig. 1b and Table 1): Menez Gwen (850 m depth) and Lucky Strike (1700 m depth), where only very few specimens were observed (Gebruk et al. 2000; Pond et al. 2000a, b). It also occurs on two sites of the south MAR, at depths between 2300 and 4200m.

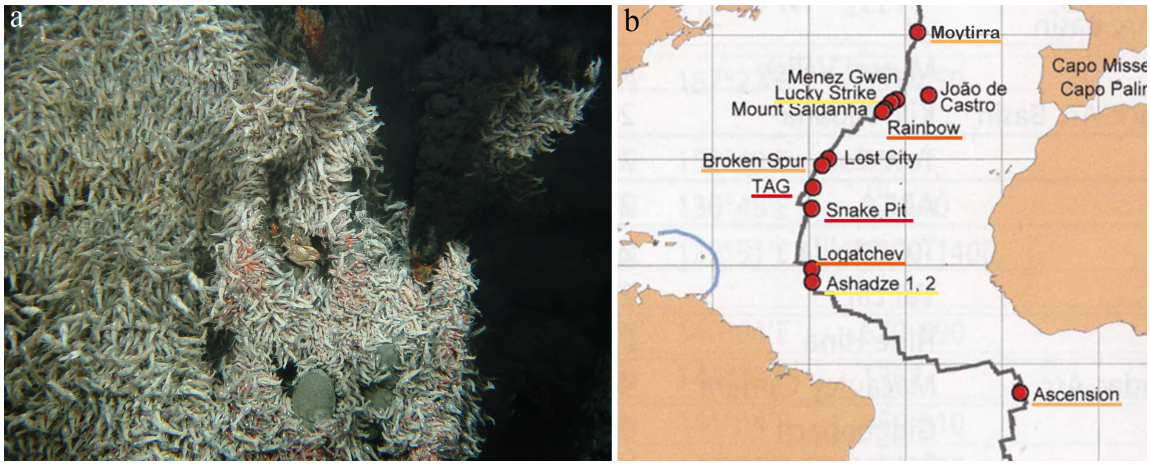

Figure 1: a) *Rimicaris exoculata* swarm at the TAG site (© Exomar / Ifremer) b) Distribution map of *R. exoculata* populations along the Mid-Atlantic Ridge, with density informations from the less (yellow) to the more (red) colonised sites (modified from Desbruyères et al. 2006).

Table 1 : Location of MAR vent fields hosting *Rimicaris exoculata* (data from InterRidge database: http://vents-data.interridge.org/)

Vent field	Latitude	Longitude	Depth (m)	Shrimp density	Discovery
Moytirra	45°28' N	27°51' W	2900	**	2011
Lucky Strike	37°17' N	32°16' W	1740	*	1993
Rainbow	36°16' N	33°54' W	2320	***	1986
Broken Spur	29°10' N	43°10' W	3100	**	1993
TAG	26°08' N	44°49' W	3670	****	1986
Snake Pit	23°22' N	44°57' W	3500	****	1985
Logatchev	14°45' N	44°58' W	3050	***	1994
Achadze	12°58' N	44°51' W	4200	*	2003
Ascension (Wideawake, Red Lion)	4°47' S	12°22' W	2990, 3048	**	2005

Shrimp densities based on personnal observations, Desbruyères et al. 2000 and Wheeler et al. 2013
* : very rare or not observed during the most recent cruises, ** : rare, ***: abundant, ****: very abundant

1.2. Habitat

R. exoculata, the most extensively studied hydrothermal shrimp species to date, occurs on the active chimney walls, in amazingly dense swarms that may contain 1500 to 3000 individuals per square meter (Fig. 1a), packed side by side and piled two or more deep (Van Dover et al. 1988; Segonzac 1992; Copley et al. 1997; Gebruk et al. 1997a; Gebruk et al. 2000). Adults of *Rimicaris exoculata* are generally found crawling on the substratum (Rona et al. 1986; Segonzac et al. 1993), and maintain high levels of activity on active surfaces of black smokers (Van Dover et al. 1988). When displaced from the substratum, shrimp immediately seek to re-establish themselves near the source of hydrothermal fluid (Van Dover et al. 1988; Renninger et al. 1995), resulting in a teeming swarm oriented against the current of vent fluids (Copley et al. 1997). This species lives within steep chemical and thermal gradients, where hot, reduced hydrothermal fluid mixes turbulently with oxygenated seawater (Schmidt et al. 2008b). Thermal environment within the swarms has been well documented and reported temperatures range from 2.8 to 30°C (Van Dover et al. 1988; Segonzac et al. 1993; Desbruyères et al. 2001; Geret et al. 2002; Zbinden et al. 2004; Schmidt et al. 2008a). Nevertheless the measursments achieved within a few centimetres of the shrimp (Zbinden et al. 2004; Schmidt et al. 2008a) do not exceed 18°C. Occasional shrimp occur scattered at the periphery of community, rather motionless, where temperature is just above that of ambient seawater (2.4°C) (Gebruk et al. 1993; Segonzac et al. 1993).

Rimicaris colonizes sites along the MAR with chemically contrasted environments (Table 2). Most active hydrothermal sites known to date are basaltic, i.e. based on underlying rocks of basaltic nature. Water-rock interactions at basalt-hosted vents release fluids rich in H_2S, but rather depleted in H_2 and CH_4. On the other hand, the hydrothermal circulation at ultramafic sites (Rainbow, Logatchev, Achadzé) is hosted on mantle rocks. As a result, the fluid composition departs from the basaltic end–members, and is relatively depleted in H_2S and enriched in H_2, FeII and CH_4, as a result of the serpentinization processes (Charlou et al. 2002, 2010; Douville et al. 2002). Thus, the chemical composition of the *Rimicaris* habitat varies strongly between the different sites. *In situ* measurements of temperature, pH, ferrous iron and sulphide concentrations in the shrimp's environment reflected the moderate contribution of the fluid in the mixing with seawater (Zbinden et al. 2004). Analyses on the Rainbow site give near-neutral pH (6.3-8), high level of ferrous-iron (0.13-265 µM) and low level of sulphide (0.4-22 µM) (Geret et al. 2002, Zbinden et al. 2004, Schmidt et al. 2009). Little or no data are available for other hydrothermal sites (see Schmidt et al. 2008a, b for TAG data).

1.3. Brief morphological description

Here is a brief description of specific morphological characteristics of the species, according to Williams and Rona (1986), Segonzac et al. (1993) and Komai and Segonzac (2008) (Fig. 2). The size (total length measured from the anterior tip of the cephalothorax to the end of the telson) ranges from 31.3 to 50.2 mm for males, from 42.3 to 57.4 mm for females, and from 23 to 47,4 mm for juveniles. The rostrum is strongly reduced. The antennular and antennal peduncles are hypertrophied. The cephalothorax is dorsoventrally compressed, distinctly broader than pleon, with strongly inflated branchial regions. The carapace extends forward and ventrally and encloses cephalic, but also anterior thoracic appendages up to the second pair of pereiopods, in an almost closed "prebranchial" chamber. The structure of the mouthparts is particularly modified : exopodites of the second maxilla and first maxillipeds are enormously expanded anteriorly, occupying two third of the prebranchial chamber. They are entirely covered on both sides with long and numerous setae. The mandibles have regressed. The two first pereiopods are relatively small and probably cannot extend out of the branchial chamber. The stomach is reduced in volume. The ocular region, strongly modified, is characterized by transverse ocular plates, with no eye-stalks.

The name *Rimicaris* came from the latina "*rima*", meaning rift or fissure, with reference to the Mid-Atlantic Ridge, and from the greek "*karis*", meaning shrimp. *Exoculata* came from the latina "*exoculo*", meaning deprived of eyes (Williams and Rona 1986).

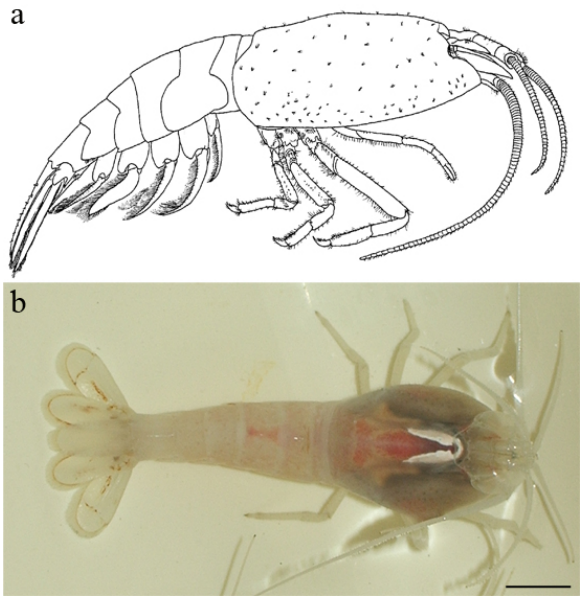

Figure 2: *Rimicaris exoculata*. a) Drawing of the lateral view (from Williams and Rona 1986). b) Dorsal view showing the carapace with a branchial region strongly inflated. Scale bar: b = 1cm

1.4. Classification

The genus *Rimicaris* was originally established (in the family Bresiliidae) for two species discovered from the hydrothermal vent field TAG (Tans- Atlantic Geotraverse) on the MAR : *Rimicaris exoculata* (Williams and Rona 1986) and *R. chacei* (Williams and Rona 1986). The former was designated as the type species of the genus. *Rimicaris chacei* was later transferred to the genus *Chorocaris* (Martin and Hessler 1990). The genus *Rimicaris* was later assigned to the family Alvinocarididae (Christoffersen 1986; Segonzac et al. 1993; Komai and Segonzac 2003), and a new subfamily (Rimicaridinae) comprising the genus *Rimicaris* was erected in 2015 by Vereshchaka and collaborators.

Two species, first described as 1) *Rimicaris aurantiaca* (Martin, Signorovich and Patel 1997), described from Snake Pit site (from 20 specimens ranging from 21.5 to 26.8 mm in total length), and 2) *Iorania concordia* (Vereshchaka 1996), described from TAG site (from 26 females ranging from 8.0 and 9.2 mm in total length), were subsequently assigned to *Rimicaris exoculata*. Nuckley et al. (1996) also assigned these small orange shrimp to *Rimicaris* sp., based on a detailed study of their unusual visual apparatus. Some workers (Segonzac et al. 1993) have early suggested that these small orange individuals may correspond to juvenile stages of *R. exoculata*. Their opinion was based on: (i) the absence of females with eggs and mature males with developed appendix interna in samples of the small orange shrimp; and (ii) maximum carapace length of the small orange shrimp which overlap with minimum carapace length of adult *R. exoculata*, suggesting the two are different stages of the same species. Allozymes and mitochondrial DNA sequences of samples from Broken Spur, TAG and Snake Pit sites further confirmed that these two small orange shrimp were indeed juveniles of *R. exoculata* (Creasey et al. 1996; Shank et al. 1998). The very different coloration (bright orange, due to the high content in astaxanthin carotenoidin pigments in the hepatopancreas, Nègre-Sadargues et al. 2000) and morphology (the slightly inflated branchiostegites and oval rather wing-shaped dorsal organ in juveniles (Vereshchaka 1996; Nuckley et al. 1996; Shank et al. 1998)) explain these taxonomic confusions (Martin and Haney 2005). It is now established that *Rimicaris aurantiaca* and *Iorania concordia* indeed correspond to one of the four stages of *R. exoculata* juveniles described by Komai and Segonzac (2008).

Up to 2015, there were 3 species is this genus : *R. exoculata*, *R. kairei* (decribed from hydrothermal vent fields "Kairei" on the Central Indian Ridge, Watabe and Hasimoto 2002) and *R. hybisae* (decribed from hydrothermal vent fields on the Mid-Cayman Spreading Centre, Nye et al. 2011). In 2015, using both morphological and molecular (COI and 16S ribosomal markers) approaches on all the 31 known species of Alvinocarididae, Vereshchaka and collaborators synonymized all the genus *Chorocaris* with *Rimicaris* (which was already proposed by Creasey et al. in 1996, Shank et al. 1999 and Teixeira et al. in 2013, and discussed by Komai and Tsuchida in 2015). This included 6 new species in this genus : *R. chacei* (its initial classification in 1986 by Williams and Rona), *R. paulexa* (Martin and Shank 2005), *R. parva* (Komai and Tsuchida 2015), *R. vandoverae* (Martin and Hessler 1990), *R. variabilis* (Komai and Tsuchida 2015) and *R. susannae* (Komai, Giere and Segonzac 2007). None of these 6 new *Rimicaris* possess the enlarge gill chamber observed in *R. exoculata*, *R. kairei* and *R. hybisae*. Their scaphognathites are moderately broad and devoid of facial bacteriophore setae (except for *R. vandoverae* and *R. chacei*) and no bacterial colonisation of the gill chamber was described for these species until now, except for *R. chacei* (Casanova et al. 1993; Gebruk et al. 2000).

2. A double symbiosis

Two microbial epibiotic community have been described associated with *R. exoculata*. One is located located in the gut, the other in the gill chamber.

2.1. Digestive tract

Morphological descriptions of the digestive tract of *R. exoculata* reveal a small stomach with few grinding structures, arguing for a low mechanical digestive activity (Segonzac et al. 1993; Durand et al. 2010). The midgut, i.e. the central digestive absorption zone deprived of a cuticle, represents two thirds of the total length of the digestive tract, and is significantly longer than in most crustaceans (Durand et al. 2010).

The first studies examining the digestive tract of *R. exoculata* reported together a high sulfur mineral content, typical of chimney walls (chalcopyrite $CuFeS_2$, pyrite FeS_2 and sphalerite ZnS), along with iron oxides (Van Dover et al. 1988; Segonzac et al. 1993) (Fig. 3a, b). Elevated bacterial densities was also reported in the stomach (10^9 cells per ml of stomach content, Van Dover et al. 1988) and increasing still in the mid- and hindgut (Polz et al. 1988). A high CO_2 fixation rate in the mid- and hindgut suggested that a highly active chemoautotrophic bacterial population in the gut could be a nutritional source (Polz et al. 1998), using the polymetallic sulphide content of the gut as an energy source.

Shrimp cuticle fragments were also observed in the gut content (Zbinden et al. 2004). A possible eating of freshly moulted exuviae to ingest associated bacteria was suggested, but as the bacterial coverage decreases beneath the iron oxyde crust before moult (Zbinden et al. 2004; Corbari et al. 2008a), it seem more likely that *Rimicaris* eats the exuvium to recover the minerals (e.g. calcium) contained in the cuticle, as it happens in other crustaceans (Steel 1993; Corbari et al. 2008a).

Stomach bacteria seem to be under a digestion process, as bacterial DNA and lipopolysaccharids were detected (Van Dover et al. 1988; Durand et al. 2010) but SEM and TEM observations failed to show intact microorganisms (Van Dover et al. 1988; Zbinden and Cambon-Bonavita 2003). On the other hand, midgut bacteria were shown to belong both to a transient and a specific resident gut microflora (Zbinden and Cambon-Bonavita 2003; Durand et al. 2010). A dense bacterial population of long thin (0.2 µm x 15 µm) single-celled bacteria is present between the microvilli of the midgut epithelium (Durand et al. 2010) (Fig. 3c, d). This population is separated from the bolus by the peritrophic membrane and is thus not part of the shrimp diet, at least through a digestion process. As the midgut is deprived of cuticle, and thus not subject to exuviation, this probably favours long-term microbial colonization and

interactions of this resident microbial community with its host (Durand et al. 2010). Intact rods and cocci were also observed within the gut content (Zbinden and Cambon-Bonavita 2003). Pond et al. (1997a) suggested that the gut bacteria could contribute to the animal's diet not through a digestion process but rather through the provision of essential dietary components.

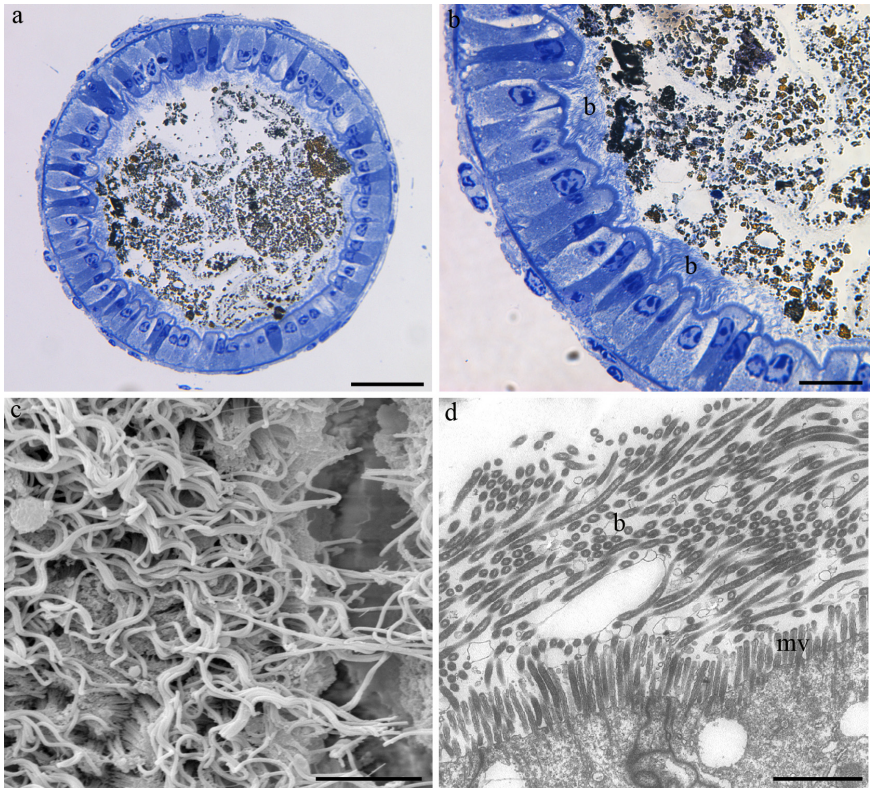

Figure 3: *R. exoculata* gut epibionts. a) Semi-thin section in the midgut showing the mineral black and brown mineral particles (respectively iron sulphides and oxides). b) Closer view on the epithelium showing the abundance of filamentous epibiotic bacteria (b) all around the section. c) SEM view of the epibionts (picture L. Durand). d) TEM observations of the bacterial gut epibionts (b) inserted bewtween the microvilli (mv). Scale bars : a = 50µm, b = 20 µm, c = 5 µm, d = 2 µm

The bacterial diversity in the midgut is dominated by only 3 major groups, *Defferibacteres*, *Mollicutes* and *Epsilonproteobacteria* (and to a lesser extent *Gammaproteobacteria*) (Zbinden and Cambon-Bonavita 2003, Durand et al. 2010), and is low compared to that of the environment (Durand et al. 2015). Those 3 lineages were also still present after a 72 h starvation experiment leading to a completely empty gut, and were then designated as resident epibionts (Durand et al. 2010) rather than transient microflora. The two former phylotypes, absent from the environment (except for one clone collected close to shrimp aggregates (Hügler et al. 2011)), could be specific and selected bacterial resident community (Zbinden and Cambon-Bonavita 2003; Durand et al. 2010, 2015). Conversely, *Epsilonproteobacteria* gut and gill chamber epibionts were similar, suggesting a part of it could be directly acquired from the gill chamber and may thus be a transient community remaining thanks to a permanent ingestion process (Durand et al. 2015). As no clear hybridization response could be obtained on the thin filamentous bacteria inserted between the microvilli, their phylotype assignation remains uncertain (Durand et al. 2010). Starvation experiments emptying the bolus eliminate most of the *Deferribacteres*, arguing that the filaments do not belong to this group. *Mollicutes* are suspected, based on their morphology, but this has not been proved (Durand et al. 2010).

Beside the trophic role, a detoxification role of minerals or heavy metals has been proposed for the gut bacteria (Durand et al. 2010).

2.2. Cephalothorax

2.2.1. Localisation

Bacteria colonise almost all the available surfaces of the branchial chamber (Fig. 4a), with the notable exceptions of the gills and the inner side of the branchiostegites facing them (Zbinden et al. 2004). Bacteria are mostly present on the bacteriophore setae of the dorsal and ventral sides of hypertrophied exopodites of the second maxilla (scaphognathites) and first maxillipeds (Fig. 4b, c), as well as on the internal tegument of the carapace (branchiostegite) at the level of the prebranchial chamber (Fig. 4d, e) (Casanova et al. 1993; Segonzac et al. 1993).

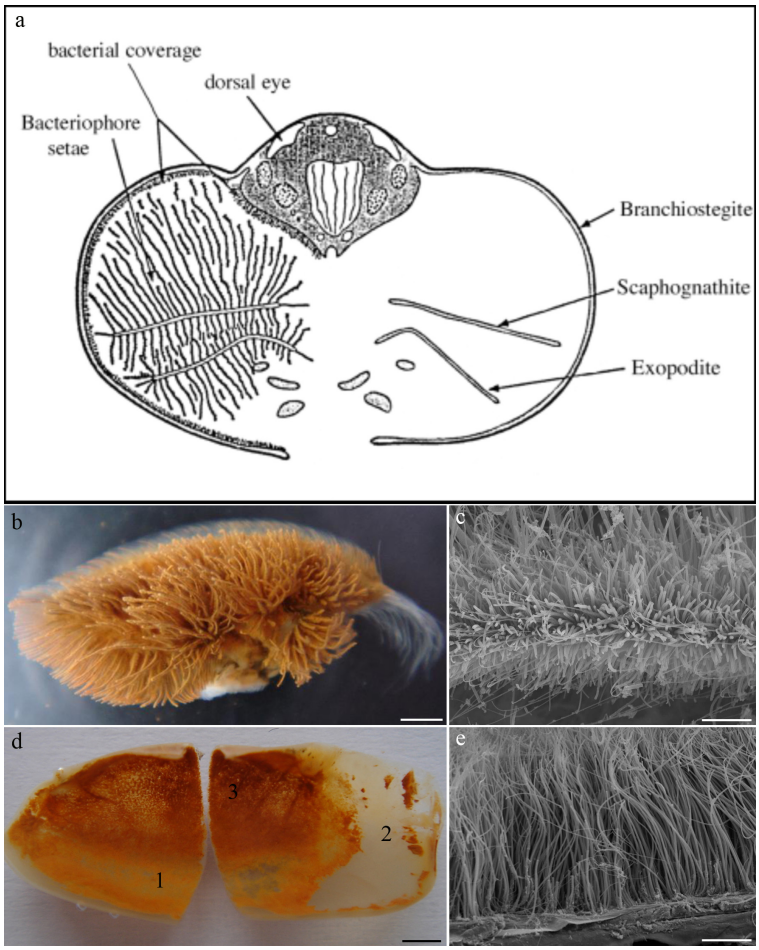

Figure 4 : *R.exoculata* epibiotic bacteria of the cephalothorax. a) Schematic cross-section of the cephalothorax (modified from Segonzac et al. 1993). b) Scaphognathite covered by bacteriophore setae. c) SEM close-up on a seta covered by filamentous bacteria. d) Inner side of the banchiostegite (where we can see the 3 area described below : 1, 2, 3) (picture P. Compère). e) SEM close-up on the mat of filamentous bacteria of the third area. Scale bars : b, d = 2 mm, c = 20 µm, e = 100 µm

Investigation of bacteria by Scanning Electron Microscopy (SEM) on the inner side of the branchiostegite revealed 3 distinct compartments in the gill chamber (Fig. 4d): (1) the lower pre-branchial chamber, housing only a thin bacterial coverage; (2) the 'true' branchial chamber, containing the gills and completly devoid of bacteria; and (3) the upper pre-branchial chamber, housing the main ectosymbiotic bacterial community. The limit between the upper and lower pre-branchial chamber corresponds to the position of the exopodites of the first maxillipeds, the scaphognathites being entirely enclosed in the upper pre-branchial chamber (Zbinden et al. 2004). The water current, generated by the beating of the scaphognathites, enters ventrally, passes from the lower pre-branchial chamber (first compartment), to the gills (second compartment), and then through the upper pre-branchial chamber containing the epibiont community (third compartment), bringing both oxygenated

seawater to the shrimp gills and dissolved reduced compounds to bacteria (Casanova et al. 1993; Segonzac et al. 1993; Zbinden et al. 2004).

Using oligonucleotide slot-blot hybridization, Polz and Cavanaugh (1995) estimated that an average shrimp would carry $8.5x10^6$ bacteria, which would correspond to 2 to $4x10^{11}$ bacteria per m^2 in the swarms.

2.2.2. Chemosynthetic symbiosis

As light does not penetrate deeper than the first few hundreds meters depth of the ocean, hydrothermal ecosystems are devoid of local photosynthetic production, which usually fuels the ecosystems on Earth. It was quickly evidenced that bacterial chemosynthesis was the major, if not the sole, food source for the unusually rich bottom fauna clustered around the vents (Jannasch and Wirsen 1979). The food web of these communities is based on chemoautotrophic bacteria living upon reduced compounds (mainly sulphur and methane, Nelson and Fischer 1995) that are leached by superheated water from surrounding rocks. If suspension feeders or grazers consume bacteria directly, one of the most striking feature of the hydrothermal environment is the number of species that have established symbioses, cultivating their bacteria either within their tissues or on the external surface of their bodies. For Jannasch (1985), chemosynthetic symbioses account for the major part of the total primary production at the deep-sea vent sites.

One of the best studied symbioses of these ecosystems is that of *Rimicaris exoculata* which harbors a dense bacterial community within its cephalothorax and on its buccal appendages. While several endosymbioses had already been studied and demonstrated at the time of *Rimicaris* discovery (as in the vestimentiferan tubeworms or the vesicomyid clams, Cavanaugh et al. 1981; Cavanaugh 1983), ectosymbioses were not commonly reported and had only been described from EPR species like the polychaete *Alvinella pompejana* (Desbruyères et al. 1983) or the limpet gastropod *Lepetodrilusus fucensis* (de Burgh & Singla 1984).

2.2.3. Trophic symbiosis

The enormous densities of *R. exoculata* on the MAR, and their dominance on many sites rapidly raised questions on how these populations were sustained. Furthermore, these shrimp cluster close to the zone of mixing between the hot fluid and seawater, displaying an intense activity, quite unusual for deep-sea organisms (Segonzac 1992). This peculiar behaviour led several authors to question benefit shrimp could obtain from it.

The first investigations on the feeding biology of *Rimicaris exoculata* led Van Dover et al. (1988) to propose that these shrimp were normal heterotrophs, grazing on free-living microorganisms colonizing the black smoker chimneys. This conclusion comes from: 1) the results of lipopolysaccharide assays that revealed large amount of bacterial cell-wall material in the stomach content, along with the fact that the gut is filled by sulphides particles; 2) the $\delta^{15}N$ and $\delta^{34}S$ isotopes; and 3) the fact that they were unable to detect trace of chemoautotrophy (i.e. ribulose-1,5-bisphosphate carboxylase activity) in the studied tissues (gut, hepatopancreas, gonads, abdominal muscles). These authors, looking only for chemoautotrophic endosymbiotic bacteria, nevertheless acknowledged that they possibly had not identified the correct host tissues. They also reported the occurrence of a dense coating of filamentous microorganisms on the setae of the exopodites of the second maxilla and first maxilliped, which they proposed to constitute a second nutritional source.

It rapidly became obvious that if shrimp occupied a substratum directly exposed to the flow of hydrothermal flow, it was to sustain chemosynthetic primary production of the epibiotic chemosynthetic bacterial community that they harvest in their cephalothorax (Gebruk et al. 1993; Polz and Cavanaugh 1995). Indeed, some authors proposed that the amount of bacteria present on chimney walls was not enough to support the shrimp population and rather suggested an alternative hypothesis to that of Van Dover, which is that *Rimicaris*

exoculata gained most of its carbon from the epibiotic bacteria living within its carapace, by scraping and grazing on them (Wirsen et al. 1993; Gebruk et al. 1993; Casanova et al. 1993; Polz et al. 1988; Rieley et al. 1999). Furthermore, the morphology of the two pairs of chelipeds, which are relatively small, suggested that they probably could not extend out of the branchial chamber to graze the chimney wall. On the other hand, they are able to reach and clean the surfaces of all appendages within the chamber, as well as the internal wall of the carapace, and then carry the scraped particles to the mouth (Van Dover et al. 1988).

The highly specialized morphological features of *Rimicaris* (hypertrophied branchial chamber and mouthparts, bacteriophore setae, Fig. 4) suggest a real bacterial culture in the shrimp pre-branchial chamber and argue for a trophic symbiosis (Gebruk et al. 1993). A number of lines of evidence converged towards the present consensus, i.e. that the epibionts are the major source of carbon (80% according to a calculation by Polz et al. 1998): i) close $\delta^{13}C$ values of the saturated and monounsaturated fatty acids isolated from the muscle tissues of *R. exoculata* (-13‰) and the epibionts (-12‰), ii) the very high level of polyunsaturated (n-7) and (n-4) fatty acids, both in the epibionts and the *R.exoculata* samples (Pond et al. 1997a; Allen-Copley et al. 1998; Rieley et al. 1999; Pond et al. 2000a, b). Many studies have reached similar conclusions considering the close $\delta^{13}C$ signature between the epibiotic bacteria (-9.3 to -12.4‰, Polz et al. 1988; Gebruk et al. 2000) and *Rimicaris* tissues (-10 to -12.5‰, Van Dover et al. 1988; Polz et al. 1988; Gebruk et al. 1997b, 2000; Pond et al. 1997a; Vereshchaka et al. 2000).

Few year later, a third hypothesis argued for a trans-epidermal transfer of dissolved organic matter from the epibiotic bacteria through the branchiostegite cuticle (Casanova et al. 1993; Zbinden et al. 2004; Corbari et al. 2008a). Rejected by some authors (Gebruk et al. 2000) on the basis of previous studies that have shown that transport of dissolved organic matter across the chitinous exoskeleton in Crustacean is unlikely (Stephens, 1988), this hypothesis was nevertheless supported by several points: i) The thinness of the cuticle (up to 0.5 µm) and the important haemolymphatic lacunas underlying it, as well as the numerous membrane infoldings and mitochondria in branchiostegites epithelium beneath the bacteria (Martinez et al. 2005) suggest epidermal transport activity; ii) Despite a considerable number of observations, no areas scrapped by the animal, nor free of bacteria on the inner side of branchiostegites or on scaphognathites were never showed (Zbinden et al. 2004; Corbari et al. 2008a). Although supporting the hypothesis that the shrimp grazed off their epibionts, Polz et al. (1998) noticed that only slightly more than 20% of the rRNA detected in the gut correspond to that of the epibionts. In order to test the trans-tegumental hypothesis, Ponsard et al. (2013) performed *in vivo* shrimp incubations in a pressurised aquarium with isotope-labelled inorganic carbon ($NaH^{13}CO_3$ and $NaH^{14}CO_3$), complemented with different electron donors (sulphide $Na_2S_2O_3$ and iron Fe^{2+}). These experimentations provided direct evidence that bacterial epibionts are chemoautotrophs, and showed that the carbon incorporation rates increase in the presence of the two electron donors, indicating that both sulphide and iron oxidation metabolism occur among the epibionts (Fig. 5a). They showed above all that a direct nutritional transfer of soluble bacterial by-products to the host occurs, from the bacteria to the host, by transtegumental absorption across the gill chamber integument (Fig. 5b-d), rather than via the digestive tract. They thus provided the first direct evidence of a true mutualistic nutritional bacteria–host interactions.

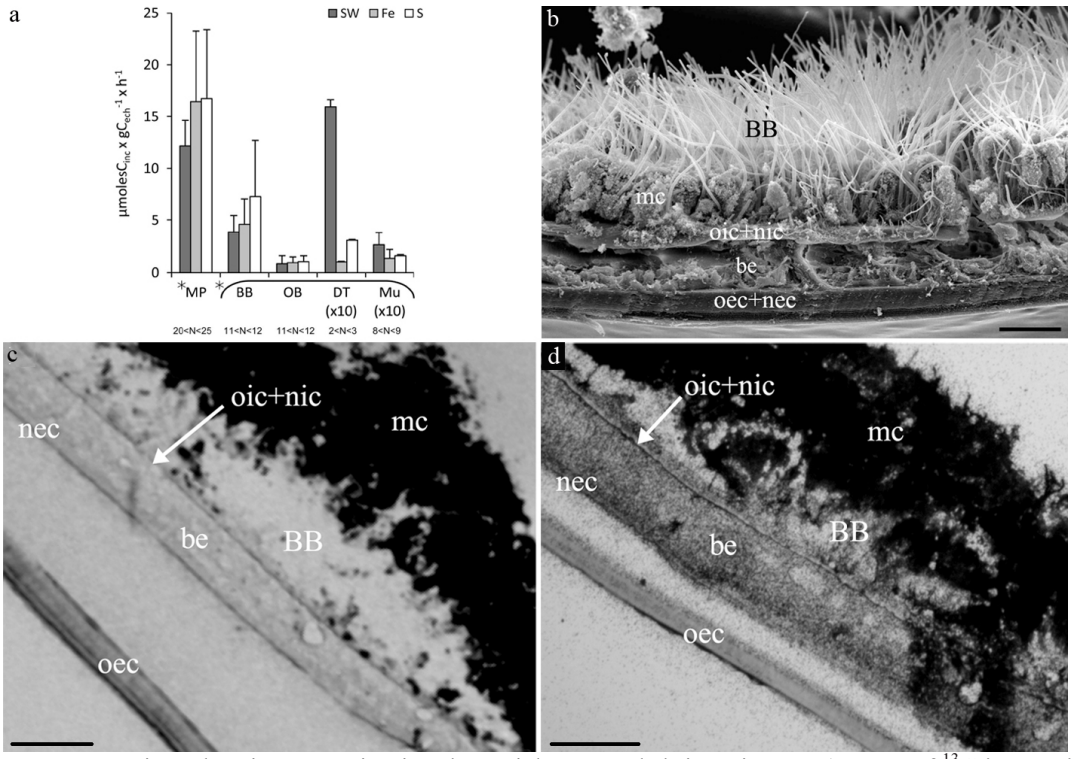

Figure 5: Inorganic carbon incorporation into bacterial mats and shrimp tissues. a) Rates of ^{13}C inorganic carbon incorporation. The shrimp were incubated for 4 or 10 h in $NaH^{13}CO3$ in pure seawater (dark grey), supplemented with reduced iron (light grey) or thiosulphate (white). MP: mouthparts, BB: bacterial biofilm of the branchiostegite, OB: outer branchiostegite, DT: digestive tract, Mu: muscles (from Ponsard et al. 2013). c-d) SEM and autoradiography of the branchiostegite of a specimen incubated with ^{14}C-acetate after only 3 days (c) and after 11 days of exposure (d). oic: old internal cuticle, be: branchiostegite epidermis, nic, nec; new internal and external cuticles, oec: old external cuticle. Scale bars : a = 1 cm, c = 50 µm, e-f = 100 µm.

2.2.4. Morphological diversity

Using SEM (Scanning Electron Microscopy) observations, several authors described three bacterial morphotypes: 2 filamentous types (one thin of 0.2 to 1 µm and one thick of 1 to 3 µm in diameter, both up to 250 µm length) and 1 rod-shaped type (0.5 x 1.5 µm) (Gebruk et al. 1993; Casanova et al. 1993; Segonzac et al. 1993; Zbinden et al. 2004).

Additionnal observations with TEM (Transmission Electron Microscopy) on Rainbow samples refined these data and defined 6 different types (Zbinden et al. 2008). Two sub-types of rods were distinguished based on size and aspect of the intracellular contents : 1) short and thick rods (0.6 x 1.25 µm), with a dense dark intracellular content and 2) longer and thinner rods (0.3 x 3 µm), with a light intracellular content. Two sub-types of thin filaments were also described based on their cell morphology and intracellular aspect: 1) thin filaments with rectangular cells, no marked narrowing between two adjacent cells and a homogeneous and dense content and 2) thin filaments with ovoid–shaped cells, with a marked narrowing between two adjacent cells, a more heterogeneous intracellular content and occurence of intracellular electron dense granules. Finally, in addition to the previously described thick filaments, these authors reported the occurence of bacteria with stacks of intracytoplasmic membranes typical of type I methanotrophs, bringing the diversity to at least 6 morphotypes (Fig.6).

Intracellular granules were observed in the thin filaments (and not in the other morphotypes). EDX (Energy Dispersive X-ray) microanalysis revealed two types of granules: one containing phosphorus and iron, probably as iron polyphosphate; the second type containing only sulphur (Zbinden et al. 2008). Globules of elemental sulphur were already reported in the *R. exoculata* filamentous bacteria by Gebruk et al. (1993). Shrimp maintenance in a pressurized aquarium lead to the emptying of most of the granules, thereby suggesting a storage role (Zbinden et al. 2008).

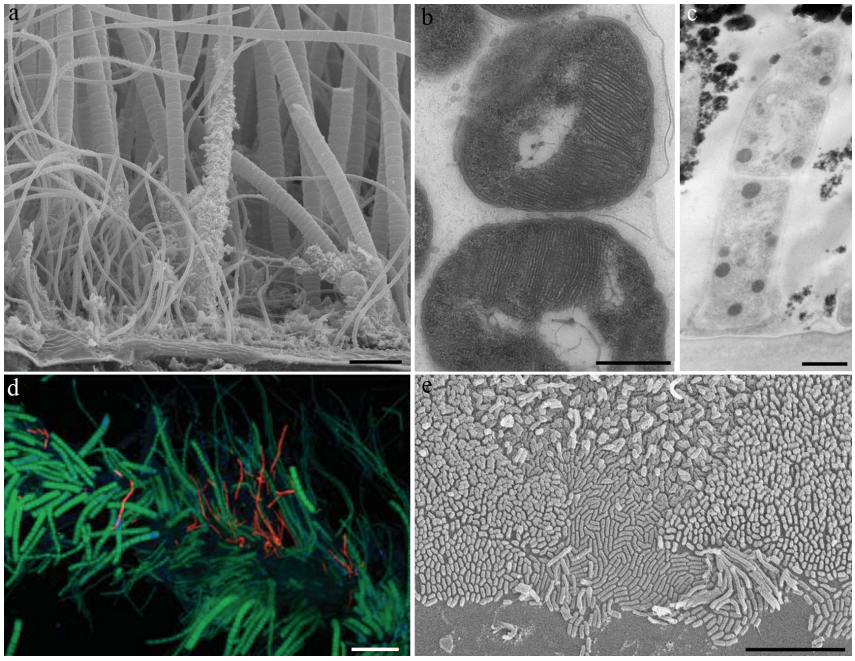

Figure 6: Diversity of gill chamber bacterial epibionts. a) SEM view of the thick and thin filamentous bacteria on the inner face of the branchiostegite. b) TEM view of a methanotrophic bacteria characterized by their stacks of intracytoplasmic membranes. c) TEM view of intracellular granules in the thin filaments (from Zbinden et al. 2008). d) FISH view of a scaphognathite setae showing *Epsilonproteobacteria* thick filament (green) and *Gammaproteobacteria* thin filament (red) (from Guri et al. 2012). e) SEM view of a monolayer of prostrate and erect rod-shaped bacteria. Scale bars : a, d, e = 10 µm, b, c = 0.5 µm

2.2.5. Phylogenetic diversity

If hydrothermal endosymbioses often rely on a limited number of symbionts (for example, only one symbiont, a sulphur-oxidizing *Gammaproteobacteria*, was found in *Riftia pachyptila*, *Calyptogena magnifica* or *Bathymodiolus thermophilus*, Distel et al. 1988), ectosymbioses are often composed of a highly diverse bacterial community, both phylogenetically and metabolically.

A first phylogenetic study (Polz and Cavanaugh, 1995) showed that all three morphotypes of *R. exoculata* epibionts belonged to a single bacterial phylotype of *Epsilonproteobacteria*. The high morphological diversity observed among the *R. exoculata* symbiotic community (see references above) rather pleads for a higher phylogenetic diversity, a hypothesis raised by Polz and Cavanaugh (1995) themselves. Advances in sequencing technologies has helped to refine the initial data and show a much larger diversity with bacteria belonging mostly to the Proteobacteria (78%) with two dominant groups : Epsilon- (39%) and Gamma- (30%) and lower abundance of *Alpha-*, *Beta-*, *Delta-*, and *Zetaproteobacteria*, as well as *Flavobacteria*, *Methanoccocci*, *Bacilli*, *Clostridia* and *Aquificae* (Zbinden et al. 2008; Petersen et al. 2010; Hügler et al. 2011; Guri et al. 2012; Jan et al. 2014). 2% of the sequences obtained from the metagenome of *R. exoculata* epibionts are affiliated with Archaea (Jan et al. 2014).

Fluorescent *in situ* hybridization (FISH) allowed to intersect the data of morphology and molecular biology and confirmed the predominance of *Epsilonproteobacteria* with thick and thin filamentous morphologies and *Gammaproteobacteria* related exclusively to some thin filamentous morphologies (Petersen et al. 2010; Guri et al. 2012). Type-I methanotrophic *Gammaproteobacteria* appear like circular "donuts" in FISH (Guri et al. 2012).

2.2.6. Metabolic diversity

Although the single phylotype described was initially infered to be sulphur-oxidizer, because of its morphological resemblance to *Thiothrix* (Wirsen et al. 1993) and the occurence

of sulphur granules within the cells (Gebruk et al. 1993), several authors suggested that a number of other reduced inorganic compounds could be used as electron donors for chemosynthesis, such as hydrogen, ammonia, nitrite and heavy metals such as iron or manganese (Jannash and Wirsen 1979). Segonzac et al. (1993) proposed that, owing to the numerous energy sources available on different MAR vent sites, it would be likely for *R. exoculata* symbionts to display different autotrophic metabolisms. Attempts to cultivate these symbionts (and beyond, all currently known symbionts) still remained unsuccessful and potential metabolism can only be inferred from occurence of specific genes or other indirect assumptions. Several studies revealed that the metabolic abilities of the *R. exoculata* symbiotic community were indeed much more diverse than initially thought.

Fluid chemistry

Chemoautotrophic metabolisms rely on bacterial oxidation of reduced compounds available in fluids. Vent fluids on the MAR exhibit varied chemical compositions (Table 2), resulting from temperature and pressure conditions and the nature of the source rocks hosting the hydrothermal convection (Desbruyères et al. 2000). In particular, fluid emissions occurring in ultramafic rocks (Rainbow, Logatchev, Achadzé) are characterised by fluids enriched in metals and gases (H_2: up to 19 mM and CH_4: 2.5 mM) resulting from serpentinization and relatively impoverished in H_2S (Charlou et al. 2010). The fluid from the Rainbow site is also characterized by a very high quantity of Fe (24 mM). On the other hand, basalt-hosted sites such as TAG, Broken Spur, Snake Pit expel endmember fluids that are enriched in H_2S (up to 11 mM) but impoverished in H_2, CH_4 or Fe (Charlou et al. 2002).

Table 2 : Concentration of the main electron donors in the end-member fluid of different sites colonised by *R. exoculata* populations (data from Desbruyères et al. 2000, Douville et al; 2002, Charlou et al. 2002, 2010).

	SW	Rainbow	Broken Spur	TAG	Snake Pit	Logatchev	Achadzé
type		ultramafic	basaltic	basaltic	basaltic	ultramafic	ultramafic
pH	7.8	2.8-3.1	-	2.5-3.4	3.7-3.9	3.3-3.9	3.1
H_2S (mM)	0	1.2-1.4	8.5-11	2.5 - 6.7	6.7	1.1-1.4	1
CH_4 (mM)	0.0003	1.6-2.5	0.065-0.13	0.124 - 0.147	0.046 - 0.062	2-2.6	0.5-1.2
H_2 (mM)	0.0004	13-16	0.43-1.03	0.15-0.37	-	9-12.5	8-19
Fe (µM)	<0.001	24	1.68 - 2.16	1.64 - 5.45	2400	1825/2500	9300

Chemoautotrophy

Chemoautotrophy of the gill-chamber bacterial population was early established by reports of both ^{14}C-labelled bicarbonate incorporation and high Rubisco activity in the bacteria covering the shrimp mouthparts and carapace (Wirsen et al. 1993; Polz et al. 1998; Ponsard et al. 2013). Two carbon fixation pathways co-occur in the epibotic community: the Calvin-Benson-Bassham (CBB) cycle and the reductive tricarboxylic acid (rTCA) cycle, as highlighted by the gene detection of their respective key enzymes (the ribulose-1,5-bisphosphate carboxylase/oxygenase (RubisCO) and the ATP-dependent citrate lyase (ACL) (Hügler et al. 2011; Jan et al. 2014). The rTCA cycle is used by the *Epsilonproteobacteria*, as in all chemoautotrophic *Epsilonproteobacteria* investigated to date (Campbell and Cary 2004; Hügler et al. 2005, 2011), whereas the CBB cycle is mediated by the *Gammaproteobacteria* (Hügler et al. 2011; Jan et al. 2014). The *Zetaproteobacteria* also contain genes for the CBB cycle (Jan et al. 2014).

Only genes coding for the RubisCO type II were identified (Hügler et al. 2011; Jan et al. 2014), which is consistent with the isotopic data. Invertebrate-chemoautotroph symbioses fall into two main groups based on stable carbon isotope ratios: the "-30‰" group and the "-11‰"

group (Robinson and Cavanaugh 1995). The "-11‰" group (the *Rimicaris* group, see reference above) express the RubisCO type II. This form is adapted to low oxygen and medium to high carbon dioxide concentrations (Jan et al. 2014).

Incorporation of radio-labelled small organic molecules (^{14}C-acetate and ^{3}H-lysine) in thick and thin filaments indicates that at least a fraction of the symbionts can switch to a mixotrophic metabolism, depending on available energy and/or carbon sources (Ponsard et al. 2013)

Sulphide oxidation

Sulphide oxidation was initially proposed as the sole metabolism of the symbiotic population (Wirsen et al. 1993), based on i) the phylogeny of the symbionts (thought to belong to a single phylotype, Polz and Cavanaugh 1995), ii) the high level of H_2S in the Snake Pit site from where the shrimp and bacteria were first described, and iii) the observation of internal sulphur globules in shrimp ectosymbionts (Gebruk et al. 1993).

Successful amplification of several genes coding for subunits of key enzymes involved in the sulphur compounds oxidation confirmed the occurrence of this metabolism within the epibiotic community: genes coding for the adenosine-5'-phosphosulphate reductase (*aprA*), related to *Gammaproteobacteria* (Zbinden et al. 2008; Hügler et al. 2011) and genes coding for a sulphate thiohydrolase (*SoxB*), related to *Epsilonproteobacteria* (Hügler et al. 2011). Other *Sox* genes (*SoxAZYX*, *SoxB*, *SoxW*) affiliated to *Gammaproteobacteria* were also found (Jan et al. 2014). *Dsr* genes (coding for the dissimilatory sulphate reductase) were found in *Gammaproteobacteria* (Jan et al. 2014). This enzyme is known to promote the oxidation of stored elemental sulphur, and could in this case be used to take advantage of the reserves of intracellular elemental sulphur (Zbinden et al. 2008).

Hügler et al. (2011) highlighted the co-occurrence of sulphur-oxidizing and sulphur-reducing epibionts among the symbiont community suggesting that they may be involved in a syntrophic exchange of sulphur compounds, which could increase the overall efficiency of this epibiotic community.

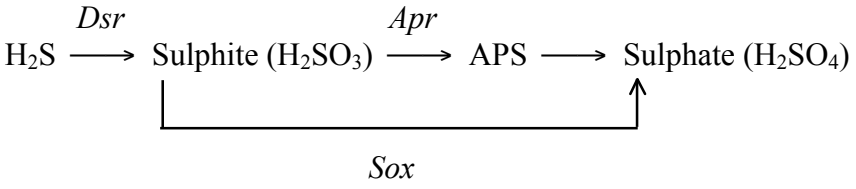

Methane oxidation

Bacteria with stacks of intracytoplasmic membranes typical of type I methanotrophs were observed in *R. exoculata* epibionts from the Rainbow site, using transmission electron microscopy (Zbinden et al. 2008) and fluorescence in situ hybridization (Guri et al. 2012). Bacterial sequences obtained from these samples clearly belong to known methanotrophic *Gammaproteobacteria* symbionts (like *Bathymodiolus* symbionts) (Zbinden et al. 2008). Furthermore, successfull amplification of particulate methane monoxygenase (*pmoA*) genes gave sequences that belong to the methylotrophic *Gammaproteobacteria* class (*Methylomonas* sp., *Methylobacter* sp. and *Bathymodiolus pmoA* gene sequences) (Zbinden et al. 2008).

Using ^{14}C-labelled methane incubation, Polz et al. (1998) did not detect any methane utilization in shrimp branchiostegites or scaphognathites from Snake Pit samples. The levels of CH_4 in the fluid, and consequently proportion of this metabolism among the bacterial community are probably too low at Snake Pit to detect any activity. Such an activity could probably be measured for ultramafic site like Rainbow or Logatchev. It has been shown for mussels (*Bathymodiolus azoricus*) that if the ratio CH_4/H_2S in the fluids is less than 1 (like in Snake Pit), the thiotrophic symbionts dominate, whereas if this ratio is higher than 2 (like in

Rainbow or Logatchev, Charlou et al. 2002), the methanotrophs dominate (Salerno et al. 2005). This is probably true for *R. exoculata* symbionts too.

Iron oxidation

The oxidation of sulphide and methane have long remained the only bacterial autotrophic chemosynthetic metabolisms described in hydrothermal vents symbionts. But the study of *R. exoculata* symbiosis highlighted the iron oxidation as another potential metabolism (Zbinden et al. 2004). Indeed, a striking feature of the epibiosis of *R. exoculata* of Rainbow site is the fairly abundant, rusty, mineral deposits surrounding the bacteria of the shrimp gill chamber, leading to the question of their origin. Long based on indirect suggestions, a large body of evidences now indicates that iron oxidation would be present within the epibiosis. In oxic environments, spontaneous ferrous iron oxidation is extremely rapid at ambient temperature (25°C) and neutral pH (Emerson and Moyer 1997, Neubauer et al. 2002). Under these conditions, Fe-oxidizing bacteria may find it difficult to compete with the abiotic process. However, in the shrimp environment, the temperature is usually lower than 25°C and oxygen is reduced to about two-thirds of its level in air-saturated seawater (Zbinden et al. 2004). Under such conditions abiotic oxidation is much slower. Based on the kinetic study of Millero et al. (1987), Zbinden et al. (2004) calculated that the FeII half-life would be about 35 h in a shrimp environment. Considering that the upper pre-branchial chamber (housing the main ectosymbiotic bacterial community) is located downstream of the gills in the water flow, leading to a pH reduction, a CO_2 increase and an O_2 decrease due to shrimp respiration, the abiotic oxidation rate should thus be even slower (Zbinden et al. 2004). And since the minerals only appear after a recolonization of the gill chamber by bacteria after each moult (Corbari et al. 2008a) and because of their tight association with microbial cells (Gloter et al. 2004; Anderson et al. 2008; Corbari et al. 2008b), a neutrophilic iron-oxidizing bacterial origin is highly suspected.

Other data are in line with a bacterial origin of iron oxides: i) The very homogeneous composition, along with the uncommon mixed-valence of the nanocristalline 2-line ferrihydrite (Gloter et al. 2004) of these iron oxides are characteristic of bacteriogenic iron oxyhydroxides (Kennedy et al. 2004). ii) Iron polyphosphate granules were detected inside some thin filamentous epibionts (Zbinden et al. 2008). Such granules are widely distributed in prokaryotes and could serve as ATP substitute, energy storage or chelator of metal ions (Kornberg 1995). An iron storage role has been suggested here to fuel the metabolism in case of iron depletion in the environemnt (shrimp maintenance in a pressurized aquarium without iron supply indeed led to the emptying of most of the granules) (Zbinden et al. 2008). iii) Finally, this hypothesis is supported by the fact that shrimp incubation in the presence of Fe^{2+} increases the ^{14}C-carbon fixation rate showing that Fe^{2+} contributes to fuelling *R. exoculata* epibionts (Ponsard et al. 2013)

Recently, more direct data have been paid to this issue: members of the *Zetaproteobacteria* were identified among the shrimp epibiosis, through a metagenomic approach and FISH observations (Jan et al. 2014). All the characterized *Zetaproteobacteria* are iron oxidizers, able to grow at circumneutral pH and under microaerophilic conditions, resulting in the precipitation of large amounts of Fe-oxyhydroxides (Emerson et al. 2007; Jan et al. 2014; Scott et al. 2015; Henri et al. 2016). Furthermore, homologues of genes expressed during iron oxidation by *A. ferrooxidans* (a molybdopterin oxidoreductase Fe_4S_4 region and ferredoxin encoding genes) were identified in the *Zetaproteobacteria* (Jan et al. 2014)

Based on geochemical calculations, Schmidt et al. (2008a) showed that at the Rainbow site, iron oxidation appears to be the major energy source, due its exceptional enrichment in the fluid. But kinetic modeling (Schmidt et al. 2009) suggested successive stages of first microbially driven, then abiotic iron oxidation. In the earliest stage of the moulting cycle, the formation of iron oxyhydroxides would be dominated by iron-oxidizing bacteria, the resulting accumulation of biogenic iron oxide would subsequently favor abiotic iron oxidation and inhibit microbial growth.

Hydrogen

Hydrogen was recently showed to also power primary production in bacterial symbionts of the hydrothermal vent mussel *Bathymodiolus puteoserpentis*, from the Logatchev site on MAR (Petersen et al. 2011). High concentrations of hydrogen are present in the fluids of ultramafic systems. It is a particularly favourable electron donor as the energy yield from hydrogen oxidation is much higher than from methane oxidation, sulphur oxidation and all other potential electron donors for chemolithoautotrophic growth under standard condition (Petersen et al. 2011).

The key enzymes involved in hydrogen metabolism are hydrogenases, which catalyse the reaction: $H_2 \rightarrow 2H^+ + 2e^-$. The *HynL* gene, encoding the large subunit of a [NiFe] hydrogenase, has been successfully amplified in *Rimicaris exoculata* (Hügler et al. 2011) and sequences fell in different clusters that contain *Epsilonproteobacteria* and *Deltaproteobacteria* sequences (Hügler et al. 2011). Jan et al. (2014) also found hydrogenases in *Gammaproteobacteria*.

Metabolism plasticity

As this shrimp colonizes chemically contrasted environments, these different metabolic pathways are likely to occur among the epibiotic community of *R. exoculata*, and their relative abundance could vary according to the local availability of reduced compounds. The energy budget provided by the oxidation of the various potential electron donors greatly depends on environmental conditions, notably their concentrations, the temperature and the local pH (Zbinden et al. 2004), which will define the energy that can be derived from the different oxidative pathways (Schmidt et al. 2008a). Using geochemical calculations, Schmidt et al. (2008a) determined the most favorable energy metabolism for the Rainbow and TAG sites. At Rainbow, iron oxidation appears to be the major energy source, due its exceptional enrichment in the fluid. The energetical yield of hydrogen oxidation depends on how fast it reacts with oxygen, but could be in the same range as for iron oxidation. Sulphide and methane only represent secondary energy sources for the shrimp epibionts at that site. Conversely, at TAG, Schmidt et al. (2008a) found that sulphide oxidation is the major energy source, and that iron oxidation could still be substantial, while methane represents only a minor part of the primary production. A thermodynamic model by Petersen et al. (2011) predicts that at the Logatchev vent field, aerobic hydrogen oxidation could provide up to 7 times more energy per kilogram of vent fluid than methane oxidation, and up to 18 times more energy per kilogram of vent fluid than sulphide oxidation. These data suggest that the chemical energy sources used by *R. exoculata* symbionts differ substantially depending on the site and a metabolic plasticity among the epibiosis may occur as a response to varying vent fluid composition.

In the light of all these results, we can now consider the gill chamber epibiont populations of *R. exoculata* as a functional consortium, composed of different morphotypes and phylotypes, and possessing different metabolisms. In summary, compiling all these data, the following scheme can be drawn (Fig.7): the bacterial population is numerically dominated by filamentous *Epsilon-* and *Gammaproteobacteria* (respectively 39 and 30% of the bacterial sequences of the metagenome (Jan et al. 2014)). *Gammaproteobacteria* appears as thin filaments and rod-shaped bacteria. They are chemoautotrophic sulphur-oxidizers, using the APS pathway for energy generation and the CBB cycle for carbon fixation (*aprA* and *cbbM* gene sequences, respectively). They are present mostly on the mouthparts. *Gammaproteobacteria* also occur as coccoid-shaped cells with intracytoplasmic membranes, caracteristic of type I methanotrophs, using methane oxidation for energy generation and probably also using the CBB cycle for carbon fixation. *Epsilonproteobacteria* appear as thick filaments and some thin filaments. Both are chemoautotrophic sulphur-oxidizers, using the

SOX pathway for energy generation and the rTCA cycle for carbon fixation (*SoxB* and *aclA* gene sequences, respectively). Part of the *Epsilonproteobacteria* also posses hydrogenase genes and could use hydrogen oxidation for energy generation. *Zetaproteobacteria* (2.2% of the bacterial sequences of the metagenome (Jan et al. 2014)) appear as rods and are chemoautotrophic iron-oxidizers (identified by a molybdopterin oxidoreductase Fe_4S_4 region and ferredoxin encoding genes), using the CBB cycle for carbon fixation (*cbbM* genes). *Deltaproteobacteria* (1% of the bacterial sequences of the metagenome (Jan et al. 2014)) possess *aprA* and hydrogenase genes, suggesting they can grow lithotrophically using hydrogen as electron donor for sulphate reduction.

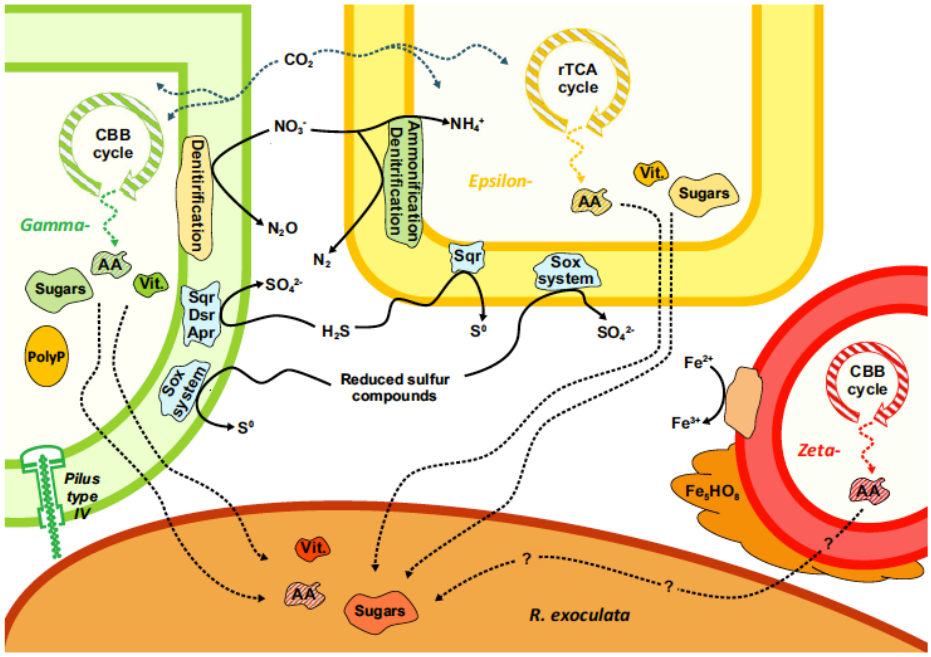

Figure 7 : Scheme of the proposed functioning of the *R. exoculata* gill chamber symbiosis. AA: amino acids; Sqr: sulphide-quinone oxidoreductase; Vit.: vitamins; PolyP: polyphosphates. Dotted arrows indicate indirect synthesis (for amino acids), diffusion (for CO2) or transfer (for amino acids, sugars and vitamins) (From Jan et al. 2014)

2.3. Symbionts transmission

Regarding the gut symbionts, free-living *Epsilonproteobacteria* and *Gammaproteobacteria* are commonly identified in hydrothermal ecosystems, but gut population displayed a diversity clearly reduced compared to the environmental one. They could thus be acquired from the environnment but with a selective filtering process (Durand et al. 2015). On the other hand, only one *Deferribacteres* and three *Mollicutes* OTUs were retrieved in gut libraries whatever the site considered, but none of the *Deferribacteres* (Durand et al. 2015), and only one of *Mollicutes* (Hügler et al. 2010) sequences were retrieved from the environment. Moreover, the high similarity level between all *Deferribacteres*-related sequences (>99%) associated with shrimp, regardless of the site, suggests a long-term, specific association between these bacteria and their host (Durand et al. 2010). Both their absence in the environment and the long term association plead for a vertical transmission of these symbionts. Nevertheless, bacteria were never observed to date in the eggs (Guri et al. 2012). Another horizontal transmission way was suggested : epibionts could be acquired at early juvenile stages by processes such as oral or anal trophallaxis (Durand et al. 2015), as it has been shown to ensure symbiont transmission among nest members, thereby contributing to maintenance of a beneficial microbiota in various groups of social insects (ants, termites, bees, Salem et al. 2015).

Regarding the cephalothorax symbionts, no bacterial symbionts are present within the eggs, or in the cephalothorax of larvae (Guri et al. 2012; Hernandez-Avila et al. 2015) or juveniles (Komai and Segonzac 2008) in *R. exoculata*. The cyclic occurrence of aposymbiotic (before the symbiont acquisition) and symbiotic phases in the host's life cycle is intrinsic to horizontally transmitted symbionts (Bright and Bulgheresi 2010). And when present, larvae are also aposymbiotic during their pelagic dispersal (Bright and Bulgheresi 2010). Furthermore, some *Epsilonproteobacteria* and *Gammaproteobacteria* sequences retrieved from the Rainbow seawater sample were closely related (99% similarity) to epibiont sequences from the gill chamber of shrimp from the same site (Guri et al. 2012). A free-living form of the *Epsilon* symbiont has been also shown to make up a substantial proportion of the free-living community on sulphides at the Snake Pit vent site (Polz and Cavanaugh 1995). These results would rather plead for the existence of horizontal (environmental) transmission for the shrimp cephalothorax epibionts, acquired at each generation and after each moult (Petersen et al. 2010). As concentrations of potential symbionts are not always high in the environment, many aquatic hosts therefore actively pump water along their tissues, enhancing their chances of entrapping potential symbionts (Bright and Bulgheresi 2010). This is the case with the water currents generated by scaphognathite beating in the gill chamber of *R. exoculata*. This epibiont transmission pathway would be in adequacy with the large colonization of the MAR by *R. exoculata* because horizontal transmission is believed to promote dispersal as compared with vertical transmission (Chaston and Goodrich-Blair 2010).

2.4. Host-symbiont interaction

The first essential step in the establishment of a symbiosis with horizontal transmission is the bilateral recognition of the host and the symbiont, which usually occurs through lectin-like surface molecules. This also implies to cope with the immunitary system of the partner. These very specific mecanisms are the result of a long common evolutionary history between the bacteria and its host. The diversity of the epibiotic community of *R. exoculata* cephalothorax is very stable in time and space (Zbinden et al. 2008, Petersen et al. 2010, Guri et al. 2012), and reduced compared to the environmental one (Flores et al. 2011). It can therefore be assumed that a selection takes place during the stages of colonization, carried out by the host or between the epibionts themselves. In a biofilm, bacteria communicate with each other through the secretion of signaling molecules, and use this quorum sensing to coordinate the formation of biofilms, exopolysaccharide production, virulence, or cell aggregation. Signaling molecules could either be N-acyl homoserine lactones (AHL or autoinducer 1) synthetized by the LuxI enzyme, or an autoinducer 2 synthetized by a LuxS enzyme, according to bacterial type (Montgomery et al. 2013). When the signaling molecules exceed a threshold concentration, they bind to a LuxR receptor, which activates the transcription of certain genes.

In 2014, a metagenomic study of *R. exoculata* cephalothoracic epibionts (Jan et al. 2014) revealed virulence gene homologues in *Epsilonproteobacteria*, as well as genes linked to quorum sensing in *Epsilonproteobacteria* (*luxS*) and *Gammaproteobacteria* (*luxR*). These categories of genes may be involved in host-symbiont interactions and recognition of bacteria by the host. Genes encoding proteins involved in attachment to surfaces have also been demonstrated in this study (type IV pili, O antigen), reflecting the ability of these bacteria to form a biofilm within the cephalothorax of the shrimp (Le Bloa et al. 2017). The expression of *luxS* and *luxR* genes in the cephalothoracic community was only detected for the late moulting stages (Le Bloa et al. 2017). The expression of these quorum-sensing genes at the peak of the bacterial colonization could indicate that the bacteria start to regulate themselves to avoid invasion or competition, but could also be involved in the dispersal of the epibiont biofilm just before the moult (Le Bloa et al. 2017). As neither *luxI,* nor the autoinducer-1 were found within the bacterial community (Jan et al. 2014, Le Bloa et al. 2017), the epibiotic community may not use the LuxI/LuxR quorum sensing system, but rather the other, more

universal, LuxS/LuxR system (Montgomery et al. 2013).

To maintain its epibiosis, the shrimp must at the same time select its epibionts and regulate their proliferation, and also prevent the installation of non beneficial bacteria or pathogens. Permanently exposed to a large density and diversity of microbes, marine animals in general and *R. exoculata* in the present case must have an effective immune system in microbial growth inhibition. Devoid of specific immune system, shrimp rely only on innate immunity, a non-specific, rapid defense oriented towards all the external aggressions (Rosa and Barraco 2010). Part of this defense occurs through antimicrobial peptides (AMPs), small sized molecules naturally produced by bacteria, protists, fungi, plants and animals, which act as a first line of defense against bacterial infection (Rosa and Barraco 2010; Tasiemski et al. 2014). The first AMP of hydrothermal species was described in the polychaete *Alvinella pompejana* (Tasiemski et al. 2014), which harbors a dense epibiotic community on dorsal expansions of its tegument (Gaill et al. 1984) and therefore shares similarities with *R. exoculata* (Segonzac et al. 1997). Tasiemski et al. (2014) show that AMP targets specially one type of bacteria (the most abundant) but has no effects on the others, and thus suggest that this AMP (*alvinellacin*) selects and shapes the epibiotic microflora and prevents microbiota from over-proliferating. Le Bloa et al. (2017) identified in *R. exoculata* the first AMP in a hydrothermal shrimp, named *Re*-crustin. It is mainly synthesized by tissues that are in contact with the environment, and is particularly highly expressed in the tissues colonized by the symbionts (branchiostegite and scaphognathite) and at the juvenile stage. But the role of the AMP is still not clearly elucidated.

All this leads to the hypothesis that there could be a recognition system and a strict control allowing a phylogenetically identical recolonization in the cephalothorax after each moult (Le Bloa et al. 2017).

2.5. Ectosymbiosis and moult cycle

In shrimp, as in other arthropods, growth occurs through cyclic moults, during which the cuticle is regularly renewed. At ecdysis, when the entire old cuticle is shed, the bacterial population of the cephalothorax is shed with it, and a new bare cuticle covers the freshly moulted shrimp. As direct continuous observations along the moult cycle are not possible at hydrothermal sites, estimation of the moult cycle duration can only be determined indirectly. The percentages of individuals at each moult stage was determined using the Drach method (Drach and Tchernigovtzeff 1967) and correspond to the relative duration of the stage in the moult cycle (Corbari et al. 2008a). By compiling data from the literature, Corbari et al. (2008a) showed that the anecdysal period (stage C_4) varies considerably in different shrimp species of comparable size, whereas the preecdysial period (stage D_0-D_4) is similar. Comparison with known cycles of similar size coastal shrimp allowed these authors to estimate the absolute duration of the *R. exoculata* moult cycle to 10 days (Fig. 8a).

The abundance and distribution of the bacterial coverage are related to the moulting cycle and depend on the period of time elapsed since the last moult (Zbinden et al. 2004; Corbari et al. 2008a). The bacterial re-colonisation begins just after the exuviation, with only scarce and randomly distributed patches of short thin filaments and rods (Fig. 8b, c). A rapid bacterial growth quickly leads to a dense bacterial mat composed of long thin and thick filaments. According to Petersen et al. (2010), freshly molted shrimp would be first colonized by *Epsilonproteobacteria* while later stages would be dominated by *Gammaproteobacteria*. The maximum bacterial coverage is reached in early preecdysial individuals, within no more than 2 days (Corbari et al. 2008a). Evolution until the next moult consists mainly in the development of the mineral deposits which finally turn into a thick crust isolating the bacterial population of the external environment (Fig. 8d, e) (Corbari et al. 2008a). A high moulting rate is usually regarded as an antifouling mechanism contributing to the elimination of epibiotic bacteria (Bauer 1989). The high moulting frequency in *R. exoculata* (10 days compared to 21 days for *Penaeus japonicus* or 48 to 91 days for *Macrobrachium rosenbergii*)

was rather seen as a mean to eliminate the mineral crust that isolates the bacteria from the necessary reduced compounds of the fluid and allow the reinstallation of a new and efficient symbiotic community (Corbari et al. 2008a).

As shrimp colours gradually evolved throughout the moult cycle due to progressive iron oxides deposits in the gill chamber, colour can thus be used as an convenient proxy to determine specimen moult stage (Corbari et al. 2008a). The gradation evolves from white individuals in postecdysis (Fig. 8b) to dark red specimens in preecdysis (Fig. 8d) at the high iron content Rainbow site. At TAG site (where the fluid contains high amount of sulphide and less iron), grey specimen intercalate between white and light red in early preecdysial individuals, due to iron sulphides deposits, but late preecdysial individuals are dark red (Corbari et al. 2008a).

The bacterial community of the digestive tract is located in the midgut, which is devoid of cuticle, and thus not submitted to the moult cycle, meaning that this part of the symbiosis is not renewed regularly.

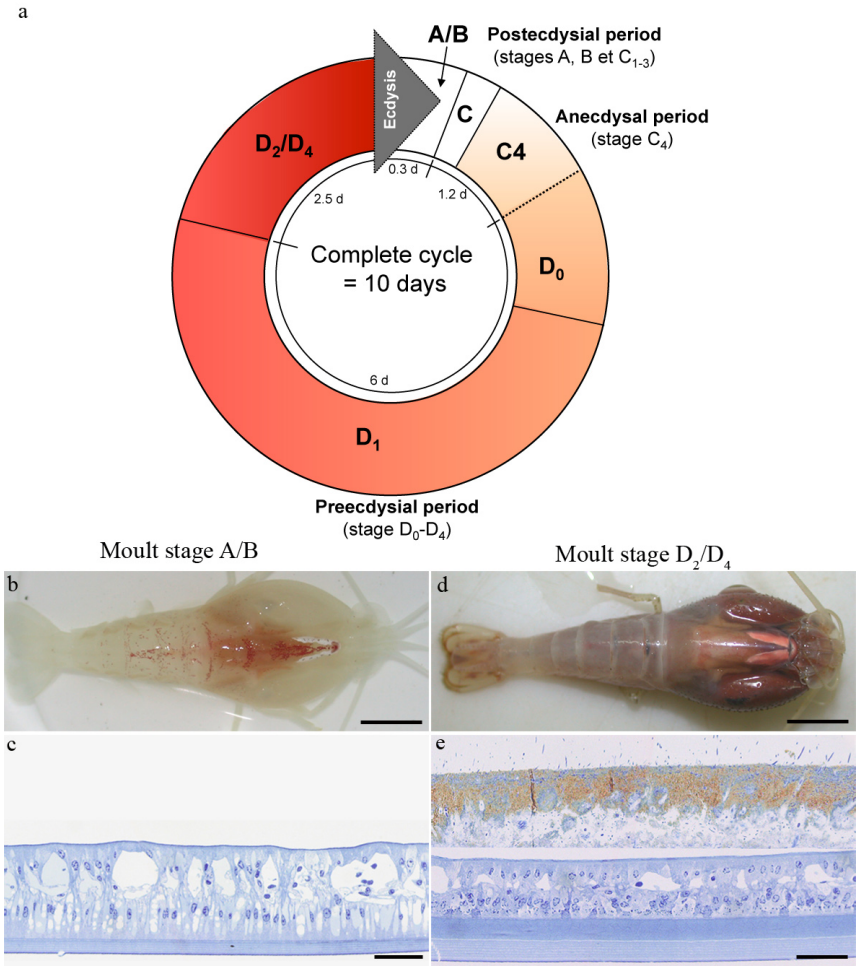

Figure 8 : a) *R. exoculata* moult cycle with duration of the different stages (courtesy of L. Corbari). Colour pattern and semi-thin sections of the branchiostegite illustrating the bacterial colonisation of a specimen with white (b-c) and red (d-e) branchiostegites (modified from Corbari et al. 2008a). Scale bars : b, d = 1 cm, c, e = 50 µm.

3. Reproduction and Dispersal

Knowledge on reproduction and dispersal in *R. exoculata* has long been scattered. One of the main mysteries of this species long remained that almost no reproducing individuals, nor early developmental stages (larvae) were collected throughout fairly extensive samplings on all colonized sites since its discovery in 1986 (Tyler and Young 1999). Vereshchaka (1998) for example noted that *R. exoculata* is represented in Russian collections by thousands of

individuals, among which spawn-bearing females were absent. This absence has been linked to seasonal breeding and sampling efforts almost entirely restricted to the summer months (Gebruk et al. 1997a; Vereshchaka et al. 1998; Herring 1998; Ramirez-Llodra et al. 2000; Guri et al. 2012; Hernandez-Avila, 2015). It has also been proposed that ovigerous *R. exoculata* leave the swarms around high temperature vents, where samples are generally collected, to protect the embryos from hydrothermal fluids and from the risk of mechanical damages caused in the highly active aggregation of shrimp (Ramirez-Llodra et al. 2000). However, a few brooding females, eggs and hatched eggs were collected in March 2007 from females collected among the shrimp aggregates at the Logatchev site (Guri et al. 2012). And a consequent number of brooding females and hatched larvae were also collected, also from aggregates, in January 2014 at the TAG site (Hernandez-Avila et al. 2015). This supports the first hypothesis of seasonal reproduction.

Nevertheless, due to the very small number of ovigerous females and larvae obtained to date, only scattered data are available for the life cycle of *R. exoculata* and many unresolved questions remained (Fig. 9).

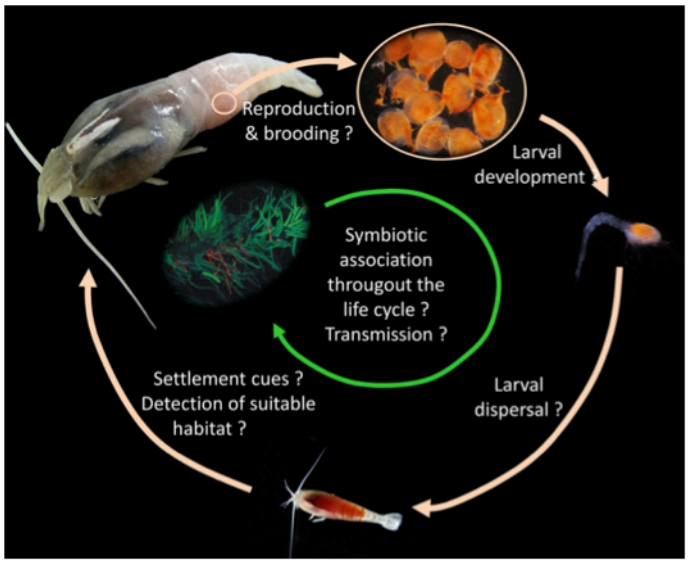

Figure 9 : Scheme of the life-cycle of the vent shrimp *Rimicaris exoculata* and its symbionts with unresolved key questions (courtesy of F. Pradillon)

3.1. Reproduction cycle

Based on samples recovered at two different periods of the year (September and November, or July and September), Copley et al. (2007) and Ramirez-Llodra et al. (2000) respectively observed a continuous range in oocyte size–frequency distributions, from individuals with only small oocytes (76–108 μm) to individuals with much larger ones (466–601 μm), leading them to conclude to an asynchronous gametogenesis. Copley et al. (2007) also suggested a lack of seasonal reproduction in *R. exoculata* due to similar median sizes of oocytes in their two samplings, whereas Ramirez-Llodra et al. (2000) observed that females collected in September had larger oocytes than those collected in June, arguing for a more advanced stage of development. Samplings in August to October revealed that many of the females had well-formed eggs in their gonads and were ready to lay them shortly (TAG and Broken Spur sites: Vereshchaka et al. 1998), whereas samplings in January and Mars showed brooding females, eggs, and hatched larvae (Logatchev site: Guri et al. 2012; TAG site: Hernadez-Avila et al. 2015). Combining all this data argue for a seasonal reproduction with spawning occuring in late fall (October - November), females brooding embryos during winter and hatching of larvae in the late winter - early spring (Januray - March), close to what has been described in another Alvinocaridid species, *Alvinocaris stactophila*, from the Brine Pool cold seep in the Gulf of Mexico (Copley and Young 2006). Post-larvae were collected in the water column around Broken Spur in August and September (Herring and Dixon 1998),

without knowing if they were dispersing from the vent site or converging on it (Herring 1998).

In Decapods, mature oocytes are transferred to the female pleopods where they are fertilized by the sperm. Copulation takes place after the ecdysis and the ovigerous females incubate the eggs on the pleopods, between lateral sclerites that are usually enlarged at the pre-spawning moult to create a brood chamber (Ramirez-Llodra et al. 2000). Within a brood, the embryos developp synchronously and all the eggs are at the same stage, but can differ from one female to another (Ramiez-Llodra et al. 2000; Guri et al. 2012). The eggs were always hatched beneath the female abdomen so that only free larvae would be released into the environment (Guri et al. 2012). Few fecundity values have been published to date : 988 eggs for a female (Ramirez-Llodra et al. 2000, which also reported the value of 836 eggs for one female from J. Copley's pHD thesis). Egg sizes ranging from 0.2 to 1 mm were reported (Vereshchaka et al. 1988; Ramirez-Llodra et al. 2000; Guri et al. 2012).

The high number of small size eggs (Ramirez-Llodra et al. 2000), together with the rich lipid reserves (Pond et al. 1997b; Allen Copley et al. 1998) and genetic data showing high gene flow between MAR sites (Creasey et al. 1996; Shank et al. 1998; Tokuda et al. 2006) plead for a short embryonic developemnt and a long planktotrophic phase, giving a high dispersal and colonisation potential for this species.

3.2. Larvae

For the first time, significant numbers of brooding females and hatched larvae were collected in January 2014, at the TAG site (Hernandez-Avila et al. 2015). This allowed the first detailed description of the first larval stage (zoea I) of *R. exoculata* which bring important cues about the early life history of the species. This study highlighted the absence of both masticatory processes in the mandible and setation in mouthparts that could participate in the process of capture and manipulation of food, suggesting that the alvinocaridid first larval stage is a non-feeding larva. Gebruk et al. (2000) also noted that bathypelagic caridean shrimp generally have non-feeding zoeal stages.

These undeveloped mouthparts (Hernandez-Avila et al. 2015) and the accumulation of wax esters and monounsaturated fatty acids support the occurrence of primary lecithotrophy in the early stage of alvinocaridids (Pond et al. 1997b; Allen Copley et al. 1998; Gebruk et al. 1997b; Hernandez-Avila et al. 2015). Size and high lipid content of postlarvae collected by Herring and Dixon (1988) around Broken Spur vent field nevertheless led these authors to conclude that they must have fed and grown extensively since they hatched. Wax esters and photosynthetically-derived fatty acids found in the juveniles indicate that in their early life stages they may feed and survive for extended periods in the euphotic zone (Pond et al. 1997b; Allen Copley et al. 1998). Combining these data lead to suggest that the early lecithotrophic period would be followed by a feeding period during the larval development (Hernandez-Avila et al. 2015).

It also has to be noted that alvinocaridid first larval stage is very distinctive from other decapod crustaceans because of the combination of undeveloped mouth parts and lack of pereiopods and pleopods, which suggest lecithotrophy but extended larval development, whereas usually lecithotrophy is rather associated to abbreviated development and some degree of larval retention (Hernandez-Avila et al. 2015).

3.3. Dispersal

Given the discontinuous nature of vent sites along the MAR (one field per 175 km from 11°N to 40°N, German et al. 1996), vent shrimp populations are continually faced with the threat of local exctinction due to the ephemeral nature of hydrothermal emissions (Dixon et al. 1998). The strong convection current of hot water rising from the vents forms a buyant plume that is likely to transport eggs or larvae away from vents in the water column (Tyler and Young 2003). Along the MAR, the flow remains in the axis of the ridge, constrained by the steep walls of the graben (Tyler and Young 2003). Nevertheless, several structures could

act as barriers againt larval dispersal (Atlantis and Kane Fracture Zone, the Azores islands). Using a midwater trawl, Herring and Dixon (1998) collected alvinocarididae shrimp post-larvae up to 100 km away from the Broken Spur site, showing they can extend into the next MAR segment beyond the Atlantis Fracture Zone. Active swimming and changes of buoyancy seem necessary to rise above the basin and then sink down to a new site (Herring and Dixon 1998). Genetic analysis of adult *Rimicaris exoculata* from the TAG and Broken Spur vent sites (~370 km) showed no significant genetic differenciation (Creasey et al. 1996; Teixeira et al. 2010), supporting high gene flow among vent MAR sites and effective dispersal potential. Numerous studies of lipid profiles (Pond et al. 1997b; Allen Copley et al. 1998; Dixon et al. 1998, Herring 1998; Pond et al. 2000b) revealed, in post-larvae and juveniles, high amounts of wax-ester lipids, which let these authors suggest that they spend a substantial period of their early life stages as planktotrophic organisms, feeding on photosynthetic material and accumulating substantial reserves, before returning to a suitable vent site.

Although larval stages of some alvinocarid shrimp appear to feed on photosynthetically-derived organic matter (Allen Copley et al. 1998), it is still unclear which habitat the larval stages use (Hernandez-Avila et al. 2015). Post-larval stages of Alvinocarididae have been collected at long distances (> 100 km) from their potential origin, in bathypelagic habitat between 1990 and 3060 m (Herring and Dixon 1998). Based on laboratory experiments Tyler & Dixon (2000) nevertheless reported that 1 atm pressure (surface) and 20°C are fatal to larvae of the shrimp *Mirocaris fortunata*. The larvae probably do not rise that high in the water column, staying rather below the thermocline (~200m depth), feeding on particles descending to the aphotic zone (Hernandez-Avila et al. 2015).

3.4. Settlement

The settlement stage is a key step in reproduction, where larvae have to find a location which confers high probability of survival and successful reproduction (Rittschoff et al. 1998). Environmental (chemical and physical) cues, such as inorganic and organic compounds like co-specific odors, surface energy, vibration or light, determine where the larvae settle (Rittschof et al. 1998). At hydrothermal vents, sulphide, as an obvious signature for hydrothermal habitats, was proposed to be a settlement cue (Rittschof et al. 1998). *In situ* experiments at the Juan de Fuca Ridge confirmed attraction of alginate gels containing sulphide on larvae of vent polychaete worms (Cuomo et al. 1985). But to date, nothing is known on *R. exoculata* larvae settlement cues or sensory habilities. Vereshchaka (1997) indicated a settling stage between 3 and 7 mm of carapace length.

3.5. Juveniles

Upon examination of the abundant material of postlarval stages, covering a wide range of size (rostral carapace length between 4.8 and 17.4 mm), Komai and Segonzac (2008) have described 4 ontogenic stages, and have shown that *R. exoculata* exhibits dramatic morphological change at size of 7.0–9.0 mm in carapace length. During these stages, they noted that there was no significant increase of size, the shrimp probably spending much energy for great morphological change rather than increase of body size. The most notable changes are the progressive reduction of the rostrum, the fusion of the eye-stalk, the inflation of the branchiostegite and the apparition of numerous plumose setae on the swelling exopodites of the second maxilla and first maxilliped (Komai and Segonzac 2008). Vereshchaka (1996) observed voluminous colonies of the *Thiotrix*-like bacteria on plumose setae of the mouthparts on specimens of 8.0 to 9.2 mm in carapace length.

The juvenile vent shrimp colonize the vents at total length ranging from 14 to 25 mm. Aggregations of juveniles were often reported at lower habitat temperatures than the adults (10°C vs. 28°C) in chimney areas with lower hydrothermal flow, these juveniles being also less active than the adults (Nuckley et al. 1996; Shank et al. 1998). Among the 519 juveniles

examined from the July 1997 expedition, Shank et al. (1998) found no males and suggest that male sexual characteristics are not displayed by juveniles, or *R. exoculata* may be a protogynous hermaphrodite.

When arriving at vents, juveniles carry abundant stores of lipids. Carbon stable isotopes showed a graded increase from the juveniles, through the smaller adults to the older specimens (Polz et al. 1998; Gebruk et al. 1997b; Gebruk et al. 2000), corresponding to the development of bacterial growth and their gradual introduction in the diet. There is also an increase in the proportion of the heavy isotope of nitrogen between the juvenile and the adult stages. The lipid data (Pond et al. 2000a, b; Allen et al. 2001), showing an evolution from photosynthetically-derived n-3 fatty acids to bacterially-derived n-4 fatty acids, also evidence a change in diet during metamorphosis and maturation (Gebruk et al. 2000).

4. Biogeography and connectivity

4.1. Host biogeography and connectivity

The discovery and faunal descriptions of vent sites all around the world gave rise to the description of biogeographic provinces based on faunal distribution (Van Dover et al. 2002). Due to the discontinuous and ephemeral nature of these habitats, questions about geographical structure and dispersal capabilities of hydrothermal vent populations arose. Indeed high rate of large-scale dispersal, although potentially generating a significant loss of larvae in the water column, ensure long term persistence in these fragmented ephemeral habitats (Teixeira et al. 2010). Discontinuities of the ridges (transform faults and fracture zones), as well as hydrological barriers, are supposed to impede the along-axis dispersal of a number of vent species and favour allopatric speciation (Vrijenhoek 2010, Bachraty et al. 2010). The first study of *R. exoculata* biogeography (Creasey et al. 1996) was conducted using allozyme polymorphisms, between TAG and Broken Spur, two sites separated by 370 km. The results showed no significant genetic differenciation, indicating a high gene flow between the two populations. The authors calculated a high migration rate between the two vent field exceeding 100 individuals per generation. Using the mitochondrial COI gene from juveniles and adults from Broken Spur, TAG and Snake Pit, Shank et al. (1998) came to the same conclusion that the different individuals analyzed were conspecific. Several studies using mtDNA haplotypes (Teixeira et al. 2010), different mitochondrial marker genes (COI and CytB, Petersen et al. 2010) and microsatellites (Teixeira et al. 2012) from shrimp from 5 sites along the MAR (Rainbow, TAG, Achadzé, Logatchev, South MAR) showed an overall high genetic diversity within the populations, but a lack of genetic structure among the different populations along the 8500 km of the MAR portion encompassing the sampled sites. Their data also revealed no genetic differentiation among samples separated by up to eleven years for two vent sites (Logatchev and Rainbow). Teixeira et al. (2010, 2012) suggested that such pattern can be explained by a recent (about 250 Kyr ago) common bottleneck or (re)colonization event of *R. exoculata* populations along the MAR, followed by an ongoing population extension, with a large panmixia and high dispersal capacity.

All these results indicated that neither the distance between vent fields (up to 1000s km, Vrijenhoek 2010), nor the broad range of depths (850 - 3650 m) and the occurence of the different transform faults or fracture zones along the MAR were obstacles to dispersal and gene flow between the studied *R. exoculata* populations. Teixeira et al. (2012) even reported that of all the species studied to date on hydrothermal vent habitats, *R. exoculata* is the first to exhibit no barriers to dispersal across such a high geographic extent.

4.2. Symbionts biogeography

4.2.1. Gill chamber symbionts.

In contrast with the hosts, a phylogenetical analyse of 16S rRNA gene of *R. exoculata* gill chamber epibionts from 3 vent sites (Rainbow, Logatchev and South MAR) showed spatial

clustering of bacterial sequences. This genetic differenciation is correlated with geographic distance between the sites rather than with vent geochemistry (i.e. ultramafic- vs. basalt-hosted vent fields) (Petersen et al. 2010). The authors proposed two hypotheses to explain the spatial structuring of symbiont population, without being able to decide in favor of one or the other, due to too limited data on free-living relatives of the shrimp symbionts : 1) free-living symbiont populations are genetically isolated due to the existence of barriers to gene flow between vent fields and the spatial structuring of symbiont populations reflects the diversity of free-living forms of the symbionts; 2) the free-living symbiont populations are not spatially structured along the MAR and the structuring of symbiont populations at each vent site reflects a specific colonization of the hosts by their symbionts from the pool of diverse free-living forms. Using lux genes, Le Bloa et al. (2017) also showed a geographical clustering of the epibionts according to their vent site origins (Rainbow, TAG, Snake Pit and Logatchev).
Geographical segregation of the symbionts compared to host homogeneity may be attributable either to the influence of environment on symbionts or to the very recent common history of *R. exoculata* populations, with recent divergence detectable only on short-generation symbionts and still undetectable on the genetics of their hosts (Teixeira et al. 2010).

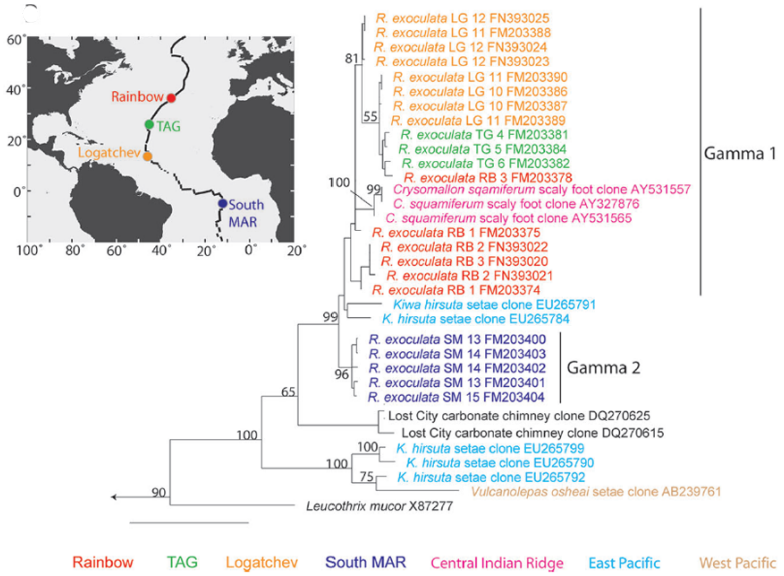

Figure 10 : 16S rRNA Phylogeny of the *R. exoculata Gammaproteobacteria* symbionts and their close relatives, both invertebrate-associated and free-living. Colours indicate the geographic location of the sampling. Bar indicates 5% estimated sequence divergence. Only bootstrap values (100 re-samplings) over 60 are shown (from Petersen et al. 2010).

4.2.2. Gut symbionts

Deferribacteres and *Mollicutes*, phyla that have not been retrieved the environment (seawater and chimney samples, Durand et al. 2015, Flores et al. 2011), as well as *Epsilon-* and *Gammaprotebacteria* gut symbionts showed a pattern of phylogenetic differenciation very similar to that of the host, revealing no geographical differenciation for TAG, Logatchev and Achadzé sites. These results are interpreted, for hosts and symbionts, as a significant recurrent genes flow and/or a recent and common bottleneck-expansion history across MAR sites (Teixeira et al. 2011, 2012). Only at Rainbow, the epibiont divergence pattern at the ribotype level contrasts with that of the hosts (Durand et al. 2015). Both physical (the shallow depth compared to the other sites and its peculiar position at the intersection between the nontransform fault system and the ridge fault, Charlou et al. 2010), as well as the unique geochemical conditions prevailing in Rainbow could be a factor affecting the selective pressures acting on epibionts (Durand et al. 2015).

5. Physiology

5.1. Respiration

R. exoculata features 10 pairs of phyllobranchiate gills, with single-layered branchial lamellae bordered by a thin cuticle (0.3–0.5 µm) (Martinez et al. 2005). The gills do not seem involved in osmoregulation (which seem only mediated by the epipodites in the branchial chamber), considering the lack of Na^+-K^+ ATPase (Martinez et al. 2005). Gills are mainly involved in respiration, but a detoxication activity was also shown to occur in the gills through sulphide oxidizing bodies (Compère et al. 2002, see paragraph below).

Living within steep chemical and thermal gradients, where hot, reduced hydrothermal fluid mixes turbulently with oxygenated seawater (Schmidt et al. 2008a), shrimp are exposed to highly fluctuating oxygen conditions, sometimes to hypoxic conditions. For example, O_2 concentrations of 63 to 236 µM were measured in discrete samples of fluid in vicinity of shrimp swarms (Zbinden et al. 2004). For comparison, concentrations of 242 µM and 12.4 µM were measured from ambiant seawater and a black smoker outlet of Rainbow site respectively (Zbinden et al. 2004). Few studies were devoted to respiratory adaptations of *Rimicaris exoculata* (Lallier and Truchot 1997; Lallier et al. 1998), and to a broader extend to crustaceans at hydrothermal vents (Arp and Childress 1981; Sanders et al. 1988; Lallier et al. 1998; Chausson et al. 2001, 2004). In 2003, Ravaux and collaborators measured oxygen consumption rates of 0.837 to 1.094 mg O_2 g^{-1} dry mass h^{-1} for *R. exoculata* at *in situ* pressure conditions ($230x10^5$ Pa) and at oxygen levels of the deep seawater surrounding the north Atlantic vent sites. These values are in good accordance with the relationship between oxygen consumption and dry mass obtained for Crustaceans (see references in Ravaux et al. 2003).

The respiratory pigment of decapod crustaceans is haemocyanin (Hc) that binds reversibly oxygen to a pair of copper atoms. The Hc of *R. exoculata* is composed mostly of hexameric molecules (89%) of 469 ± 9 kDa (Lallier et Truchot 1997). For a majority of crustaceans, haemocyanin–oxygen (Hc–O_2) affinity is relatively low, with P_{50} (oxygen partial pressure at half-saturation) values >10 Torr under physiological conditions (Truchot 1992). For example, P_{50} = 27 Torr at pH 7.8, 10°C for the coastal shrimp *Palaemon elegans* (Bridges et al. 1984). But it has been shown (Truchot 1992; Sanders and Childress 1990) that Hc–O_2 affinity is well correlated with ambient oxygen content of the environment, and that heamocyanin affinity for oxygen of species living in hypoxic environments is higher than those living in normoxic conditions. Lallier and Truchot (1997) showed indeed that *R. exoculata* haemocyanin has a high oxygen affinity (P_{50} = 3 Torr at pH 7.5, 15°C), which is also the case for *Segonzacia mesatlantica*, the endemic crab of the MAR vent sites (P_{50} = 2.2 Torr at pH 7.5, 15°C, Chausson et al. 2004). *R. exoculata* haemocyanin also showed almost no temperature effect on the P_{50} in the range 15-35°C, a large Bohr effect (oxygen affinity increases with pH) and a moderate lactacte (main end-product of anaerobiosis in Crustacea) effect (oxygen affinity increases with lactate) (Lallier and Truchot 1997), which is favourable in a medium where temperature and oxygen contents fluctuate considerably (Lallier et al. 1998). Lallier and Truchot (1997) also highlighted, that native hemolymph (i.e. not dialysed) show a lower affinity for O_2 (P_{50} = 6), suggesting the occurrence of a factor in *R. exoculata* hemolymph that decreases Hc oxygen affinity. The high affinity would thus allow good oxygen-scavenging by the pigment in a frequently hypoxic environment, the presence of factor in return would increase the release of the oxygen to the tissue by decreasing the affinity of haemocyanin for oxygen (Lallier et al. 1998).

5. 2. Sensory perception

Since the very first publications describing hydrothermal vents, the question of the location of vent emission was recognized. Corliss et al. (1979) noted “there are many questions to be answered about these animal communities. One concerns how they locate and colonize new

vents".

Rimicaris exoculata depends on hydrothermal emissions to feed its symbionts and thus faces recognition of active hydrothermal sites at different time of its life. After dispersal in the water column, sometimes tens or hundreds of miles from their starting point, larvae need to find a vent site to settle and begin their adult life (Herring and Dixon 1998; Pond et al. 1997). As adults, shrimp have to locate in the environment, find fluid to feed their symbiotic bacteria, interact with conspecifics or just to remain in an appropriate range of physicochemical conditions (Desbruyères et al. 2000, 2001). Fluid chemical compounds like sulphide, temperature and dim light emitted by vents have been proposed to be potential attractants for detection of hydrothermal emissions (Van Dover et al. 1989; Renninger et al. 1995; Gaten et al. 1998a, b). Shrimp were also proposed to use acoustic vibrations induced by hydrothermal fluid emissions as navigational cues (Segonzac et al. 1993, Crone et al. 2006). Nevertheless, sensory perception in general has been very little studied in hydrothermal species. And chemical senses have been unequally studied. As hydrothermal environment is devoid of light and as shrimp eyes presented obvious modifications related to their habitat, they have been relatively well studied, while fewer data are available on chemoreception or thermoreception.

Works on vision have shown that adults of *Rimicaris exoculata* (as well as *Mirocaris fortunata*, *Chorocaris chacei* and *Alvinocaris markensis*) lacks the usual externally differenciated eye (eye-stalk) of shrimp, having instead a pair of large, highly reflective, dorsal organs (Van Dover et al. 1989). These unusual eyes have no image-forming optics, but a solid wall of light-sensitive rhabdom consisting of 3500 photoreceptors (containing rhodopsin). Beneath the rhabdomeral segments, a thick white diffusing layer (tapetum) increases, by reflection, the quantity of light captured by the retina (O'Neill et al. 1995; Nuckley et al. 1996; Kuenzler et al. 1997; Lakin et al. 1997; Wharton et al. 1997; Jinks et al. 1998; Chamberlain, 2000). These features are mostly understood as an adaptation for detection of extremely faint sources of light emmitted by the vents (thermal radiations or sonoluminescence (i.e. glow produced by imploding bubbles of gas at high pressures), Pelli and Chamberlain 1989; Van Dover et al. 1989, 1996). The shrimp eyes present a clear evolution between the larvae and the adults (also observed in the hydrothermal vent crab *Bythograea thermidron,* Jinks et al. 2002) from an imaging retina to the non-imaging retina of the adults: the zoeal eye is similar (eye-stalk) to those of other surface-dwelling decapod larvae (Gaten et al. 1998a, b), suggesting that the early stages are planktonic (Gaten et al. 1998b). Intense lights (and notably those of submersible used for the collect) have been shown to induce irreversible retinal damage in the hydrothermal shrimp eyes (*Rimicaris exoculata* and *Mirocaris fortunata*). When freshly collected and little exposed to submersible or sun light, shrimp have pink-colored eyes, with normal extensive rhabdom layer. Once exposed for a certain time to light, specimens have white eyes, with severe breakdown, often with complete loss of the rhabdom layer (Herring et al. 1999).

Concerning chemoreception, as far as we know, only one study was published to date, focused on olfaction in *Rimicaris exoculata* (Renninger et al. 1995). Chemoreception in decapods encompasses: "olfaction" mediated by olfactory receptor neurons (ORNs) housed in specialized unimodal olfactory sensilla (the aesthetascs), restricted to the lateral flagella of the antennules (Laverack 1964; Grünert and Ache 1988; Cate and Derby 2001) and "distributed chemoreception" mediated by numerous bimodal sensilla (containing mecano- and chemo-receptor neurons) occurring on all appendages (Schmidt and Mellon 2011; Mellon 2014; Derby et al. 2016). Renninger and collaborators (1995) reported behavioral observations of shrimp showing *in situ* strong orientation behavior to a piece of sulphide removed from the chimney. They also reported unpublished data of CL Van Dover and N Sofranko showing an avoidance response of the coastal shrimp *Palaemonetes vulgaris* to an H_2S solution < 0.08 mM. Their microscopic observations oddly focused on the second antennae, thus missing the primary olfactory sensilla (the aesthetascs) located on the lateral flagella of the antennules

(Laverack 1964). They described non-aethetascs sensilla of first (antennule) and second antennae, with an open pore at their tips. Each sensillum is innerved by 10 to 14 sensory dendrites. The sensilla density on the second antenna of *R. exoculata* is 4-5 times higher than in a coastal shrimp (*P. aztecus*), which suggested to the authors enhanced sensory capabilities. They then examined the physiological responses of antennal nerves to various chemical stimulants. Antennal flagella (i.e. medial and lateral flagella of the first antennae and flagella of the second antennae) respond to a variety of chemical stimuli, including homogenates of bacteria, a mixture of amino acids, and solutions of Na_2S. Even if the 3 flagella respond to an exposure to Na_2S, the largest and most robust response was registred in the flagella of the second antennae, while the lateral flagella responded little, if not at all, to Na_2S.

Recently, Zbinden and collaborators (2017) presented a morphological description of the sensilla on the antennules and antennae in *Rimicaris exoculata* (as well as in *Mirocaris fortunata*, *Chorocaris chacei* and *Alvinocaris markensis*). These observations revealed no specific adaptation regarding the size or number of aesthetascs between hydrothermal and coastal species. These authors also identified an olfactory co-receptor (named Ionotropic Receptors, IR), the IR25a, which is mostly expressed in the lateral antennular flagella, bearing the aesthetascs olfactory sensilla, but also to a lesser extent in the medial antennular flagella and the antennae.

Even if the thermal biology of *Rimicaris exoculata* has been investigated (see below), very few studies were conducted on thermosensibility. Peripheral specific or putative multimodal thermoreceptors are not known in Crustaceans (Ache 1982). Nevertheless *Rimicaris* shrimp seem able to detect thermal differences, as they avoid extreme thermal temperatures, showing quick escape behavior when coming in contact with the hydrothermal fluid (Segonzac et al. 1993). And behavioural studies show attraction to hot water (Ravaux, Shillito and Zbinden, unpublished results).

5.3. Thermal biology

The extreme trophic specialization of *Rimicaris* would force shrimp to live at the very edge of the hot discharges (Gebruk et al. 1997a). Damages (black burnt cuticles) caused by contact with superheated fluid has been observed on many specimens (Van Dover et al. 1988; Gebruk et al. 1993, 2000; Segonzac et al. 1993). The proportion of damaged specimens with burnt pereopods, pleopods or antennae at TAG site ranged from 33 to 50% of the population (Vereshchaka et al. 2000; Gebruk et al. 1997a). Shrimp were often observed deviating very suddenly when entering in contact with hot fluid. Vereshchaka et al. (2015) related the efficiency of the shrimp escape behaviour to a morphological characteristic of *Rimicaris* which possess two strong movable spines instead of one on the tail fan.

As for its counterpart of the Pacific vent site, the polychaete *Alvinella pompejana*, that also thrive also on active chimney walls, close to superheated fluid exits, an important question that has long intrigued scientists is to know the upper thermal limit tolerated by the shrimp. Answers to these questions came with the development of pressure aquariums that have allowed *in vivo* experiments (Ravaux et al. 2003; Ravaux et al. 2009; Cottin et al. 2010a, b; Shillito et al. 2014). *R. exoculata* upper thermal limit (critical thermal maximum, CTmax) was first proposed to be in the 33-37°C range (Ravaux et al. 2003), but was later recalculated by Shillito et al. (2006) as 38.5 ± 2°C. This species can therefore not sustain prolonged exposure at this temperature, and was also proved to trigger a heat stress response through the over-expression of stress gene hsp70 when exposed to 30°C for 1h (Ravaux et al. 2007; Cottin et al. 2010a). First observations of the thermal behaviour showed a possible escape response at temperature of about 25°C, and an attraction for temperature of about 10°C (Ravaux et al. 2003; Ravaux et al. 2009). *R. exoculata* may therefore choose a microhabitat in a relatively narrow thermal window that would be defined by both the shrimp nutritional demands, the thermal tolerance and thermal preference.

As their host, *Rimicaris* epibionts are punctually subjected to bursts of very hot

temperatures. To date, however, only few data are available on their thermal sensitivity. Genes encoding heat shock proteins were recently identified in the metagenome for *Epsilonproteobacteria*, *Gammaproteobacteria* and *Zetaproteobacteria* epibionts, indicating their ability to cope with the fluctuating conditions of the hydrothermal habitat (Jan et al. 2014).

5.4. Detoxication

Hydrothermal vent invertebrates are surrounded by fluids containing numerous potential chemical threats, such as sulphide (a cellular respiration poison), methane and dissolved metals like iron, copper, zinc, cadmium, lead, mercury. An excessive accumulation of metals in the cells can lead to the formation of reactive oxygen species (ROS) and cause severe cell damages. Hydrothermal fauna have developed adaptations to deal with these toxic compounds, excreting them from their bodies or storing them in less toxic forms (Childress and Fisher 1992, Rousse et al. 1998). The question of detoxication is all the more a topical issue in the present circumstances where the various metals (e.g. Cu, Ni, Zn, Mn, Co, Ag, Au) contained in the hydrothermal massive sulphide deposits are of growing economic interest to mining industries (Grameling 2014, Mengerink et al. 2014). It is likely that the exploitation activities will expose the local fauna to intense plumes of sediments, metals and various chemical compounds (Van Dover 2014). Various detoxification mecanisms have been suggested or described for *Rimicaris*.

Metals can be stored as insoluble, non-circulating forms, thus avoiding disturbance of essential metabolic functions (Geret et al. 2002). For example, copper and sulphur are accumulated in the epithelial cells of the hepatopancreas as insoluble granules, thus decreasing the potential toxic effect of Cu present in the cytoplasm of cells (Auguste et al. 2014). Hepatopancreas and gills were shown to be the two tissues that accumulate the most trace metals, in concentration that reflect their concentration in the vent fluid (Geret et al. 2002, Kadar et al. 2006, Auguste et al. 2014). The most accumulated metals in *R. exoculata* soft tissues were Fe, Zn, Mn and Cu, whilst Ag and Cd were the less accumulated (Gonzalez-Rey et al. 2008). But compared with the concentration in the environment, only Cu and Cd are bioaccumulated (Geret et al. 2002). Shrimp experimental exposure to 0.4 and 4 µM of Cu in pressurized aquaria do not show significant differences between the two treatments which could indicate a potential regulation mechanism of metal metabolism by the shrimp (Auguste et al. 2014). Low levels of arsenic (Larsen et al. 1997, Taylor et al. 2012) and mercury (Kadar et al. 2006, Martins et al. 2001), compared with coastal shrimp, have been detected in *R. exoculata*, probably related to their short food chain, limiting the accumulations of toxic compounds in tissues. Moreover, compared to *Mirocaris fortunata* that lives further away from vent fluids, *R. exoculata* had similar or often less metals accumulated in selected organs, possibly thanks to a higher degree of adaptation to hydrothermal conditions (Kadar et al. 2006).

Sulphide detoxication was proposed to occur in the gill epithelium of the shrimp thanks to sulphide-oxidising bodies (SOB), electron-dense organelles containing membranes stacks (Compère et al. 2002). Such structures were already observed in different tissues of organisms from sulphide-rich habitats, like in the gill of the clam *Solemya reidi* or in the hindgut and tegumental tissues of the echiuran worm *Urechis caupo*, in which enzymatic oxidation of sulphide to less toxic thiosulphate was demonstrated (Compère et al. 2002 and references therein).

Another detoxification process, the methallothioneins (MTs), cystein-rich, low molecular weight proteins with a high affinity for physiological (Zn, Cu, Se) or xenobiotic (Cd, Hg, As, Ag) metal cations, have been proposed to be involved in detoxication by binding metals and can also act as oxyradicals scavengers protecting cells against ROS (Roesijadi 1992). Induction of methallothioneins was observed in the shrimp gill after an experimental exposure to 4 µm of Cu, probably linked to the role of MTs in the detoxification and/or storage of Cu

(Auguste et al. 2016). But presence of MTs, as well as activities of several antioxydant enzymes in control shrimp showed the existence of constitutive mecanisms of protection against metal toxicity (Auguste et al. 2016). Compared to *Mirocaris fortunata*, *R. exoculata* showed much higher MT levels (approximately six fold higher) than those found in *M. fortunata*, suggesting a higher exposition to metals, but lower antioxydant activities (Gonzalez-Rey et al. 2007). This can be explained as metal-induced reactive oxygen species are less likely to be formed when MT synthesis increases, leading to a natural decrease in the antioxidant enzymatic protections (Gonzalez-Rey et al. 2007).

Following hypothesis proposed for *Alvinella pompejana* filamentous epibionts on the EPR (Cosson-Mannevy et al. 1986), detoxicating properties have also been proposed for the shrimp symbiotic bacteria at MAR (Segonzac et al. 1993, Jan et al. 2014).

Perspectives

Our knowledge of *R.exoculata* has increased greatly since its description in 1986 by Williams and Rona. But study on hydrothermal fauna long remained and still are limited due to the remotness of the sites, the difficulty to perform *in vivo* experiment on animals shocked by the decompression during ascent to the surface, as well as the low frequency of cruises, usually scheduled during spring/summer due to weather conditions. These blockages are about to be overcome by the development of pressurised equipment which allow recovery and maintenance at native pressure to tackle physiological issues by *in vivo* experiments on animals in good physiological condition. Long-term rearing of deep-sea fauna would now be possible thanks to aquariums like AbyssBox, allowing studies of species interactions and behaviour, sensorial adaptations, reproduction, and larval development (Shillito et al. 2015). Cruise scheduling, in the recent past years, other than during the summer months allowed, for example, sampling during the shrimp breeding season, and to obtain the first eggs and early larval stages.

In the future, technological developments will undoubtedly help to answer the still unresolved questions about the biology and physiology of this shrimp, such as the relative importance of the different metabolic pathways within the epibiosis, according to the harvest site, the nature of the molecules exchanged between bact and hosts, the establishment of symbiosis and host-symbionte recognition mechanisms, the life span of shrimp and their full life cycle or the way how shrimp locate in their environment and communicate with each other**.**

Acknowledgments

The authors wish to thank the chief scientists of the numerous cruises, as well as captains and crews of the research vessels and the submersibles for their invaluable assistance in providing *R. exoculata* samples. The authors thank J. Ravaux, B. Shillito for their corrections on this manuscript. This work was supported in part by UPMC Sorbonne Universités and indirectly by the following grants: the European Union Seventh Framework Programme (FP7/2007–2013) under the MIDAS project [grant agreement n°603418] and the National program BALIST ANR-08-BLAN- 0252.

References

Ache B (1982) Chemoreception and thermoreception. In: Bliss D (ed) The Biology of Crustacea, Vol 3 Academic Press, ew York

Allen C, Copley J, Tyler P (2001) Lipid partitioning in the hydrothermal vent shrimp *Rimicaris exoculata*. Marine Ecology 22(3):241-253

Allen Copley C, Tyler P, Varney M (1998) Lipid profiles of hydrothermal vent shrimps. Cahiers de Biologie Marine 39:229-231

Anderson L, Halary S, Lechaire JP, Boudier T, Frébourg G, Marco S, Zbinden M, Gaill F (2008) Tomography of bacteria-mineral associations within the deep sea hydrothermal vent shrimp *Rimicaris exoculata*. Comptes rendus Chimie 11:268-280

Arp A, Childress J (1981) Functional characteristics of the blood of the deep-sea hydrothermal vent Brachyuran crab. Science 214:559-560

Auguste M, Mestre N, Rocha T, Cardoso C, Cueff-Gauchard V, Le Bloa S, Cambon-Bonavita M-A, Shillito B, Zbinden M, Ravaux J, Bebianno M (2016) Development of an ecotoxicological protocol for the deep-sea fauna using the hydrothermal vent shrimp *Rimicaris exoculata*. Aquatic Biology 175:277-285

Bachraty C, Legendre P, Desbruyères D (2009) Biogeographic relationships among deep-sea hydrothermal vent faunas at global scale. Deep-sea Research I 56:1371-1378

Bauer R (1989) Decapod crustaceans grooming : functional morphology, adaptive value, and phylogenetic significance. In: Felgenhauer B, Watling L, Thistle A (eds) Functional morphology of feeding and grooming in Crustacea. Balkema, AA, Rotterdam

Bridges C, Morris S, Grieshaber M (1984) Modulation of haemocyanin oxygen affinity in the intertidal prawn *Palaemon elegans* (rathke). Respiration Physiology 57:189-200

Bright M, Bulgheresi S (2010) A complex journey: transmission of microbial symbionts. Nature Reviews Microbiology 8(3):218-230

Campbell B, Cary S (2004) Abundance of reverse Tricarboxylic Acide cycle genes in free-living microorganisms at deep-sea hydrothermal vents. Applied and Environmental Microbiology 70(10):6282-6289

Casanova B, Brunet M, Segonzac M (1993) L'impact d'une épibiose bactérienne sur la morphologie fonctionnelle de crevettes associées à l'hydrothermalisme médio-Atlantique. Cahiers de Biologie Marine 34:573-588

Cate H, Derby C (2001) Morphology and distribution of setae on the antennules of the Caribbean spiny lobster *Panulirus argus* reveal new types of bimodal chemo-mechanosensilla. Cell Tissue Research 304:439-454

Cavanaugh C (1983) Symbiotic chemoautotrophic bacteria in marine invertebrates from sulphide-rich habitats. Nature 302:58-61

Cavanaugh C, Gardiner S, Jones M, Jannasch H, Waterbury J (1981) Prokaryotik cells in the hydrothermal vent tube worm *Riftia pachyptila* Jones: possible chemoautotrophic symbionts. Science 213:340-342

Chamberlain S (2000) Vision in hydrothermal vent shrimp. Philosophical Transactions of teh Royal Society B 355:1151-1154

Charlou JL, Donval JP, Fouquet Y, Jean-Baptiste P, Holm N, Caccavo F (2002) Geochemistry of high H_2 and CH_4 vent fluids issuing from ultramafic rocks at the Rainbow hydrothermal field (36°14'N, MAR). Chemical Geology 191:345-359

Charlou J, Donval J, Konn C, Ondréas H, Fouquet Y, Jean-Baptiste P, Fourré E (2010) High production and fluxes of H_2 and CH_4 and evidence of abiotic hydrocarbon synthesis by serpentinization in ultramafic-hosted hydrothermal systems on the Mid-Atlantic Ridge. In: Rona P, Devey C, Dyment J, Murton B (eds) Diversity of Hydrothermal Systems on Slow Spreading Ocean Ridges. American Geophysical Union, Washington, D. C

Chaston J, Goodrich-Blair H (2010) Common trends inmutualism revealed by model associations between invertebrates and bacteria. FEMS Microbiology Reviews Rev 34:41-58

Chausson F, Bridges C, Sarradin P, Green B, Riso R, Caprais J, Lallier F (2001) Structural anf functional properties of hemocyanin from *Cyanagraea praedator*, a deep-sea hydrothermal vent crab. Proteins: Structure, Function, and Genetics 45:351–359

Chausson F, Sanglier S, Leize E, Hagège A, Bridges C, Sarradin PM, Shillito B, Lallier F, Zal F (2004) Respiratory adaptations to the deep-sea hydrothermal vent environment: the case of *Segonsacia mesatlantica*, a crab from the Mid-Atlantic Ridge. Micron 35:31-41

Childress J, Fischer C (1992) The biology of hydrothermal vent animals: physiology, biochemistry and autotrophic symbioses. Oceanographic Marine Biology Annual Review 30:337-441

Christoffersen M (1986) Phylogenetic relationships between Oplophoridae, Atyidae, Pasiphaeidae, Alvinocarididae fam. n., Bresiliidae, Psalidopodidae and Disciadidae (Crustacea Caridea Atyoidea). Boletim de Zoologia, Univ S Paolo 10:273-281

Compère P, Martinez A, Charmantier-Daures M, Toullec J, Goffinet G, Gaill F (2002) Does sulphide detoxication occur in the gills of the hydrothermal vent shrimp, *Rimicaris exoculata*? Comptes Rendus Biologies 325:591-596

Copley J, Tyler P, Murton B, Van Dover C (1997) Spatial and interannual variation in the faunal distribution at Broken Spur vent field (29°N, Mid-Atlantic Ridge). Marine Biology 129:723-733

Copley J, Young C (2006) Seasonality and zonation in the reproductive biology and population structure of the shrimp *Alvinocaris stactophila* (Caridea: Alvinocarididae) at a Louisiana Slope cold seep. Marine Ecology Progress Series 315:199-209

Copley J, Jorgensen P, Sohn R (2007) Assessment of decadal-scale ecological change at a deep Mid-Atlantic hydrothermal vent and reproductive time-series in the shrimp *Rimicaris exoculata*. Journal of Marine Biological Association of the UK 87:859-867

Corbari L, Zbinden M, Cambon-Bonavita M-A, Gaill F, Compère P (2008a) Bacterial symbionts and mineral deposits in the branchial chamber of the hydrothermal vent shrimp *Rimicaris exoculata*: relationship to moult cycle. Aquatic Biology 1:225-238

Corbari L, Cambon-Bonavita M-A, Long Garry J, Grandjean F, Zbinden M, Gaill F, Compère P (2008b) Iron oxide deposits associated with the ectosymbiotic bacteria in the hydrothermal vent shrimp *Rimicaris exoculata*. Biogeosciences 5:1295-1310

Corliss J, Dymond J, Gordon L, Edmond J, Von Herzen R, Ballard R, Kenneth G, Williams D, Bainbridge A, Crane K, Van Andel T (1979) Submarine thermal springs on the Galapagos Rift. Science 203:1073-1083

Cottin D, Shillito B, Chertemps T, Thatje S, Léger N, Ravaux J (2010a) Comparison of heat-shock responses between the hot vent shrimp *Rimicaris exoculata* and the related coastal shrimp *Palaemonetes varians*. Journal of Experimental Biology 393:9-16

Cottin D, Shillito B, Tanguy A, Léger N, Ravaux J (2010b) Identification of differentially expressed genes in the hydrothermal vent shrimp *Rimicaris exoculata* exposed to heat stress. Marine Genomics 3:71-78

Creasey S, Rogers A, Tyler P (1996) Genetic comparison of two populations of the deep-sea vent shrimp *Rimicaris exoculata* (Decapoda: Bresiliidae) from the Mid-Atlantic Ridge. Marine Biology 125:473-482

Crone, T., Wilcock, W., Barclay, A., Parsons, J., 2006. The sound generated by mid-ocean ridge black smoker hydrothermal vents. PLoS ONE 1(1), e133. doi:110.1371/journal.pone.0000133.

Cuomo C (1985) Sulphide as a larval settlment cue for *Capitella* spI. Biogeochemistry 1:169-181

de Burgh M, Singla C (1984) Bacterial colonization and endocytosis on the gill of a new limpet species from a hydrothermal vent. Marine Biology 84:1-6

Derby C, Kozma M, Senatore A, Schmidt M (2016) Molecular mechanisms of reception and perireception in custacean chemoreception: a comparative review. Chemical Senses 41(5):381-398

Desbruyères D, Gaill F, Laubier L, Prieur D, Rau G (1983) Unusual nutrition of the "Pompeii worm" *Alvinella pompejana* (polychaetous annelid) from a hydrothermal vent environment: SEM, TEM, ^{13}C and ^{15}N evidence. Marine Biology 75:201-205

Desbruyères D, Almeida A, Biscoito M, Comtet T, Khripounoff A, Le Bris N, Sarradin PM, Segonzac M (2000) A review of the distribution of hydrothermal vent communities along the northern Mid-Atlantic Ridge: dispersal vs. environmental controls. Hydrobiologia 440:201-216

Desbruyères D, Biscoito M, Caprais JC, Colaço A, Comtet T, Crassous P, Fouquet Y, Khripounoff A, Le Bris N, Olu K, Riso R, Sarradin PM, Segonzac M, Vangriesheim A (2001) Variations in deep-sea hydrothermal vent communities on the Mid-Atlantic Ridge near the Azores plateau. Deep-Sea Research I 48:1325-1346

Desbruyères, D., Segonzac, M., Bright, M., 2006. Handbook of deep-sea hydrothermal vent fauna. Second completely revised edition. Biologiezentrum Linz, Austria.

Distel D, Lane D, Olsen G, Giovannoni S, Pace B, Pace N, Stahl D, Felbeck H (1988) Sulfur-oxidizing bacterial endosymbionts: analysis of phylogeny and specificity by 16S rRNA sequences. Journal of Bacteriology 170(6):2506-2510

Dixon DR, Dixon L, Pond DW (1998) Recent advances in our understanding of the life history of bresiliid vent shrimps on the MAR. Cahiers de Biologie Marine 39:383-386

Douville E, Charlou JL, Oelkers EH, Bienvenu P, Jove Colon CF, Donval JP, Fouquet Y, Prieur D, Appriou P (2002) The rainbow vent fluids (36°14'N, MAR): the influence of ultramafic rocks and phase separation on trace metal content in Mid-Atlantic Ridge hydrothermal fluids. Chemical Geology 184:37-48

Drach P, Tchernigovtzeff C (1967) Sur la méthode de détermination des stages d'intermue et son application générale aux Crustacés. Vie et Milieu 18A:595-609

Durand L, Zbinden M, Duperron S, Roussel E, Cueff-Gauchard V, Shillito B, Cambon-Bonavita M-A (2010) Microbial diversity associated with the hydrothermal vent shrimp *Rimicaris exoculata* gut and occurrence of a resident microbial community. FEMS Microbiology Ecology 71:291-303

Durand L, Roumagnac M, Cueff-Gauchard V, Jan C, Guri M, Tessier C, Haond M, Crassous P, Zbinden M, Arnaud-Haond S, Cambon-Bonavita M-A (2015) Biogeographical distribution of *Rimicaris exoculata* gut epibiont communities along the Mid-Atlantic Ridge hydrothermal vent sites. FEMS Microbiology Ecology 91(10): fiv101

Emerson D, Moyer C (1997) Isolation and characterization of novel iron-oxidizing bacteria that growt at circum neutral pH. Applied and Environmental Microbiology 63 (12):4784-4792

Flores G, Campbell J, Kirshtein J, Meneghin J, Podar M, Steinberg J, Seewald J, Tivey M, Voytek M, Yang Z, Reysenbach A (2011) Microbial community structure of hydrothermal deposits from geochemically different vent fields along the Mid-Atlantic Ridge. Environmental Microbiology 13(8):2158-2171

Gaill F, Desbruyères D, Prieur D, Gourret J (1984) Mise en évidence de communautés bactériennes épibiontes vu "Ver de Pompéï" (*Alvinella pompejana*). Comptes Rendus de l'Académie des Sciences de Paris, série III 298:553-558

Gaten E, Herring P, Shelton P, Johnson M (1998a) Comparative morphology of the eyes of postlarval bresiliid shrimps from the region of hydrothermal vents. Biological Bulletin 194:267-280

Gaten E, Herring P, Shelton P, Johnson M (1998b) The development and evolution of the eyes of vent shrimps (Decapoda: Bresiliidae). Cahiers de Biologie Marine 39:287-290

Gebruk A, Pimenov N, Savvichev A (1993) Feeding specialization of bresiliid shrimps in the TAG site hydrothermal community. Marine Ecology Progress Series 98:247-253

Gebruk A, Galkin S, Vereshchaka A, Moskalev L, Southward A (1997a) Ecology and Biogeography of the Hydrothermal Vent fauna of the Mid-Atlantic Ridge. Advanced in Marine Biology 32:93-144

Gebruk A, Lein A, Galkin S, Miller Y, Pimenov N, Moskalev L, Ivanov M (1997b) Trophic structure of the Broken Spur Hydrothermal community shown by carbon stable isotope and C:H:N:S data. BRIDGE Newsletter 12:40-45

Gebruk A, Southward E, Kennedy H, Southward A (2000) Food sources, behaviour, and distribution of hydrothermal vent shrimp at the Mid-Atlantic Ridge. Journal of Biological Association of the UK 80:485-499

Geret F, Riso R, Sarradin PM, Caprais JC, Cosson R (2002) Metal bioaccumulation and storage forms in the shrimp, *Rimicaris exoculata*, from the Rainbow hydrothermal field (Mid-Atlantic Ridge); preliminary approach to the fluid-organism relationship. Cahiers de Biologie Marine 43:43-52

German C, Parson L, Team HS (1996) Hydrothermal exploration near the Azores Triple Junction: tectonic control of venting at slow-spreading ridges? Earth and Planetary Science Letters 138:93-104

Gloter A, Zbinden M, Guyot F, Gaill F, Colliex C (2004) Formation and stabilization of mixed valence ferrihydrite on bacterial surfaces from hydrothermal vents. Earth and Planetary Science Letters 222:947-957

Gonzalez-Rey, M., Serafim, A., Company, R., bebianno, M., 2007. Adaptation to metal toxicity: a comparison of hydrothermal vent and coastal shrimps. Mar Ecol 28, 100-107.

Gonzalez-Rey M, Serafim A, Company R, Gomes T, Bebianno M (2008) Detoxification mechanisms in shrimp: Comparative approach between hydrothermal vent fields and estuarine environments. Marine Environmental Research 66:35-37

Gramling, C., 2014. Seafloor Mining Plan Advances, Worrying Critics. Science 344, 463.

Grünert U, Ache B (1988) Ultrastructure of the aesthetasc (olfactory) sensilla of the spiny lobster, *Panulirus argus*. Cell Tissue Research 251:95-103

Guri M, Durand L, Cueff-Gauchard V, Zbinden M, Crassous P, Shillito B, Cambon-Bonavita M-A (2012) Acquisition of epibiotic bacteria along the life cycle of the hydrothermal shrimp *Rimicaris exoculata.* ISME Journal 6:597-609

Henri P, Rommevaux-Jestin C, Lesongeur F, Mumford A, Emerson D, Godfroy A, Ménez B (2016) Structural Iron (II) of Basaltic Glass as an Energy Source for Zetaproteobacteria in an Abyssal Plain Environment, Off the Mid Atlantic Ridge. Frontiers in Microbiology 6:1518

Hernandez-Avila I, Cambon-Bonavita M-A, Pradillon F (2015) Morphology of First Zoeal Stage of Four Genera of Alvinocaridid Shrimps from Hydrothermal Vents and Cold Seeps: Implications for Ecology, Larval Biology and Phylogeny. . PLoS ONE 10(12):e0144657.

Herring P (1998) North Atlantic midwater distribution of the juvenile stages of hydrothermal vent shrimps (Decapoda : Bresilidae). Cahiers de Biologie Marine 39:387-390

Herring P, Dixon DR (1998) Extensive deep-sea dispersal of postlarval shrimp from a hydrothermal vent. Deep-Sea Research Part I 45:2105-2118

Herring P, Gaten E, Shelton P (1999) Are the shrimp blinded by science? Nature 398:116

Hügler M, Petersen J, Dubilier N, Imhoff J, Sievert S (2011) Pathways of carbon and energy metabolism of the epibiotic community associated with the deep-sea hydrothermal vent shrimp *Rimicaris exoculata.* PLoS One 6(1): e16018. doi:16010.11371/journal.pone.0016018

Hügler M, Wirsen C, Fuchs S, Taylor C, Sievert S (2005) Evidence for autotrophic CO2 fixation via the reductive tricarboxylic acid cycle by members of the epsilon subdivision of Proteobacteria. Journal of Bacteriology 187:3020-3027

Jan C, Petersen J, Werner J, Huang S, Teeling H, Glöckner F, Golyshina O, Dubilier N, Golyshin P, Jebbar M, Cambon-Bonavita M (2014) The gill chamber epibiosis of deep-sea shrimp *Rimicaris exoculata*: an in-depth metagenomic investigation and discovery of *Zetaproteobacteria*. Environ Microbiol 16(9):2723-2738

Jannasch H (1985) The chemosynthetic support of life and the microbial diversity at deep-sea hydrothermal vents. Proceedings of the Royal Society of London 25 (1240):277-297

Jannasch H, Wirsen C (1979) Chemosynthetic primary production at east Pacific sea Floor spreading centers. Bioscience 29(10):592-598

Jinks R, Battelle B, Herzog E, Kass L, Renninger G, Chamberlain S (1998) Sensory adaptations in hydrothermal vent shrimps from the Mid-Atlantic Ridge. Cahiers de Biologie Marine 39:309-312

Kádár, E., Costa, V., Santos, R.S., 2006. Distribution of micro-essential (Fe, Cu, Zn) and toxic (Hg) metals in tissues of two nutritionally distinct hydrothermal shrimps. Science of The Total Environment 358 (1–3), 143-150.

Kennedy C, Scott S, Ferris F (2004) Hydrothermal phase stabilization of 2-line ferrihydrite by bacteria. Chemical Geology 212:269–277

Komai T, Giere O, Segonzac M (2007) New record of alvinocarid shrimps (Crustacea: Decapoda: Caridea) from hydrothermal vent fields on the southern Mid-Atlantic Ridge, including a new species of the genus Opaepele. Species Diversity 12:237–253

Komai T, Segonzac M (2003) Review of the hydrothermal vent shrimp genus Mirocaris, redescription of M. fortunata and reassessment of the taxonomic status of the family Alvinocarididae (Crustacea: Decapoda: Caridea). Cahiers de Biologie Marine 44:199-215

Komai T, Segonzac M (2008) Taxonomic review of the hydrothermal vent shrimp genera *Rimicaris* Williams and Rona and *Chorocaris* Martin and Hessler (Crustacea: Decapoda; Caridea: Alvinocarididae). Journal of

Shellfish Research 27 (1):21-41
Komai T, Tsuchida S (2015) New records of Alvinocarididae (Crustacea: Decapoda: Caridea) from the southwestern Pacific hydrothermal vents, with descriptions of one new genus and three new species. Journal of Natural History 49 (29-30):1789-1824
Kornberg A (1995) Inorganic polyphosphate : toward making a forgotten polymer unforgettable. Journal of Bacteriology 177 (3):491-496
Kuenzler R, Kwasniewski J, Jinks R, Lakin R, Battelle B, Herzog E, Kass L, Renninger G, Chamberlain S (1997) Retinal anatomy of new bresiliid shrimp from Lucky Strike and Broken Spur hydrothermal vent fields on the Mid-Atlantic Ridge. Journal of Marine Biological Association of the UK 77 (3):707-725
Lakin R, Jinks R, Battelle B, Herzig P, Kass L, Renninger G, Chamberlain S (1997) Retinal anatomy of *Chorocaris chacei*, a deep-sea hydrothermal vent shrimp from the Mid-Atlantic Ridge. Journal of Comparative Neurology 385:503-514
Lallier F, Truchot J (1997) Hemocyanin oxygen-binding properties of a deep-sea hydrothermal vent shrimp – evidence for a novel cofactor. Journal of Experimental Biology 277(5):357-364
Lallier F, Camus L, Chausson F, Truchot J (1998) Structure and function of hydrothermal vent crustacean haemocyanin: an update. Cahiers de Biologie Marine 39(3-4):313-316
Larsen E, Quétel C, Munoz R, Fiala-Médioni A, Donard O (1997) Arsenic speciation in shrimp and mussel from the Mid-Atlantic hydrothermal vents. Marine Chemistry 57:341-346
Laverack M (1964) The antennular sense organs of *Panulirus argus*. Comparative Biochemistry and Physiology 13:301-321
Le Bloa S (2016) Mode de reconnaissance hôte-symbionte en milieux extrêmes: cas du modèle symbiotique, la crevette *Rimicaris exoculata*, pHD thesis Université de Bretagne occidentale,
Le Bloa S, Durand L, Taupin L, Marteau C, Cueff-Gauchard V, Bazire A, Cambon-Bonavita M-A (2017) Highlighting of Quorum Sensing lux genes and their expression in the hydrothermal vent shrimp *Rimicaris exoculata* ectosymbiontic community. Possible used as markers of biogeography. PLoS ONE 12(3):e0174338. https://doi.org/0174310.0171371/journal.pone.0174338
Lonsdale P (1977) Clustering of suspension-feeding macrobenthos near abyssal hydrothermal vents at oceanic spreading centers. Deep Sea Research 24:857-863
Markert S, Arndt C, Felbeck H, Becher D, Sievert S, Hügler M, Albrecht D, Robidart J, Bench S, Feldman R, Hecker M, Schweder T (2007) Physiological proteomics of the uncultured endosymbiont of *Riftia pachyptila*. Science 315:247-250
Martin J, Hessler R (1990) *Chorocaris vandoverae*, a new genus and species of hydrothermal vent shrimp (Crustacea, Decapoda, Bresiliidae) from the Western Pacific. Contributions in Science 417:1-11
Martin J, Haney T (2005) Decapod crustaceans from hydrothermal vents and cold seeps: a review through 2005. Zoological Journal of the Linnean Society 145:445-522
Martin J, Shank T (2005) A new species of the shrimp genus Chorocaris (Decapoda: Caridea: Alvinocarididae) from hydrothermal vents in the eastern Pacific Ocean. Proceedings of the Biological Society of Washington 118:183-198
Martin J, Signorovitch J, Patel H (1997) A new species of Rimicaris (Crustacea: Decapoda: Bresiliidae) from the Snake Pit hydrothermal vent field on the Mid-Atlantic Ridge. Proceedings of the Biological Society of Washington 110 (3):399-411
Martinez AS, Charmantier G, Compère P, Charmantier-Daures M (2005) Branchial chamber tissues in two caridean shrimps: the epibenthic *Palaemon adspersus* and the deep-sea hydrothermal *Rimicaris exoculata*. Tissue and cell 37:153-165
Martins I, Porteiro F, Cravo A, Santos R (2001) Mercury concentrations in invertebrates from Mid-Atlantic Ridge hydrothermal vent fields. Journal of Marine Biological Association of the UK 81:913-915
Mellon D (2014) Sensory Systems of Crustaceans. In: Derby C, Thiel M (eds) The Natural History of the Crustacea- Vol 3: Nervous Systems and Control Behavior. Oxford Univ. Press., New York
Mengerink, K., Van Dover, C., Ardron, J., Baker, M., Escobar-Briones, E., Gjerde, K., Koslow, J., Ramirez-Llodra, E., Lara-Lopez, A., Squires, D., Sutton, D., Sweetman, A., Levin, L., 2014. A Call for Deep-Ocean Stewardship. Science 344, 696-698.
Millero F, Sotolongo S, Izaguirre M (1987) The oxidation kinetics of Fe (II) in seawater. Geochimica et Cosmochimica Acta 51:793–801
Montgomery K, Charlesworth J, LeBard R, Visscher P, Burns B (2013) Quorum Sensing in extreme environments. Life:https://doi.org/10.3390/life3010131
Nègre-Sadargues G, Castillo R, Segonzac M (2000) Carotenoid pigments and trophic behaviour of deep-sea shrimps (Crustacea, Decapoda, Alvinocarididae) from a hydrothermal area of the Mid-Atlantic Ridge. Comparative Biochemistry and Physiology Part A 127:293-300
Nelson D, Fischer C (1995) Chemoautotrophic and methanotrophic endosymbiotic bacteria at deep-sea vents and seeps. In: Karl D (ed) The microbiology of deep-sea hydrothermal vents. CRC Press, Boca Raton - New York - London - Tokyo
Neubauer SC, Emerson D, Megonigal JP (2002) Life at the energetic edge: kinetics of circumneutral iron oxidation by lithotrophic iron-oxidizing bacteria isolated grom the wetland-plant rhizosphere. Applied and

Environmental Microbiology 68 (8):3988-3995
Nuckley D, Jinks R, Battelle B, Herzog E, Kass L, Renninger G, Chamberlain S (1996) Retinal anatomy of a new species of Bresiliid shrimp from a hydrothermal vent field on the Mid-Atlantic Ridge. Biol Bull 190:98-110
Nuckley D, Jinks R, Battelle B, Herzog E, Kass L, Renninger G, Chamberlain S (1996) Retinal Anatomy of a New Species of Bresiliid Shrimp From a Hydrothermal Vent Field on the Mid-Atlantic Ridge. Biological Bulletin 190:98-110
Nye V, Copley J, Plouviez S (2011) A new species of *Rimicaris* (Crustacea: Decapoda: Caridea: Alvinocarididae) from hydrothermal vent fields on the Mid-Cayman Spreading Centre, Caribbean. Journal of Marine Biological Association of the UK 92(5):1057-1072
O'Neill P, Jinks R, Herzog E, Battelle B, Kass L, Renninger G, Chamberlain S (1995) The morphology of the dorsal eye of thehydrothermal vent shrimp, *Rimicaris exoculata*. . Visual Neuroscience 12:861-875
Pelli D, Chamberlain S (1989) The visibility of 350°C black-body radiation by the shrimp *Rimicaris exoculata* and man. Nature 337:460-461
Petersen J, Ramette A, Lott C, Cambon-Bonavita M-A, Zbinden M, Dubilier N (2010) Dual symbiosis of the vent shrimp *Rimicaris exoculata* with filamentous gamma- and epsilonproteobacteria at four Mid-Atlantic Ridge hydrothermal vent fields. Environmental Microbiology 12(8):2204-2218
Petersen J, Zielinski F, Pape T, Seifert R, Moraru C, Amann R, Hourdez S, Girguis P, Wankel S, Barbe V, Pelletier E, Fink D, Borowski C, Bach W, Dubilier N (2011) Hydrogen is an energy source for hydrothermal vent symbioses. Nature 476:176-180
Polz M, Cavanaugh C (1995) Dominance of one bacterial phylotype at a Mid-Atlantic Ridge hydrothermal vent site. Proceedings of the National Academy of Sciences of the United States of America 92:7232-7236
Polz M, Robinson J, Cavanaugh C, Van Dover C (1998) Trophic ecology of massive shrimp aggregations at a mid-Atlantic Ridge hydrothermal vent site. Limnology and Oceanography 43(7):1631-1638
Pond D, Dixon D, Bell M, Fallick A, Sargent J (1997a) Occurence of 16:2(n-4) and 18:2 (n-4) fatty acids in the lipids of the hydrothermal vent shrimps *Rimicaris exoculata* and *Alvinocaris markensis*: nutritional and trophic implications. Marine Ecology Progress Series 156:167-174
Pond DW, Dixon DR, Sargent JR (1997b) Wax-ester reserves facilitate dispersal of hydrothermal vent shrimps. Marine Ecology Progress Series 146:289-290
Pond D, Sargent J, Fallick A, Allen C, Bell M, Dixon D (2000a) δ13C values of lipids from phototrophic zone microplankton and bathypelagic shrimps at the Azores sector of the Mid-Atlantic Ridge. Deep-Sea Research I 47:121-136
Pond DW, Gebruk A, Southward E, Southward A, Fallick A, Bell M, Sargent J (2000b) Unusual fatty acid composition of storage lipids in the bresilioid shrimp *Rimicaris exoculata* couples the photic zone with MAR hydrothermal vent sites. Marine Ecology Progress Series 198:171-179
Ponsard J, Cambon-Bonavita M-A, Zbinden M, Lepoint G, Joassin A, Corbari L, Shillito B, Durand L, Cueff-Gauchard V, Compère P (2013) Inorganic carbon fixation by chemosynthetic ectosymbionts and nutritional transfers to the hydrothermal vent host-shrimp, *Rimicaris exoculata.* ISME Journal 7:96-109
Ramirez-Llodra E, Tyler P, Copley J (2000) Reproductive biology of three caridean shrimp, *Rimicaris exoculata*, *Chorocaris chacei* and *Mirocaris fortunata* (Caridea : Decapoda), from hydrothermal vents. Journal of Marine Biological Association of the UK 80:473-484
Ravaux J, Gaill F, Le Bris N, Sarradin PM, Jollivet D, Shillito B (2003) Heat-shock response and temperature resistance in the deep-sea vent shrimp *Rimicaris exoculata*. Journal of Experimental Biology 206:2345-2354
Ravaux J, Toullec JY, Léger N, Lopez P, Gaill F, Shillito B (2007) First hsp70 from two hydrothermal vent shrimps, *Mirocaris fortunata* and *Rimicaris exoculata* : characterization and sequence analysis. Gene 386:162-172
Ravaux J, Cottin D, Chertemps T, Hamel G, Shillito B (2009) Hydrothermal vent shrimps display low expression of heat-inducible hsp70 gene in nature. Marine Ecology Progress Series 396:153-156
Renninger G, Kass L, Gleeson R, Van Dover C, Battelle B, Jinks R, Herzog E, Chamberlain S (1995) Sulfide as a chemical stimulus for deep-sea hydrothermal vent shrimps. Biological Bulletin 189:69-76
Rieley G, Van Dover C, Hedrick D, Eglinton G (1999) Trophic ecology of *Rimicaris exoculata*: a combined lipid abundance/stable isotope approach. Marine Biology 133:495-499
Rittschof D, Forward R, Cannon G, Welch J, McClary M, Holm E, Clare A, Conova S, McKelvey L, Bryan P, Van Dover C (1998) Cues and context: Larval responses to physical and chemical cues. Biofouling 12(1-2):31-44
Robinson J, Cavanaugh C (1995) Expression of form I and form II Rubisco in chemoautotrophic symbioses: Implications for the interpretation of stable carbon isotope values. Limnology Oceanography 40(8):1496-1502
Roesijadi G (1992) Metallothioneins in metal regulation and toxicity in aquatic animals. Aquatic Toxicology 22:81-113
Rona P (1986) Direct observations of Atlantic black smokers. Eos Transactions, American Geophysical Union 67 (46):1327
Rosa R, Barracco M (2010) Antimicrobial peptides in crustaceans. Invertebrate Survival Journal 7(2):262-284

Rousse N, Boulègue J, Cosson R, Fiala-Médioni A (1998) Bioaccumulation des métaux chez le mytilidae hydrothermal *Bathymodiolus* sp. de la ride médio-Atlantique. Oceanologica Acta 21(4):597-607

Salem H, Florez L, Gerardo N, Kaltenpoth M (2015) An out-of-body experience: the extracellular dimension for the transmission of mutualistic bacteria in insects. Proceedings of the Royal Society B 282:20142957

Salerno L, Macko S, Hallam S, Bright M, Won Y, McKiness Z, Van Dover C (2005) Characterization of symbiont populations in life history stages of mussels from chemosynthetic environments. Biological Bulletin 208:145-155

Sanders N, Arp A, Childress J (1988) Oxygen binding characteristics of the hemocyanins of two deep-sea hydrothermal vent crustaceans. Respiration Physiology 71:57-68

Sanders N, Childress J (1990) Adaptations to the deep-sea oxygen minimum layer: Oxygen binding by the hemocyanin of the bathypelagic mysid, *Gnathophausia ingens* Dohrn. Biological Bulletin 178:286–294

Schmidt C, Vuillemin R, Le Gall C, Gaill F, Le Bris N (2008a) Geochemical energy sources for microbial primary production in the environment of hydrothermal vent shrimps. Marine Chemistry 108:18-31

Schmidt C, Le Bris N, Gaill F (2008b) Interactions of deep-sea vent invertebrates with their environment: the case of *Rimicaris exoculata*. Journal of Shellfish Research 27(1):79-90

Schmidt C, Corbari L, Gaill F, Le Bris N (2009) Biotic and abiotic controls on iron oxyhydroxide formation in the gill chamber of the hydrothermal vent shrimp *Rimicaris exoculata*. Geobiology 7:1-11

Schmidt M, Mellon D (2011) Neuronal processing of chemical information in crustaceans. In: Breithaupt T, Thiel M (eds) Chemical communication in Cristaceans. Springer Science+ Business Media, New York

Scott J, Breier J, Luther III G, Emerson D (2015) Microbial iron mats at the Mid-Atlantic Ridge and evidence that Zetaproteobacteria may be restricted to iron-oxidizing marine systems. PLoS ONE 10(3):e0119284. doi:0119210.0111371/journal.pone.0119284

Segonzac M (1992) Les peuplements associés à l'hydrothermalisme océanique du Snake Pit (dorsale médio-Atlantique, 23°N, 3480m): composition et microdistribution de la mégafaune. Compte-Rendus de l'Académie des Sciences 314, série III:593-600

Segonzac M, de Saint-Laurent M, Casanova B (1993) L'énigme du comportement trophique des crevettes Alvinocarididae des sites hydrothermaux de la dorsale médio-atlantique. Cahiers de Biologie Marine 34:535-571

Segonzac M, Comtet T, Chevaldonné P (1997) Epibiosis in two invertebrate species associated to oceanic hydrothermalism: an example of adaptative convergence. Cahiers de Biologie Marine 38:139-140

Shank T, Lutz R, Vriejenhoek C (1998) Molecular systematics of shrimp (Decapoda: Bresiliidae) from deep-sea hydrothermal vents. I. Enigmatic "small orange" shrimp from the Mid-Atlantic Ridge are juvenile *Rimicaris exoculata*. Molecular Marine Biology and Biotechnology 7:88-96

Shank T, Black M, Halanich K, Lutz R, Vriejenhoek C (1999) Miocene radiation of deep-sea hydrothermal vent shrimp (Caridea: Bresiliidae): Evidence from mitochondrial cytochrome oxydase subunit I. Molecular Phylogenetics and Evolution 13:244-254

Shillito B, Le Bris N, Hourdez S, Ravaux J, Cottin D, Caprais JC, Jollivet D, Gaill F (2006) Temperature resistance studies on the deep-sea vent shrimp *Mirocaris fortunata.* The Journal of Experimental Biology 209:945-955

Shillito B, Gaill F, Ravaux J (2014) The Ipocamp pressure incubator for deep-sea fauna. Journal of Marine Science and Technology 22(1):97-102

Shillito B, Ravaux J, Sarrazin J, Zbinden M, Barthélémy D, Sarradin P (2015) Long-term Maintenance and Public Exhibition of Deep-Sea Fauna : The AbyssBox Project. Deep-sea Research I 121: 137-145

Steel C (1993) Storage and translocation of integumentary calcium during the moult cycle of the terrestrial isopod *Oniscus asellus* (L.). Canadian Journal of Zoology 714:4-10

Stephens G (1988) Epidermal amino acid transport in marine invertebrates. Biochimica and Biophysica Acta 947:113-138

Tasiemski A, Jung S, Boidin-Wichlacz C, Jollivet D, Cuvellier-Hot V, Pradillon F, Vetriani C, Hecht O, Sönnichsen F, Gelhaus C, Hung C, Tholey A, Leippe M, Grötzinger J, Gaill F (2014) Characterization and function of the first antibiotic isolated from a vent organism: the extremophile metazoan *Alvinella pompejana*. PLoS ONE 9(4):e95737. doi:95710.91371/journal.pone.0095737

Taylor, V., Jackson, B., Siegfried, M., Navratilova, J., Francesconi, K., Kirshtein, J., Voytek, M., 2012. Arsenic speciation in food chains from mid-Atlantic hydrothermal vents. Environmental Chemistry 9(2), 130-138.

Teixeira S, Cambon-Bonavita M-A, Serrao E, Desbruyères D, Arnaud-Haond S (2010) Recent population expansion and connectivity in the hydrothermal shrimp *Rimicaris exoculata* along the Mid-Atlantic Ridge. . Journal of Biogeography 38 (3):564–574

Teixeira S, Serrao EA, Arnaud-Haond S (2012) Panmixia in a Fragmented and Unstable Environment: The Hydrothermal Shrimp *Rimicaris exoculata* Disperses Extensively along the Mid-Atlantic Ridge. PLoS One 7

Teixeira S, Olu K, Decker C, Cunha R, Fuchs S, Hourdez S, EA S, Arnaud-Haon S (2013) High connectivity across the fragmented chemosynthetic ecosystems of the deep Atlantic Equatorial Belt: efficient dispersal mechanisms or questionable endemism? Marine Ecology 22:4663–4680

Tokuda G, Yamada A, Nakano K, Arita N, Yamasaki H (2006) Occurrence and recent long-distance dispersal of deep-sea hydrothermal vent shrimps. Biology Letters 2:257-260

Truchot J-P (1992) Respiratory function of Arthropod hemocyanins. In: Mangum C (ed) Blood and Tissues Oxygen Carriers. Springer Verlag, Berlin, Heidelberg

Tyler P, Dixon DR (2000) Temperature/pressure tolerance of the first larval stage of Mirocaris fortunata from Lucky Strike hydrothermal vent field. Journal of Marine Biological Association of the UK 80:739-740

Tyler P, Young C (1999) Reproduction and dispersal at vents and cold seeps. Journal of Marine Biological Association of the UK 79:193-208

Tyler P, Young C (2003) Dispersal at hydrothermal vents : a summary of recent progress. Hydrobiologia 503:9-19

Van Dover C, Fry B, Grassle J, Humphris S, Rona P (1988) Feeding biology of the shrimp *Rimicaris exoculata* at hydrothermal vents on the Mid-Atlantic Ridge. Marine Biology 98:209-216

Van Dover C, Szuts E, Chamberlain S, Cann J (1989) A novel 'eyeless' shrimp from hydrothermal vents of the Mid-Atlantic Ridge. Nature 337:458-460

Van Dover C, Reynolds G, Chave A, Tyson J (1996) Light at deep-sea hydrothermal vents. Geophysical Research Letters 23(16):2049-2052

Van Dover C, German C, Speer K, Parson L, Vrijenhoek R (2002) Evolution and Biogeography of Deep-Sea Vent and Seep Invertebrates. Science 295:1253-1257

Van Dover C (2014) Impacts of anthropogenic disturbances at deep-sea hydrothermal vent ecosystems: A review. Marine Environmental Research 102:59-72

Vereshchaka A (1996) A new genus and species of Caridean shrimp (crustacea: decapoda: alvinocarididae) from north Atlantic hydrothermal vents. Journal of Marine Biological Association of the UK 76:951-961

Vereshchaka A (1997) Comparative morphological studies on four populations of the shrimp *Rimicaris exoculata* from the Mid-Atlantic Ridge. Deep-sea Research I 44 (11):1905-1921

Vereshchaka A, Vinogradov G, Ivanenko V (1998) General properties of the reproductive biology of some hydrothermal crustacea (shrimp, amphipods, copepods). Doklady Biological Sciences 360:269-270

Vereshchaka A, Vinogradov G, Lein A, Dalton S, Dehairs F (2000) Carbon and nitrogen isotopic composition of the fauna from the Broken Spur hydrothermal vent field. Marine Biology 136:11-17

Vereshchaka A, Kulagin D, Lunina A (2015) Phylogeny and new classification of hydrothermal vent and seep shrimps of the family Alvinocarididae (Decapoda). PLoS ONE 10(07):e0129975. doi:0129910.0121371/journal.pone.0129975

Vriejenhoek C (2010) Genetic diversity and connectivity of deep-sea hydrothermal vent metapopulations. Molecular Ecology 19(20):4391-4411

Watabe H, Hashimoto J (2002) A New Species of the genus *Rimicaris* (Alvinocarididae: Caridea: Decapoda) from the active hydrothermal vent field, "Kairei Field," on the Central Indian Ridge, the Indian Ocean. Zoological Science 19:1167-1174

Vriejenhoek C (2010) Genetic diversity and connectivity of deep-sea hydrothermal vent metapopulations. Molecular Ecology doi: 10.1111/j.1365-294X.2010.04789.x

Wharton D, Jinks R, Herzog E, Battelle B, Kass L, Renninger G, Chamberlain S (1997) Morphology of the eye of the hydrothermal vent shrimp *Alvinocaris markensis.* Journal of Marine Biological Association of the UK 77:1097-1108

Wheeler, A., Murton, B., Copley, J., Lim, A., Carlsson, J., Collins, P., Dorschel, B., Green, D., Judge, M., Nye, V., Benzie, J., Antoniacomi, A., Coughlan, M., Morris, K., 2013. Moytirra: Discovery of the first known deep-sea hydrothermal vent field on the slow-spreading Mid-Atlantic Ridge north of the Azores. Geochemistry, Geophysics, Geosystems 14(10), 4170-4184.

Williams A, Rona P (1986) Two new caridean shrimps (Bresiliidae) from a hydrothermal field on the Mid-Atlantic Ridge. Journal of Crustacean Biology 6(3):446-462

Wirsen C, Jannasch HW, Molyneaux S (1993) Chemosynthetic microbial activity at Mid-Atlantic Ridge hydrothermal vent sites. Journal of Geophysical Research 98 (B6):9693-9703

Zbinden M, Cambon-Bonavita M-A (2003) Occurence of *Deferribacterales* and *Entomoplasmatales* in the deep-sea shrimp Rimicaris exoculata gut. FEMS Microbiology Ecology 46:23-30

Zbinden M, Le Bris N, Gaill F, Compère P (2004) Distribution of bacteria and associated minerals in the gill chamber of the vent shrimp *Rimicaris exoculata* and related biogeochemical processes. Marine Ecology Progress Series 284:237-251

Zbinden M, Shillito B, Le Bris N, De Vilardi de Montlaur C, Roussel E, Guyot F, Gaill F, Cambon-Bonavita M-A (2008) New insights on the metabolic diversity among the epibiotic microbial community of the hydrothermal shrimp *Rimicaris exoculata*. Journal of Experimental Marine Biology and Ecology 159 (2):131-140

Zbinden M, Berthod C, Montagné N, Machon J, Léger N, Chertemps T, Shillito B, Ravaux J (2017) Comparative study of chemosensory organs of shrimp from hydrothermal vent and coastal environments. Chemical senses doi:10.1093/chemse/bjx007

1. Etude des symbioses chez d'autres espèces d'Alvinocarididae des sources hydrothermales, grâce notamment au co-encadrement de la thèse de Vincent Apremont (2014-2017) avec Marie-Anne Cambon-Bonavita.

Trois autres espèces d'Alvinocarididae occupent les sites hydrothermaux de la dorsale médio-Atlantique avec *Rimicaris exoculata*: *Chorocaris chacei* (récemment ré-assigné au genre *Rimicaris*), *Mirocaris fortunata* et *Alvinocaris markensis*. Ces espèces présentent des différences morphologiques, anatomiques et physiologiques, ainsi que différents profils de comportements et distributions. L'espèce *Rimicaris exoculata*, de loin la plus abondante sur ces sites, est aussi la plus étudiée du point de vue symbiose (cf. synthèse ci-dessus). Jusqu'ici, comparativement, peu d'études se sont intéressées aux autres espèces, numériquement moins importantes. Ces publications ont mis en évidence différents degrés d'interactions et de dépendance vis à vis de bactéries symbiotiques, depuis *Rimicaris*, qui est hautement spécialisée jusqu'à *Alvinocaris*, le plus proche en apparence des crevettes brésilidés non hydrothermales (Segonzac, 1992; Segonzac et al. 1993; Casanova et al. 1993; Gebruk et al. 1993, 1997b, 2000; Colaço et al. 2002). Afin d'étudier plus en détail ces espèces marginales, nous disposons d'échantillons de différentes espèces (*Mirocaris fortunata*, *Chorocaris chacei*, *Alvinocaris markensis*, *Alvinocaris lusca*, *Alvinocaris chelys*, *Alvinocaris komai*, *Alvinocaris muricola*, *Nautilocaris* sp.) provenant des différents environnements (sites hydrothermaux de la dorsale Médio-Atlantique, de la dorsale Est-Pacifique, du Bassin de Lau, des suintements froids du Golf de Guinée…).

La thèse de Vincent Apremont s'est focalisée sur l'étude de *Rimicaris* (*Chorocaris) chacei* et de ses symbiontes. Pour cette étude, il a combiné des approches moléculaires et des analyses phylogénétiques, et des approches en microscopies (photonique, FISH, électronique à balayage et à transmission) réalisées à l'Ifremer de Brest, sous le co-encadrement de Marie-Anne Cambon-Bonavita ou à l'UPMC sous mon encadrement. Ses résultats ont montré chez *R. chacei* une épibiose au niveau de la cavité céphalothoracique moins développée que celle de *R. exoculata* (surfaces occupées par les bactéries moindres, scaphognathites moins développés et présentant moins de soies bactériophores), mais une diversité morphologique et phylogénétique assez proche, dominée par des *Epsilon*- et des *Gammaprotéobactéries*. Le tube digestif (mésentéron) est, comme chez *R. exoculata*, le siège d'une épibiose, avec là aussi des bactéries assez proches morphologiquement et phylogénétiquement de sa consoeur. Ces résultats font l'objet d'une publication en cours de rédaction pour FEMS Microbiology Ecology. Une approche de séquençage haut débit et traitement des données via oligotyping (étude de la diversité présente au sein d'un jeu de données en deçà du seuil de l'OTU) est en cours pour essayer d'affiner les différences entre les communautés bactériennes associées à *R. exoculata* et *R. chacei* et essayer d'expliquer la coexistence de 2 espèces soeurs, avec des symbioses très proches, occupant quasiment la même niche écologique, mais sans compétition apparente.

La campagne océanographique Bicose 2, prévue pour Février 2018, permettra de réaliser sur *R. chacei* des expérimentations *in vivo* en aquarium pressurisés similaires à celles réalisées sur *R. exoculata*: des incubations en présence de marqueurs froids et radioactifs (^{13}C-bicarbonate et ^{14}C-bicarbonate) et de différents donneurs d'électrons (sulfures, fer, methane,…). Cela permettra de déterminer certains métabolismes bactériens, et de mettre en évidence d'éventuels transferts nutritionnels bactéries-hôte à la base de la symbiose et de déterminer la ou les voies par lesquelles ces transferts s'effectuent. De petites molécules organiques type ^{14}C-acétate et de ^{3}H-lysine pourront également être utilisées afin de vérifier la possibilité d'absorption et d'incorporation de molécules organiques solubles par la crevette *R. chacei*.

Comparaison de la couverture bactérienne chez *R. exoculata* (à gauche) et *R. chacei*

2. Etude de la perception sensorielle chez les crevettes hydrothermales, grâce notamment au co-encadrement de la thèse de Julia Machon (2015-2018) avec Juliette Ravaux.

En 2013, nous avons lancé, avec Juliette Ravaux, et en collaboration avec deux collègues spécialistes de l'olfaction des insectes (N. Montagné et T. Chertemps, UPMC, UMR1272 Physiologie des insectes: signalisation et de communication), une nouvelle thématique de recherche sur la perception sensorielle chez les crevettes hydrothermales. Les adaptations sensorielles (en dehors de la vision) ont globalement été très peu étudiées chez les organismes hydrothermaux (une publication de Renninger et al. en 1995), et ce champ d'étude reste donc quasiment vierge malgré son importance capitale dans la compréhension du cycle de vie de ces espèces, leur dispersion, leur maintien et leur évolution à long terme.

Les sites hydrothermaux profonds forment des habitats clairsemés et instables le long des dorsales océaniques, chaque site étant séparé du suivant de quelques kilomètres à plusieurs centaines de kilomètres. La dispersion de ces habitats imposent donc des moyens efficaces de détection des sites pour les espèces hydrothermales à différentes étapes de leur cycle de vie, que ce soit à l'état larvaire pour le recrutement, ou à l'état adulte pour la colonisation de nouveaux sites après extinction d'une source active, ou tout simplement pour se situer par rapport au fluide. Les mécanismes qui permettent aux crevettes de retrouver des signes de l'activité hydrothermale, possiblement située à des dizaines de kilomètres de leur point de départ, restent une énigme. L'objectif de ce projet est d'étudier les adaptations sensorielles chez les crevettes des sources hydrothermales profondes, en se focalisant particulièrement sur la chimio- et la thermoréception, via des études morphologiques, moléculaires, comportementales et électrophysiologiques.

Deux espèces hydrothermales, *Mirocaris fortunata* et *Rimicaris exoculata*, ont été choisies dans le cadre de la thèse de Julia Machon, pour leur abondance et leurs différences écologiques: *R. exoculata* vit sur la paroi des cheminées actives (à des températures de 20-30°C), de façon à rester à proximité du fluide hydrothermal, où ses bactéries symbiotiques trouvent les éléments réduits nécessaires à la chimiosynthèse. *M. fortanata*, qui est détritivore,

vit plus en périphérie des sites, dans des zones de fluides diffus, à des températures de 8 à 14°C, et est donc moins directement dépendante du fluide. Toutes les études sont conduites en parallèle sur une crevette côtière apparentée, *Palaemon elegans*, afin d'étudier les éventuelles adaptations spécifiques à l'environnement hydrothermal.

Ces travaux ont jusqu'ici fait l'objet de 3 rapports de Master (1 M1 et 2 M2) apportant des données sur la morphologie des soies sensorielles et en particulier olfactives (aesthétasques), sur la recherche de récepteurs olfactifs (IR25a) dans les antennes et antennules, sur les comportements des crevettes face à certains stimuli olfactifs. Ces données ont été publiées en 2017 (Zbinden et al. 2017, Chemical Senses). Le Master 2, puis la thèse de Julia Machon ont permis d'aborder des aspects plus fonctionnels et d'étudier la réponse des neurones olfactifs à différents stimuli, à la fois sur la crevette côtière *Palaemon elegans* et sur la crevette hydrothermale *Mirocaris fortunata*, grâce à la maintenance de ces animaux à l'aquarium Océanopolis de Brest. Les travaux de Julia ont permis de mettre au point la première technique d'électroantennographie sur crevette en milieu marin (Machon et al. 2015, Journal of Experimental Biology). Les résultats obtenus montrent des réponses positives des l'antennules portant les aesthétasques, mais aussi des antennes, aux sources de nourritures (granulés alimentaires, jus de crabe ou de crevettes mortes), ainsi qu'à des concentrations élevées de sulfures (concentrations dans le fluide pur et au delà). Ces résultats, couplés à une étude ultrastructurale des aesthétasques (épaisseur de la cuticule, nombre de neurones…) sont en cours de rédaction (Machon et al. in prep).

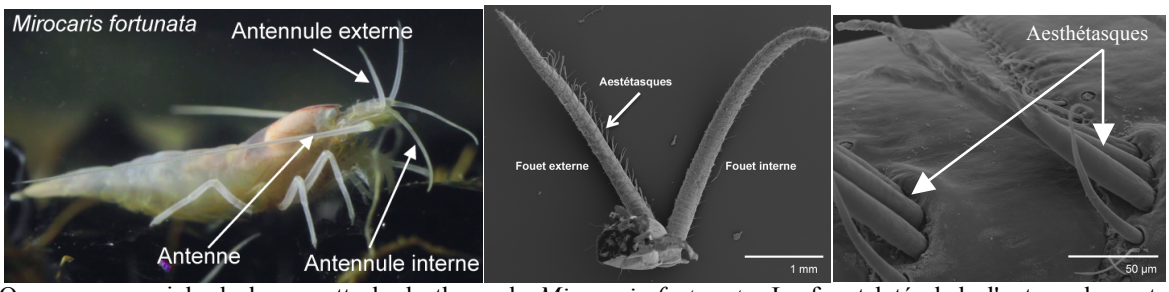

Organes sensoriels de la crevette hydrothermale *Mirocaris fortunata*. Le fouet latéral de l'antennule porte les sensilles spécialisées dans l'olfaction (aesthétasques).

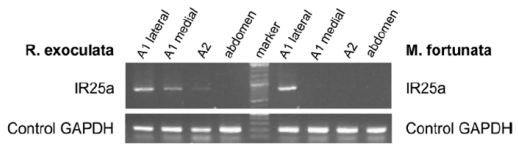

Le co-récepteur IR25a, impliqué dans la transduction olfactive, est exprimé majoritairement dans le fouet latéral chez *Rimicaris* et *Mirocaris*, et en plus faible proportion dans le fouet médian et l'antenne de *Rimicaris.*

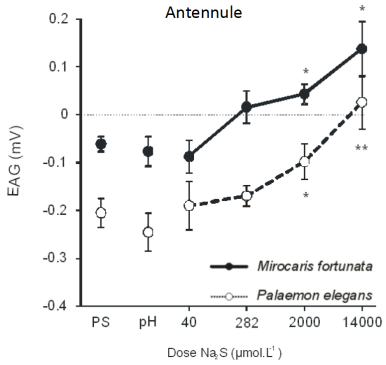

Les enregistrements d'éléctroantennographie montrent la détection de sulfures par l'antennule des 2 espèces étudiées (figure J. Machon).

Ces études seront poursuivies selon différents axes:

1) Tout d'abord un transcriptome par séquençage Illumina des ARNs extraits des deux fouets des antennules, des antennes et des muscles de l'abdomen de *M. fortunata, R. exoculata, A. markensis* et *C. chacei* a été réalisé et est en cours d'analyse en collaboration avec Thomas Chertemps et Nicolas Montagné (iEES, Paris). Ces données permettront de trouver d'autres IRs (notamment IR8 a et IR93a, déjà identifiés chez certaines des espèces étudiées). Nous comptons aussi rechercher des Transient Receptor Potential channels (TRPs) associés à la détection des hautes températures, notamment à partir des TRPs déjà identifiés

chez la drosophile et la daphnie (*TRPA1*, *painless*, *pyrexia*) et dont certains domaines sont relativement bien conservés (Neely et al. 2001, Lee et al. 2005, Fowler and Montell 2013).

2) Comportement : Julia a testé de nombreux protocoles, sur *Mirocaris* et *Palaemon*, pour étudier les comportements d'attraction ou de répulsion vis à vis de la température et de différentes sources d'odeurs représentatives de stimuli hydrothermaux et environnementaux (ex: nourriture, sulfures). Ses essais ont clairement montré une attraction de *Mirocaris* à la température, contrairement à *Palaemon*. Les tests sur l'olfaction sont en cours de réalisation sur *Palaemon*, et seront testés ensuite testés sur le nouvel arrivage de crevettes *Mirocaris fortunata* attendu à Océanopolis fin Juillet suite à la mission Momarsat/Biobaz. L'attraction / répulsion aux sulfures sera également testée chez les deux espèces.

3) La détection de signaux chimiques est impliquée dans de nombreux aspects du comportement des crustacés : la recherche et l'évaluation de la nourriture, l'orientation dans l'environnement, mais aussi diverses interactions sociales, comme les interactions prédateur-proie, la recherche de partenaire pour la reproduction ou l'établissement de hiérarchie sociale.
Le rôle de la communication chimique dans le phénomène d'agrégation chez *Rimicaris exoculata* pourra être étudié en se basant sur des études réalisées sur d'autres crustacés grégaires (Rittschof et al. 1992, Ratchford and Eggleston 2000, Briones-Fourzan and Lozano-Alvarez 2008).

4) En fonction du matériel obtenu lors de la campagne Bicose en 2018, l'étude des capacités sensorielles des autres stades de développement pourra être étudiée, notamment les larves, qui dispersent dans la colonne d'eau et doivent détecter des signes l'activité hydrothermale afin de s'y installer. Cela se fera en collaboration avec F. Pradillon de l'Ifremer, qui travaille sur le cycle de reproduction de la crevette *R. exoculata*.

Références bibliographiques non trouvées dans la review ou ma liste de publications

Briones-Fourzan P, Lozano-Alvarez E (2008) Coexistence of congeneric spiny lobsters on coral reefs: differences in conspecific aggregation patterns and their potential antipredator benefits. Coral Reefs 27:275-287

Colaço A, Dehairs F, Desbruyères D (2002) Nutritional relations of deep-sea hydrothermal fields at the Mid-Atlantic Ridge: a stable isotope approach. Deep-Sea Res Part I 49:395-412

Fowler M, Montell C (2013) Drosophila TRP channels and animal behavior. Life Sciences 92:394-403

Julian D, Gaill F, Wood E, Arp A, Fisher C (1999) Roots as a site of hydrogen sulfide uptake in the hydrocarbon seep vestimentiferan *Lamellibrachia* sp. J Exp Biol 202:2245-2257

Lee Y, Lee Y, Lee J, Bang S, Hyun S, Kang J, Hong S, Bae E, Kaang B, Kim J (2005) Pyrexia is a new thermal transient receptor potential channel endowing tolerance to high temperatures in *Drosophila melanogaster*. Nat Genet 37(3):305-310

Neely G, Keene A, Duchek P, Chang E, Wang Q, Aksoy Y, Rosenzweig M, Costigan M, Woolf C, Garrity P, Penninger J (2011) *TrpA1* regulates thermal nociception in *Drosophila*. PLoS One 6(8):e24343

Ratchford S, Eggleston D (2000) Temporal shift in the presence of a chemical cue contributes to a diel shift in sociality. Anim Behav 59:793-799

Rittschof D, Tsai D, Massey P, Blanco L, Kueber GJ, Haas RJ (1992) Chemical mediation of behavior in hermit crab : alarm and aggregation cues. J Chem Ecol 18(7):959-984

Curriculum vitae

ZBINDEN Magali – Enseignant-Chercheur Université Pierre & Marie Curie

Née le 12 Janvier 1973 à FONTAINEBLEAU (77)

Laboratoire actuel
UMR 7208 BOREA (Direction S. Dufour)
Equipe Adaptations aux Milieux Extrêmes (Direction B. Shillito)
7, Quai St Bernard, Bât A, 75005 Paris

Tél : 01 44 27 37 93 / Fax : 01 44 27 52 50
E-mail : magali.zbinden@upmc.fr

1. Formation / Expérience professionnelle

Depuis 2014	**Maître de Conférence, section 68, Université Pierre et Marie Curie, Paris VI.** Laboratoire Biologie des Organismes et Ecosystèmes Aquatiques (BOREA), UMR 7208
2004 - 2013	**Maître de Conférence, section 68, Université Pierre et Marie Curie, Paris VI.** Laboratoire Systématique, Adaptation, Evolution (SAE), UMR 7138
2002-2004	**ATER** (section 68) Université Pierre et Marie Curie, Paris VI.
2002	**Post-doctorat** au Laboratoire de Biologie Générale et de Morphologie Ultrastructurale, Institut de Zoologie, Université de Liège, Belgique (Bourse FNRS, Convention n°2.4533.01).
2001	**Post-doctorat** au Laboratoire de Biologie Cellulaire et Moléculaire du Développement, UMR 7622 ; Université Pierre et Marie Curie (Contrat Européen Ventox EVK3-CT-1999-0003).
1998-2000	Technicienne (mi-temps) en microscopie au Laboratoire de Biologie Végétale Yves Rocher, Issy-les-Moulineaux.

1997-2001	**Doctorat de l'Université Aix-Marseille II**, Spécialité : Physiologie Soutenue le 28 Mars 2001, à Marseille. Mention Très Honorable Titre : " Données sur les interactions biogéochimiques en milieu hydrothermal : l'exemple d'*Alvinella pompejana* ".
1996-1997	**DEA "Adaptations et survie en environnements extrêmes".** Université Aix-Marseille II. Mention Bien.

2. Activités d'enseignement

2.1. Principaux enseignements depuis ma nomination

Licence
UE Des organismes aux molécules (L1), UE Diversité du Vivant (L1), UE Organisation Fonctionnelle des Animaux (L2), UE Biologie Comparée et Evolution des Animaux (L3), UE Interactions Durables, Ecologie, Evolution (L3).

Master
UE Physiologie Environnementale (M1), UE Biologie Intégrée des Organismes (M1), UE Ecophysiologie (M1), UE Biologie et Adaptations en Milieux Extrêmes (M2)

Autres
Formation continue : Initiation à la Biologie: de la molécule à l'organisme
CAPES : Préparation au CAPES (SVT), Sciences de la Vie, Sciences de la Terre et de l'Univers

2.2. Responsabilités administratives

Depuis 2009	Responsable des TP-TD de l'UE obligatoire de L2: Organisation Fonctionnelle des Animaux (LV201 devenu 2V312). UE obligatoire de 800 étudiants (29 groupes)
Depuis 2016	Co-responsable de l'UE optionnelle de L3 « Interactions Durables, Ecologie et Evolution ». (75 étudiants, 3 groupes)
Depuis 2012	Membre de la commission de spécialistes de la section 68, UPMC
2013 - 2017	Membre élu du Conseil d'Administration de l'UFR 927 de l'UPMC
	Membre nommé du Conseil d'Enseignement de l'UFR 927 de l'UPMC
2014 - 2015	Membre nommé de la Commission d'attribution de la Prime d'Investissement en Innovations Pédagogiques (PIIP)

3. Encadrements d'étudiants

3.1. Thèses

2015 – 2018 : Julia Machon : Thèse de Doctorat de l'Université Pierre et Marie Curie.
Titre : « « Adaptations sensorielles chez les crevettes hydrothermales profondes : Comparaison des facultés sensorielles de la crevette hydrothermale *Mirocaris fortunata* et de l'espèce côtière *Palaemon elegans* ». Co-encadrement avec Juliette Ravaux, UPMC.
2 publications en liaison avec l'encadrement

2014 – 2017 : Vincent Apremont : Thèse de Doctorat de l'Université de Bretagne Occidentale. Ecole Doctorale des Sciences de la Mer.
Titre : "Etude fonctionnelle d'ectosymbioses chimiosynthétiques chez des crustacés de milieux marins réducteurs et implication du tégument de l'hôte dans les transferts nutritionnels ". Thèse en co-financement UPMC / Ifremer. Co-encadrement avec Marie-Anne Cambon-Bonavita, Ifremer.
1 publication en préparation en liaison avec l'encadrement

2007 – 2010 : Marie Pailleret : Thèse De Doctorat de l'Université Pierre Et Marie Curie. Ecole Doctorale Diversité du Vivant
Titre : « Étude intégrée des interactions entre bois coulés et organismes associés dans le domaine marin profond ». Mention Très Honorable.
4 publications en liaison avec l'encadrement, dont 1 en dernier auteur.

3.2. Masters 2

2017: Alisson Galet : Stage de Master 2, mention SDUEE, spécialité OEM. Co-encadrement S. Duperron.

2015 : Julia Machon : Stage de Master 2, Mention SDUEE spécialité EPET. Co-encadrement J. Ravaux (cf thèse pour les publications)

2013 : **Gaëlle Honnaert** : Stage de Master 2, Master mention SDUEE spécialité OEM. Co-encadrement J. Ravaux

2012 : **Lise Marqué** : Stage de Master 2, Master mention SDUEE spécialité OEM.
2 publications en liaison avec l'encadrement, dont 1 en dernier auteur

2011 : **Christine Fauveau** : Stage de Master 2 (Développement, INteractions et Evolution du Vivant - DINEV), Perpignan. (Encadrement pour la partie microscopie).

2010 : **Marie-Anne Pottier** : Stage de Master 2, Mention BIP
1 publication en liaison avec l'encadrement, dont 1 en dernier auteur

2006 : **Marie Pailleret** : Stage de Master 2, Mention SDUEE Spécialité SEP. Co-encadrement : C. Privé-Gil, UMR 5143 (Laboratoire de Paléobotanique et Paléoécologie). (cf thèse pour les publications)

+ 8 encadrements de M1 depuis 2004 dont **2 avec publications en liaison avec l'encadrement**

4. Activités de recherche

4.1. Communications scientifiques / Listes des publications

Indice Google Scholar du 12/06/17

- **45 publications** parues dans des revues à comité de lecture pour l'ensemble de la carrière (2001-2016)
- Participation à 14 congrès et workshops nationaux et internationaux. Présentation de 18 posters et 10 communications orales.

Dans la liste ci-dessous, le nom de l'étudiant encadré est souligné.

45. **Zbinden M**, Berthod C, Montagné N, Machon J, Léger N, Chertemps T, Sarrazin J, Barthélémy D, Shillito B, Ravaux J (2017) Comparative study of chemosensory organs of shrimp from hydrothermal vent and coastal environments. Chemical senses. doi:10.1093/chemse/bjx007. IF: 2,5
44. Machon J, Ravaux J, **Zbinden M**, Lucas P (2016) New electroantennography method on a marine shrimp in water. Journal of Experimental Biology 219: 3696-3700. IF: 2,91
43. Ravaux J, Léger N, Rabet N, Fourgous C, Voland G, **Zbinden M**, Shillito B (2016) Plasticity and acquisition of the thermal tolerance (upper thermal limit and heat shock response) in the intertidal species *Palaemon elegans*. Journal of Experimental Marine Biology and Ecology 484: 39-45. IF: 1,79
42. Auguste M, Mestre N, Rocha T, Cardoso C, Cueff-Gauchard V, Le Bloa S, Cambon-Bonavita M-A, Shillito B, **Zbinden M**, Ravaux J, Bebianno M (2016) Development of an ecotoxicological protocol for the deep-sea fauna using the hydrothermal vent shrimp *Rimicaris exoculata*. Aquatic Biology 175 : 277-285. IF : 3,45
41. Durand L, Roumagnac M, Cueff-Gauchard V, Jan C, Guri M, Tessier C, Haond M, Crassous P, **Zbinden M**, Arnaud-Haond S, Cambon-Bonavita M-A (2015) Biogeographical distribution of *Rimicaris exoculata* resident gut epibiont communities along the Mid-Atlantic Ridge hydrothermal vent sites. *FEMS Microbiology Ecology* 91(10): fiv101. IF : 3,56
40. Matabos M, Cuvelier D, Brouard J, Shillito B, Ravaux J, **Zbinden M**, Barthélémy D, Sarrazin J (2015) Behavioural study of two hydrothermal crustacean decapods: *Mirocaris fortunata* and *Segonzacia mesatlantica*, from the Lucky Strike vent field (Mid Atlantic Ridge). *Deep-sea Research II* 121: 146-158. IF : 2,82
39. Shillito B, Ravaux J, Sarrazin J, **Zbinden M**, Barthélémy D, Sarradin P (2015) Long-term Maintenance and Public Exhibition of Deep-Sea Fauna : The AbyssBox Project. *Deep-sea Research II* 121: 139-145. IF : 2,82
38. Gaudron S, Marqué L, Thiébaut E, Riera P, Duperron S, **Zbinden M** (2015) Trophic ecology of eight gastropod species from East Pacific Rise hydrothermal vents. *Marine Ecology* 36 (Suppl 1) : 18-34. IF : 1,84
37. Aznar-Cormano L, Brisset J, Chan T, Corbari L, Puillandre N, Utge J, **Zbinden M**, Zuccon D, Samadi S (2015) Hierarchical taxonomic sampling is a necessary but not sufficient condition for resolving inter-families relationships in decapods. *Genetica* 143 : 195-205. IF : 1,74

36. **Zbinden M**, Marqué L, Gaudron S, Ravaux J, Duperron S (2015) Epsilonproteobacteria as gill epibionts of the gastropod *Cyathermia naticoides* from sites 9°N and 13°N on the East-Pacific Rise. *Marine Biology* 162: 435-448. IF : 2,39

35. Ravaux J, Hamel G, **Zbinden M**, Tasiemski A, Boutet I, Léger N, Tanguy A, Jollivet D, Shillito B (2013) Thermal limit for metazoan life in question: *in vivo* heat tolerance of the Pompeii worm. *PLOS One* 8(5): e64074. doi:10.1371/journal.pone.0064074. IF : 3,53

34. Holovachov O, Rodrigues C, **Zbinden M**, Duperron S (2013) *Trophomera conchicola* n. sp. (Nematoda: Benthimermithidae) from chemosymbiotic bivalves *Idas modiolaeformis* and *Lucinoma kazani* (Mollusca: Mytilidae and Lucinidae) in Eastern Mediterranean. *Russian Journal of Nematology* 21(1): 1-12

33. Ponsard J., Cambon-Bonavita M.-A., **Zbinden M**., Lepoint G., Joassin A., Corbari L., Shillito B., Durand L., Cueff-Gauchard V. and Compère P. (2013) Inorganic carbon fixation by chemosynthetic ectosymbionts and nutritional transfers to the hydrothermal vent host-shrimp, *Rimicaris exoculata. ISME Journal* 7 : 96-109. IF : 6,15

32. Duperron S., Pottier M.-A., Léger N., Gaudron S., Puillandre N., Le Prieur S., Sigwart J., Ravaux J. and **Zbinden M.** (2013) A tale of two chitons: is habitat specialisation linked to distinct associated bacterial communities? *FEMS Microbiology Ecology* 83: 552-567. IF : 3,408

31. Fagervold S., Galand P., **Zbinden M**., Gaill F., Lebaron P. and Palacios C. (2012) Sunken woods on the ocean floor provide diverse specialized habitats for microbes. *FEMS Microbiology Ecology* 82:616-628. IF : 3,039

30. Ravaux J., Léger N., Rabet N., Morini M., **Zbinden M**., Thatje S. and Shillito B. (2012) Adaptation to thermally variable environments: capacity for acclimation of thermal limit and heat shock response in the shrimp *Palaemonetes varians*. *Journal of Comparative Physiology - B* 182: 899–907. IF : 1,966

29. Guri M., Durand L., Cueff-Gauchard V., **Zbinden M.**, Crassous P., Shillito B. and Cambon-Bonavita M.-A. (2012) Acquisition of epibiotic bacteria along the life cycle of the hydrothermal shrimp *Rimicaris exoculata. ISME Journal* 6: 597-609. IF : 6,15

28. Hoyoux C., **Zbinden M**., Samadi S., Gaill F. and Compère P. (2012) Diet and gut microorganisms of *Munidopsis* squat lobsters associated with natural woods and mesh-enclosed substrates in the deep south Pacific. *Marine Biological Research* 8 (1): 28-47. IF : 1,48

27. **Zbinden M**., Pailleret M., Ravaux J., Gaudron S., Hoyoux C., Lorion J., Halary S., Warén A. and Duperron S. (2010) Bacterial communities associated with the wood-feeding gastropod *Pectinodonta* sp. (Patellogastropoda, Mollusca). *FEMS Microbiology Ecology* 74: 450-463. IF : 3,039

26. Durand L., **Zbinden M**., Duperron S., Roussel E., Cueff-Gauchard V., Shillito B. and Cambon-Bonavita M.-A. (2010) Microbial diversity associated with the hydrothermal vent shrimp *Rimicaris exoculata* gut and occurrence of a resident microbial community. *FEMS Microbiology Ecology* 71: 291-303. IF : 3,039

25. Petersen J., Ramette A., Lott C., Cambon-Bonavita M.-A., **Zbinden M**. and Dubilier N. (2010) Dual symbiosis of the vent shrimp *Rimicaris exoculata* with filamentous gamma- and epsilonproteobacteria at four Mid-Atlantic Ridge hydrothermal vent fields. *Environmental Microbiology* 12(8): 2204-2218. IF : 4,7

24. Dupont J., Magnin S., Rousseau F., **Zbinden M**., Frébourg G., Richer de Forges B. and Samadi S. (2009) Molecular and ultrastructural characterization of two Ascomycetes found on sunken wood off Vanuatu Islands in the deep Pacific Ocean. *Mycological Research* 113: 1351-1364. IF : 1,861

23. Palacios C., **Zbinden M**., Pailleret M., Gaill F. and Lebaron P. (2009) High similarity in the microbial community structure of sunken woods at shallow marine waters and deep-sea sites across the oceans. *Microbial Ecology* 58: 737-752. IF : 2.56

22. Hoyoux C., **Zbinden M**., Samadi S., Gaill F. and Compère P. (2009) Wood-based diet and gut microflora of a galatheid crab associated with Pacific deep-sea wood falls. . *Marine Biology* 156: 2421-2439.IF : 2.215

21. Becker P., Samadi S., **Zbinden M**., Hoyoux C., Compère P. and De Ridder C. (2009) First insights into the gut microflora associated with an echinoid from wood falls environments. *Cahiers de*

Biologie Marine 50: 343-352.

20. Duperron S., De Beer D., **Zbinden M**., Boetius A., Schipani V., Kahil N. and Gaill F. (2009) Molecular characterization of bacteria associated with the trophosome and the tube of *Lamellibrachia* sp., a siboglinid annelid from col seeps in the eastern Mediterranean. *FEMS Microbiology Ecology* 69: 395-409. IF: 3,039

19. Pradillon F., **Zbinden M**., Le Bris N., Hourdez S., Barnay A.S. and Gaill F. (2009). Development of assemblages associated with alvinellid colonies on the walls of high-temperature vents at the East Pacific Rise. *Deep-sea Research part II*, 56, pp. 1622-1631. IF : 1,17

18. **Zbinden M**., Shillito B., Le Bris N., De Vilardi de Montlaur C., Roussel E., Guyot F., Gaill F. and Cambon-Bonavita M.-A. (2008). New insights on the metabolic diversity among the epibiotic microbial community of the hydrothermal shrimp *Rimicaris exoculata*. *Journal of Experimental Marine Biology and Ecology*, 159 (2), pp.131-140. IF : 1,75

17. Anderson L., Lechaire J.P., Boudier T., Halary S., Frébourg G., **Zbinden M**., Marco S. et Gaill F. (2008). Tomography of bacteria-mineral associations within the deep sea hydrothermal vent shrimp *Rimicaris exoculata*. *Comptes-Rendus de Chimie*, 11(3), pp. 268-280. IF : 1,305

16. Corbari L., Cambon-Bonavita M.A., Long Garry J., Grandjean F., **Zbinden M**., Gaill F., Compère P. (2008) Iron oxide deposits associated with the ectosymbiotic bacteria in the hydrothermal vent shrimp *Rimicaris exoculata*. *Biogeosciences* 5:1295-1310. IF: 2.813

15. Corbari L., **Zbinden M.**, Cambon-Bonavita M-A., Gaill F., Compère P. (2008) Bacterial symbionts and mineral deposits in the branchial chamber of the hydrothermal vent shrimp *Rimicaris exoculata*: relationship to moult cycle. *Aquatic Biology* 1:225-238. IF : 1,26

14. Pailleret M., Saedlou N., Palacios C., **Zbinden M**., Lebaron P., Gaill F., Privé-Gill C. (2007). Identification of natural sunken wood samples. *Comptes-Rendus Palevol*., 6, pp. 463-468. IF: 0.88

13. Pailleret M, Petit P, Privé-Gill C, Saedlou N, Gaill F, **Zbinden M** (2007) Sunken woods from the Vanuatu Islands: identification of wood substrates and preliminary description of associated fauna. *Marine Ecology*, 28, pp. 233-241. IF: 1,14

12. Palacios C., **Zbinden M**., Baco A., Treude T., Smith C., Gaill F., Lebaron P., Boetius A. (2006) Microbial ecology of deep-sea sunken wood: quantitative measurements of bacterial biomass and cellulolytic activities. *Cahiers de Biologie Marine*, 47, pp. 415-420. IF : 0,47

11. Pradillon, F., **Zbinden, M**., Mullineaux, L., Gaill, F., (2005). Colonisation of newly-opened habitat by a pioneer species, *Alvinella pompejana* (Polychaeta: Alvinellidae), at East Pacific Rise vent sites. *Marine Ecology Progress Series* 302, 147-157. IF: 2,54

10. Le Bris N., **Zbinden M**. et Gaill F. (2005) Processes controlling physico-chemical gradients associated to Alvinella pompejana at the interface of hydrothermal smokers. *Deep-sea Research I*, 52, pp. 1071-1083. IF : 1,795

9. **Zbinden M.**, Le Bris N., Gaill F. et Compère P. (2004) Distribution of bacteria and associated minerals in the gill chamber of the vent shrimp *Rimicaris exoculata* and related biogeochemical processes. *Marine Ecology Progress Series*, 284, 237-251. IF : 2,54

8. Gloter A., **Zbinden M**., Guyot F., Gaill F. et Colliex C. (2004) TEM-EELS study of natural ferrihydrite from geological–biological interactions in hydrothermal systems. *Earth and Planetary Science Letters*, 222, pp. 947-957. IF: 3,87

7. Alain K., **Zbinden M**., Le Bris N., Lesongeur F., Querellou J., Gaill F. et Cambon-Bonavita M.-A. (2004) Early steps of colonisation processes at deep-sea hydrothermal vents. *Environmental Microbiology*, 6, pp.227-241. IF: 4,929

6. **Zbinden M**. et Cambon-Bonavita M.-A. (2003) Occurence of *Deferribacterales* and *Entomoplasmatales* in the deep-sea shrimp *Rimicaris exoculata* gut. *FEMS Microbiology Ecology*, 46, pp. 23-30. IF : 3,039.

5. **Zbinden M**., Le Bris N., Compère P., Martinez I., Guyot F. et Gaill F. (2003) Mineralogical gradients induced by Alvinellids at hydrothermal vents (9°N, EPR). *Deep-sea Research I*, 50, pp. 269-280. IF: 1,795

4. Alain K., Rolland S., Crassous P., Lesongeur F., **Zbinden M**., Le Gall C., Godfroy A., Pagé A., Juniper K., Cambon-Bonavita M.-A., Duchiron F. et Querellou J. (2003) *Desulfurobacterium crinifex* sp. nov., a novel thermophilic, pinkish-streamers forming, chemolithoautotrophic

bacterium isolated from a Juan de Fuca ridge hydrothermal vent. Emendation of the genus *Desulfurobacterium*. *Extremophiles*, 7, pp.361-370. IF: 2,317

3. Ravaux J.* et **Zbinden M.***, Voss-Foucart M., Compère P., Goffinet G. et Gaill F. (2003) Comparative degradation rates of chitinous exoskeletons from deep-sea environments. *Marine Biology*, 143, pp. 405-412. * Ces deux auteurs ont contribué également à ce travail. IF : 2,215

2. Alain K, Pignet P, **Zbinden M**, Quillevere M, Duchiron F, Donval JP, Lesongeur F, Raguenes G, Crassous P, Querellou J, Cambon-Bonavita M-A (2002) *Caminicella sporogenes* gen. nov., sp. nov., a novel thermophilic spore-forming bacterium isolated from an East-Pacific Rise hydrothermal vent. *Int J Syst Evol Microbiol* 52: 1621-1628. IF: 2,384

1. **Zbinden M**., Martinez I., Guyot F., Cambon-Bonavita M.A. et Gaill F. (2001). Zinc-iron sulphide mineralization in tubes of hydrothermal vent worms. *European Journal of Mineralogy*, 13, pp.653-658. IF: 1,206

4.2. Implications dans des programmes nationaux / internationaux

Participation à des programmes nationaux

- Membre du GDR **Ecchis** (2004-2012) – Coordination François Lallier, UPMC
- Membre du Réseau Ecologie des Interactions Durables (**REID**)
- **ATM** (Action Transversale du Muséum National d'Histoire Naturelle) pour un projet "Recherche symbiose bactérienne chez crustacés décapodes hydrothermaux"

Participation à des programmes internationaux

- Partenaire du projet européen **CAREX** (Coordination Action for Research Activities on life in Extreme Environments (2008-2010) – Seventh Framework Program (FP7) – Coordinateur N. Walter
- Participant du projet européen **HERMIONE** Hotspot Ecosystem Research and Man's Impact On European Seas (2009-2012) – Coordinateur du projet : Prof. Philip P.E. Weaver (National Oceanography Centre, Southampton, UK)
- Participant de l'ANR Blanc International **TFDeepEvo** (Taiwan France : Exploration de la biodiversité et évolution de la faune marine profonde) (2012-2015) – Coordinateur du projet : S. Samadi, MNHN, France
- Partenaire du projet européen **MIDAS** (Managing Impacts of Deep-seA reSource exploitation) (2014-2016) – Coordinateur du projet : Coordinateur du projet : Prof. Philip P.E. Weaver (National Oceanography Centre, Southampton, UK)

4.3. Participation à des missions océanographiques

- Participation à **16 campagnes hauturières nationales et internationales.** Participation à **5 plongées** (2 Nautile (France), 2 Alvin (EU), 1 Shinkai (Japon))
- **Co-chef de projet sur la campagne Bicose en 2014**

2014 **BICOSE**, mission océanographique française, Dorsale médio-Atlantique (23-26°N). Navire: Pourquoi Pas ?, submersible: ROV Victor 6000. Chef de mission : MA Cambon-Bonavita.

2013 **BIOBAZ Centrale**, mission océanographique française, Dorsale médio-Atlantique (36-38°N). Navire: Pourquoi Pas ?, submersible: ROV Victor 6000. Chef de mission : F. Lallier.

2012 **MESCAL 2**, mission océanographique française, Dorsale est-Pacifique (13°N). Navire: Atalante, submersible : Nautile. Chef de mission: N. Le Bris.

2011 **MOMASAT**, mission océanographique française, Dorsale médio-Atlantique (36-37°N). Navire: Pourquoi Pas ?, submersible: ROV Victor 6000. Chefs de mission : M Cannat et PM Sarradin.

2010 **MESCAL**, mission océanographique française, Dorsale est-Pacifique (13°N). Navire: Atalante, submersible : Nautile (participation à 1 plongée). Chef de mission: F. Lallier
2009 **NT09-10**, mission océanographique japonaise, Nansei Shoto Trench. Navire : Natsushima, submersible : ROV Hyper Dolphin. Chef de mission : Y. Fujiwara
2008 **MOMAR08**, mission océanographique française, Dorsale médio-Atlantique (36-37°N). Navire: Atalante, submersible: ROV Victor 6000. Chefs de mission : F. Gaill et J. Dyment.
2007 **MOMARDREAM**, mission océanographique française, Dorsale médio-Atlantique (36-37°N). Navire: Pourquoi Pas?, submersible: Nautile (participation à 1 plongée). Chefs de mission: F. Gaill et J. Dyment.
2006 **SANTOBOA**, mission océanographique française, Vanuatu. Navire: Alis. Chef de mission : Sarah Samadi, IRD.
2005 **EXOMAR**, mission océanographique française, Dorsale médio-Atlantique (36-37°N). Navire: Atalante, submersible: ROV Victor 6000. Chef de mission : A. Godfroy, Ifremer.
2004 **BOA 0**, mission océanographique française, Vanuatu. Navire: Alis. Chef de mission : F. Gaill.
2002 **PHARE**, mission océanographique française, Dorsale est-Pacifique (13°N). Navire: Atalante, submersible : ROV Victor 6000. Chef de mission: N. Le Bris.
2001 **ATOS**, mission océanographique française, Dorsale médio-Atlantique (36-37°N). Navire: Atalante, submersible : ROV Victor 6000. Chef de mission : PM Sarradin.
1999 **EPR 99**, mission océanographique américaine, Dorsale est-Pacifique (9°N). Navire: Atlantis II, submersible Alvin (participation à 1 plongée). Chef de mission : C. Fisher.
1998 **BIOACCESS 98**, mission océanographique japonaise, Bassin de Manus. Navire : Natsushima, submersible Shinkai 2000 (participation à 1 plongée). Chef de mission : J. Hashimoto.
1995 **LARVA 95**, mission océanographique américaine Dorsale Est Pacifique (site 9°N). Navire : Atlantis II, submersible Alvin (participation à 1 plongée). Chef de mission : L. Mullineaux.

4.4. Responsabilité de recherche

- **Reviewer pour les revues** : FEMS Microbiology Ecology, PLOS One, Marine Ecology, Deep-sea Research, Central European Journal of Biology, Cahiers de Biologie Marine, Journal of Basic Microbiology.

- **Participation à des jurys de thèse / comité de thèse**:
  - Pierre Méthou : Thèse de Doctorat de l'Université de Bretagne occidentale. Mention Océanologie Biologique. Ecole Doctorale des Sciences de la Mer. "Cycle de vie de la crevette *Rimicaris exoculata*". Membre du comité de thèse. Thèse en cours.
  - Ivan Hernandez-Avila: Thèse de Doctorat de l'Université de Bretagne occidentale. Mention Océanologie Biologique. Ecole Doctorale des Sciences de la Mer : "Larval dispersal and life cycle in deep-water hydrothermal vents : the case of Rimicaris exoculata and related species". Membre du comité de thèse et Examinateur. Thèse soutenue le 28 Novembre 2016.
  - Hsin Lee : Thèse de Doctorat en cotutelle entre le MNHN et l'Université Nationale de Taiwan. «Clarifier la systématique des Cocculinidae et comprendre le rôle de la spécialisation à l'habitat dans la diversification de ces gastéropodes du milieu profond». Membre du comité de thèse. Thèse en cours
  - Julie Ponsard : Thèse de Doctorat de l'Université de Liège. « Etude fonctionnelle d'ectosymbioses chimiosynthétiques chez des crustacés de milieux marins réducteurs et implication du tégument de l'hôte dans les transferts nutritionnels ». Membre du comité de thèse. Thèse non soutenue.
  - Mathieu Guri : Thèse de Doctorat de l'Université de Bretagne occidentale/Université Européenne de Bretagne. « Etude de la diversité des épibiontes bactériens associés au céphalothorax de la crevette hydrothermale *Rimicaris exoculata*». Examinateur. Thèse soutenue le 19 Décembre 2011, Brest.

- Caroline Hoyoux : Thèse de Doctorat de l'Université de Liège. « Crustacés décapodes des bois coulés en océan profond : régimes alimentaires et symbioses microbiennes». Membre du comité de thèse. Thèse soutenue le 4 Octobre 2010, Liège.
- Marie Pailleret : Thèse de Doctorat de l'Université Pierre et Marie Curie. « Étude intégrée des interactions entre bois coulés et organismes associés dans le domaine marin profond ». Directrice de thèse. Thèse soutenue le 10 Mars 2010, UPMC.
- Lucile Durand : Thèse de Doctorat de l'Université de Brest/Université Européenne de Bretagne. « Etude de la diversité des peuplements épibiontes associés au tractus digestif de la crevette hydrothermale *Rimicaris exoculata* : une possible association mutualiste ». Examinateur. Thèse soutenue le 26 Février 2010, Brest.

- **Expert** externe pour la Commission Nationale Flotte Hauturière

5. Actions de médiation scientifique

2016
- Conseiller scientifique pour l'exposition temporaire du Muséum National d'Histoire Naturelle "Mondes Marins" prévue pour Octobre 2018.

2015
- Référent scientifique pour l'exposition temporaire "Cyclops, explorateur de l'océan" à Océanopolis, Parc de découverte des océans, à Brest (2015-2017).

2014
- Participation au festival Pariscience (festival international du film scientifique). Débat avec le public suite à la projection du film de JY Collet "Abysses, alliances des profondeur". Octobre 2014, Paris.
  http://www.pariscience.fr/fr/showing/484/abysses-les-alliances-des-profondeurs/?festival_id=13&date=2014-10-06

- Participation à la **communication autour de la campagne océanographique Bicose** 2014
  - Conférence Science à Cœur à l'UPMC (15 Mai 2014)
  http://www.upmc.fr/fr/culture/sciences_a_coeur_saison_6/grand_quizz_sciences_a_coeur.html
  - Podcast sur Indéscience, blog d'informations scientifiques par des étudiants en science: https://soundcloud.com/indesciences-podcast/01-plong-e-au-coeur-des

- Participation à la soirée "**La nuit des abysses**": Plongée en direct du submersible Victor 6000 à 3500m de fond et échanges en triplex entre les scientifiques sur le navire océanographique Pourquoi Pas? et l'UPMC à Paris et l'Ifremer de Brest: http://www.upmc.fr/fr/culture/nuit_des_abysses.html, http://video.upmc.fr/differe.php?collec=CS_nuit_abysses

2013
- Participation à la **communication autour de la campagne océanographique Biobaz** 2013
  - Articles sur la page Recherche / En direct des laboratoires de l'UPMC: http://www.upmc.fr/fr/recherche/actualites_de_la_recherche/en_direct_des_laboratoires/actualite_pole_vie_sante/magali_zbinden_biobaz.html

- Page facebook de la campagne: https://www.facebook.com/pages/Campagne-Biobaz-2-21-ao%C3%BBt-2013/552751104786791

- Conseillère scientifique et participation sur le **film « Abysses, les alliances des profondeurs »**. Réalisation JY Collet / Com On Planet. Diffuseurs : France 5 (Août 2014) et Ushuaïa TV. http://jeanyvescollet.com/productions-en-cours/144-la-symbiose-des-abysses

- Participation à la réalisation du portfolio du magazine DOC Sciences (N°16-nov 2013, série "Biodiversité" n°2). Portfolio "Oasis de vie dans les abysses, p. 62). http://www.docsciences.fr/Oasis-de-vie-dans-les-abysses

2012

- Participation à la conception et la création de **l'Exposition permanente** à Océanopolis, Parc de découverte des océans, à Brest : **« Voyage abyssal, un regard sur l'extrême. AbyssBox, la vie sous pression »**. Ouverture Avril 2012.

- Participation au **film « AbyssBox, la vie sous pression »**. Réalisation JY Collet / Com On Planet. http://jeanyvescollet.com/les-films-extraits-dossiers/143-abyssbox-la-vie-sous-pression

Autres

- Rencontres avec les élèves dans le cadre des appels à projet "Jeunes Reporters des Arts et des Sciences", organisés par Océanopolis, Parc de découverte des océans, à Brest, en 2012, 2013, 2014, 2016.
  http://www.oceanopolis.com/Enseignants/Arts-et-Sciences-2012-2013/Rencontres-avec-les-chercheurs

- Collaboration (avec Lionel Guérin, professeur de SVT) sur un projet annuel d'étude autour des sources hydrothermales avec une classe du lycée EABJM (École Active Bilingue Jeannine Manuel). 2015, 2016.

- Participation au **film « Phare 2002, la campagne océanographique »**. Réalisation JF Ternay / CRNS Images média. http://videotheque.cnrs.fr/index.php?urlaction=doc&id_doc=1053

6. Selection de publications

1. Zbinden M., Le Bris N., Gaill F. et Compère P. (2004) Distribution of bacteria and associated minerals in the gill chamber of the vent shrimp *Rimicaris exoculata* and related biogeochemical processes. *Marine Ecology Progress Series*, 284, 237-251. IF : 2,54
2. Zbinden M., Shillito B., Le Bris N., De Vilardi de Montlaur C., Roussel E., Guyot F., Gaill F. and Cambon-Bonavita M.-A. (2008). New insights on the metabolic diversity among the epibiotic microbial community of the hydrothermal shrimp *Rimicaris exoculata*. *Journal of Experimental Marine Biology and Ecology*, 159 (2), pp.131-140. IF : 1,75
3. Ponsard J., Cambon-Bonavita M.-A., Zbinden M., Lepoint G., Joassin A., Corbari L., Shillito B., Durand L., Cueff-Gauchard V. and Compère P. (2013) Inorganic carbon fixation by chemosynthetic ectosymbionts and nutritional transfers to the hydrothermal vent host-shrimp, *Rimicaris exoculata. ISME Journal* 7 : 96-109. IF : 6,15
4. Zbinden M, Berthod C, Montagné N, Machon J, Léger N, Chertemps T, Sarrazin J, Barthélémy D, Shillito B, Ravaux J (2017) Comparative study of chemosensory organs of shrimp from hydrothermal vent and coastal environments. Chemical senses. doi:10.1093/chemse/bjx007. IF: 2,5
5. Zbinden M., Pailleret M., Ravaux J., Gaudron S., Hoyoux C., Lorion J., Halary S., Warén A. and Duperron S. (2010) Bacterial communities associated with the wood-feeding gastropod *Pectinodonta* sp. (Patellogastropoda, Mollusca). *FEMS Microbiology Ecology* 74: 450-463. IF : 3,039
6. Zbinden M, Marqué L, Gaudron S, Ravaux J, Duperron S (2015) Epsilonproteobacteria as gill epibionts of the gastropod *Cyathermia naticoides* from sites 9°N and 13°N on the East-Pacific Rise. *Marine Biology* 162: 435-448. IF : 2,39

Vol. 284: 237–251, 2004 | MARINE ECOLOGY PROGRESS SERIES
Mar Ecol Prog Ser | Published December 21

Distribution of bacteria and associated minerals in the gill chamber of the vent shrimp *Rimicaris exoculata* and related biogeochemical processes

Magali Zbinden[1,2,*], Nadine Le Bris[3], Françoise Gaill[1], Philippe Compère[2]

[1]Systématique, Adaptation et Evolution, CNRS IRD MNHN UPMC, 7 Quai Saint Bernard, 75252 Paris cedex 05, France
[2]Département des Sciences de la Vie, Institut de Zoologie, Université de Liège, 22 Quai Van Beneden, 4020 Liège, Belgium
[3]Département Environnement Profond, IFREMER DRO, BP 70, 29280 Plouzané, France

ABSTRACT: The shrimp *Rimicaris exoculata* dominates the megafauna of some Mid-Atlantic Ridge hydrothermal vent fields. This species harbours a rich bacterial epibiosis inside its gill chamber. At the 'Rainbow' vent site (36° 14.0' N), the epibionts are associated with iron oxide deposits. Investigation of both bacteria and minerals by scanning electron microscopy (SEM) and X-ray microanalysis (EDX) revealed 3 distinct compartments in the gill chamber: (1) the lower pre-branchial chamber, housing bacteria but devoid of minerals; (2) the 'true' branchial chamber, containing the gills and devoid of both bacteria and minerals; and (3) the upper pre-branchial chamber, housing the main ectosymbiotic bacterial community and associated mineral deposits. Our chemical and temperature data indicated that abiotic iron oxidation appears to be kinetically inhibited in the environment of the shrimps, which would explain the lack of iron oxide deposits in the first 2 compartments. We propose that iron oxidation is microbially promoted in the third area. The discrepancy between the spatial distribution of bacteria and minerals suggests that different bacterial metabolisms are involved in the first and third compartments. A possible explanation lies in the modification of physico-chemical conditions downstream of the gills that would reduce the oxygen content and favours the development of bacterial iron-oxidizers in this Fe^{II}-rich environment. A potential role of such iron-oxidizing symbionts in the shrimp diet is suggested. This would be unusual for hydrothermal ecosystems, in which most previously described symbioses rely on sulphide or methane as an energy source.

KEY WORDS: Crustacea · Deep-sea · Moulting cycle · Biomineralisation · Symbiosis · Iron oxidation

INTRODUCTION

Caridean shrimps belonging to the Alvinocarididae family dominate the megafauna of many of the MAR (Mid-Atlantic Ridge) vent sites. *Rimicaris exoculata* (Williams & Rona 1986) is particularly abundant, forming dense, motile swarms around the chimney walls (Segonzac 1992, Gebruk et al. 1993). *R. exoculata* carries a rich bacterial epibiosis that develops on different parts of the gill chamber (i.e. the inner side of the branchiostegites and the hypertrophied mouthparts) (Van Dover et al. 1988, Casanova et al. 1993, Gebruk et al. 1993, Segonzac et al. 1993). Molecular analyses of such bacteria, from Snake Pit (MAR) samples, suggested that the epibiont community consists of 1 single bacterial phylotype, belonging to the ε-Proteobacteria (Polz & Cavanaugh 1995). They were hypothesised to acquire their metabolic energy from sulphide oxidation, but cultivation was unable to confirm this (Gebruk et al. 1993, Wirsen et al. 1993). Most of the studies on these epibionts have concerned their possible role in the shrimp diet. It was proposed that *R. exoculata* grazed either on bacteria living on the surface of the chimney (Van Dover et al. 1988), or on its epibiotic bacteria, regarded as ectosymbionts (Gebruk et al. 1993, 2000, Segonzac et al. 1993, Rieley et al. 1999) It has also been suggested that an autotrophic bacterial population living in the shrimp's gut might serve as a

*Email: magali.zbinden@snv.jussieu.fr

nutritional source (Pond et al. 1997, Polz et al. 1998, Zbinden & Cambon-Bonavita 2003).

Previous studies have provided morphological descriptions of *Rimicaris exoculata* and its alvinocaridid-ae relatives, and described the morphology of the epibionts (Casanova et al. 1993, Segonzac et al. 1993), but have neither focused on their spatial distribution, nor considered the development of the bacterial community in relation to the shrimp moulting stages. As with other arthropods, shrimps undergo cyclic moults, where the cuticle is regularly renewed. At ecdysis, when the entire old cuticle of the shrimp is shed, all the bacteria are shed with it, and a new cuticle covers the newly moulted shrimp. The abundance and distribution of the bacterial coverage seems to be related to the moulting cycle of the shrimp and to depend on the period of time elapsed since the last moult. Although nothing is known about the moulting cycle of *R. exoculata* and the duration of its moulting stages, in Crustacea the anecdysial period (taken as reference) is generally regarded as the longest stage of the moulting cycle, corresponding to a period of tegumental stability (for reviews see Vernet & Charmantier-Daures 1994 and Compère et al. 2004).

Another important point that has not received special attention is the presence of mineral deposits within the gill chamber. Whereas at the TAG (trans-Atlantic geotraverse) site, the carapace area of some shrimps was described as dark, or even black, from the presence of sulphide particles associated with the bacteria by Gebruk et al. (1993), other authors (Wirsen et al. 1993) described filamentous bacteria on the inner cephalothorax surface associated either with rusty brown or black material. At the 'Rainbow' site, fairly abundant, rusty, mineral deposits surround the bacteria of the gill chamber of the shrimp. These rusty, bacteria-associated deposits were reported only recently in a paper that focused on their mineralogy (Gloter et al. 2004) and emphasised the very homogeneous and specific mineralogical composition of these iron oxide deposits, suggesting a direct role of bacteria in mineral formation.

Numerous authors have reported the occurrence of iron oxide deposits of putative microbial origin at deep-sea hydrothermal vents (e.g. Wirsen et al. 1993, Juniper et al. 1995, Fortin et al. 1998). More recent studies have highlighted the direct role of bacteria in the deposition of iron and suggested a major contribution of chemoautotrophic iron-oxidisers in this process (Emerson & Moyer 2002, Kennedy et al. 2003). To date, however, the occurrence of such iron-oxidisers in association with animals has never been described. Our first aim was to undertake a detailed map of the distribution of both epibiotic bacterial and associated minerals within the whole gill chamber of *Rimicaris exoculata* including the mouthparts (i.e. the hypertrophied exopodites of the second maxilla, called scaphognathites, and the exopodites of the first maxillipeds) of shrimps in anecdysis. Our observations revealed 3 distinct areas on the gill chamber walls, which differed from each other not only in the abundance of bacteria and mineral deposits, but also in the nature of the minerals. Taking into consideration the water pathway through the gill chamber and the geochemical characteristics of the shrimp environment revealed by our *in situ* analysis and sampling data, this suggests the existence of three functionally different compartments. On this basis, we present further insights into the questions of the origin of these minerals, the spatial and functional relations between bacteria and minerals, and the biological role of the epibiosis.

MATERIALS AND METHODS

Shrimp collection and selection. Specimens of *Rimicaris exoculata* were collected during the French 'ATOS' cruise (June 2001), at the Rainbow vent site (36° 14.0' N, Mid-Atlantic Ridge, 2300 m depth). Shrimps were collected with the suction sampler of the ROV 'Victor 6000' operating from the RV 'Atalante'. Immediately after retrieval, living specimens were dissected into body components (branchiostegites, scaphognathites, exopodites, gills, stomach and digestive tract). The samples were fixed either in a 2.5% glutaraldehyde/sodium cacodylate-buffered solution and later post-fixed in osmium tetroxide for morphological observations, or in a 2.5% glutaraldehyde/seawater solution, without post-fixation, for X-ray microanalysis.

Shrimps in anecdysis were selected for observation according to the moult-staging method of Drach & Tchernigovtzeff (1967), by examination of bristle-bearing appendages (uropods) under the light microscope. The moulting stage was later confirmed by examination of the branchiostegite integument by light microscopy (LM) and transmission electron microscopy (TEM).

LM and TEM. Samples fixed for morphological observation were dehydrated in an ethanol and propylene oxide series and then embedded in an epoxy resin (Serlabo). Semi-thin and ultra-thin sections were obtained from a Reichert-Jung Ultramicrotome (Ultracut E) using a diamond knife. Semi-thin sections were stained with toluidine blue for observations by light microscopy (using a Nikon Optiphot-pol microscope and a Zeiss Opton photomicroscope). Ultra-thin sections were contrasted with uranium acetate and lead citrate, and observed on a Jeol (JEM 100-SX) transmission electron microscope operating at 80 kV.

SEM and X-ray microanalysis. Before preparation, samples were observed with a stereomicroscope and photographed. Large samples were carefully dissected into small pieces that were dehydrated through an ethanol series, critical-point-dried and platinum-coated in a Balzers SCD-030 sputter-unit prior to observation in a scanning electron microscope (JEOL JSM-840A), operating at 20 kV.

Elemental energy-dispersive X-ray microanalyses (EDX) were performed either on the platinum-coated bulk samples prepared for SEM observation as previously described, or on carbon-coated semi-thin sections, cut at 1 to 2 µm and mounted on carbon stubs. X-ray microanalyses and elemental mappings were performed in the SEM fitted with a Link Pentafet detector and a Link eXl-10 analyser.

Chemical analysis. Sulphide and ferrous iron were analysed *in situ* in the surroundings of shrimp swarms, using a submersible flow analyser mounted on the ROV 'Victor' (Le Bris et al. 2000). The analyser drew the sample from a deported inlet up to the colorimetric detection unit, located on the submersible. Analyses were performed within 5 min after sample collection at the ambient seawater temperature of 5°C, thus preventing any oxidation of sulphide or ferrous iron with oxygen in the sample prior analysis. Probes for pH and temperature (MICREL, France) were combined with the analyser inlet (Le Bris et al. 2001). The sensors were positioned by the ROV manipulator to within a few centimetres of the shrimps, as confirmed by close-up video pictures. Only a coarse estimation of the pH (± 0.5) could be obtained from *in situ* measurements, because of unusual baseline instabilities.

To complement the *in situ* analyses, water samples were collected in the vicinity of shrimps using the sequential fluid sampling system of the ROV and analysed on board ship for pH, H_2S, O_2 and later onshore for total iron. A colorimetric flow-injection analysis method, adapted from Coale et al. (1991), was used for the determination of the total iron content in acidified subsamples. For the other parameters, standard laboratory analytical methods were used as described in Sarradin et al. (1998).

RESULTS

Macroscopic observations of *Rimicaris exoculata*

Macroscopic observations of *Rimicaris exoculata* revealed obvious morphological differences between individuals in anecdysis. The colour of the pre-branchial pouch of the gill chamber varied from beige to dark orange-brown and was visible through the translucent branchiostegite carapace. Stereomicroscopic observations showed that the coloration was related to the extent of the mineral deposits that covered the inner side of the branchiostegites, as well as the scaphognathite and exopodite surfaces that bear long bacteriophore setae. In beige individuals, the mineral deposits were scarce or absent. In dark orange-brown individuals, heavy mineral deposits appeared, located on all the cuticular surfaces in the upper pre-branchial chamber (above the exopodites), including both sides of the scaphognathites and the upper side of the exopodites. The mineral seemed to be much less abundant in the lower part of the pre-branchial chamber and was almost completely absent from the gills and the walls of the 'true' posterior branchial chamber surrounding the gills. Observations of the inner side of the branchiostegites showed 3 well-delimited areas forming 3 distinct compartments (Figs. 1 & 2a): (1) an antero-ventral area, which was relatively clear; (2) a posterior area, which always remained light beige; (3) an antero-dorsal area, which was intensely coloured.

SEM and X-ray microanalysis

Morphology of bacteria

Bacterial colonisation occurred on the shrimp mouth-parts and the inner side of the branchiostegites in the form of a more or less thick mat of filaments (Figs. 3a–c & 4a,b), whose density varied between areas

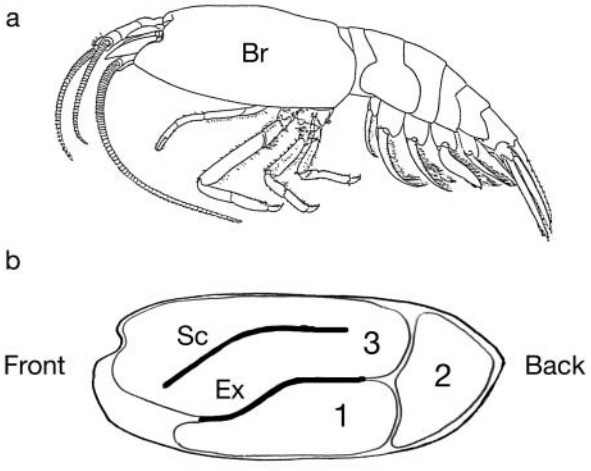

Fig. 1. *Rimicaris exoculata*. (a) Lateral view (from Williams & Rona 1986); Br: branchiostegite. (b) Line-drawing of inner side of branchiostegite (right side), showing location of scaphognathite (Sc), exopodite of 1st maxilliped (Ex) and delimiting 3 areas corresponding to 3 different compartments of the chamber: 1, antero-ventral area corresponding to lower pre-branchial chamber; 2, posterior area facing gills and corresponding to 'true' branchial chamber; 3, antero-dorsal area corresponding to upper pre-branchial chamber

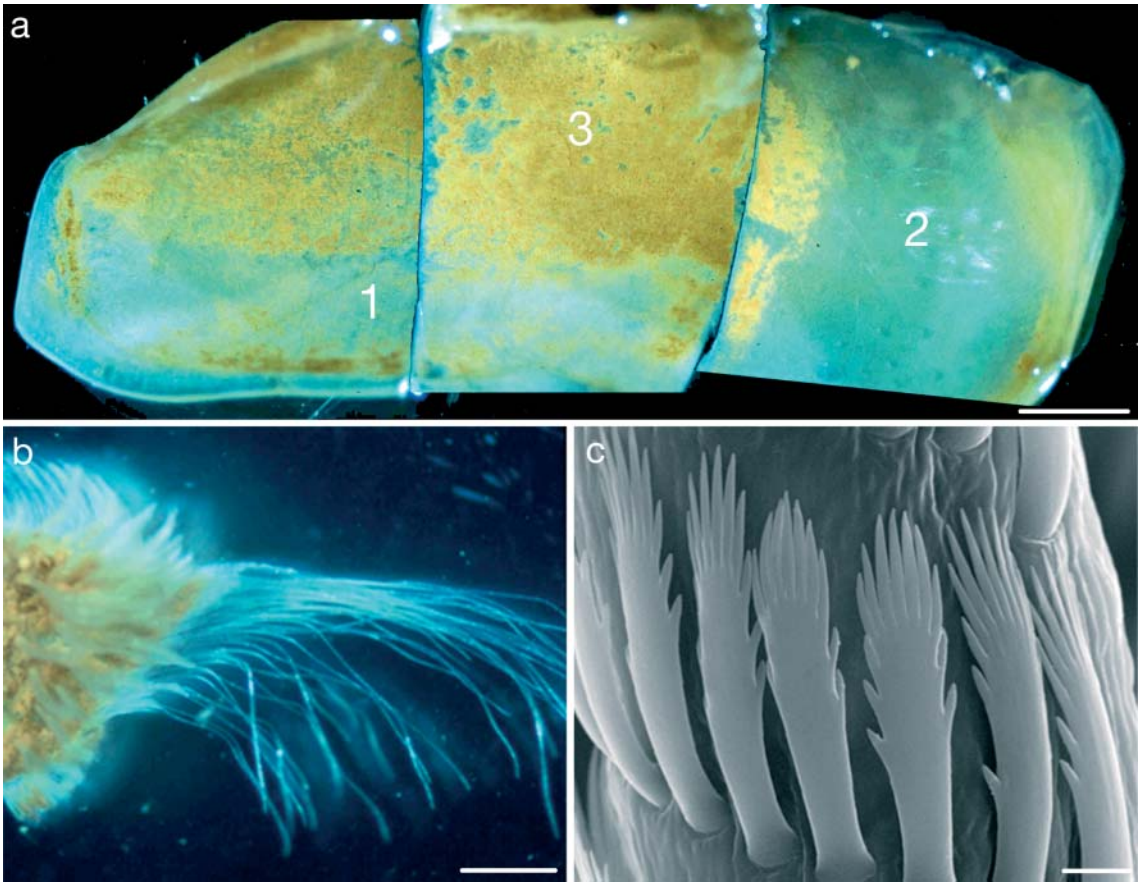

Fig. 2. *Rimicaris exoculata*. (a) Stereomicroscopic view of inner face of right side branchiostegite of a shrimp in anecdysis (comprising 3 photos), showing the 3 areas in Fig. 1(b) and medium amounts of rusty mineral deposits (iron oxides): 1, antero-ventral area characterised by few mineral deposits and bacteria; 2, posterior area facing gills and devoid of mineral deposits and bacteria; 3, antero-dorsal area characterised by thick rusty crust of minerals associated with a heavy bacterial mat. (b) Dorsal stereomicroscopic view of right scaphognathite showing posterior end bearing long multidenticulate gill-cleaning setae. (c) SEM view of digitate scale setules of multidenticulate gill-cleaning setae of scaphognathite. Scale bars: (a, b) = 2.5 mm; (c) = 2 µm

(see subsection 'Distribution of bacteria and the mineral deposits'). There were 2 types of filaments of different diameter and length: thick filaments 2.5 to 3.0 µm in diameter, and thin filaments 0.5 to 1.0 µm (Fig. 4g). Length was more dificult to measure but, for both types, could range up to 250 µm. Individual rods were also observed (0.5 × 1.5 µm) at the base of the filamentous bacteria (Fig. 4f,h), as a mono- or bi-layer on the inner branchiostegite cuticle (Fig. 5) and on the bacteriophore setae of the mouthparts (not shown). In places where a monolayer occurred, it was either formed by prostrate or erect rod-shaped bacteria (Fig. 5d,e).

Morphology of mineral deposits

Mineral deposits observed macroscopically (Figs. 2a & 3a,e,f) mostly consisted of round-shaped particles of small size (200 to 1000 nm diameter) or as small bothroidal concretions that seemed to have an amorphous texture (Fig. 4e,f). In TEM sections (not illustrated), these particles displayed a multilayered inner structure, characteristic of bothroidal concretions. They were fairly coalescent, filling the spaces between the bases of the large filamentous bacteria (Fig. 4e), and were always associated with rod-shaped bacteria (Fig. 4f).

Rarer objects, mostly encountered on the lower face of the exopodites, were also observed as large black, angular particles with a crystalline appearance (Fig. 3e). These particles were only very occasionally observed in other areas of the gill chamber.

Distribution of bacteria and mineral deposits

Bacteria colonised almost all the available surfaces of the branchial chamber, with the notable exceptions of the gills and the inner side of the branchiostegites

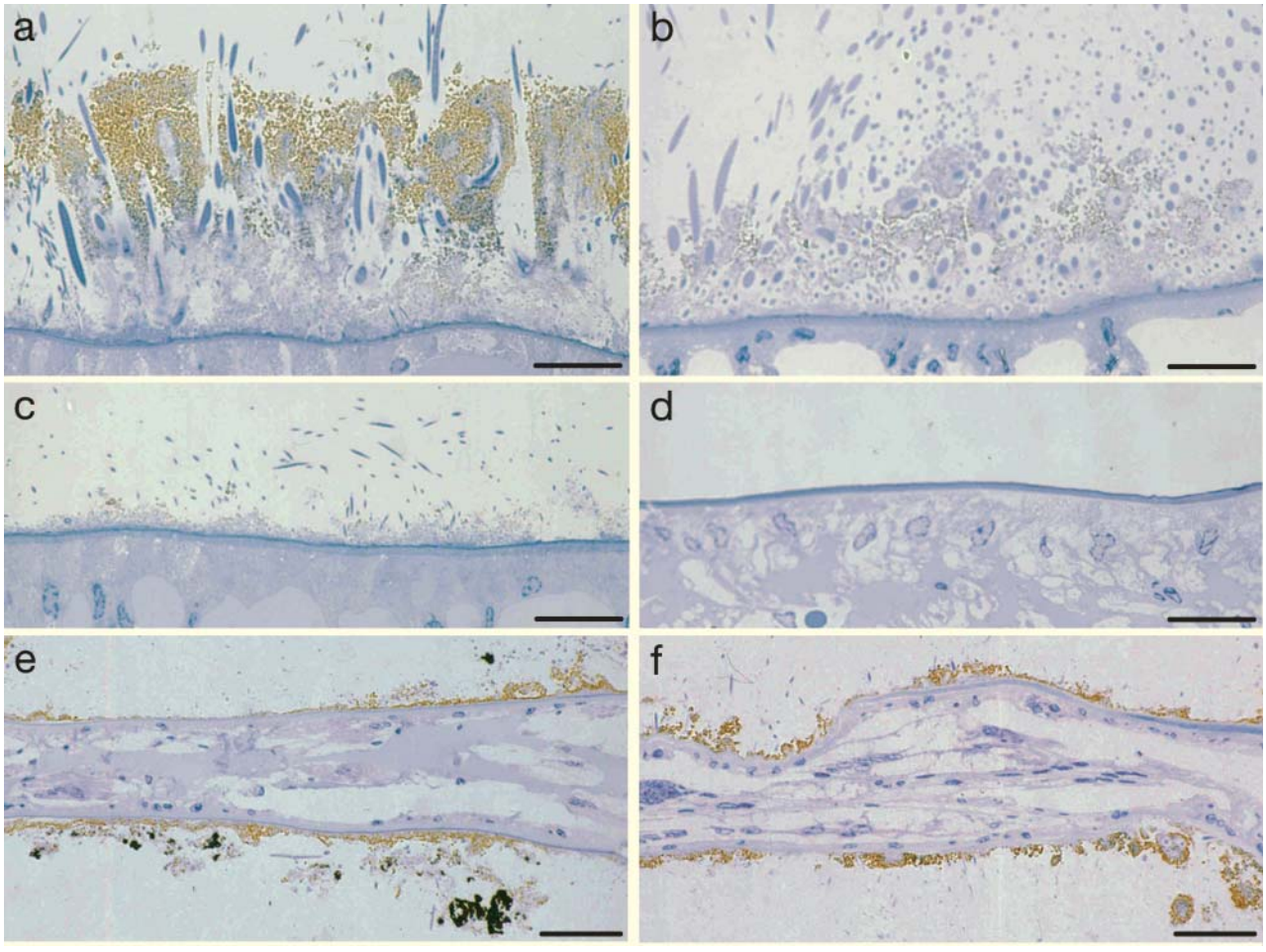

Fig. 3. *Rimicaris exoculata*. Semi-thin sections from 3 areas—inner branchiostegite integument, scaphognathite, and exopodite of the 1st maxilliped. (a, b) Antero-dorsal area of branchiostegite of (a) heavily and (b) weakly mineralised individual, with particulate orange-brown iron oxides.; (c) antero-ventral area of branchiostegite; (d) posterior area of the branchiostegite; (e) exopodite of first maxilliped of a heavily mineralised individual, showing occurrence of iron oxide (orange-brown) on both sides and of sulphides (black) mainly on ventral side; (f) scaphognathite of heavily mineralised individual, showing occurrence of iron oxides (orange-brown) on both sides. Scale bars: (a to d) = 50 µm; (e & f) = 100 µm

facing the gills. SEM observations revealed the complete absence of both bacterial coverage and mineral deposits from these areas (Figs. 3d & 5a). In the rest of the gill chamber, bacteria were present, sometimes in association with mineral deposits, but their distribution was not uniform. On the inner side of the branchiostegites, distribution of bacteria and minerals clearly defined the 3 distinct areas already observed macroscopically (Fig. 2a) and shown as a line-drawing (Fig. 1b).

The first area, occupying the antero-ventral part of the branchiostegites, was characterised by a thin bacterial coverage and the rare occurrence of mineral deposits (Fig. 3c). The density of bacteria was highest near the upper limit of this area and gradually decreased ventrally towards the epimeral fold of the branchiostegite (Fig. 5), where bacterial coverage was absent except in the groove close to the epimeral border. As stated earlier, the dorsal (upper) limit of this area corresponded to the position of the hypertrophied exopodites of the first maxillipeds, which horizontally divide the pre-branchial chamber into an upper and lower compartment (see Fig. 1b).

In the second area, on the posterior part of the branchostegite facing the gills, the cuticle was bare, being totally devoided of bacteria and mineral deposits (Fig. 3d). This surface varied between individuals, being relatively rough, folded, or almost smooth (not illustrated).

The third area was the antero-dorsal region of the branchiostegites; this was characterised by a thick bacterial mat and varying amounts of mineral particles (orange-brown particles of iron oxide, see next subsection) in different individuals (cf. Fig. 3a with 3b and Fig. 4a with 4b). The intensity of the rusty colouration

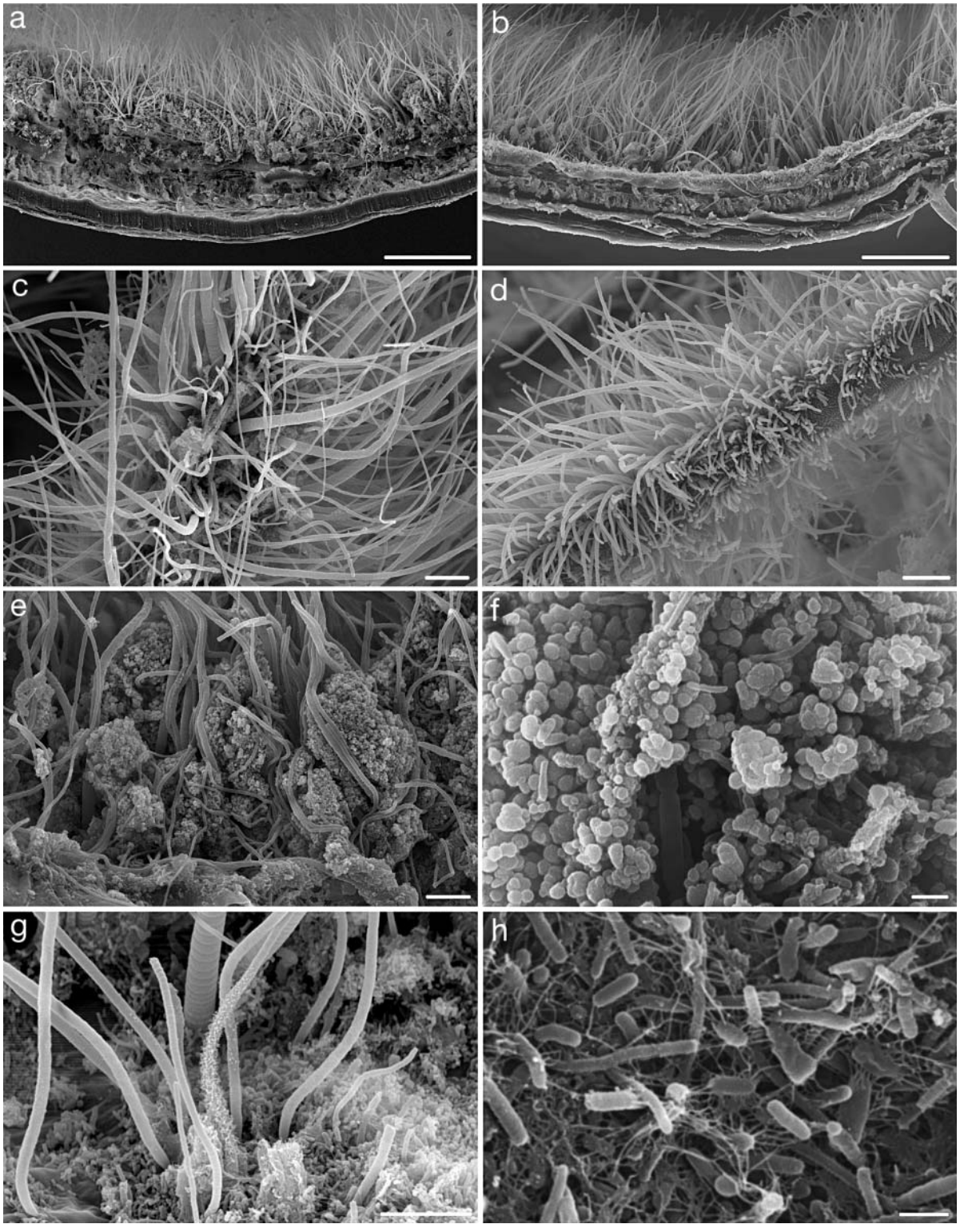

Fig. 4. *Rimicaris exoculata*. SEM micrographs of inner branchiostegite and bacteriophore setae of scaphognathite. (a, b) Vertical fracture in antero-dorsal area of branchiostegite showing bacterial coverage and mineral deposit in (a) heavily and (b) weakly mineralised individual; (c, d) bacterial mats and mineral deposits on bacteriophore setae of the scaphognathites in (c) heavily and (d) weakly mineralised individual; (e, f) details of mineral deposits in antero-dorsal area of branchiostegite; (g, h) details of bacterial diversity in antero-dorsal area of branchiostegite showing rod-shaped bacteria and thick and thin filaments. Scale bars: (a, b) = 100 µm; (c, d, e, g) = 10 µm; (f, h) = 1 µm

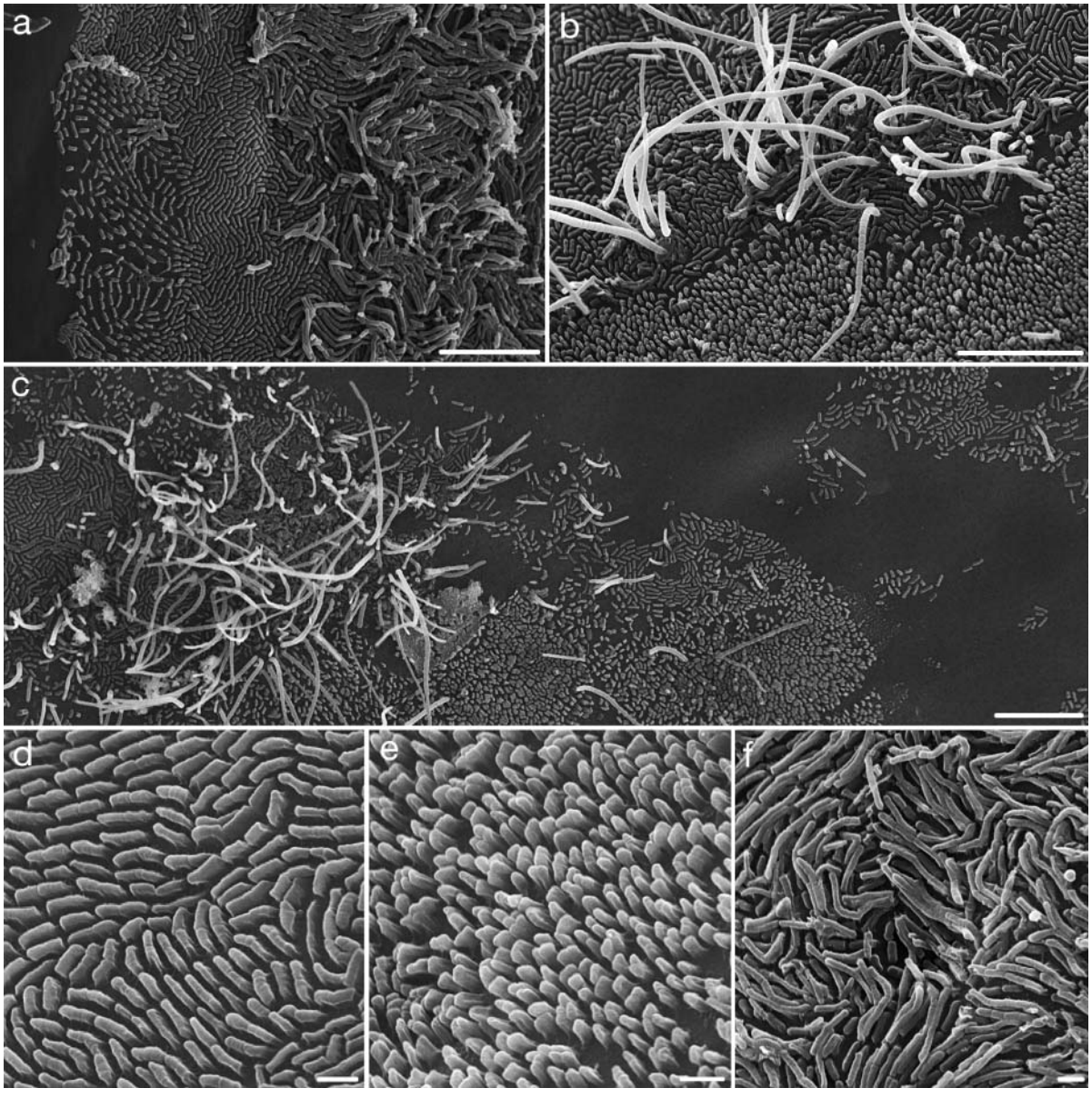

Fig. 5. *Rimicaris exoculata*. SEM micrographs of increasing bacterial coverage at boundary of the antero-dorsal and posterior areas of inner branchiostegite. (a) Emergence of monolayer of rod-shaped bacteria followed by bilayer of bacteria, the latter comparising short prostrate filaments. (b) Detail of short erect filaments emerging from bilayer of prostrate filaments and surrounded by monolayers of prostrate and erect rod-shaped bacteria. (c) General view of boundary area showing free surface, monolayers, and erect short filaments. (d–f) Details of bacterial morphotypes: monolayers of prostrate (d) and erect (e) rod-shaped bacteria, and bi-layer of short prostrate filaments (f). Scale bars: (a–c) = 10 µm; (d–f) = 1 µm

observed macroscopically (Fig. 2a) was directly related to the thickness of the mineral crust; abundance of bacteria and thickness of bacterial coverage varied inversely with thickness of the mineral crust. Abundant long bacterial filaments were encountered in beige individuals with few mineral deposits on the gill chamber walls and mouthparts (Figs. 3b & 4b); in these individuals, thickness of the bacterial coverage reached a maximum of 150 µm. In contrast, in heavily mineralised individuals, in which the mineral crust reached a maximum thickness of 60 µm, filamentous bacteria emerging from the mineral crust were rarer (Figs. 3a & 4a), and rod-shaped bacteria occurred between the mineral particles.

At the boundaries between the areas of thick bacterial mats and the zones that remained free (i.e. between the antero-dorsal area and the posterior or antero-ventral areas), bacterial coverage was progressive,

showing gradual steps of colonisation. In direct contact with the free zones, there first appeared a monolayer of isolated rod-shaped bacteria (0.5 to 1 µm in length) (Fig. 5a to c) that either adopted a prostrate (Fig. 5b,d) or erect (Fig. 5b,e) position. Then followed a bilayer (Fig. 5a,f) formed by short prostrate filaments (up to 2 µm) of 2 or 3 cells that seemed to be in division. In some places, thin erect filaments (Fig. 5b,c) arose from the bilayer through growth of the prostrate filaments. They appeared multicellular, but remained relatively short (from 2.5 to 20 µm). The spatial density of these thin erect filaments rapidly increased towards the zones of thick bacterial mats, which included thick erect filaments in addition to thin filaments and isolated bacteria (Fig. 4e,g). On the outer face of the branchiostegites, bacteria were few, with only small mono-layered patches of rods and small mats of short filaments near the base of the sensory setae (not shown).

Entirely enclosed in the upper pre-branchial chamber, the scaphognathites showed on both sides the same bacterial coverage and mineral deposits (Fig. 3f) as the antero-dorsal area of the branchiostegites. Bacteria (rods and filaments) densely covered the cuticular surface as well as the long bacteriophore setae (Fig. 4c,d). As on the branchiostegites, the density of the mineral deposits and the importance of the bacterial coverage on the scaphognathites varied widely between individuals, but presented the same features on both sides.

Separating the upper and lower compartments of the pre-branchial chamber, the expodites showed on both sides a bacterial coverage roughly similar to that of the scaphognathites. On the dorsal side, the mineral deposit was also similar to that on the scaphognathites, and mainly consisted of iron oxide (see next subsection); it was often less marked on the ventral side which, in contrast, displayed a number of black angular particles (Fig. 3e).

Element composition of particles (Fig. 6)

X-ray spectra (Fig. 6j) and maps (Fig. 6b,c,d,e) of the orange-brown deposit particles revealed the dominance of iron (Fe) (major peaks Kα at 6.400 keV and Kβ at 7.059 keV), but also the occurrence of calcium (Ca) (minor peaks Kα at 3.690 keV and Kβ at 4.012 keV) and traces of silica (Si) (Kα at 1.740 keV), phosphorus (P) (Kα at 2.013 keV) and sulphur (S) (Kα at 2.307 keV). The element maps also show that the distribution of these elements within the mineral crust was uniform. The mineralogy of the amorphous particles forming the deposit was investigated in a previous study by means of TEM and electron energy loss spectroscopy (EELS), and it was concluded that these particles consisted of iron oxyhydroxides in the form of ferrihydrite (Gloter et al. 2004).

X-ray spectra (Fig. 6k) and maps (Fig. 6g,h,i) of the black mineral particles on the lower side of the exopodites revealed 4 elements only: S (major Kα peak at 2.307 keV), Fe (Kα at 6.400 keV and Kβ at 7.059 keV), Cu (Kα at 8.041 keV and Kβ at 8.907 keV) and/or Zn (Kα at 8.681 keV and Kβ at 9.572 keV), according to the particles analysed. These particles thus appeared to be composed of zinc/iron and copper/iron sulphides.

Chemical and thermal environment of *Rimicaris exoculata*

In situ measurements of temperature, pH, ferrous iron and sulphide concentrations in the shrimp's environment reflected mixing of the vent fluid with seawater, with a moderate contribution of the fluid (Table 1). The mean temperature was several degrees above that of ambient seawater (2°C). The *in situ* pH ranged from that of the alkaline seawater (pH ~8) to a near-neutral level. The most important feature was the high level of ferrous iron in this environment (more than 100 µM). In comparison, sulphide was only slightly enriched (<3 µM). Discrete samples were consistent with the *in situ* ranges, also displaying approximately neutral pH and iron enrichment (Table 2). Their sulphide range was even slightly below the *in situ* range, probably due

Table 1. *In situ* temperature, pH, ferrous iron (Fe^{II}) and sulphide (S^{-II}) concentrations in environment of *Rimicaris exoculata* swarms. Values are means ± SD and (ranges)

T (°C)	pH	Fe^{II} (µM)	S^{-II} (µM)
8.7 ± 2.3		134 ± 60	1.6 ± 1.4
(3.8–14.7)	(7–8)	(56–265)	(0.4–6.3)
(n = 327)	(n = 327)	(n = 24)	(n = 17)

Table 2. pH (at 25°C, 1 atm), O_2, total sulphide (S^{-II}) and total iron (Fe^{II} + Fe^{III}) concentrations in discrete samples of ambient seawater and of fluid in vicinity of *Rimicaris exoculata* swarms, and at outlet of a black smoker. nd: no data

Sample	pH	O_2 µM	S^{-II} µM	Fe^{II} + Fe^{III} µM
Ambient seawater	7.8	242	<0.1	<0.5
	(n = 2)	(n = 2)	(n = 2)	(n = 2)
Shrimp swarms	7.0	166	–	73
	6.8–7.3	63–236	<0.1–2.7	45–101
	(n = 4)	(n = 3)	(n = 4)	(n = 4)
Smoker output	5.6	12.4	nd	5197
	5.3–6.1	<0.1–37		1620–8425
	(n = 3)	(n = 3)		(n = 3)

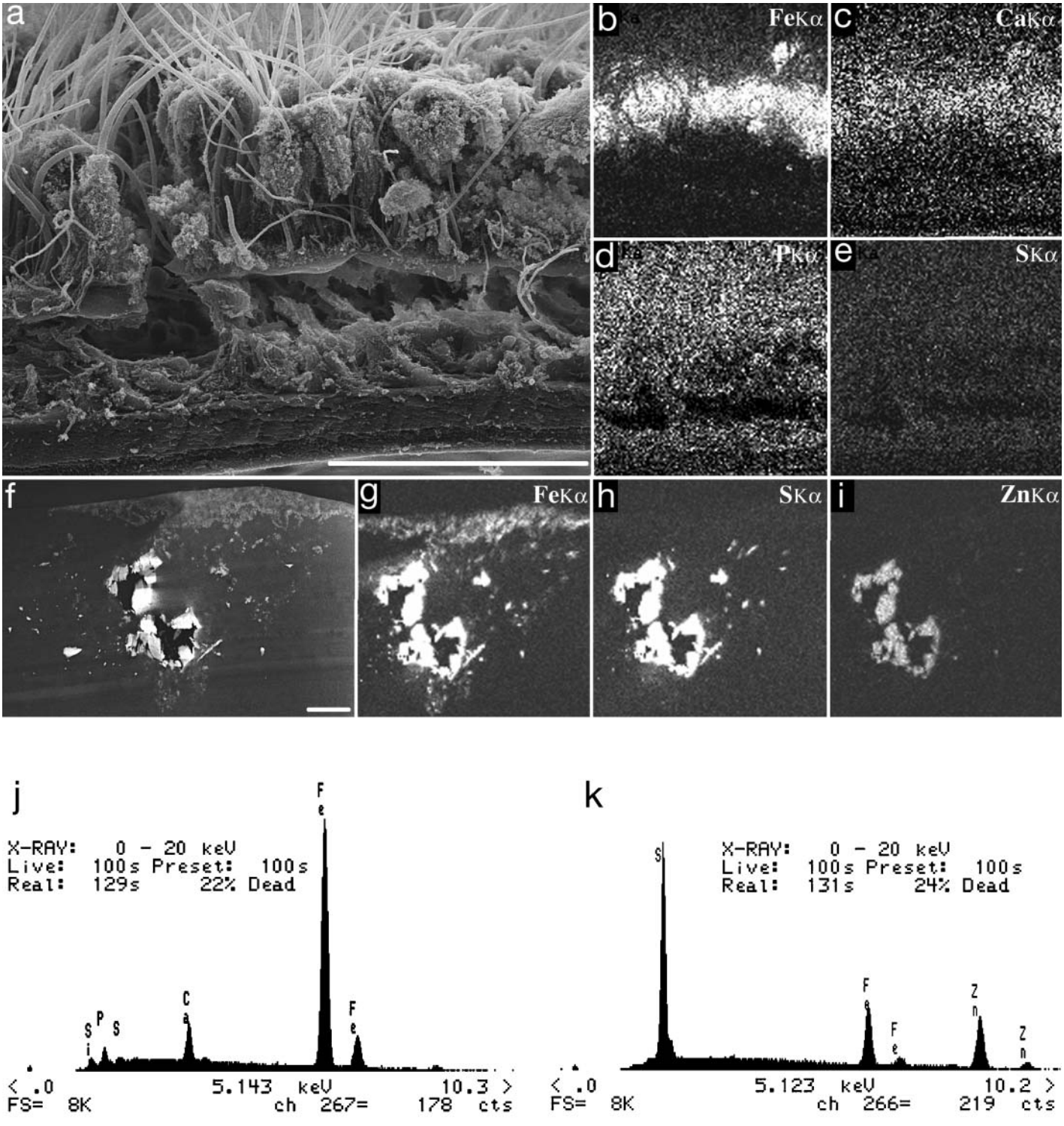

Fig. 6. *Rimicaris exoculata*. Element X-ray microanalyses and maps of mineral deposits in gill chamber (a) SEM image: (b)–(e); and X-ray maps of vertical fracture in antero-dorsal area of inner branchiostegite from heavily mineralised individual, showing (b) distribution of iron associated with (c) calcium and (d) phosphorus. (e) Sulphur is totally absent. (f)–(i) Semi-thin sections of resin-embedded exopodite of first maxilliped showing mineral deposits adhering to its lower face, including large black sulphide particle. (f) SEM image. (g) Elemental maps of iron, (h) sulphur and (i) zinc; largest particle is black zinc/iron sulphide particle surrounded by small iron sulphide particles. In contact with the cuticle is a thin crust of small iron-oxide particles. (j) X-ray spectrum of mineral deposit on the face of branchiostegite (as in a) showing major Fe peaks and minor peaks of Ca, Si, P and S. (k) X-ray spectrum of the black sulphide particle (f), showing S, Fe and Zn. Scale bars: (a) = 100 µm; (f) = 20 µm

to sulphide oxidation in the sampling vials during collection. It is interesting to note that the total iron (i.e. Fe^{II} + Fe^{III}) in the samples was of the same order of magnitude as the average ferrous iron content determined *in situ*, indicating that ferric iron did not represent a substantial fraction of iron in the fluid phase surrounding shrimp swarms. Even though the oxygen content in samples could have been underestimated, since oxygen uptake can occur in the sample bottles during retrieval to the surface, its level in these samples was still about two-thirds of the atmospheric-saturation level for seawater (at 25°C). The oxygen content in the environment of the shrimps thus remained quite high, in comparison to the largely oxygen-depleted conditions at the smoker outlets (Table 2). All these results indicated chemical conditions in the immediate surroundings of the shrimp as being intermediate between ambient seawater conditions and the more acidic and reduced fluid at the black smoker outlets. They reflected a metastable state in which reduced species (Fe^{II}, sulphide) coexisted with oxidized species (oxygen), similar to the situation described for other vent habitats (Johnson et al. 1988). The large predominance of iron over sulphide in the mixing zone was however atypical in comparison to the other vent habitats studied (Johnson et al. 1988, Luther et al. 2001, Le Bris et al. 2003).

DISCUSSION

Spatial distribution of the bacteria/mineral association in the branchial chamber

According to the literature on water flow in the branchial chamber of *Rimicaris exoculata* (Casanova et al. 1993), the water current generated by the beating of the scaphognathites runs through the gill chamber, entering ventrally and exiting anteriorly. The flow thus passes from the lower pre-branchial chamber (first compartment), to the gills (second compartment), and then through the upper pre-branchial chamber containing the epibiont community (third compartment). Analysis of the mineral distribution in the gill chamber revealed 2 important factors: (1) Metal sulphide particles occur almost solely on the lower face of the exopodites and on the surface of the antero-ventral area of the branchiostegites. These sulphide particles have a structure and composition typical of high-temperature plume particles (James & Elderfield 1996), indicating that the lower pre-branchial compartment may serve as a barrier against ambient particles. The long setae at the lower side of the exopodites would act as a filter to prevent penetration of particles and their accumulation in the gill chamber. Our results clearly confirm that water enters the gill chamber along the ventral side and flows out along the dorsal side. (2) Iron oxides are abundant in the upper pre-branchial compartment, whereas they are almost totally absent from the lower pre-branchial and posterior branchial compartments. The spatial variability in the mineral-deposit distribution is clearly related to the direction of the water flow, the upper pre-branchial compartment with the epibionts being located downstream of the gills in the water flow.

The absence of bacteria from the posterior area of the branchiostegites facing the gills, as well as from the gills themselves, is surprising in this environment, in which nearly all available surfaces are colonised by the epibionts. This absence of bacteria probably results from movement of the scaphognathites, which may act as gill-cleaners. They bear long multidenticulate setae with digitate scale setules at their posterior end (Fig. 2c). Such scaphognathites features are reported to comprise one of the passive gill-cleaning mechanisms in crustaceans, as described for caridean atyid shrimps by Suzuki & McLay (1998) and the mud-lobster *Thalassina anomalia* by Batang & Suzuki (1999). The functional importance of the gills as exchange surfaces in the shrimp's metabolism requires them to remain free of any microorganism and deposit, which would increase the diffusion distance between the haemolymph and the external medium.

The absence of bacteria from the outer face of the branchiostegites (except for small depressions around the bases of the setae) is also puzzling. Attempts to submerge the branchiostegites in aqueous fixatives have shown that the outer face is highly hydrophobic. The outer membrane of the bacteria is a lipid bilayer, containing proteins and sugars that give it a hydrophilic character. This could explain why bacteria are not able to colonise the hydrophobic outer face of the branchiostegites. The same could be true for the whole cephalothoracic shield and the abdominal tergites, which macroscopically always appear smooth and free of encrusting organisms.

Biogeochemical processes

Metazoan-associated bacteria have been reported to lead to the formation of iron minerals at hydrothermal vents (Zbinden et al. 2001, 2003, Lechaire et al. 2002), but until now never to the formation of iron oxides. The precipitation and accumulation of iron oxides in association with bacterial cells is common in aqueous environments, where high concentrations of Fe^{III} are produced by the oxidation of the reduced form Fe^{II} (Juniper & Tebo 1995, Ferris et al. 2000). The formation

of epicellular iron oxides by bacteria can occur either passively or actively. In the first case, bacteria provide nucleation sites for iron oxides through the electrostatic binding of dissolved ferric species to the anionic structural polymers of the cellwall. These bacteria-associated iron oxides have a chemical composition similar to those produced abiotically in solution (Konhauser 1998). Alternatively, bacteria can induce ferric oxide precipitation as a result of their metabolism. This can be done indirectly, by local alteration of the pH and redox conditions around the cell (Konhauser 1998), or by production of extracellular organic polymers that bind ferric iron and promote oxide nucleation and growth; or directly, by oxidation of Fe^{II} as an electron donor in their metabolism (Emerson & Moyer 1997, 2002, Straub et al. 2001, Neubauer et al. 2002).

The spatial heterogeneity of the mineral/bacteria association observed in this study indicates that precipitation is not just a passive nucleation process. Furthermore, the uncommon mixed-valence ferrihydrite mineralogy described for iron oxide (Gloter et al. 2004) suggests bacterial iron oxidation (Edwards et al. 2003). A direct role of the epibionts in the formation of the deposits is thus strongly suggested.

In oxic environments, spontaneous ferrous iron oxidation is extremely rapid at ambient temperature (25°C) and neutral pH (Emerson & Moyer 1997, Neubauer et al. 2002). Under these conditions, Fe-oxidizing bacteria may find it difficult to compete with the abiotic process. In the present study, however, the temperature was low and oxygen was reduced to about two-thirds of its level in air-saturated seawater. Abiotic oxidation is much slower under such conditions. As calculated from the kinetic study of Millero et al. (1987), the Fe^{II} half-life would be about 35 h in a shrimp environment, whereas it is only of a few minutes in air-saturated seawater at 25°C. Our *in situ* analyses confirmed that iron mostly remains in its metastable reduced form in the surroundings of the shrimp. The absence of iron oxides from the first chamber is consistent with this slow abiotic oxidation rate and denotes the absence of a nucleation effect at the bacterial cell surface. In contrast, the abundance of iron oxides in the third chamber indicates that iron oxidation is promoted in this microenvironment.

In the upper pre-chamber, i.e. downstream of the gills in the water flow, a pH reduction, a CO_2 increase and an O_2 decrease can be expected as a result of shrimp respiration. According to Millero et al. (1987) and King (1998), all these changes should lead to a decrease in the abiotic oxidation rate. This further supports the idea of a microbially-mediated oxidation, at least for the first mineral deposition stage. Iron-oxidizing microorganisms have been shown to require micro-aerophilic conditions for growth at ambient temperature (Emerson & Moyer 1997, Neubauer et al. 2002). It is not known whether such a low oxygen requirement is also valid at low temperatures, where competion with the abiotic process is not so critical, but a possible explanation to the observed dissimilarity between the 2 chambers would be the presence of a gradient in oxygen content in the shrimp branchial cavity.

It has been previously reported, for the Snake Pit site, that the bacteria in the whole gill chamber of the shrimp belong to the same phylotype (Polz & Cavanaugh 1995). If this is also the case for shrimp from our study site, it would appear that the bacteria of the pre-branchial chamber resort to a different metabolism because of local conditions. As described for *Acidothiobacillus ferrooxidans* (Rawlings & Kusano 1994), some bacteria are able to obtain their energy through the oxidation of either ferrous iron or reduced inorganic sulphur compounds, depending on the availability of these elements in the surrounding fluid. However, without further investigations, it is hazardous to extrapolate the conclusion drawn for shrimp epibionts at the Snake Pit vent site to those at the Rainbow site. The Rainbow hydrothermal fluid chemistry is indeed highly different from that at the Snake Pit, especially with respect to its exceptionally high iron enrichment and quite low sulphide content (Charlou et al. 2002, Douville et al. 2002). It is also conceivable that a different and more diversified microflora inhabits the gill chamber of *Rimicaris exoculata* at the Rainbow site.

As discussed in Emerson & Moyer (1997) and referenced herein, ferrous iron oxidation under neutral and microaerophilic conditions can provide enough energy to drive chemoautotrophic CO_2 fixation. The energy budget of iron oxidation greatly depends on environmental conditions, and especially pH (Straub et al. 2001, Emerson & Moyer 2002). Using the standard Gibbs free-energies listed in Buffle & De Vitre (1994), we obtained a first estimation of the energy available from the different redox pathways. At pH 7 and under standard conditions, the energy available from the oxidation of ferrous iron to amorphous iron oxyhydroxide is 228 kJ mol^{-1} (while it is only 44 kJ mol^{-1} at pH 2 for ferric iron in dissolved form). This energy budget would be even larger if a more crystalline phase were formed. In comparison, oxidation of sulphide to sulphate would provide 797 kJ mol^{-1} and oxidation of sulphide to elemental sulphur only 209 kJ mol^{-1}. As iron is on average 85-fold higher than sulphide in the environment of the Rainbow shrimp swarms, the energy available for chemoautotrophic primary production in these conditions would be 25 to 100 higher with iron as electron donor than with sulphide.

Potential biological role of epibiosis

The epibiotic bacteria appear to take advantage of a specific microenvironment in the gill chamber, where conditions are optimal for their growth; this may not be the case on the mineral surfaces exposed to the outer medium. Some direct or indirect benefits for the shrimp are not necessarily involved, but several hypotheses have been raised and are discussed below.

Detoxification

In comparison to ambient seawater, the Rainbow hydrothermal fluid is enriched in toxic heavy metals and radioactive elements (Douville et al. 2002). These compounds adsorb onto iron oxides (Ferris et al. 2002), and their elimination from the dissolved phase results in the lowering of their capacity to pass through biological membranes and, hence, reduces their toxicity. In the present study, the absence of iron oxides from the branchial chamber or the lower pre-branchial chamber upstream of the gills does not support the idea of a 'detoxification mechanism' with respect to the respiratory organs. If detoxification occurs through adsorption onto the iron oxide particles, it would be only significant in the last chamber, i.e. in the upper pre-branchial chamber situated downstream of the gills.

Shrimp diet

One hypothesis concerning the role of the epibionts suggests that *Rimicaris exoculata* gains most of its carbon from the epibiotic bacteria living within its carapace (Rieley et al. 1999), by scraping and grazing on them (Gebruk et al. 1993). Our observations on numerous specimens however did not reveal scraped areas on the walls of the pre-branchial chamber (inner side of the branchiostegites) nor on the mouthparts. The bacterial biofilm never seems damaged mechanically by the appendages (with the exception of its complete removal from the gills and branchial chamber walls by the gill-cleaning setae of the scaphognathites). It is thus unlikely that the shrimps graze on their own bacteria. In order for shrimp to obtain carbon from their epibionts, 3 processes are suggested. (1) The shrimps could consume their exuviae (i.e the old moulted cuticle) and thus ingest the epibionts. Our observations of gut contents did reveal the presence of cuticle fragments (data not shown) in a shrimp in late anecdysis, which had heavy mineral oxide deposits in its pre-branchial chamber. Maintainance of shrimps in a pressure vessel (Shillito et al. 2001) for 24 or 30 h has shown that digestive transit in *Rimicaris exoculata* is fairly rapid (guts are completely empty of minerals and organic residues after this time; M. Zbinden unpubl.). It is thus unlikely that the individual we observed had ingested its own exuvium, but rather that the cuticle fragments originated from the exuviae of other shrimp. Questions that arise are: are there sufficient bacteria on the exuviae and are moults frequent enough to feed the shrimp, taking into account the metabolic cost of moulting and the fact that bacterial coverage increasingly regresses in shrimps approaching their next moult ?

(2) Trans-epidermal transfer of dissolved organic matter from the epibiotic bacteria could occur through the branchiostegite cuticle. This hypothesis has already been suggested for the filamentous bacteria present on the mouthparts of this shrimp (Casanova et al. 1993). Although, Gebruk et al. (2000) did not agree with this hypothesis (on the basis of studies on other Crustacea which showed the active transport of dissolved organic matter to be unlikely), the hypothesis is supported by recent TEM observations of the epithelium lining the inner face of the branchiostegites of *Rimicaris exoculata*. The epidermal cells exhibit apical membrane infoldings (Martinez 2001) and are rich in mitochondria, suggesting epidermal transport activity (J. B. Braquenier & P. Compère unpubl. data).

(3) Absorption of hydrolysates resulting from bacterial activity in the gut has also been suggested to occur through the hindgut cuticle of the deposit-feeding shrimp *Nyotrypaea californiensis* (Lau et al. 2002). On the basis of the presence of an intact bacterial microflora in *Rimicaris exoculata* gut, a trans-epithelial transfer through the gut endoderm has also been suggested (Zbinden & Cambon-Bonavita 2003), but this remains to be demonstrated.

If such trans-epidermal nutrition does occur at the upper pre-branchial chamber level then the *Rimicaris exoculata* ectosymbiosis would appear to be unique in comparison to other vent symbioses, not only in regard to the nature of the host (such symbioses have never been reported for other crustaceans), but also in regard to its iron oxidative microbial metabolism, since most symbioses studied so far rely only on sulphide or methane oxidation (Nelson & Fisher 1995).

On the basis of their morphological resemblance to *Thiotrix* spp., these epibionts were previously inferred to be sulphur-oxidisers (Gebruk et al. 1993), but until now, attempts to cultivate these bacteria have remained unsuccessful. Chemoautotrophic growth activity of the filamentous bacteria from the inner cephalothorax surface has nevertheless been demonstrated (Wirsen et al. 1993), with higher values measured in the rusty brown bacterial films than in the more reduced blackish films. Furthermore, CO_2 incorporation was detected on scrapings of shrimps cara-

paces and scaphognathites, but no significant increase in fixation was observed in the presence of reduced sulphur compounds (Polz et al. 1998).

As previously discussed (Emerson & Moyer 1997, 2002), iron redox gradients in advective systems can constitute ideal habitats for aerobic neutrophilic iron oxidisers. Our *in situ* and discrete-sample chemical analyses indicate that the environment of shrimp swarms meets these requirements. The shrimp's gill chamber provides a large surface for microbial growth with a controlled and constantly renewed access to reduced iron and oxygen. Iron oxidation could constitute a significant energetic option in a medium where ferrous iron is unusually enriched whereas sulphide (a main electron donor at most Mid-Atlantic Ridge or East Pacific Rise vent sites) is low.

Among the sites explored to date, the Rainbow hydrothermal fluid is exceptionally rich in iron (24 mmol kg^{-1}; Douville et al. 2002), and is considered an atypical hydrothermal fluid in this respect (Allen & Seyfried 2003). Its high iron content gave us unique opportunity of demonstrating the possibility of diverse metabolic pathways of the microbial epibiosis associated with *Rimicaris exoculata*. However, the iron-oxidiser epibionts of *R. exoculata* may not be restricted to this site. Rusty minerals associated with *R. exoculata* epibionts have also been described from other Mid-Atlantic sites (Wirsen et al. 1993), and deserve further investigation. At the TAG site, particularly, the iron content of its hydrothermal fluid, although not so dominant over sulphide, reaches values of 5.5 mmol kg^{-1}. This is substantially higher than that of the other MAR sites, except for Rainbow. A newly discovered vent site on the Indian Ridge, where megafauna biomass is dominated by shrimp swarms of the genus *Rimicaris*, was also reported to have an end-member fluid iron-content as high as 14 mmol kg^{-1} (Van Dover et al. 2001). This is lower that at Rainbow but much higher than this is generally the case at MAR sites (Von Damm 1995, Douville et al. 2001). Abundant iron-oxide microbial mats were reported for the new Indian Ridge site, suggesting that microbial iron-oxidation may be an important chemoautotrophic process there (Emerson & Moyer 2002). Nothing is known about the shrimp epibionts or associated minerals at the new site, but the occurrence of iron-oxidising epibionts could be postulated in this case also .

Conclusions

The distribution of bacteria and mineral deposits in the branchial chamber of the shrimp defines 3 compartments, which differ in bacterial and mineral abundance, and in the nature of the minerals. These 3 compartments are functionally different. They represent distinct microenvironments, probably providing different chemical conditions, which may promote different bacterial metabolisms. We propose that the epibiotic bacteria of the antero-dorsal part of the branchial chamber relies on iron-oxidation for growth. If this is true, this symbiosis would appear unique, as most previously studied symbioses at deep-sea vents rely on sulphide or methane oxidation. Further microbiological investigations are required to confirm this hypothesis, and to determine if this bacteria—*Rimicaris exoculata* association is widespread or specific to the peculiar chemical environment of the Rainbow vent field.

Acknowledgements. The authors want to thank P. M. Sarradin, chief scientist of the ATOS cruise, as well as the captain and crew of the RV 'Atalante', the ROV 'Victor' team, and P. Rodier for technical assistance. The authors wish also to express their appreciation to N. Decloux (microtomy and SEM preparation) for her excellent technical assistance. We also thank the 4 reviewers for providing constructive comments for rewriting this paper. This work was partly funded with the help of the Dorsales Programm (INSU, CNRS SDV, Ifremer), the VENTOX program (EVK3 CT-1999-0003) and the Geomex program (CNRS). A fellowship for M.Z. and part of this work were supported by the Belgian Fund for Joint Basic Research (F.R.F.C Belgium, convention no. 2.4533.01.F).

LITERATURE CITED

Allen DE, Seyfried WE (2003) Compositional controls on vent fluids from ultramafic-hosted hydrothermal systems at mid-ocean ridges: an experimental study at 400°C, 500 bars. Geochim Cosmochim Acta 67:1531–1542

Batang ZB, Suzuki H (1999) Gill-cleaning mechanisms of the mud-lobster *Thalassina anomalia* (Decapoda: Thalassinidea: Thalassinidae). J Crustac Biol 19:671–683

Buffle J, De Vitre R (1994) Chemical and biological regulation of aquatic systems. Lewis Publishers, Boca Raton, FL

Casanova B, Brunet M, Segonzac M (1993) L'impact d'une épibiose bactérienne sur la morphologie fonctionnelle de crevettes associées à l'hydrothermalisme médio-Atlantique. Cah Biol Mar 34:573–588

Charlou JL, Donval JP, Fouquet Y, Jean-Baptiste P, Holm N, Caccavo FJ (2002) Geochemistry of high H_2 and CH_4 vent fluids issuing from ultramafic rocks at the Rainbow hydrothermal field (36° 14′ N, MAR). Chem Geol 191:345–359

Coale KH, Chin CS, Massoth GJ, Johnson KS, Baker ET (1991) In situ chemical mapping of dissolved iron and manganese in hydrothermal plumes. Nature 352:325–328

Compère P, Jeuniaux C, Goffinet G (2004) Chapter 3, The integument: morphology and biochemistry. In: Forest J, von Vaupel Klein JC (eds) Treatise on zoology 1. Anatomy, taxonomy, biology. Vol Crustacea. Koninklijke Brill, Leiden, p 1–85

Douville E, Charlou JL, Oelkers EH, Bienvenu P and 5 others (2002) The rainbow vent fluids (36° 14′ N, MAR): the influence of ultramafic rocks and phase separation on trace metal content in Mid-Atlantic Ridge hydrothermal fluids. Chem Geol 184:37–48

Drach P, Tchernigovtzeff C (1967) Sur la méthode de détermi-

nation des stades d'intermue et son application générale aux Crustacés. Vie Milieu 18A:595–609
Edwards KJ, McCollom TM, Konishi H, Buseck PR (2003) Seafloor bioalteration of sulphide minerals: results from in situ incubations studies. Geochim Cosmochim Acta 67: 2843–2856
Emerson D, Moyer CL (1997) Isolation and characterization of novel iron-oxidizing bacteria that grow at circumneutral pH. Appl Environ Microbiol 63:4784–4792
Emerson D, Moyer CL (2002) Neutrophilic Fe-oxidizing bacteria are abundant at the Loihi seamount hydrothermal vents and play a major role in Fe oxide deposition. Appl Environ Microbiol 68(6):3085–3093
Ferris FG, Hallberg RO, Lyven B, Pedersen K (2000) Retention of strontium, cesium, lead and uranium by bacterial iron oxides from a subterranean environment. Appl Geochem 15:1035–1042
Fortin D, Ferris FG, Scott SD (1998) Formation of Fe-silicates and Fe-oxides on bacterial surfaces in samples collected near hydrothermal vents on the southern Explorer Ridge in the northeast Pacific Ocean. Am Mineralogist 83: 1399–1408
Gebruk AV, Pimenov NV, Savvichev AS (1993) Feeding specialization of bresiliid shrimps in the TAG site hydrothermal community. Mar Ecol Prog Ser 98:247–253
Gebruk AV, Southward EC, Kennedy H, Southward AJ (2000) Food sources, behaviour, and distribution of hydrothermal vent shrimp at the Mid-Atlantic Ridge. J Mar Biol Assoc UK 80:485–499
Gloter A, Zbinden M, Guyot F, Gaill F, Colliex C (2004) Formation and stabilization of mixed valence ferrihydrite on bacterial surfaces from hydrothermal vents. Earth Planet Sci Lett 222:947–957
James RH, Elderfield H (1996) Dissolved and particulate trace metals in hydrothermal plumes at the Mid-Atlantic Ridge. Geophys Res Lett 23:3499–3502
Johnson KS, Childress J, Hessler RR, Sakamoto-Arnold C (1988) Chemical and biological interactions in the Rose Garden hydrothermal vent field. Deep-Sea Res Part A 35: 1723–1744
Juniper SK, Tebo BM (1995) Microbe–metal interactions and mineral deposition at hydrothermal vents. In: Karl D (ed) The microbiology of deep-sea hydrothermal vents. CRC Press, Boca Raton, FL, p 219–253
Juniper SK, Martineu P, Sarrazin J, Gelinas Y (1995) Microbial mineral floc associated with nascent hydrothermal activity on Coaxial segment, Juan de Fuca Ridge. Geophys Res Lett 22:179–182
Kennedy CB, Scott SD, Ferris FG (2003) Ultrasutructure and potential sub-seaflor evidence of bacteriogenic iron oxide from Axial Volcano, Juan de Fuca Ridge, north-east Pacific Ocean. FEMS Microbiol Ecol 43:247–254
King DW (1998) Role of carbonate speciation on the oxidation rate of Fe(II) in aquatic systems. Environ Sci Technol 32: 2997–3003
Konhauser KO (1998) Diversity of bacterial iron mineralization. Earth-Sci Rev 43:91–121
Lau WW, Jumars PA, Armbrust EV (2002) Genetic diversity of attached bacteria in the hindgut of the deposit-feeding shrimp *Neotrypaea* (formerly *Callianassa*) *californiensis* (Decapoda: Thalassinidae). Microb Ecol 43:455–466
Le Bris N, Sarradin PM, Birot D, Alayse AM (2000) A new chemical analyser for in situ measurement of nitrate and total sulphide over hydrothermal vent biological communities. Mar Chem 72:1–15
Le Bris N, Sarradin PM, Pennec S (2001) A new deep-sea probe for *in situ* pH measurement in the environment of hydrothermal vent biological communities. Deep-Sea Res Part I 48:1941–1951
Lechaire JP, Shillito B, Frébourg G, Gaill F (2002) Elemental characterization of microorganism granules by EFTEM in the tube wall of a deep-sea vent invertebrate. Biol Cell 94: 243–249
Luther GW, Rozan TF, Taillefert M, Nuzzio DB, Meo CD, Shank TM, Lutz RA, Cary SC (2001) Chemical speciation drives hydrothermal vent ecology. Nature 410:813–816
Martinez AS (2001) Adaptations morphofonctionnelles des crustacés caridés et brachyoures. La salinité du milieu hydrothermal profond. PhD thesis, University of Montpellier II
Millero FJ, Sotolongo S, Izaguirre M (1987) The oxidation kinetics of Fe(II) in seawater. Geochim Cosmochim Acta 51:793–801
Nelson DC, Fischer CR (1995) Chemoautotrophic and methanotrophic endosymbiotic bacteria at deep-sea vents and seeps. In: Karl D (ed) The microbiology of deep-sea hydrothermal vents. CRC Press, Boca Raton, FL, p 125–166
Neubauer SC, Emerson D, Megonigal JP (2002) Life at the energetic edge: kinetics of circumneutral iron oxidation by lithotrophic iron-oxidizing bacteria isolated from the wetland-plant rhizosphere. Appl Environ Microbiol 68(8): 3988–3995
Polz MF, Cavanaugh CM (1995) Dominance of one bacterial phylotype at a Mid-Atlantic Ridge hydrothermal vent site. Proc Natl Acad Sci USA 92:7232–7236
Polz MF, Robinson JJ, Cavanaugh CM, Van Dover CL (1998) Trophic ecology of massive shrimp aggregations at a mid-Atlantic Ridge hydrothermal vent site. Limnol Oceanogr 43:1631–1638
Pond DW, Dixon DR, Bell MV, Fallick AE, Sargent JR (1997) Occurrence of 16:2(n-4) and 18:2(n-4) fatty acids in the lipids of the hydrothermal vent shrimps *Rimicaris exoculata* and *Alvinocaris markensis*: nutritional and trophic implications. Mar Ecol Prog Ser 156:167–174
Rawlings DE, Kusano T (1994) Molecular genetics of *Thiobacillus ferrooxidans*. Microbiol Rev 58:39–55
Rieley G, Van Dover CL, Hedrick DB, Eglinton G (1999) Trophic ecology of *Rimicaris exoculata*: a combined lipid abundance/stable isotope approach. Mar Biol 133:495–499
Sarradin PM, Caprais JC, Briand P, Gaill F, Shillito B, Desbruyères D (1998) Chemical and thermal description of the environment of the Genesis hydrothermal vent community (13° N, EPR). Cah Biol Mar 39:159–167
Segonzac M (1992) Les peuplements associés à l'hydrothermalisme océanique du Snake Pit (dorsale médio-Atlantique, 23° N, 3480 m): composition et microdistribution de la mégafaune. CR Acad Sci Sér III 314:593–600
Segonzac M, de Saint-Laurent M, Casanova B (1993) L'énigme du comportement trophique des crevettes Alvinocarididae des sites hydrothermaux de la dorsale médio-atlantique. Cah Biol Mar 34:535–571
Shillito B, Jollivet D, Sarradin PM, Rodier P, Lallier F, Desbruyères D, Gaill F (2001) Temperature resistance of *Hesiolyra bergi*, a polychaetous annelid living on vent smoker walls. Mar Ecol Prog Ser 216:141–149
Straub KL, Benz M, Schinck B (2001) Iron metabolism in anoxic environments at near neutral pH. FEMS Microbiol Ecol 34:181–186
Suzuki H, McLay CL (1998) Gill-cleaning mechanisms of *Paratya curvirostris* (Caridea: Atyidae) and comparison with seven species of Japanese atyid shrimps. J Crustac Biol 18:253–270
Van Dover CL, Fry B, Grassle JF, Humphris SE, Rona PA (1988) Feeding biology of the shrimp *Rimicaris exoculata*

at hydrothermal vents on the Mid-Atlantic Ridge. Mar Biol 98:209–216

Van Dover CL, Humphris SE, Fornari D, Cavanaugh CM and 23 others (2001) Biogeography and ecological setting of Indian Ocean hydrothermal vents. Science 294:818–823

Vernet G, Charmentier-Daures M (1994) Mue, autotomie et régénération. In: Forest J (ed) Traité de zoologie 7, Crustacés (1), Morphologie, physiologie, reproduction, embryologie. Masson, Paris, p 107–194

Von Damm KL (1995) Controls on the chemistry and temporal variability of seafloor hydrothermal fluids. In: Humphris S, Zierenberg R, Mullineaux L, Thomson R (eds) Seafloor hydrothermal systems. Physical, chemical, biological and geological interactions. American Geophysical Union, Washington, p 222–247

Williams AB, Rona PA (1986) Two new caridean shrimps (Bresiliidae) from a hydrothermal field on the Mid-Atlantic Ridge. J Crustac Biol 6:446–462

Wirsen CO, Jannasch HW, Molyneaux SJ (1993) Chemosynthetic microbial activity at Mid-Atlantic Ridge hydrothermal vent sites. J Geophys Res B 98:9693–9703

Zbinden M, Cambon-Bonavita MA (2003) Occurrence of *Deferribacterales* and *Entomoplasmatales* in the deep-sea shrimp *Rimicaris exoculata* gut. FEMS Microbiol Ecol 46: 23–30

Zbinden M, Martinez I, Guyot F, Cambon-Bonavita MA, Gaill F (2001) Zinc–iron sulphide mineralization in tubes of hydrothermal vent worms. Eur J Mineral 13:653–658

Zbinden M, Le Bris N, Compère P, Martinez I, Guyot F, Gaill F (2003) Mineralogical gradients associated with alvinellids at deep-sea hydrothermal vents. Deep-Sea Res Part I 50:269–280

Editorial responsibility: Otto Kinne (Editor), Oldendorf/Luhe, Germany

Submitted: January 26, 2004; Accepted: July 8, 2004
Proofs received from author(s): December 7, 2004

Journal of Experimental Marine Biology and Ecology 359 (2008) 131–140

Contents lists available at ScienceDirect

Journal of Experimental Marine Biology and Ecology

journal homepage: www.elsevier.com/locate/jembe

New insigths on the metabolic diversity among the epibiotic microbial communitiy of the hydrothermal shrimp *Rimicaris exoculata*

Magali Zbinden [a,*], Bruce Shillito [a], Nadine Le Bris [b], Constance de Villardi de Montlaur [a], Erwan Roussel [c], François Guyot [d], Françoise Gaill [a], Marie-Anne Cambon-Bonavita [c]

[a] UMR CNRS 7138, Systématique, Adaptations et Evolution, UPMC, 7 Quai Saint Bernard, 75252 Paris cedex 05, France
[b] Ifremer Brest, Département Environnement Profond, BP 70, 29280 Plouzané, France
[c] Ifremer Brest, Laboratory of Microbiology of Extreme Environments, LM2E, UMR 6197, BP 70, 29280 Plouzané, France
[d] Institut de Physique du Globe de Paris, Laboratoire de Minéralogie-Cristallographie, Université Paris-Jussieu, Tour 16, Case 115, 4, place Jussieu, 75 252 Paris Cedex 05, France

ARTICLE INFO

Article history:
Received 6 November 2007
Received in revised form 19 March 2008
Accepted 20 March 2008

Keywords:
High pressure experiments
Hydrothermal vent shrimp
Intracellular granules
Iron
Methane
Sulfur

ABSTRACT

The *Rimicaris exoculata* dominates the megafauna of some of the Mid Atlantic ridge hydrothermal vent sites. This species harbors a rich community of bacterial epibionts inside its gill chamber. Literature data indicate that a single 16S rRNA phylotype dominates this epibiotic community, and is assumed to be a sulfide–oxidizing bacteria. However attempts of cultivation were not successful and did not allow to confirm it. The aim of our study was to test the hypothesis of sulfide oxidation in the gill chamber, by a multidisciplinary approach, using *in vivo* experiments at *in situ* pressure in the presence of sulfide, microscopic observations and a molecular survey. Morphology of microorganisms, before and after treatment, was analyzed to test the effect of sulfide depletion and re-exposure. Our observations, as well as molecular data indicate a wider diversity than previously described for this shrimp's epibiotic community. We observed occurrence of bacterial intracellular sulfur– and iron–enriched granules and some methanotrophic–like bacteria cells for the first time. Genes that are characteristic of methane–oxidizing (*pmoA*) and sulfide–oxidizing (APS) bacteria were identified. These results suggest that three metabolic types (iron, sulfide and methane oxidation) may co–occur within the epibiont community associated with *Rimicaris exoculata*. As this shrimp colonizes chemically contrasted environments, the relative abundance of each metabolic type could vary according to the local availability of reduced compounds.

1. Introduction

Hydrothermal vent communities along the Mid–Atlantic Ridge (MAR) are dominated by large populations of caridean shrimps. Found in dense clusters of 40 000 individuals per m3 (Segonzac et al., 1993), *Rimicaris exoculata* (Williams and Rona, 1986) is the most abundant species on some of these sites. This shrimp has been found to host a dense bacterial epibiosis on the internal walls (branchiostegites) of its branchial chamber and on its mouthparts (scaphognathites and exopodites of the first maxillipeds) (Van Dover et al., 1988; Casanova et al., 1993; Segonzac et al., 1993; Zbinden et al., 2004). This indicates an intimate association between these organisms. The main source of dietary carbon could originate: 1) from bacteria ingested with the sulfide scraped from the chimney (Van Dover et al., 1988), 2) from their epibiotic bacteria (Segonzac et al., 1993; Gebruk et al., 2000) or 3) from an autotrophic bacterial population living in the shrimp's gut (Pond et al., 1997; Polz et al., 1998; Zbinden and Cambon-Bonavita, 2003). Fatty acid abundances and carbon isotopic composition recently provided strong evidence that mature *R. exoculata* gain most of their carbon from the epibiotic bacteria within their carapace rather than from bacteria grazed on the chimney walls (Rieley et al., 1999). For shrimps sampled from the Snake Pit site, three bacterial morphotypes were described (Segonzac et al., 1993) which all belonged to the same phylotype of Epsilon*proteobacteria* (Polz and Cavanaugh, 1995). Although attempts to cultivate these microorganims failed until now, they were hypothesized to acquire their metabolic energy from sulfide oxidation (Gebruk et al., 1993; Wirsen et al., 1993). Chemosynthetic activity of the filamentous bacteria from the inner cephalothorax surface has been shown (Wirsen et al., 1993), but no significant increase of CO_2 incorporation was observed in the presence of reduced sulfur compounds (Polz et al., 1998).

More recently, Zbinden et al. (2004) suggested that another metabolic pathway, iron oxidation, could be involved at the iron–rich Rainbow ultramafic site. Unlike most active hydrothermal sites known to date, the hydrothermal circulation at Rainbow is hosted on mantle rocks. As a

* Corresponding author. Tel.: +33 1 44 27 35 02; fax: +33 1 44 27 52 50.
E-mail address: magali.zbinden@snv.jussieu.fr (M. Zbinden).

0022-0981/$ – see front matter © 2008 Elsevier B.V. All rights reserved.
doi:10.1016/j.jembe.2008.03.009

result, its fluid composition departs from the common range of hydrothermal end–members, and is relatively depleted in H_2S and enriched in H_2, FeII and CH_4, as a result of the serpentinization processes (Charlou et al., 2002; Douville et al., 2002).

During the ATOS cruise, shrimps were all collected from the Rainbow site. The main objective of our work was to test the hypothesis that all the shrimp epibionts were sulfide–oxidizers. To overcome the inability to cultivate the epibionts, we performed *in vivo* experiments. For the first time, pressurized aquaria were used to gain information on the bacterial epibionts' metabolism. The aspect and ultrastructure of the bacteria were checked after incubations at 230 bars (*in situ* pressure), at 15 °C (*in situ* temperature) with or without sulfide–enriched seawater (thereafter called sulfide pulses), and compared to in situ reference shrimps. A molecular survey was undertaken to get new insights on possible metabolic type of the epibiotic microbial communities of *Rimicaris exoculata*, particularly thiotrophy using the 5′-adenylylsulfate (APS) reductase gene.

2. Materials and methods

2.1. Animal collection and selection

Specimens of *Rimicaris exoculata* were collected during the French ATOS cruise (June 2001), on the Rainbow vent site (36°14.0′ N, Mid–Atlantic Ridge, 2320 meter depth). Shrimps were collected with the suction sampler of the ROV "Victor 6000", operated from the R/V "L'Atalante". Once on board, some live specimens were immediately dissected into body components. These samples are referred to as "reference shrimps" further in the text. Alternatively, some shrimps were placed in pressure vessels (IPOCAMP™) for *in vivo* experiments (see below) and in this case dissected immediately after removal from the vessel. Scaphognathite samples were fixed in a 2.5% glutaraldehyde–sodium cacodylate buffered solution and later post–fixed in osmium tetroxide for morphological observations. Samples for X–ray analyses were not postfixed. For each treatment, shrimps in anecdysis were selected for observation according to the moult–staging method of Drach and Tchernigovtzeff (1967), by examination of bristle–bearing appendages (uropods) under a light microscope. The moulting stage was later confirmed by examination of the branchiostegite integument by light microscopy and Transmission Electron Microscopy (TEM). For molecular studies, shrimps were frozen immediately after recovery under sterile conditions. Once in the lab, the scaphognathites and branchiostegites were dissected and DNA extraction was performed.

2.2. Pressurized incubator IPOCAMP™

The stainless steel pressure vessel has an internal volume of approximately 19 liters (see Shillito et al., 2001 for detailed description and diagrams). This is a flow–through pressure system, with flow rates that can reach 20 l.h–1. Pressure oscillations arising from pump strokes (100 rpm) are less than 1 bar at working pressure. The temperature of the flowing seawater (filtered at 1 μm mesh) is constantly measured, at pressure, in the inlet and outlet lines (±1 °C). Temperature regulation is powered by a regulation unit (Huber CC 240) that circulates ethylene–glycol through steel jackets surrounding the pressure vessel and around the seawater inlet line.

In vivo experiments. Re–pressurization at 230 bars was achieved in about 2 min after closure of the vessel. As the shrimps were sampled at the end of the dive, less than 2 h passed between the time the samples began decompression (submersible ascent) and the moment they were re–pressurized. At atmospheric pressure, just after the submersible recovery, the shrimps (except for some individuals, which may have been damaged by the suction sampler) were alive and active. Pressure vessel experiments were carried out at *in situ* pressure (230 bars) and at 15 °C, according to the literature data: 10–15 °C (Segonzac et al., 1993); 3.8–14.7 °C (Zbinden et al., 2004); 13.2±5.5 °C (Desbruyères et al., 2001). Previous *in vivo* experiments showed a good physiological state of the shrimps when re–pressurized at these temperature and pressure conditions (Ravaux et al., 2003). Only alive and active shrimps after treatment were used for the present study.

Two experiments at 230 bars were performed:

(1) Sample incubation at 15 °C in surface seawater, to investigate the effect of depletion of electron donors on the shrimps and their epibionts. Twelve shrimps were placed in the pressure vessel, for 30 h. The seawater was regularly (5 times) renewed, by replacing a quarter of the total volume. Surface seawater oxygen level (253 μM) lies slightly above the concentration measured in the environment of the shrimps (Schmidt et al., 2008). These samples are referred to as "non–sulfide shrimps" further in the text.

(2) Incubation at 15 °C, with exposure to sulfide pulses. Nine shrimps were placed in the pressure vessel for 32 h. During the 32 h of the experiment, we first maintained the shrimps in normal sea–water for 8 hours. Then, 4 pulses were performed as follows: i) the inlet of the flow–through pressure system was fed with a reservoir containing 20 l of a solution of 25 μM sulfide in natural surface seawater. This concentration roughly corresponds to the maximum of estimated from the shrimps environment at Rainbow (Schmidt et al., 2008). This moderate concentration also ensured that the oxygen is not fully depleted from the medium. When the reservoir was almost empty, the outlet line was connected to the inlet line, in order to recirculate the sulfide–enriched seawater; ii) After an exposure of one hour, seawater was then pumped into the vessel for 2 h; iii) finally the vessel was closed for 3 h before the next pulse started with a freshly prepared 25 μM sulfide solution. These samples are referred to as "sulfide shrimps" further in the text. The term "re–pressurised shrimps" englobes both "non sulfide" and "sulfide" shrimps.

Survival of the re–pressurized shrimps was determined at the end of the pressure experiments, by identifying each individual and witnessing its movements.

2.3. Light microscopy and transmission electron microscopy (TEM)

Samples were dehydrated in ethanol and propylene oxide series and then embedded in an epoxy resin (Serlabo). Semi–thin and ultra–thin sections were made on a Reichert–Jung Ultramicrotome (Ultracut E) using a diamond knife. Semi–thin sections were stained with toluidine blue for observations by light microscopy (using a Nikon Optiphot–pol microscope and a Zeiss Opton photomicroscope). For ultrastructural observations, thin sections were laid on copper grids and stained with uranyl acetate and lead citrate. Observations were carried out on a Philips 201 TEM, operating at 80 kV.

2.4. Energy dispersive X–ray microanalyses (EDX)

Microanalysis was carried out using a JEOL JEM 2100F transmission electron microscope, operating at 200 kV, and acquired with an energy dispersive X–ray detection system (Tracor 5400 FX), equipped with a Si (Li) diode, using a 2.4 nm probe.

2.5. Ultrastructural analyses and enumeration of bacteria

Exhaustive analysis and enumeration of bacteria and their intracellular granules were undertaken on one individual for each treatment. For each shrimp, bacteria associated to 5 setae of the scaphognathite were analyzed. For each seta, an overall picture was taken and picture of all the bacteria were then captured at a magnification of 20000. Bacteria cells were then counted and described. The occurrence of intracellular granules was noted for each cell. Granules were defined as electron–dense spots larger than 1.5 mm on the pictures (i.e. 75 nm), as numerous dark spots of various sizes occur in the cells. Due to their small size, spots

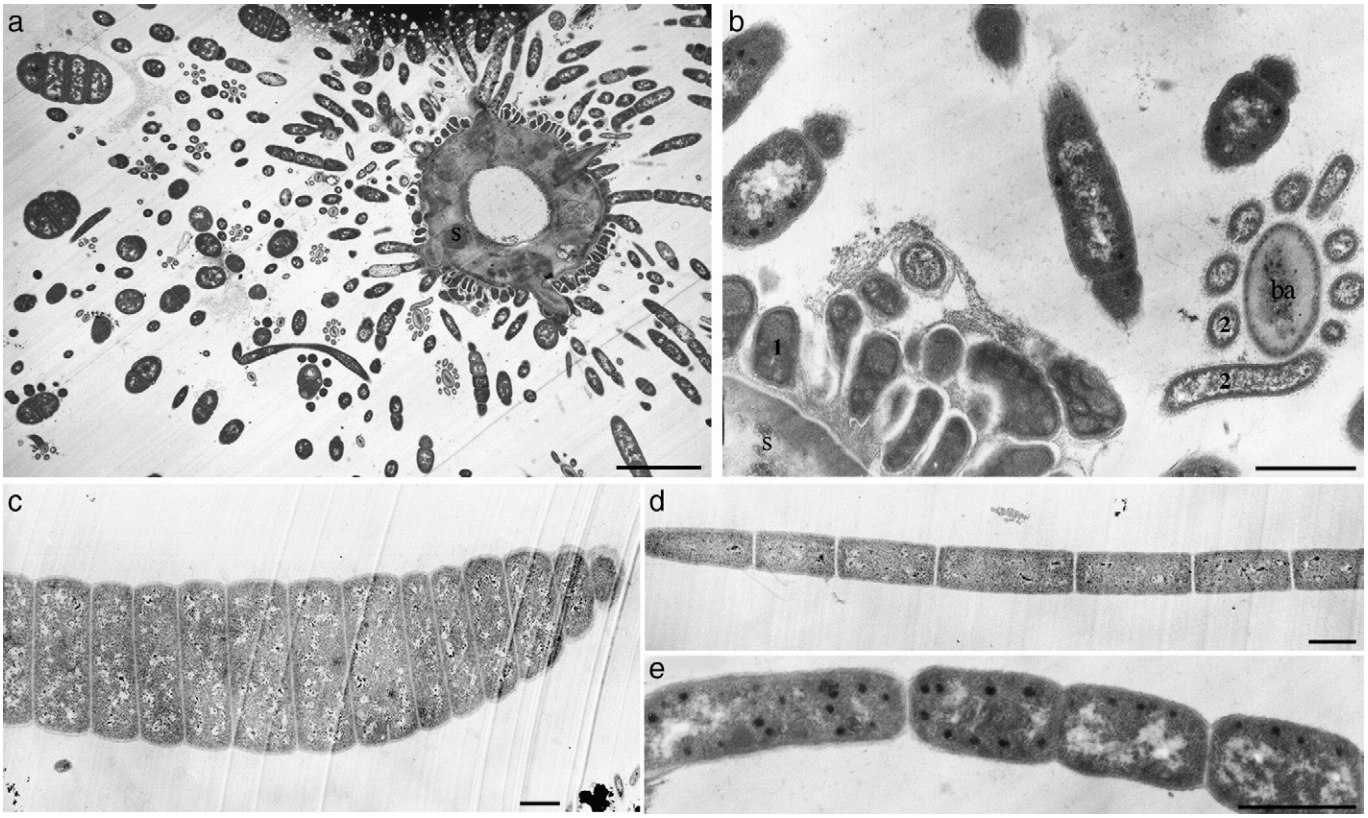

Fig. 1. Bacteria associated with a scaphognathite seta of a reference shrimp. a) General view of the seta (s) and the associated bacteria. b to e) Observed morphotypes: b) rods type (1) attached to the seta (s) and rods type (2) attached to the barbula (ba); c) large filaments; e) thin filaments without granules inside the cells; d) thin filaments with granules. Scale bars: a=5 μm, b, c, d, e=1 μm.

smaller than 75 nm cannot be analyzed by EDX and were not taken into account in this study because of the uncertainty on their nature.

2.6. Statistical analyses

A one–way ANOVA was used to test differences in the state of the bacteria (i.e. percentage of full granules) among treatments. Normality was judged visually from normal probability plots and homogeneity of variances was verified with the Levene test. A multiple range test using the Student-Newman-Keuls (SNK) procedure was performed to investigate the difference between treatments for significant results. All data analyses were carried out using Statistica v. 6 software.

2.7. DNA extraction

One *in situ* reference shrimp was dissected under sterile conditions. DNAs from scaphognathite (SC) and branchiostegite (LB), were extracted using the FastDNA SPIN kit for soil samples (Bio 101 System, Qbiogen) following the kit protocols.

2.8. PCR and cloning

PCR were performed using the universal primers for Bacteria or Archaea 16S rDNA on both (SC and LB) extracted DNA samples: E8F (AGA GTT TGA TCA TGG CTC AG) and U1492R (GTT ACC TTG TTA CGA CTT) for Bacteria and A8F (CGG TGG ATC CTG CCG GA) and A1492R (GGC TAC CTT GTT ACG ACT T) for Archaea. PCR cycles were as follows: 1 cycle of 3 min at 94 °C, 30 cycles of 1 min at 94 °C, 1 min 30 at 49 °C and 2 min at 72 °C and 1 cycle of 6 min at 72 °C.

The gene encoding particulate methane monooxygenase subunit A (*pmoA*) was amplified on the SC DNA using the primers described by Duperron et al. (2007) A189F (GGN GAC TGG GAC TTC TGG) and MB661R (cg gmg caa cgt cyt tac C). PCR cycles were as follows: 1 cycle of 4 min at 92 °C, 30 cycles of 1 min at 92 °C, 1 min 30 at 55 °C and 1 min at 72 °C and 1 cycle of 9 min at 72 °C.

The gene encoding the APS reductase gene was amplified on the SC DNA using the primers designed before (Blazejak et al., 2005). PCR cycles were as follows: 1 cycle of 4 min at 92 °C, 30 cycles of 1 min at 92 °C, 1 min 30 at 58 °C and 1 min at 72 °C and 1 cycle of 9 min at 72 °C.

Approximately 100 ng of bulk DNA was amplified in a 50 μl reaction mix containing (final concentration): 1X Taq DNA polymerase buffer (Q biogen Starsbourg, France), 2 μM of each dNTP, 20 μM of each primer and 2.5 U of Taq DNA polymerase (Q Biogen France). PCR products were then visualized on an agarose gel containing ethidium bromide before cloning. The PCR products were cloned with the TOPO TA Cloning kit (Invitrogen Corp., San Diego CA USA) following to the manufacturer's protocol. PCR products were purified using the QIAquick PCR purification kit (Qiagen SA, Grenoble, France) following the manufacturer's instructions. Clone libraries were constructed by transforming *E. coli* TOP10F'. Clones were selected on Petri dishes containing ampicilline (50 μg/ml) and XGAL and IPTG for the white–blue selection. White clones were then cultured and treated for sequencing at the "Ouest Genopole Plateforme" (Roscoff, France, http//www.sb-roscoff.fr/SG/) on a Abi prism 3100 GA (Applied Biosystem), using the Big–Dye

Table 1
Cell sizes of the various bacterial morphotype observed (values are given in μm and correspond to the upper values measured)

	Cell diameter	Cell height
Large filament	5,5	2,45
Thin filament (1)	1,1	2,35
Thin filament (2)	1,5	2,75
Thick rods (type 1)	0,6	1,25
Thin rods (type 2)	0,3	3

Terminator V3.1 (Applied Biosystem) following the manufacturer's instructions.

2.9. Phylogenetic analyses

To determine approximate phylogenetic affiliations, sequences were compared to those available in databases using the BLAST network service (Altschul et al., 1990). Alignments of 16S rDNA sequences were performed using CLUSTALW (Thompson et al., 1994), further refined manually using SEAVIEW (Galtier et al., 1996). The trees were constructed by PHYLO-WIN (Galtier et al., 1996). Only homologous positions were included in the phylogenetic comparisons. For the 16S rDNA phylogenetic reconstruction, the robustness of inferred topology was tested by bootstrap resampling (500) (Felsentein, 1985) of the tree calculated on the basis of evolutionary distance (Neighbor-Joining-algorithm; Saitou and Nei 1987) with Kimura 2 correction. Sequences displaying more than 97% similarity were considered to be related, and grouped in the same phylotype. Phylogenies of amino acid sequences of the *pmoA* (154 aa) and APS (129 aa) were reconstructed using PHYLO–WIN with Neighbor-Joining-algorithm and PAM distance (according to Dayhoff's PAM model). The robustness of the inferred topology was tested by bootstrap resampling (500).

Nucleotide sequence accession numbers. Sequences have been deposited at EMBL with accession numbers: from AM412507–AM412521 and from AM902724–AM902731 for partial 16S rDNA sequences; from AM412502–AM412506 for partial *pmoA* (particulate methane monooxygenase subunit A) gene; and from AM902732–AM902736 for APS reductase gene.

3. Results

3.1. Morphology and ultrastructure of the epibionts

A total of 315 pictures was analyzed on which 6567 bacterial cells were counted. On *in situ* reference shrimps, TEM observations of the scaphognathite bacteria revealed more morphological diversity (Fig. 1) than previously described by Scanning Electron Microscopy (SEM) studies (Segonzac et al., 1993; Zbinden et al., 2004).

We observed 3 types of filaments (two thin types and one large) and two types of rods. Dimensions are in the range of those previously found (Table 1). Two types of rods can be distinguished based on size, location and aspect of the intracellular contents. The first type (Fig. 1b) is characterized by short and thick cells, with a dense dark intracellular content. They are mainly located on the setae. The second type (Fig. 1b) is longer and thinner, with a light intracellular content. These rods are mainly located on the barbula that emerge from the setae. Two types of thin filaments can be distinguished based on the aspect of the intracellular contents: i) a small number of thin filaments exhibit rectangular cells with no marked narrowing between two adjacent cells. Cells in these filaments show a homogeneous and dense content, with few electron light areas and no granules (Fig. 1d); ii) the others, more numerous, exhibit ovoid–shaped cells, with marked narrowing between two adjacent cells. Cells of these filaments have a more heterogeneous intracellular content (which seems denser at the periphery and more diffuse in the center) and contain granules (Fig. 1e).

Ultrastructural changes are observed between the bacteria of re–pressurised shrimps and those of reference shrimps (Fig. 2). No

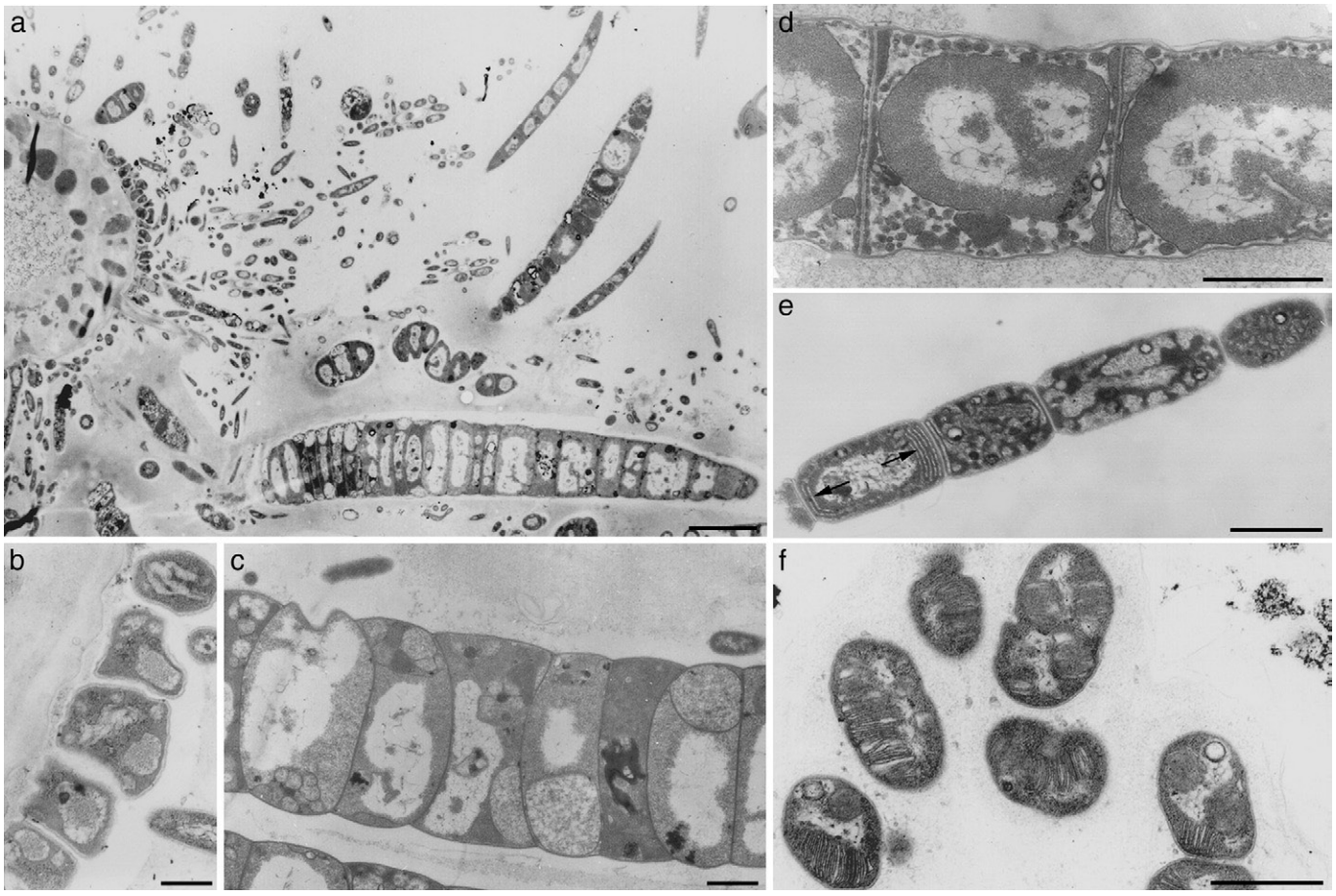

Fig. 2. Bacteria associated with a scaphognathite seta of the re–pressurised shrimps. a) General view of the seta and the associated bacteria. b to e) Observed ultrastructural modifications: b) type 1 rods (type 2 does not seem to be affected); c) large filaments with heterogeneous content; d) or with globular content; e) thin filaments with heterogeneous content (d), and occasionally occurrence of membrane folds at the boundary of the cell (arrows). (f) methanotrophic bacteria characterized by their stacks of intracytoplasmic membranes. Scale bars: a=5 μm; b=0.5 μm; c, d, e, f=1 μm.

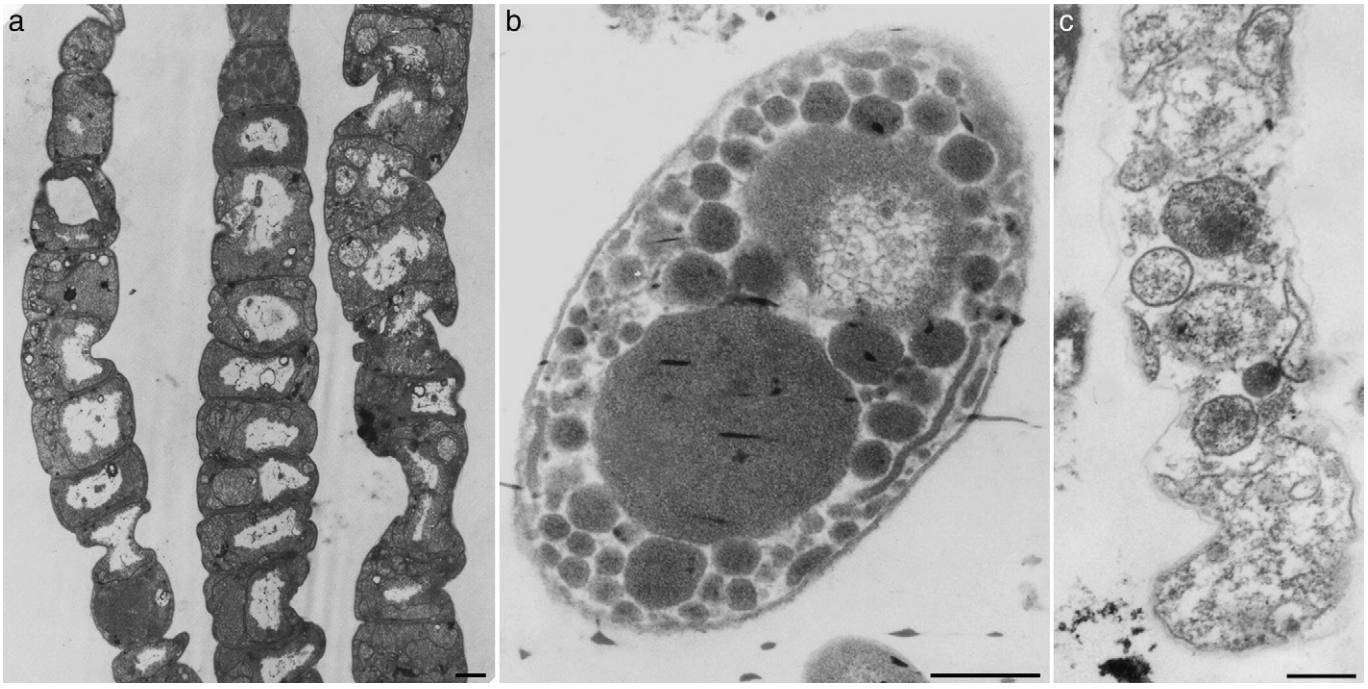

Fig. 3. Evolution of the morphotypes observed in the re–pressurised shrimps. Filament cells exhibit a mis shapen aspect (a), a completely globular content (b) or appear as ghosts (c). Scale bars: a = 1 μm; b, c = 0.5 μm.

significant morphological differences were noticed between the bacteria of the shrimps from both pressure experiments. Cells of large and thin filaments, as well as thick rods, have a less regular shape and exhibit a more heterogeneous intracellular content than those of reference shrimps (Fig. 2b–c). Only thin rods keep the ultrastructal aspect observed in reference shrimps. Some of the bacteria show a globular intracellular content (Fig. 2d) or additional membrane folds (Fig. 2e). These types are only observed among bacteria of the shrimps maintained at 230 bars. Occasionally, these morphotypes can have a very degraded aspect, with totally mis–shapen cells (Fig. 3a), completely globular cell contents (Fig. 3c) or cell ghosts (Fig. 3c). Cell ghosts are also occasionally observed among bacteria of reference shrimps where they represent 1.5 to 4% of all the bacteria, and may be due to the usual turn–over of the cells. Cells with irregular shape and contents account for up to 30% of all cells in the re–pressurised shrimps and ghosts up to 15% (intra–individual variation between the five setae is too high to test the significance of inter–individual variations and the effect of sulfide exposure). Furthermore, very few dividing cells were observed for re–pressurised shrimps, whereas they were numerous for in situ reference shrimps. Surprisingly we observed, for the first time among *R. exoculata* epibionts (in reference shrimps, as well as in re–pressurised ones), some bacteria with stacks of intracytoplasmic membranes typical of methanotrophs (Fig. 2f) in both reference and re–pressurised shrimps.

3.2. Intracellular electron dense granules

Only granules larger than 75 nm in diameter were considered, the largest measuring up to 200 nm. Spots under 75 nm were counted separately, as "spots". The number of granules and spots is higher for reference shrimps than for re–pressurised ones (Table 2). Granules occurred only in one type of thin filament, and are absent from thick filaments and rods. A given cell may contain several granules and spots (up to 7 granules and 10 spots per cell).

In the reference shrimps, most of the granules appear full (i.e they are electron dense and appear black on micrographs, Fig. 4a), whereas most appear partially or completely empty for the re–pressurised shrimps (i.e they are electron light and appear, at least partly white on micrographs, Fig. 4b). Percentage of full granules for each experiment

Table 2
Total numbers of bacteria analyzed, with number of granules and spots for each treatment

	Bacterial cells	Granules	Spots
Reference shrimps	1574	721	875
Non–sulfide shrimps	3110	911	219
Sulfide shrimps	1883	628	207

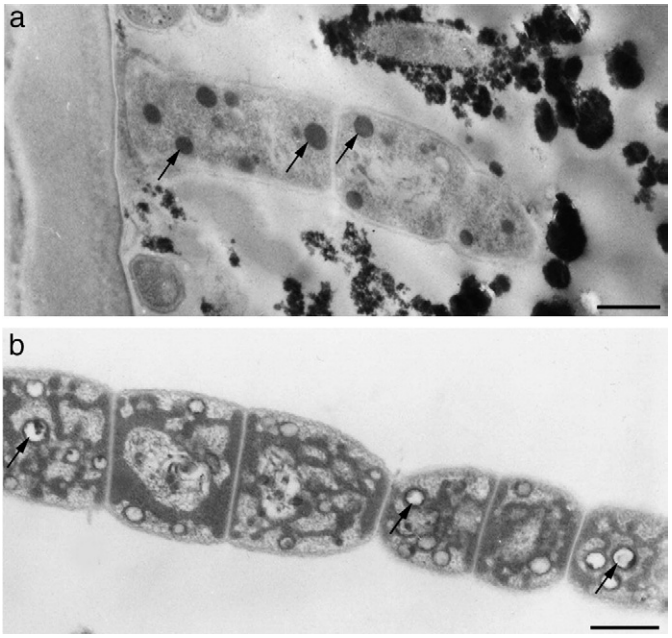

Fig. 4. Bacterial intracellular granules. Granules are full (arrows) in bacteria associated with the reference shrimp (a) and mostly empty (arrows) in those associated with re–pressurised shrimps (b). Scale bars: a, b = 0.5 μm.

are illustrated on Fig. 5. The percentage of full granules differs significantly between reference and re–pressurised shrimps (one–way ANOVA test; $F=76.942$, $p<10^{-6}$), although no significant difference was detected between sulfide and non–sulfide shrimps at 230 bars (SNK a posteriori test, $p>0.05$).

3.3. Chemical composition of granules

An EDX microanalysis was performed in order to determine the elemental composition of the granule content (Fig. 6). The control spectrum from the cytoplasmic area of the bacteria showed copper (Cu) peaks due to the support grid, uranyl (U) peaks due to uranyl acetate staining, and traces of chloride (Cl) due to the epoxy resin. Two types of granules were analyzed. The first type contains 2 main peaks: phosphorus (P) and iron (Fe), in some cases associated with small amounts of calcium (Ca) (not shown). The second type of granules shows a single peak of sulfur (S). Occasionally, traces of iron (Fe) are detected (but it can be due to the close occurrence of a thick iron oxide layer that surrounds some bacteria).

3.4. Preliminary screening of bacterial diversity

DNA was successfully extracted from scaphognathite and branchiostegite samples. PCR amplifications for Archaea failed regardless of the conditions tested, even with nested PCR. For Bacteria, 69 clones were sequenced for the scaphognathite and 56 for the branchiostegite of a reference shrimp. Only 53 clones sequences were kept for the scaphognathite sample and 46 for the branchiostegite sample, the other clone sequences being too short or of bad quality. No chimera was detected in our study.

All the sequences are related to the *Proteobacteria* cluster (Fig. 7), mainly within the Epsilon and Gamma groups, the Alpha and Delta-*proteobacteria* being less abundant. One group of 19 sequences is related to the *R. exoculata* gut clone 15, found in a previous study on the gut of a specimen from the same vent site (Zbinden and Cambon-Bonavita, 2003). A second group of 13 sequences is related to sequences retrieved from a vent gastropod coming from Rodriguez Triple junction in the Indian Ocean (Goffredi et al., 2004). A third group (5 clone sequences) is related to the *Rimicaris exoculata* epibiont (Polz and Cavanaugh, 1995). Nineteen clones sequences are related to the *Rimicaris exoculata* gut clone 22 (Zbinden and Cambon-Bonavita, 2003). Six clone sequences are related to the Delta*proteobacteria*. Twenty four sequences are affiliated

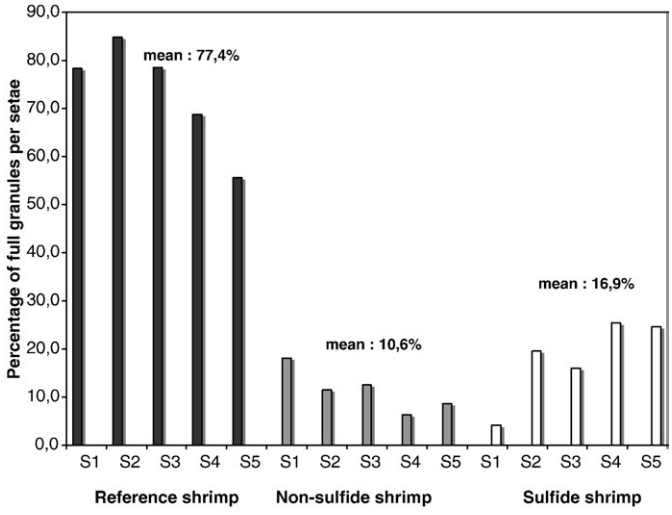

Fig. 5. Percentage of full granules in bacteria according to treatment. Diagram showing the percentage of full granules per seta for *in situ* reference shrimp, and re–pressurised shrimps either in seawater or submitted to sulfide pulses. The mean percentage for each treatment is also given.

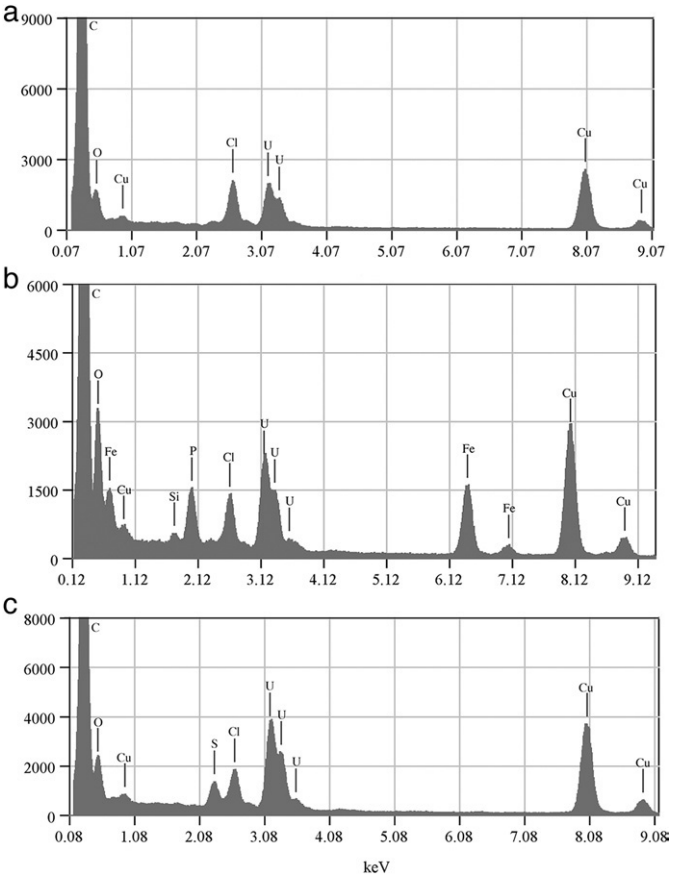

Fig. 6. Elemental X–ray microanalyzes of the bacterial intracellular granules. Spectra were obtained on a) the cytoplasm of the bacteria (as control), b) the first type of granule showing major Fe and P peaks and traces of Si, c) the second type of granule, showing one major S peak.

to the Gamma*proteobacteria*. These latter are related to sequences retrieved on a vent gastropod (Goffredi et al., 2004) and also to clone sequences retrieved on carbonate chimney from the Lost City vent field (Brazelton et al., 2006). The last group comprises eight clones, related to the Alpha*proteobacteria*, close to *Marinosulfomonas methylotropha*, and to a clone isolated from Lost City vent field (Brazelton et al., 2006).

3.5. pmoA and APS sequence analyses

We successfully amplified the *pmoA* and APS reductase genes using DNA extracted from the scaphognathite. Fifteen clones were sequenced for the *pmoA* and 5 for the APS reductase. All the sequences were kept for the phylogenetic analyses. For the *pmoA* gene (Fig. 8), two clone sequences are affiliated to the *Methylobacter* sp. group, two clones sequences are affiliated to a *Bathymodiolus* symbiont sequence and 11 clones sequences are affiliated to the *Methylomonas methanica*. For the APS reductase gene (Fig. 9), 5 sequences were related to the Delta*proteobacteria*. Ninety sequences were only marginally related to the Gamma*proteobacteria* APS gene (83% of similarity) and were related to the Idas thiotrophic clone (Duperron et al., 2008).

As no genes, until now, of the iron–oxidation pathway for neutrophilic iron–oxidizing bacteria are known, this metabolic pathway cannot be investigated by this method.

4. Discussion

4.1. Is sulfide oxidation active in the epibiotic community?

Transmission electron microscopy allowed us to refine the morphological descriptions of the epibionts on the reference shrimps, detecting

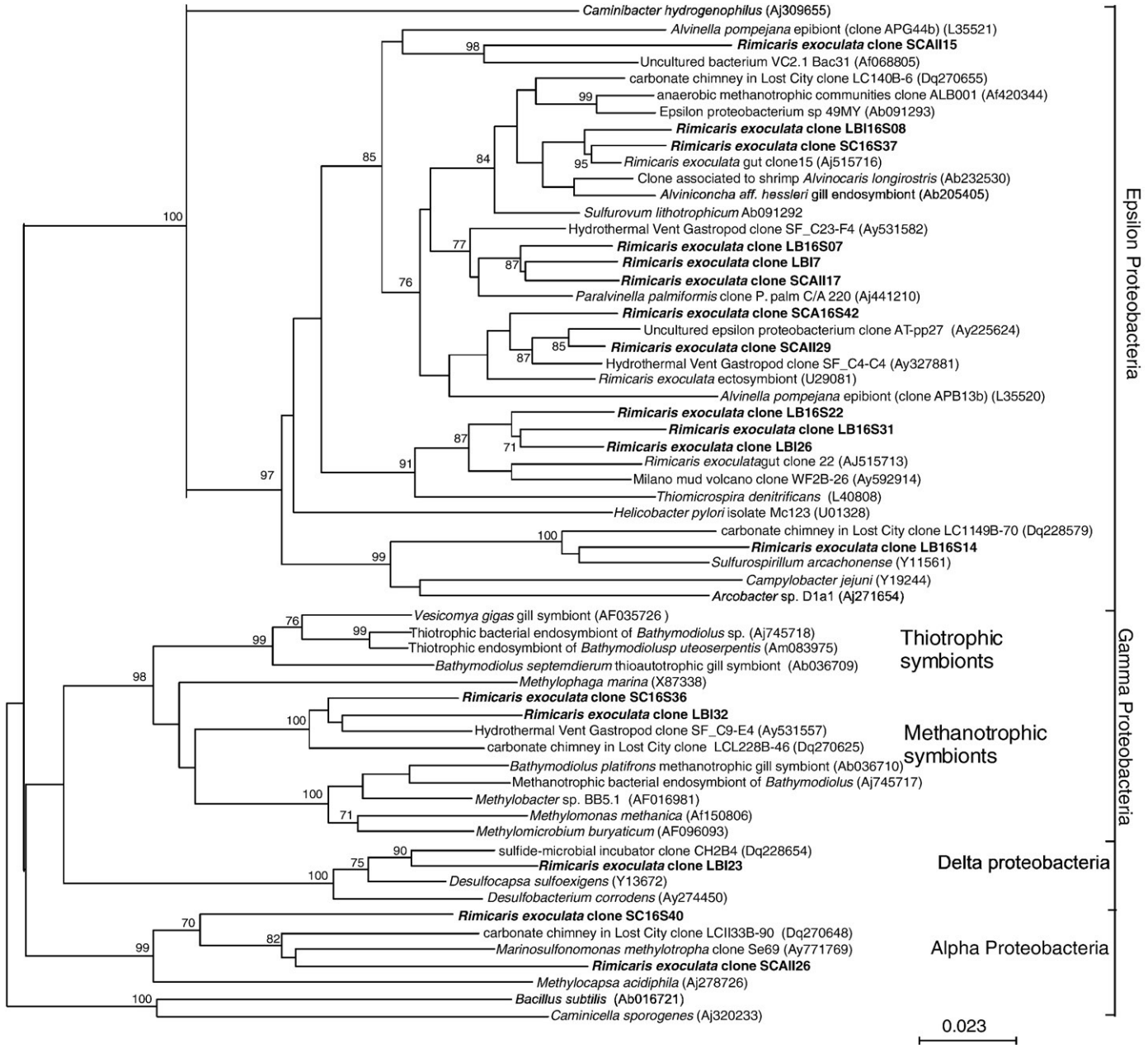

Fig. 7. Phylogenetic trees obtained using Neighbor–Joining analysis with bootstrap resampling (500 replicates). Topologies were confirmed with Maximum Parsimony method. Bootstrap values are indicated on nodes above 70%. Accession numbers of the sequences used are indicated on the tree (from AM412507–AM412521 and from AM902724–AM902731).

two types of thin filaments, and two types of rods, in addition to the thick filaments. These results indicate that the morphological diversity of bacteria associated with *R. exoculata* is higher than previously reported (Casanova et al., 1993; Gebruk et al., 1993; Zbinden et al., 2004). The molecular survey supports this result. Even though additionnal sequence investigations are needed to fully describe the microbial diversity within the gill chamber, the present study provides a preliminary overview of the epibiotic community composition. Many Epsilon*proteobacteria* sequences are related to microbial diversity usually associated with various hydrothermal invertebrates (*Alvinella pompejana*: Alain et al., 2002; *Paralvinella palmiformis*: Alain et al., 2004; gastropods: Goffredi et al., 2004; Suzuki et al., 2005; and *Rimicaris exoculata* gut: Zbinden and Cambon-Bonavita, 2003) and to the MAR environment (Lopez-Garcia et al., 2002). Only five sequences are slightly related to "*Rimicaris exoculata* ecto–epibiont". The Delta*proteobacteria* diversity is restricted to one cluster, and is related to an uncultured bacterium colonizing the mineral surfaces of a sulfide–microbial incubator. These microorganisms are usually thought to play a role in the sulfur cycle. In addition, we obtained APS reductase gene sequences that are related to those of the *Desulfobulbaceae* (Friedrich, 2002) known to be thiotroph. Most of the APS gene sequences obtained were related to the *Idas* thiotrophic symbiont gene (Duperron et al., 2008), which is a Gamma*proteobacteria*, but with a low level of similarity (83%). In our phylogenetic survey, we did not obtain 16S rDNA gene sequences related to thiotrophic Gamma*proteobacteria*, so it is unlikely that our APS gene sequences are related to these Gamma*proteobacteria*. As no Epsilon*proteobacteria* APS gene sequence is available in databanks, our APS gene sequences are more likely related to the numerous Epsilon*proteobacteria* identified in the phylogenetic survey. It is noteworthy that the APS gene can be transferred laterally among Bacteria. It is therefore not a good phylogenetic marker (Friedrich, 2002; Meyer and Kuever, 2007).

Bacteria associated with re–pressurised shrimps exhibit different ultrastructures compared to the reference shrimps. A mean of 30% of the epibionts display what we interpret as a degraded aspect (i.e.

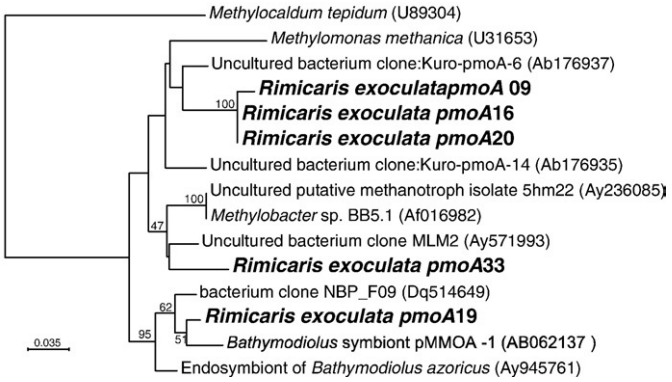

Fig. 8. Neighbor–Joining tree of *pmoA* amino acid sequences from *Rimicaris exoculata* gill chamber epibionts based on 154 amino acid positions using PAM distance (according to Dayhoff's PAM model). The robustness of the inferred topology was tested by bootstrap resampling (500). Accession numbers of the sequences used are indicated on the tree (from AM412502 to number AM412506).

heterogeneous or globular cellular content, irregular wall shapes, cell ghosts). In addition, the number of dividing cells is higher for the reference shrimps, indicating a better physiological state. These results could indicate that some of the bacteria cannot withstand the chemical environment of the re–pressurisation experiments, whether or not sulfides are present.

TEM observations of the epibionts reveal the massive occurrence of intracellular granules. Such granules are often present in prokaryotic organisms (Shively, 1974). They comprise polyglucoside, polyphosphate granules, crystals or paracrystalline arrays such as magnetosomes (Fe_3O_4), poly-β-hydroalkanoate (PHA) and sulfur globules. The main roles of these granules are hypothesized to be storage forms of energy and/or of various compounds such as carbon, sulfur and phosphates. They can also play a part in detoxification processes. X–ray analyses indicate that there are two type of granules, one type containing phosphorus (P) and iron (Fe), most probably under polyphosphate form; the other type containing mainly sulfur (S). Several granules can occur in one bacterial cell, but they are always of the same type. The maintenance in a pressurized aquarium lead to the emptying of most of the granules, which suggests a storage role. Addition of sulfide does not affect this emptying phenomenon. However, the granules were counted as a whole, as it was no longer possible to morphologically distinguish the polyphosphate from the sulfur granules. It is conceivable that the slightly higher percentage of full granules, counted in the bacteria that received sulfide pulses (see Fig. 5), is due to a better conservation of the sulfur granules. *R. exoculata* epibionts (from the Snake Pit site) were hypothesized to acquire their metabolic energy from sulfide oxidation. At the ultrastructural level, sulfur–oxidizing bacteria are characterized by the accumulation of large granules of elemental sulfur, which is known to dissolve in solvents like those commonly used for classical TEM preparations (Vetter, 1985). Consequently, these globules appear empty in thin sections (Lechaire et al., 2006). On our sections, the granule contents were not removed during preparation steps, which suggests that they are not elemental sulfur under the form usually found in sulfur–oxidizing bacteria. We can then hypothesize that these granules are rather formed of another type of more stable cristalline sulfur or are sulfur–rich organic matter. Nevertheless, sulfur–containing biopolymers are rare: they are mostly proteins containing methionine and cysteine, or complex polysaccharides that contain sulfate groups. PTE (polythioester), a new class of sulfur–containing polymer, has recently been described, (Lütke-Eversloh et al., 2001). It belongs to the polyhydroxyalkanoates (PHAs), a class of biopolymers known to occur abundantly as storage compounds for energy and carbon, in a large variety of bacteria and archaea (Anderson and Dawes, 1990).

Taken all together, the TEM observations of bacteria associated to re–pressurised shrimps show a low positive impact of sulfide re-exposure. Three hypotheses could thus be put forward to explain this: 1) the concentration and frequency of the pulses were insufficient to allow a good maintenance of the epibionts, or 2) these bacteria do not all rely on sulfide for their growth, or 3) the chemical composition of the fluid in the pressure vessel was not adapted for epibiont growth that may require more complex substrates as suggested by the lack of cultures despite many attempts. Considering the results of previous work on the epibionts of *R. exoculata* (Zbinden et al., 2004) and the chemistry of this peculiar environment: low sulfide but high iron and methane concentration (Charlou et al., 2002; Douville et al., 2002), it is possible that some bacteria do not rely on sulfide oxidation but rather on iron or methane oxidation.

4.2. Occurrence of iron oxidation among the epibiotic community

Genes involved in iron oxidation at neutral pH are still unknown and iron oxidizers show a broad diversity among the *Proteobacteria* (Edwards et al., 2003). So, iron oxidation metabolism could not be studied through a molecular approaches. Nevertheless, iron polyphosphate granules were detected inside the epibiont cells. Polyphosphate granules are widely distributed in prokaryotes, ranging in diameter from 48 nm to 1μm (Shively, 1974). Putative roles of polyphosphate are numerous: ATP substitute, energy storage or chelator of metal ions (Kornberg, 1995). Lechaire et al. (2002) described the occurrence of iron polyphosphates granules in bacteria associated with the tube of *Riftia pachyptila*, a hydrothermal vent vestimentiferan. Since polyphosphates are known to fluctuate in response to nutritional and other parameters, these authors suggest that they could act as a reservoir of

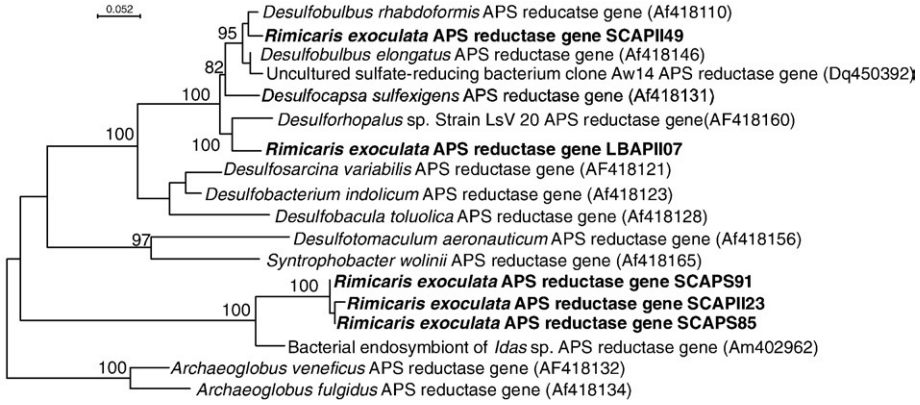

Fig. 9. Neighbor–Joining tree of APS reductase amino acid sequences from *Rimicaris exoculata* gill chamber epibionts based on 129 amino acid positions using PAM distance (according to Dayhoff's PAM model). The robustness of the inferred topology was tested by bootstrap resampling (500). Accession numbers of the sequences used are indicated on the tree (from AM902732–AM902736).

oxygen in the case of environmental anoxia. As the occurrence of iron–oxidizers among the bacteria has been suggested (Zbinden et al., 2004), these granules could be a reservoir for iron. Alternatively, if these granules occur in non–iron oxidizing bacteria, the chelation of iron by the polyphosphate granules could reduce its toxicity for the cell.

Anyway, the only way to certify the occurrence of iron–oxidizing bacteria among the epibionts is to successfully cultivate and isolate these strains. Such attempts are under progress in our lab.

4.3. A possible alternative metabolism: methanotrophy and methylotrophy

A sixth morphotype, bacteria with stacks of intracytoplasmic membranes typical of type I methanotrophs, was observed for the first time among *R. exoculata* epibionts. Moreover, our sequences cluster with known Gamma*proteobacteria* methanotrophic epibionts sequences, such as *Bathymodiolus* methanotrophic gill symbionts (Duperron et al., 2005). This is also supported by our three groups of *pmoA* sequences that clearly belong to the methylotrophic Gamma*proteobacteria* class (*Methylomonas* sp., *Methylobacter* sp. and *Bathymodiolus pmoA* gene sequences). In addition, some clone sequences are related to Alpha*proteobacteria* methylotroph species and to Epsilon*proteobacteria* clone sequences retrieved from enriched–methane environments such as the MAR Lost City and Rainbow sites, or to the Milano mud volcano (Fig. 7).

4.4. Co–occurrence of different metabolic types in the epibiotic community

Taken all together, our microscopic observations and molecular data indicate that at least three metabolic types could co–occur among the epibiotic microbial community associated to *R. exoculata* at Rainbow: iron–oxidation, methanotrophy and thiotrophy.

Desbruyères et al. (2001) tried to correlate biological diversity to the varying composition of end–member fluids. According to the amount of iron oxide closely associated to the epibionts (Zbinden et al., 2004), and to the high level of ferrous iron in the pure fluids (Charlou et al., 2002), we suggest that iron oxidation may be the dominant metabolism for this site. Recently, Salerno et al. (2005) correlated the relative microbial abundance of epibiont types of two species of mussels (*Bathymodiolus azoricus* and *B. heckerae*) with the availability of CH_4 and dissolved H_2S in the end–member fluids. They found that when the CH_4:H_2S ratio was less than 1 (as for Snake Pit, Campbell et al., 1988) then thiotrophic epibionts were dominant. If the ratio was greater than 2 (as for Lost City, Kelley et al., 2001) then methanotrophs were the dominant epibionts. For Rainbow, the ratio of CH_4:H_2S varies from 1.54 to 2.61 in pure fluids (Charlou et al., 2002). Applying the Salerno et al. (2005) empirical model to *Rimicaris* epibionts at Rainbow, would suggest that methanotrophy is an important metabolic pathway, possibly dominating sulfide oxidation. Sampling and *in situ* measurements in shrimp swarms provide nevertheless a more realistic picture of the environmental conditions experienced by the shrimps. A recent study on potential electron donors for microbial primary production within the swarms at Rainbow indicates that ferrous iron is the most favorable energy source to support epibiotic growth. Methane and sulfide would appear as secondary energy sources in this environment, where hydrogen could also represent an altenative energy source for the epibionts (Schmidt et al., 2008).

5. Conclusion

Based on TEM observations, and a preliminary molecular survey, the diversity of the *Rimicaris exoculata* epibionts (in terms of morphology and metabolism) appears to be higher than previously reported. Based on these results, we propose that the three metabolic types (iron, sulfur and methane oxidation) co–occur within the epibiont biomass associated with *Rimicaris exoculata*, and that the relative contribution of each metabolism may differ according to the local fluid chemical composition. A much wider scale study, with animals collected from chemically contrasted environments, is needed to better understand the connections of the epibiotic bacterial communities in response to the chemistry of the environment.

Acknowledgements

The authors wish to thank P.M. Sarradin, chief scientist of the ATOS cruise, as well as the captain and crew of the R/V Atalante and the Victor ROV team. The authors also thank Eric Thiébaut for his help with the statistical analyses, and Philippe Compère for his help in determination of the moulting stages. The authors are also grateful to Stephane Hourdez for his review of the manuscript. Electron microscopy was performed at the Service de Microscopie Electronique, IFR 83 de Biologie Integrative-CNRS/Paris VI. This work was partly funded with the help of the MOMARNET and VENTOX (EVK3 CT-1999-0003) programs, Ifremer research institute and Région Bretagne and Ouest Génopole. **[SS]**

References

Alain, K., Olagnon, M., Desbruyères, D., Page, A., Barbier, G., Juniper, K., Quérellou, J., Cambon-Bonavita, M., 2002. Phylogenetic characterization of the bacterial assemblage associated with the hydrothermal vent polychaete *Paralvinella palmiformis*. FEMS Microbiol. Ecol. 42, 463–476.

Alain, K., Zbinden, M., Le Bris, N., Lesongeur, F., Querellou, J., Gaill, F., Cambon-Bonavita, M.-A., 2004. Early steps of colonisation processes at deep–sea hydrothermal vents. Environ. Microbiol. 6 (3), 227–241.

Altschul, S., Gish, W., Miller, W., Myers, E., Lipman, D., 1990. Basic local alignment search tool. J. Mol. Biol. 215, 403–410.

Anderson, A., Dawes, E., 1990. Occurence, metabolism, metabolic role, and industrial uses of bacterial polyhydroxyalkanoates. Microbiol. Rev. 54 (4), 450–472.

Blazejak, A., Erseus, C., Amann, R., Dubilier, N., 2005. Coexistence of bacterial sulfide oxidizers, sulfate reducers, and spirochetes in a gutless worm (Oligochaeta) from the Peru margin. Appl. Environ. Microbiol. 71, 1553–1561.

Brazelton, W., Schrenk, M., Kelley, D., Baross, J., 2006. Methane- and sulfur–metabolizing microbial communities dominate the Lost City hydrothermal field ecosystem. Appl. Environ. Microbiol. 72 (9), 6257–6270.

Campbell, A., Palmer, M., Klinkhammer, G., Bowers, T., Edmond, J., Lawrence, J., Casey, J., Thompson, G., Humphris, S., Rona, P., Karson, J., 1988. The chemistry of springs on the Mid–Atlantic Ridge. Nature 335, 514–519.

Casanova, B., Brunet, M., Segonzac, M., 1993. L'impact d'une épibiose bactérienne sur la morphologie fonctionnelle de crevettes associées à l'hydrothermalisme médio–Atlantique. Cah. Biol. Mar. 34, 573–588.

Charlou, J.L., Donval, J.P., Fouquet, Y., Jean-Baptiste, P., Holm, N., Caccavo, F., 2002. Geochemistry of high H_2 and CH_4 vent fluids issuing from ultramafic rocks at the Rainbow hydrothermal field (36°14′N, MAR). Chem. Geol. 191, 345–359.

Desbruyères, D., Biscoito, M., Caprais, J.C., Colaço, A., Comtet, T., Crassous, P., Fouquet, Y., Khripounoff, A., Le Bris, N., Olu, K., Riso, R., Sarradin, P.M., Segonzac, M., Vangriesheim, A., 2001. Variations in deep–sea hydrothermal vent communities on the Mid–Atlantic Ridge near the Azores plateau. Deep–sea Res. Ptl 48, 1325–1346.

Douville, E., Charlou, J.L., Oelkers, E.H., Bienvenu, P., Jove Colon, C.F., Donval, J.P., Fouquet, Y., Prieur, D., Appriou, P., 2002. The rainbow vent fluids (36°14′N, MAR): the influence of ultramafic rocks and phase separation on trace metal content in Mid–Atlantic Ridge hydrothermal fluids. Chem. Geol. 184, 37–48.

Drach, P., Tchernigovtzeff, C., 1967. Sur la méthode de détermination des stages d'intermue et son application générale aux Crustacés. Vie Milieu 18A, 595–609.

Duperron, S., Nadalig, T., Caprais, J., Sibuet, M., Fiala-Médioni, A., Amann, R., Dubilier, N., 2005. Dual symbiosis in a *Bathymodiolus* sp. mussel from a methane seep on the Gabon continental margin (Southeast Atlantic): 16S rRNA phylogeny and distribution of the symbionts in gills. Appl. Environ. Microbiol. 71 (4), 1694–1700.

Duperron, S., Fiala-Médioni, A., Caprais, J.C., Olu, K., Sibuet, M., 2007. Evidence for chemoautotrophic symbiosis in a Mediterranean cold seep clam (Bivalvia: Lucinidae): comparative sequence analysis of bacterial 16S rRNA, APS reductase and RubisCO genes. FEMS Microbiol. Ecol. 59 (1), 64–70.

Duperron, S., Halary, S., Lorion, J., Sibuet, M., Gaill, F., 2008. Unexpected co–occurrence of six bacterial symbionts in the gills of the cold seep mussel *Idas* sp. (Bivalvia: Mytilidae). Environ. Microbiol. 10 (2), 433–445.

Edwards, K., Rogers, D., Wirsen, C., McCollom, T., 2003. Isolation and characterization of novel psychrophilic, neutrophilic, Fe–oxidizing, chemolithoautotrophic α- and γ-*Proteobacteria* from the deep–sea. Appl. Environ. Microbiol. 69 (5), 2906–2913.

Felsentein, J., 1985. Confidence limits on phylogenies: an approach using the bootstrap. Evolution 30, 783–791.

Friedrich, M., 2002. Phylogenetic analysis reveals multiple lateral transfers of adenosine-5′-phosphosulfate reductase genes among sulfate–reducing microorganisms. J. Bacteriol. 1 (1), 278–289.

Galtier, N., Gouy, M., Gautier, C., 1996. SEAVIEW and PHYLO_WIN: two graphic tools for sequence alignment and molecular phylogeny. Comput. Appl. Biosci. 12, 543–548.

Gebruk, A., Pimenov, N., Savvichev, A., 1993. Feeding specialization of bresiliid shrimps in the TAG site hydrothermal community. Mar. Ecol. Prog. Ser. 98, 247–253.

Goffredi, S., Waren, A., Orphan, V., Van Dover, C., Vriejenhoek, R., 2004. Novel forms of structural integration between microbes and a hydrothermal vent gastropod from the Indian Ocean. Appl. Environ. Microbiol. 70 (5), 3082–3090.

Kelley, D., Karson, J., Blackman, D., Früh-Green, G., Butterfield, D., Lilley, M., Olson, E., Schrenk, M., Roe, K., Lebon, G., Rivizzigno, P., Party, t. A.-S., 2001. An off-axis hydrothermal vent field near the Mid–Atlantic Ridge at 30°N. Nature 412, 145–149.

Kornberg, A., 1995. Inorganic polyphosphate: toward making a forgotten polymer unforgettable. J. Bacteriol. 177 (3), 491–496.

Lechaire, J.P., Shillito, B., Frébourg, G., Gaill, F., 2002. Elemental characterization of microorganism granules by EFTEM in the tube wall of a deep–sea vent invertebrate. Biol. Cell 94, 243–249.

Lechaire, J., Frébourg, G., Gaill, F., Gros, O., 2006. In situ localization of sulphur in the thiotrophic symbiotic model *Lucina pectinata* (Gmelin, 1791) by cryo–EFTEM microanalysis. Biol. Cell 98, 163–170.

Lopez-Garcia, P., Gaill, F., Moreira, D., 2002. Wide bacterial diversity associated with tubes of the vent worm *Riftia pachyptila*. Environ. Microbiol. 4 (4), 204–215.

Lütke-Eversloh, T., Bergander, K., Luftman, H., Steinbüchel, A., 2001. Identification of a new class of biopolymer: bacterial synthesis of a sulfur–containing polymer with thioester linkages. Microbiology 147, 11–19.

Meyer, B., Kuever, J., 2007. Molecular analysis of the diversity of sulfate–reducing and sulfur–oxidizing prokaryotes in the environment using aprA as functional marker gene. Appl. Environ. Microbiol. doi:10.1128/AEM.01272-07 Published online ahead of print on 5 October 2007.

Polz, M., Cavanaugh, C., 1995. Dominance of one bacterial phylotype at a Mid–Atlantic Ridge hydrothermal vent site. Proc. Natl. Acad. Sci. USA 92, 7232–7236.

Polz, M., Robinson, J., Cavanaugh, C., Van Dover, C., 1998. Trophic ecology of massive shrimp aggregations at a mid–Atlantic Ridge hydrothermal vent site. Limnol. Oceanogr. 43 (7), 1631–1638.

Pond, D., Dixon, D., Bell, M., Fallick, A., Sargent, J., 1997. Occurence of 16:2(n-4) and 18:2 (n-4) fatty acids in the lipids of the hydrothermal vent shrimps *Rimicaris exoculata* and *Alvinocaris markensis*: nutritional and trophic implications. Mar. Ecol. Prog. Ser. 156, 167–174.

Ravaux, J., Gaill, F., Le Bris, N., Sarradin, P.M., Jollivet, D., Shillito, B., 2003. Heat–shock response and temperature resistance in the deep–sea vent shrimp *Rimicaris exoculata*. J. Exp. Biol. 206, 2345–2354.

Rieley, G., Van Dover, C., Hedrick, D., Eglinton, G., 1999. Trophic ecology of *Rimicaris exoculata*: a combined lipid abundance/stable isotope approach. Mar. Biol. 133, 495–499.

Saitou, M., Nei, M., 1987. The neighbor–joining method: a new method for reconstructing phylogenetic trees. Mol. Biol. Evol. 4, 406–425.

Salerno, L., Macko, S., Hallam, S., Bright, M., Won, Y., McKiness, Z., Van Dover, C., 2005. Characterization of symbiont populations in life history stages of mussels from chemosynthetic environments. Biol. Bull. 208, 145–155.

Schmidt, C., Vuillemin, R., Le Gall, C., Gaill, F., Le Bris, N., 2008. Geochemical energy sources for microbial primary production in the environment of hydrothermal vent shrimps. Mar. Chem. 108 (1), 18–31.

Segonzac, M., de Saint-Laurent, M., Casanova, B., 1993. L'énigme du comportement trophique des crevettes Alvinocarididae des sites hydrothermaux de la dorsale médio–atlantique. Cah. Biol. Mar. 34, 535–571.

Shillito, B., Jollivet, D., Sarradin, P.M., Rodier, P., Lallier, F., Desbruyères, D., Gaill, F., 2001. Temperature resistance of *Hesiolyra bergi*, a polychaetous annelid living on vent smoker walls. Mar. Ecol. Prog. Ser. 216, 141–149.

Shively, J., 1974. Inclusion bodies in prokaryotes. Annu. Rev. Microbiol. 28, 167–187.

Suzuki, Y., Sasaki, T., Suzuki, M., Nogi, Y., Miwa, T., Takai, K., Nealson, K., Horikoshi, K., 2005. Novel chemoautotrophic endosymbiosis between a member of the epsilon–*proteobacteria* and the hydrothermal–vent gastropod *Alviniconcha* aff. *hessleri* (Gastropoda: Provannidae) from the Indian Ocean. Appl. Environ. Microbiol. 71 (9), 5440–5450.

Thompson, J., Higgins, D., Gibson, T., 1994. CLUSTAL W: improving the sensitivity of progressive multiple sequence alignment through sequence weighting, position–specific gap penalties and weight matrix choice. Nucleic Acids Res. 22, 4673–4680.

Van Dover, C., Fry, B., Grassle, J., Humphris, S., Rona, P., 1988. Feeding biology of the shrimp *Rimicaris exoculata* at hydrothermal vents on the Mid–Atlantic Ridge. Mar. Biol. 98, 209–216.

Vetter, R., 1985. Elemental sulfur in the gills of three species of clams containing chemoautotrophic symbiotic bacteria: a possible inorganic energy storage compound. Mar. Biol. 88, 33–42.

Williams, A., Rona, P., 1986. Two new caridean shrimps (Bresiliidae) from a hydrothermal field on the Mid–Atlantic Ridge. J. Crustacean Biol. 6 (3), 446–462.

Wirsen, C., Jannasch, H.W., Molyneaux, S., 1993. Chemosynthetic microbial activity at Mid–Atlantic Ridge hydrothermal vent sites. J. Geophys. Res. 98 (B6), 9693–9703.

Zbinden, M., Cambon-Bonavita, M.-A., 2003. Occurence of Deferribacterales and Entomoplasmatales in the deep–sea shrimp *Rimicaris exoculata* gut. FEMS Microbiol. Ecol. 46, 23–30.

Zbinden, M., Le Bris, N., Gaill, F., Compère, P., 2004. Distribution of bacteria and associated minerals in the gill chamber of the vent shrimp *Rimicaris exoculata* and related biogeochemical processes. Mar. Ecol. Prog. Ser. 284, 237–251.

The ISME Journal (2013) 7, 96–109

www.nature.com/ismej

ORIGINAL ARTICLE

Inorganic carbon fixation by chemosynthetic ectosymbionts and nutritional transfers to the hydrothermal vent host-shrimp *Rimicaris exoculata*

Julie Ponsard[1], Marie-Anne Cambon-Bonavita[2], Magali Zbinden[3], Gilles Lepoint[4], André Joassin[5], Laure Corbari[6], Bruce Shillito[3], Lucile Durand[2], Valérie Cueff-Gauchard[2] and Philippe Compère[1]

[1]*Laboratoire de Morphologie fonctionnelle et évolutive, Département de Biologie, Ecologie et Evolution, Centre MARE, Université de Liège, Liège, Belgium;* [2]*Laboratoire de Microbiologie des Environnements Extrêmes UMR 6197 Ifremer-CNRS-UBO, BP70, Plouzané, France;* [3]*Equipe Adaptation aux Milieux Extrêmes, UMR 7138 CNRS, Systématique, Adaptation et Evolution, Université Pierre et Marie Curie, Paris Cedex 05, France;* [4]*Laboratoire d'Océanologie, Département Biologie, Ecologie et Evolution, Centre MARE, Université de Liège, Liège, Belgium;* [5]*Laboratoire de Chimie de Coordination et Radiochimie, Département de Chimie, Université de Liège, Liège, Belgium and* [6]*Equipe Espèces et Spéciation, UMR 7138 CNRS, Systématique, Adaptation et Evolution, Muséum National d'Histoire Naturelle, Paris Cedex 05, France*

The shrimp *Rimicaris exoculata* dominates several hydrothermal vent ecosystems of the Mid-Atlantic Ridge and is thought to be a primary consumer harbouring a chemoautotrophic bacterial community in its gill chamber. The aim of the present study was to test current hypotheses concerning the epibiont's chemoautotrophy, and the mutualistic character of this association. *In-vivo* experiments were carried out in a pressurised aquarium with isotope-labelled inorganic carbon ($NaH^{13}CO_3$ and $NaH^{14}CO_3$) in the presence of two different electron donors ($Na_2S_2O_3$ and Fe^{2+}) and with radiolabelled organic compounds (^{14}C-acetate and ^{3}H-lysine) chosen as potential bacterial substrates and/or metabolic by-products in experiments mimicking transfer of small biomolecules from epibionts to host. The bacterial epibionts were found to assimilate inorganic carbon by chemoautotrophy, but many of them (thick filaments of *epsilonproteobacteria*) appeared versatile and able to switch between electron donors, including organic compounds (heterotrophic acetate and lysine uptake). At least some of them (thin filamentous *gammaproteobacteria*) also seem capable of internal energy storage that could supply chemosynthetic metabolism for hours under conditions of electron donor deprivation. As direct nutritional transfer from bacteria to host was detected, the association appears as true mutualism. Import of soluble bacterial products occurs by permeation across the gill chamber integument, rather than via the digestive tract. This first demonstration of such capabilities in a decapod crustacean supports the previously discarded hypothesis of transtegumental absorption of dissolved organic matter or carbon as a common nutritional pathway.
The ISME Journal (2013) **7,** 96–109; doi:10.1038/ismej.2012.87; published online 23 August 2012
Subject Category: microbe–microbe and microbe–host interactions
Keywords: autoradiography; chemosynthetic ectosymbiosis; Crustacea; isotopes; *Rimicaris exoculata*; transtegumental transfer

Introduction

Mostly described as endosymbioses (Dubilier *et al.*, 2008), associations between invertebrates and chemoautotrophic bacteria are regularly encountered in reducing marine habitats (Cavanaugh *et al.*, 2006). Among the Crustacea, chemosynthetic epibioses are reported in only a few hydrothermal decapods: the shrimp *Rimicaris exoculata* (Segonzac *et al.*, 1993), the galatheid crabs *Kiwa hirsuta* (Macpherson *et al.*, 2005; Goffredi *et al.*, 2008), *Kiwa puravida* (Thurber *et al.*, 2011), and *Shinkaia crosnieri* (Miyake *et al.*, 2007), and two amphipods from littoral sediments (Gillan and Dubilier, 2004; Gillan *et al.*, 2004) and sulphide-rich caves (Dattagupta *et al.*, 2009). Most of these associations are regarded as nutritional ectosymbioses, but to date, there is little direct evidence of bacterial autotrophy and no direct demonstration of mutualistic nutritional bacteria–host interactions.

Correspondence: P Compère, Laboratoire de Morphologie fonctionnelle et évolutive, Département de Biologie, Ecologie et Evolution, Centre MARE, Université de Liège, 4000 Sart-Tilman, Liège, Belgium
E-mail: pcompere@ulg.ac.be
Received 30 January 2012; revised 18 June 2012; accepted 20 June 2012; published online 23 August 2012

The shrimp *R. exoculata* (Williams and Rona, 1986) dominates the megafauna of several deep-sea hydrothermal vent sites of the Mid-Atlantic Ridge, forms dense aggregates around active chimneys (Segonzac, 1992) and harbours a luxuriant bacterial community in its enlarged gill chamber (Van Dover *et al*., 1988; Casanova *et al*., 1993; Segonzac *et al*., 1993; Polz and Cavanaugh, 1995; Zbinden *et al*., 2004) (Figure 1). The integument surfaces are periodically re-colonised during the moult cycle

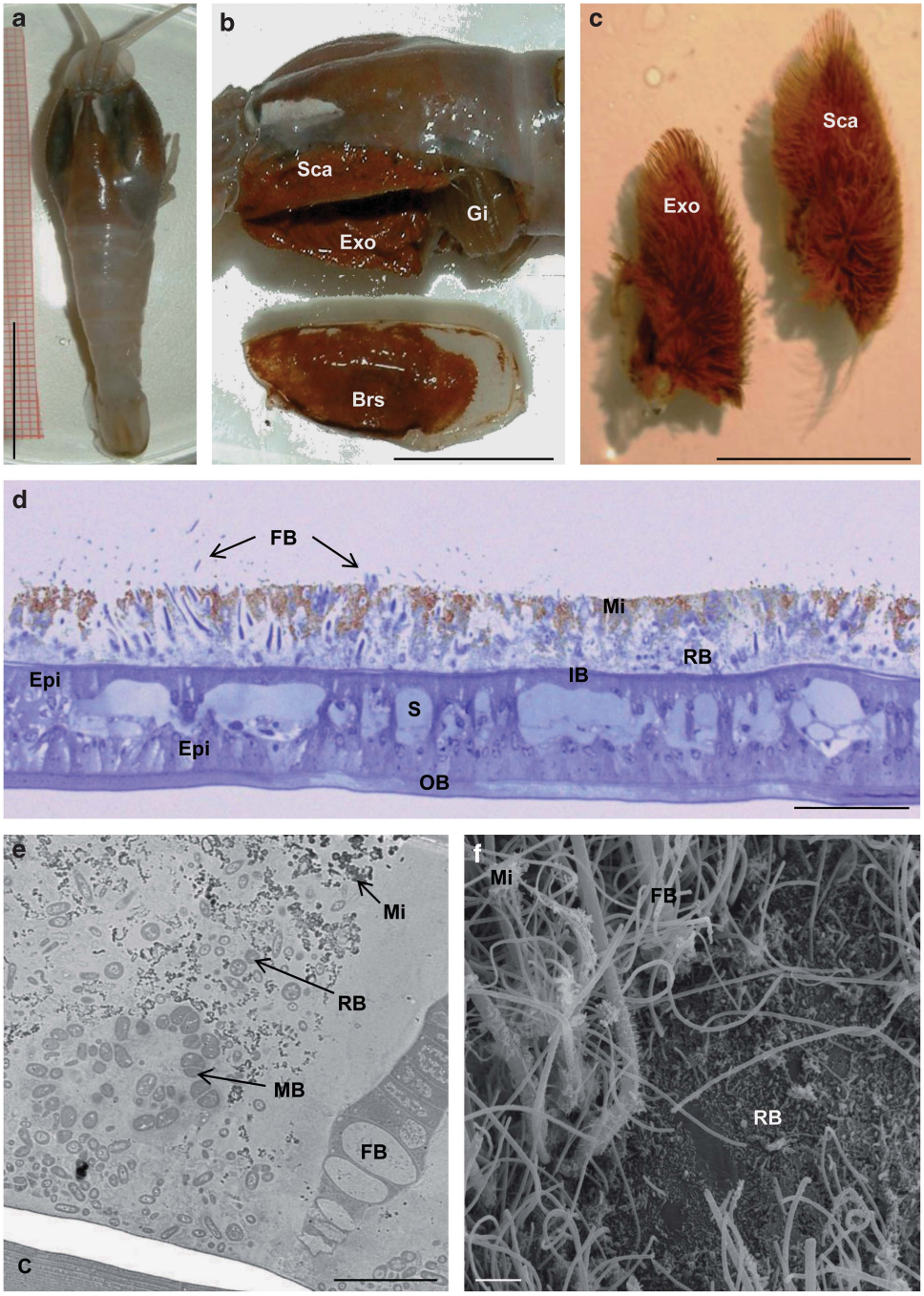

Figure 1 Illustration of the shrimp *Rimicaris exoculata* gill chamber with the associated bacterial community. (**a**) Whole shrimp with dilated gill chamber visible on both sides of the cephalothorax. (**b**) Left gill chamber opened by removal of the branchiostegite (lying below, *Brs*) and showing the very large mouthparts (scaphognathite, *Sca*, and exopodite, *Exo*) as well as the posterior gill set (*Gi*)—both the mouthparts and the inner side the branchiostegite are colonised by bacterial mats encrusted with particles of red iron oxide. (**c**) Isolated mouthparts bearing bacteriophore setae sheathed by a thick iron-oxide-encrusted biofilm. (**d**) Semi-thin cross-section (toluidine blue stained) of the branchiostegite (anterior part), showing the inner and outer integument leaflets (*IB* and *OB*) and the bacterial biofilm growing on the inner side. (**e**, **f**) Transmission electron microscopy and scanning electron microscopy images of the branchiostegite biofilm, showing several bacterial morphotypes including rods, nested methanotrophic-like bacteria, thick and thin filaments (pictures taken by Dr L Corbari). Scale bars: (**a**) 1 cm; (**b**) and (**c**) 500 mm; (**d**) 100 μm; (**e**) 5 μm; (**f**) 10 μm. *C*, cuticle; *Epi*, epidermis; *FB*, filamentous bacteria; *IB*, inner branchiostegite; *MB*, methanotrophic-like bacteria; *Mi*, mineral particles; *RB*, rod-shaped bacteria; *S*, blood sinuses.

(Corbari *et al*., 2008b), each ecdysis causing shedding of the old cuticle with its bacterial mats. The shrimp *R. exoculata*, listed as a model organism of an extreme deep-sea environment (CAREX, 2010), is exceptional among crustaceans for its association with bacteria. Recent studies suggest that *R. exoculata* gill chamber epibionts constitute a diversified community with various morphotypes, phylotypes and metabolisms (Zbinden *et al*., 2004, 2008; Petersen *et al*., 2009; Hügler *et al*., 2011; Guri *et al*., 2012), but no study has directly demonstrated which substrate(s) the bacteria oxidise to fuel their 'chemosynthetic' metabolism(s). This shrimp also harbours a digestive bacterial community (Zbinden and Cambon-Bonavita, 2003; Durand *et al*., 2010) whose role remains hypothetical (detoxification, nutrition and/or pathogen control).

There is strong evidence, based on stable isotope signatures and essential fatty acid composition, suggesting that the shrimp gets organic matter mainly from its epibionts, rather than from grazing free-living bacteria associated with chimney walls (Gebruk *et al*., 1993; Pond *et al*., 1997a, 2000; Rieley *et al*., 1999; Colaço *et al*., 2007). Yet this evidence of symbiont–host nutritional relationships is indirect, and how carbon is transferred from bacteria to shrimp remains an open question. The hypothesis of direct transfer of dissolved molecules across the shrimp integument, especially the gill chamber lining, has been proposed on the basis of morphological observations (features dedicated to bacteria farming, absence of scrape marks on the biofilm) (Zbinden *et al*., 2004; Corbari *et al*., 2008b), but the nature of the transferred molecules and the integument areas involved remain to be discovered.

The major aims of this study were to test (1) inorganic carbon fixation by active bacterial chemosynthetic metabolisms and (2) the hypothesis of bacterial organic carbon transfer (soluble molecules) to the shrimp tissues. For this, we incubated live shrimps in a pressurised vessel with different isotope-labelled molecules and electron donors, to trace carbon assimilation by the epibionts and shrimp tissues.

Materials and methods

Shrimp collection

R. exoculata specimens were collected with the slurp-gun operated from the manned submersible Nautile at the Rainbow hydrothermal vent site (36°14′N–33°54′W, 2320 m depth) during the 'MoMARDREAM-Naut' cruise, July 2007. Healthy specimens were maintained alive in a pressurised IPOCAMP incubator (Shillito *et al*., 2001) at *in-situ* pressure (230 bars) and temperature (15 °C) for *in-vivo* experiments (Zbinden *et al*., 2008). Control specimens were directly frozen at −80 °C after collection.

Experiments

Experiments were carried out only on red-coloured pre-ecdysial specimens (that is, having an established and still-growing bacterial community) (Corbari *et al*., 2008b). In the IPOCAMP, incubations with isotopic tracers were carried out in flasks filled till to the top with seawater (SW), whose volume (50 or 250 ml) was chosen according to the treatment duration and number of shrimps to ensure shrimp survival in good physiological condition at the end of the experiment (Shillito *et al*., 2001; Ravaux *et al*., 2003). Incorporation of ^{13}C- and ^{14}C-bicarbonate by the chemoautotrophic bacteria was tested with different chemical energy sources. ^{14}C-acetate and ^{3}H-lysine were chosen as representative microbial substrates and/or metabolic by-products liable to mimic transfer of small biomolecules from epibionts to host.

After each experiment, tracer excess was washed off in 0.22-μm-filtered SW: 15 min for ^{13}C and 1, 5 and 30 s, 5 and 15 min for the other experiments. The shrimps were then either directly frozen at −80 °C or dissected into body parts and tissues of interest: (1) regions colonised by the bacteria: the branchiostegites (integument folds enclosing the gill chamber), later separated into the inner bacterial biofilm (*BB*) and the outer branchiostegite (*OB*) or shrimp tissues, and the mouthparts (*MP*, scaphognathites and exopodites); (2) exchange or absorption organs: gills (*Gi*), digestive tract (*DT*) and hepatopancreas (*HP*); (3) abdominal muscles (*Mu*). In some specimens, the old abdominal cuticle (*AC*) was separated from the inner tissues (new cuticle and epidermis). In the laboratory, the samples were rinsed once again (see below) and treated to remove unfixed tracers and to preserve the labelled organic molecules before quantification.

^{13}C-bicarbonate incorporation. Four and two shrimps were incubated for 4 and 10 h, respectively, in 250-ml flasks containing 1 g/L $NaH^{13}CO_3$ (98%; Sigma 372382; St Louis, MO, USA) in filtered SW enriched or not (control) with iron (100 μM $FeCl_2$; Sigma 372870) or thiosulphate (100 μM $Na_2S_2O_3$; Sigma 72049) as chemical energy source. Before use, the dissected tissue samples were rinsed three times in distilled water before dehydration overnight at 60 °C. Dried samples were finely ground to obtain a powder to vaporise in the mass spectrometer.

^{14}C-bicarbonate incorporation. Two specimens were incubated for 6 h in 50-ml flasks containing 0.25 g/L $NaH^{12}CO_3$ labelled with 80 μM $NaH^{14}CO_3$ (4 μCi/ml; GE Healthcare CFA3-5MCI; Buckinghamshire, UK) as inorganic carbon source and dissolved in SW enriched or not with an electron donor (Fe^{2+} or $Na_2S_2O_3$) at the same concentration as above. The first shrimp for each condition was directly frozen at −80 °C for autoradiography and scintillation analysis. The second shrimp was dissected into body parts as described above before storage in

cryotubes at −80 °C. In unlabelled shrimps (control), the radioactivity level was undetectable to very low in both bacterial mats and shrimp tissues.

In the laboratory, the samples were rinsed four times in distilled water and their fresh weight was determined. After overnight digestion at 50–55 °C in glass scintillation vials containing 1 ml quaternary ammonium hydroxide (0.5 N) in toluene (BTS-450 Tissue Solubilizer; Beckman Coulter 580691; Fullerton, CA, USA), they were acidified for 2 h at room temperature by adding 250 µl acetic acid to remove any remaining ^{14}C-bicarbonate and the calcium carbonate present in the cuticle or *HP*. Scintillation liquid (Ready Organic; Beckman Coulter 586600) (10 ml) was added to all samples just before reading.

^{14}C-acetate and ^{3}H-lysine incorporation. Two sets of three to four shrimps were incubated for 1 h in 50 ml SW containing either 20 µCi/ml ^{3}H-lysine (GE Healthcare TRK520-1MCI) (that is, 0.2 µM) or 10 µCi/ml sodium ^{14}C-acetate (GE Healthcare CFA14-1MCI) (that is, 0.2 mM). In both experiments, one entire specimen was immediately frozen after rinsing (for autoradiography and analysis). The others were dissected and the pieces stored at −80 °C. Samples were treated as in the ^{14}C-bicarbonate experiment.

Stable isotope and elemental analysis
The atomic percentage of stable isotope ($\%_{at}\,^{13}C$) of each sample and its carbon content expressed as a percentage of dry weight ($\%C_{dw}$) were obtained with an isotope ratio spectrometer (Optima, Isoprime, UK) coupled to an elemental analyser (Carlo Erba, Milan, Italy) (Lepoint *et al.*, 2004).

The percentage of natural ^{13}C in control shrimps was first subtracted from the measured ^{13}C percentage in each sample to obtain the percentage of ^{13}C (or total carbon) incorporated during the experiment ($\%_{at}\,^{13}C_{inc}$). Carbon incorporation rates (C_{inc}), expressed in moles of carbon incorporated per time unit and weight unit of total carbon in the sample ($\mu molC_{inc} \times gC_{sam}^{-1} \times h^{-1}$), were calculated according to the formulas:

$$\%_{at}{}^{13}C_{inc} \cdot (DW_{sam} \cdot \ \%C_{dw}) = W^{13}C_{inc}$$

$$\frac{W^{13}C_{inc}/MM_C}{(DW_{sam} \cdot \ \%C_{dw}) \cdot t} = C_{inc}$$

where $\%_{at}\,^{13}C_{inc}$ is atomic percentage of incorporated ^{13}C; DW_{sam} is the dry weight of the sample, $\%C_{dw}$ is the carbon content expressed as a percentage of dry weight, $DW_{sam}.\%C_{dw}$ is the weight of carbon in the sample, $W^{13}C_{inc}$ is the weight of ^{13}C incorporated into the sample during the experiment, MM_C is the molar mass of carbon, t is the duration of the experiment, and C_{inc} is the carbon incorporation rate expressed in moles of incorporated carbon per time unit and weight unit of total carbon in the sample.

Measurement of incorporated radioactivity
The beta-radioactivity of the samples was measured for 15 min in liquid phase in a Beckman LS 6500 Scintillation Counter (effective resolution: 0.06 keV).

Moles of incorporated radioelement are known from the measured number of disintegrations per second (disintegrations per second × 2 half-life in seconds/Avogadro's number). The total incorporation rate, expressed in moles of incorporated molecules per time unit and weight unit of total carbon in the sample ($\mu molR_{inc} \times gC_{sam}^{-1} \times h^{-1}$), was calculated according to the formula:

$$\frac{({}^{x}E_{inc}/f)}{[(FW_{sam} \cdot p) \cdot \ \%C_{dw}] \cdot t} = R_{inc}$$

where ${}^{x}E_{inc}$ is the number of moles of incorporated radioelement, f is the ratio of radioactive to cold molecules in the incubation medium, FW_{sam} is the fresh weight of the sample, p is the dry weight/fresh weight ratio measured on control shrimps, $\%C_{dw}$ is the carbon content expressed as a percentage of sample dry weight, and R_{inc} is the total incorporation rate expressed in moles of incorporated molecules per time unit and weight of total carbon in the sample.

Autoradiography
Histological localisation of radiotracers was done by autoradiography on frozen shrimps incubated with a radiotracer. To isolate shrimp segments, each frozen shrimp was embedded in Tissue-Tek gel (Sakura 4583; Torrance, CA, USA), directly frozen in liquid nitrogen, and cut into segments 1 cm long with a hacksaw in a cryostat at −20 °C. Segments of the cephalothorax (including *MP* and gills) and the abdomen were directly thawed overnight in fixative solution (2.5% glutaraldehyde), decalcified in EDTA (0.2 M, pH 8), post-fixed in 1% OsO_4 for 2 h, rinsed in distilled water (4 × 10 min), dehydrated with ethanol, and embedded in Steedman's wax (polyethylene glycol distearate; Sigma 305413—hexadecanol 9:1; 99%; Sigma 258741). Twelve-micrometre cross-sections were obtained with a microtome (Reichert, Austria) at three levels (*MP*, gills and abdominal muscles) and deposited on gelatinised glass slides. They were rehydrated, washed in distilled water and then coated with a photographic emulsion film (Hypercoat LM-1; GE Healthcare RPN40) in the dark according to the classical wet method (Ullberg *et al.*, 1982). The slides were developed with KODAK products (KODAK D19-Revelator and KODAK-Fixator; Rochester, NY, USA) after an exposure time of 6–9 months for ^{14}C-bicarbonate or 6 h to 3 months for ^{14}C-acetate and ^{3}H-lysine. The slides were mounted in epoxy resin before being observed and photographed with an Olympus AX70 light microscope (Shinjuku, Tokyo, Japan) equipped with a Visicam 5.0 camera (Hilden, Germany).

Statistical analysis
All data are reported as mean values ± s.d. Outliers (possibly due to experimental contamination or to the absence of labelling) were eliminated with Dixon's *Q* test ($P<0.05$). One-way analysis of variance (Kruskall–Wallis) was used and all pair-wise multiple comparison procedures (Dunn's Method) performed with Sigma Plot 11.0 software (Systat Software Inc., San Jose, CA, USA) were used for sample comparisons. $P<0.05$ was taken as fiducial limit for statistical significance.

Dunn's multiple comparisons vs control group method were used to test the real incorporation of ^{14}C.

Results

^{13}C-bicarbonate experiments
The data for ^{13}C-bicarbonate incorporation are shown in Figure 2a. Bacterial mats of branchiostegites and *MP* displayed a high rate of inorganic carbon incorporation from ^{13}C-bicarbonate. Other body parts (*OB*, *DT* and *Mu*) showed lower rates. All the results appeared to be statistically significant.

After a 10-h incubation, the ^{13}C uptake measured in the bacterial mats was approximately twice as high as after 4 h (Table 1). In the *BB*, it was higher in thiosulphate-incubated shrimps (78.8 $\mu molC_{inc} \times gC_{sam}^{-1}$) than in SW-incubated specimens (52.4 $\mu molC_{inc} \times gC_{sam}^{-1}$).

The incorporation rate was higher in the *MP* (12.1–16.7 $\mu molC_{inc} \times gC_{sam}^{-1} \times h^{-1}$) than in the *BB* (3.9–7.3 $\mu molC_{inc} \times gC_{sam}^{-1} \times h^{-1}$). In shrimp tissues, it was higher in the *OB* (1.1 $\mu molC_{inc} \times gC_{sam}^{-1} \times h^{-1}$, in the presence of thiosulphate) than in the *DT* (0.3 $\mu molC_{inc} \times gC_{sam}^{-1} \times h^{-1}$) or the *Mu* (0.2 $\mu molC_{inc} \times gC_{sam}^{-1} \times h^{-1}$). The incorporation rates for *MP* and *BB* were significantly different from those of shrimp tissues ($P<0.05$).

^{14}C-bicarbonate experiments
The radioactivity levels measured in the bacteria and tissues of control shrimps appeared negligible as compared with radiotracer uptake ($P\leqslant0.001$) (Figure 2b).

High ^{14}C incorporation rates were observed in the bacterial mats of the *MP* and *BB* (Figure 2b), of the same order of magnitude as the corresponding ^{13}C-bicarbonate incorporation rates. The rate was much higher in the presence of iron or thiosulphate. In the *MP* and *BB*, respectively, it reached 10.4 and 5.4 $\mu molC_{inc} \times gC_{sam}^{-1} \times h^{-1}$ in the presence of thiosulphate and only 3.9 and 2.8 $\mu molC_{inc} \times gC_{sam}^{-1} \times h^{-1}$ for shrimps incubated in SW alone.

Most of the shrimp tissues analysed showed significant ^{14}C incorporation, whatever the incubation conditions (Figure 2b). The highest carbon incorporation rates were recorded in the tegumental tissues of the gill chambers, that is, the *OB* (2.7 $\mu molC_{inc} \times gC_{sam}^{-1} \times h^{-1}$) and the *Gi* (0.2 $\mu molC_{inc} \times gC_{sam}^{-1} \times h^{-1}$). The rates recorded for the internal tissues of all shrimps (*Mu*: 0.01; *DT*: 0.04; *HP*: 0.01 $\mu molC_{inc} \times gC_{sam}^{-1} \times h^{-1}$) were low to very low, but nevertheless significant ($P\leqslant0.001$), the digestive gland displaying the lowest values. The *AC* showed a surprisingly high incorporation rate (0.6 $\mu molC_{inc} \times gC_{sam}^{-1} \times h^{-1}$ in the presence of iron), to be explained below.

^{14}C-acetate experiments
The results for ^{14}C incorporation from acetate are shown in Figure 3a. Bacterial mats (*MP* and *BB*) showed high rates, indicating that acetate is a suitable carbon source for these bacteria. The rate recorded in SW (61.3 $\mu molAc_{inc} \times gC_{sam}^{-1} \times h^{-1}$) was 15 times the rate of carbon incorporation from ^{14}C-bicarbonate (3.9 $\mu molC_{inc} \times gC_{sam}^{-1} \times h^{-1}$ in *MP*).

High rates of ^{14}C incorporation were measured in the integument, especially in areas lining the gill

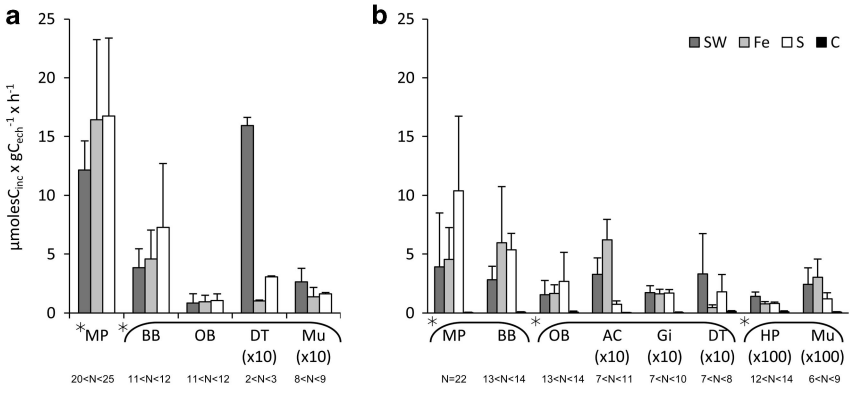

Figure 2 Rates of inorganic carbon incorporation into the bacterial mats of the mouthparts and branchiostegite and into shrimp tissues, as calculated from ^{13}C fixation (**a**) or ^{14}C fixation (**b**) data. The shrimps were incubated: (**a**) for 4 or 10 h in $NaH^{13}CO_3$ in pure seawater (dark grey), supplemented with reduced iron (light grey) or thiosulphate (white); (**b**) for 6 h in pure SW with $NaH^{14}CO_3$ (dark grey), supplemented with iron (light grey) or thiosulphate (white). The radioactivity measured in control shrimp tissues is shown (black) for comparison. Stars indicate significant differences between groups of tissues; ($\times10$, $\times100$) indicates tissues for which the values were multiplied by 10 or 100 for graph presentation; '*N*' indicates the number of samples for each data bar.

Table 1 Total amounts of inorganic carbon ($\mu molC_{inc} \times gC_{sam}^{-1} \pm$ s.d.) incorporated after 4 and 10 h into the body parts of shrimps incubated with ^{13}C-bicarbonate in the presence of seawater, or seawater supplemented with iron or thiosulphate

	Incorporated inorganic ^{13}C per g of organic C in the sample ($\mu molC_{inc} \times gC_{sam}^{-1}$) after 4 and 10 h incubations with $NaH^{13}CO_3$ in SW, SW+Fe and SW+S	
	$NaH^{13}CO_3$–4 h	*$NaH^{13}CO_3$–10 h*
Shrimp tissues		
SW		
MP	50.4 ± 10.3	103.0 ± 8.2
BB	13.3 ± 6.3	52.4 ± 3.4
OB	4.3 ± 3.3	3.1 ± 0.5
DT	/	15.9 ± 0.7
Mu	1.1 ± 0.6	2.6 ± 0.0
Fe		
MP	65.7 ± 27.3	/
BB	22.8 ± 9.8	24.0 ± 2.1
OB	4.8 ± 3.5	8.4 ± 0.3
DT	/	1.3 ± 0.5
Mu	0.8 ± 0.1	0.5 ± 0.0
S		
MP	67.9 ± 29.9	158.5 ± 7.0
BB	28.4 ± 25.0	78.8 ± 3.7
OB	5.0 ± 2.1	4.8 ± 0.4
DT	/	3.1 ± 0.1
Mu	0.6 ± 0.0	1.7 ± 0.14

Abbreviations: BB, branchiostegite biofilm; DT, digestive tract; Fe, iron condition; MP, mouthparts; Mu, muscles; OB, outer branchiostegite; S, thiosulphate condition; SW, seawater.

chamber, that is, *OB* and *Gi* (7.9 and 7.3 $\mu molAc_{inc} \times gC_{sam}^{-1} \times h^{-1}$, respectively). The level remained low but measurable in the internal tissues. In the *Mu* and *HP*, the rate did not exceed 0.1 $\mu molAc_{inc} \times gC_{sam}^{-1} \times h^{-1}$. It was slightly higher in the *DT* (0.4 $\mu molAc_{inc} \times gC_{sam}^{-1} \times h^{-1}$). In the *AC*, a distinction was made between the old, outer cuticle (AC_o) and the inner tissues (AC_n). The ^{14}C incorporation rate for the whole *AC* was mainly due to high ^{14}C uptake into the inner, living tissues (AC_n, 4.8 $\mu molAc_{inc} \times gC_{sam}^{-1} \times h^{-1}$), that is, the epidermis secreting the new cuticle, while the inert old cuticle showed low labelling (AC_o, 0.7 $\mu molAc_{inc} \times gC_{sam}^{-1} \times h^{-1}$).

^{3}H-lysine experiments

^{3}H-lysine incorporation rates were about 100 times lower than the ^{14}C-acetate incorporation rates (0.7 $\mu molLys_{inc} \times gC_{sam}^{-1} \times h^{-1}$ vs 61.7 $\mu molAc_{inc} \times gC_{sam}^{-1} \times h^{-1}$ in the *BB*) (Figure 3b). The highest rates were again found in the bacterial mats (*MP* and *BB*), suggesting that these bacteria can use lysine, probably for protein synthesis. Significant rates were measured in the gill chamber integument (*OB* and *Gi*) (34.1 and 16.1 $nmolLys_{inc} \times gC_{sam}^{-1} \times h^{-1}$, respectively), while the internal tissues (except the *Mu*: 0.8 $nmolLys_{inc} \times gC_{sam}^{-1} \times h^{-1}$) showed low labelling.

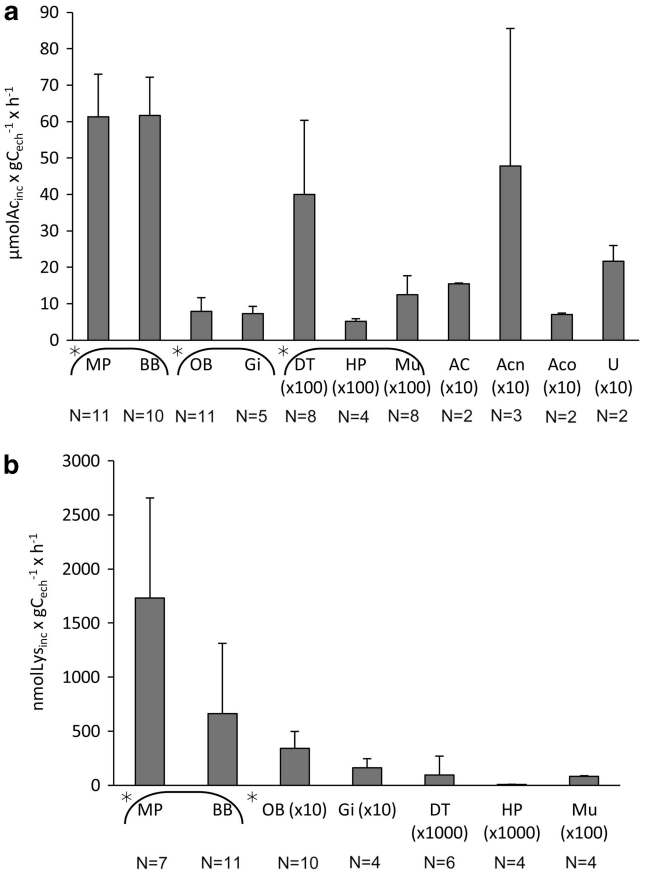

Figure 3 Rates of incorporation of ^{14}C (**a**) and ^{3}H (**b**) into the bacterial mats and inner tissues of *R. exoculata* shrimps incubated for 1 h with ^{14}C-acetate or ^{3}H-lysine in pure SW. Stars indicate significantly different groups of tissues; ($\times 10$, $\times 100$, $\times 1000$) indicates tissues for which the values were multiplied by 10, 100 or 1000 for graph presentation; '*N*' indicates the number of samples for each data bar. *U*, uropods.

Autoradiography

Our autoradiographic observations were in good agreement with the analytical data, confirming the distribution of the radiolabelled molecules among the bacterial mats and shrimp tissues (see Supplementary Information 2—Figures 7a and b for negative controls).

In the bacterial mats associated with the *MP* and branchiostegites, results for the three radiotracer incubations were quite similar. The labelling intensity depended on the specific radioactivity of the isotope, the exposure time and the amount of radiotracer incorporated. ^{3}H-lysine gave the best result with the shortest exposure time, followed by ^{14}C-acetate and ^{14}C-bicarbonate. Silver grain precipitation (in the photographic emulsion) always appeared first along the bacterial filaments (Figures 4a and c), eventually covering the whole length of the filaments as a dense black deposit (Figures 4b and d). By comparing the pictures obtained after short and long exposure times we were able to distinguish the labelled filamentous bacteria from the mineral crust of iron oxides: the

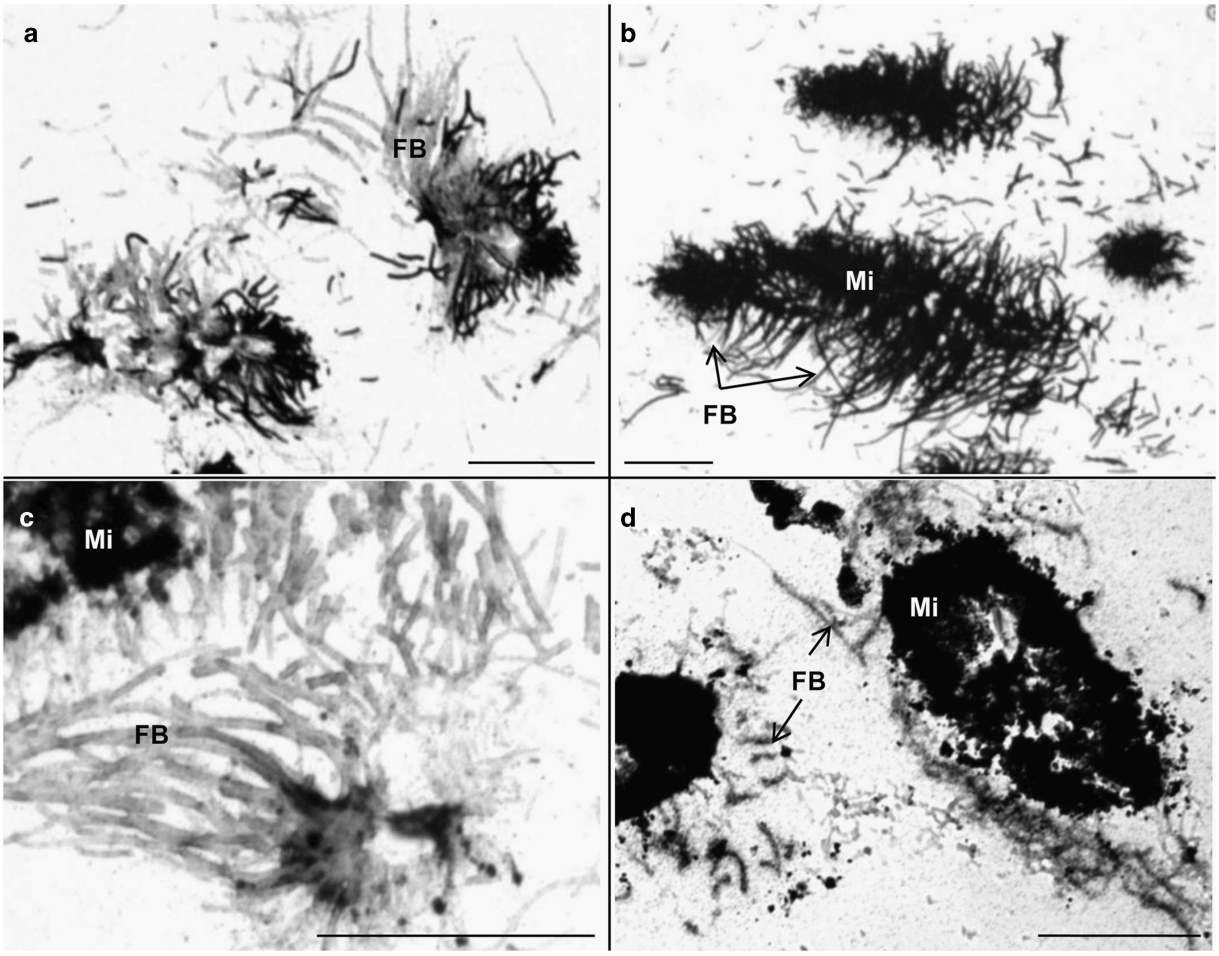

Figure 4 Autoradiographs of histological sections: cross-sectioned bacteriophore setae of the mouthparts of *R. exoculata* shrimps incubated for 1 h with ^{3}H-lysine (**a**, **b**) or for 6 h with ^{14}C-bicarbonate (**c**, **d**). (**a**) Filamentous bacteria are distinguished from mineral deposits and labelled on short segments only. (**b**) The filamentous bacteria are labelled over their entire length. (**c**) Filamentous bacteria are poorly or not labelled. (**d**) Discontinuous labelling appears on the distal part of the filamentous bacteria but does not stain them close to the setae. Exposure times: (**a**) 12 h, (**b**) 11 days, (**c**) 10 weeks and (**d**) 34 weeks. Scale bars: 100 μm. *FB*, filamentous bacteria; *Mi*, mineral.

latter also appeared as dark masses, but they were not labelled, whereas the bacteria located inside or below the mineral crust were moderately labelled (Figure 5a).

The shrimp tegumental tissues appeared densely labelled after incubation with ^{3}H-lysine or ^{14}C-acetate, but sections of shrimps incubated with ^{14}C-bicarbonate required very long exposure times before the label appeared. After 20–30 days of exposure, gills and muscles also appeared moderately labelled (Figures 5b and c), but neither the *DT* nor the *HP* showed any measurable labelling. Detailed views of the branchiostegite (Figure 5a) confirmed and explained the analytical data obtained for the abdominal integument: living tissues synthesising new cuticle and the new cuticle itself showed the most intense labelling. In contrast, the overlying old cuticle remained free of silver grains except in its lower part, which was probably infused with moulting fluid enzymes secreted by the epidermis (Compère *et al*., 2004).

Discussion

The *in-vivo* experiments presented here provide direct evidence that *R. exoculata* epibionts are autotrophic. These are the first experiments to have been carried out on live shrimps together with their epibionts, and the first to demonstrate a mutualistic relationship in this bacteria–shrimp symbiosis under *in-situ* pressure conditions.

Carbon fixation by bacterial chemosynthesis

Once thought to be a monoculture of a single, pleomorphic phylotype of *epsilonproteobacteria*, the gill chamber epibiont population of *R. exoculata* is now regarded as a functional consortium or syntrophic community (Stams and Plugge, 2009) dominated by *gamma*- and *epsilonproteobacteria*. By combining 16S rRNA and functional gene analysis with *in-situ* hybridisation and transmission electron microscopy observations on *R. exoculata*

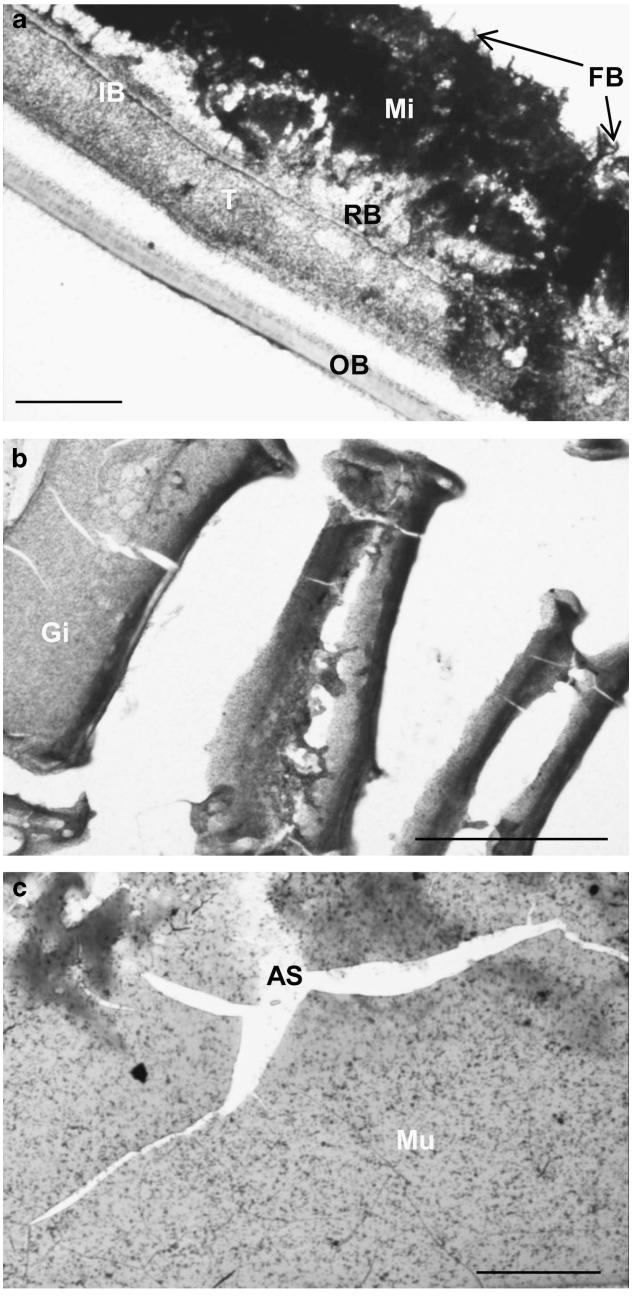

Figure 5 Autoradiographs of different cross-sectioned body parts of *R. exoculata* shrimps incubated for 1 h with ^{14}C-acetate (**a**, **c**) or ^{3}H-lysine (**b**): (**a**) branchiostegite (3-day exposure) showing intense labelling of emerging filamentous bacteria and much weaker labelling below the mineral crust, a dense silver deposit covering the living tissue, that is, both the inner and the outer epidermis and their respective new cuticles, while the old outer cuticle remains almost free of silver particles; (**b**) gills (20-days exposure); (**c**) abdominal muscles (29-days exposure) labelled moderately but more intensely than the background. Scale bar: 100 μm. *AS*, sectioning artificial space; *FB*, filamentous bacteria; *Mi*, mineral crust; *Mu*, muscles; *OB*, outer branchiostegite (old cuticle separated from the new one); *RB*, rod-shaped bacteria; *T*, tissues including the epidermis bordered by the new cuticle being deposited.

epibionts and their free-living or symbiotic relatives from vent habitats, investigators (Campbell *et al.*, 2006; Zbinden *et al.*, 2008; Petersen *et al.*, 2009; Goffredi, 2010; Hügler *et al.*, 2010, 2011; Guri *et al.*, 2012) have evidenced *epsilonproteobacteria* of Marine Groups 1 (the new family Thiovulgaceae) and 2, as thick (3-μm wide) and thin (1-μm wide) filaments, respectively. Both should oxidise sulphur compounds through the *Sox* pathway and fix carbon through the reverse tricarboxylic acid cycle (*SoxB* and *acl*A gene sequences). Authors have also identified *gamma-proteobacterial* epibionts of the Thiotrichaceae family (*Leucothrix* group), together with some free-living members and some other invertebrate ectosymbionts, mainly of crustaceans (Goffredi, 2010). These *gammaproteobacteria* appearing at least as filamentous and rod-shaped morphotypes can probably grow as sulphide oxidisers, most likely using the APS pathway for energy generation and the Calvin-Benson-Bassham cycle for carbon fixation (*apr*A and *cbb*M gene sequences, respectively) (Zbinden *et al.*, 2008; Hügler *et al.*, 2010, 2011; Guri *et al.*, 2012). In addition, coccoid-shaped cells with intracytoplasmic membrane stacks have been identified as type-I methanotrophic *gammaproteobacteria* (*pmo*A gene sequence) (Corbari *et al.*, 2008a; Zbinden *et al.*, 2008; Guri *et al.*, 2012), and *deltaproteobacteria* related to *Desulfocapsa* have been identified thanks to their *apr*A and hydrogenase gene sequences (Hügler *et al.*, 2011), suggesting they can grow lithotrophically using hydrogen as electron donor for sulphate reduction. On this basis, the authors hypothesise that an internal sulphur cycle between sulphur-oxidising *epsilon-* and *gammaproteobacteria* and sulphate-reducing *deltaproteobacteria* could take place in the shrimp gill chamber, as proposed for oligochete symbiosis (Dubilier *et al.*, 2001).

The following results of the present study support the view that shrimp-associated bacteria carry out chemosynthetic inorganic carbon fixation: (1) the carbon incorporation rates for ^{13}C- and ^{14}C-bicarbonate are in good agreement, (2) they increase in the presence of electron donors ($S_2O_3^{2-}$, Fe^{2+}), (3) they are stable over time, as confirmed by the time-related increase in ^{13}C incorporation and (4) autoradiographs of histological sections show labelling of bacterial mats.

The carbon fixation rates observed here are similar to but somewhat higher than those observed by Polz *et al.* (1998): 3.9 vs 2 $\mu molC_{inc} \times gC_{sam}^{-1} \times h^{-1}$ for the *MP* of shrimp incubated in SW. This comparison is somewhat uncertain, as we had to convert Polz's data, expressed per weight unit of protein, into values given per weight unit of total carbon, the carbon content of proteins being estimated at 45% (Rouwenhorst *et al.*, 1991). Yet, the consistently higher rates found here might be due to the incubation of live shrimps under *in-situ* pressure (230 bars in this study), as opposed to the use, in previous experiments, of pieces of dead shrimp under atmospheric pressure. Active chemoautotrophy might be promoted by preserving shrimps and

bacteria in good physiological condition (Ravaux *et al.*, 2003). Accordingly, Zbinden *et al.* (2008) observed <30% degraded epibionts in re-pressurised shrimps. The carbon fixation rates determined here are much lower, however, than those obtained for other chemosynthetic symbionts (bacterial homogenates or endobacteria of bivalve gills), for example, those of *Bathymodiolus thermophilus*: $150\,\mu molC_{inc} \times gC_{sam}^{-1} \times h^{-1}$ in SW (Nelson *et al.*, 1995), or *Solemya velum*: $2500\,\mu molC_{inc} \times gC_{sam}^{-1} \times h^{-1}$ in the presence of thiosulphate (Scott and Cavanaugh, 2007). Moreover, owing to the relatively low energy level of thiosulphate as compared with sulphide, the latter authors observed threefold higher carbon fixation rates with 0.2 mM Na_2S ($70\,\mu molC \times g_{prot}^{-1} \times min^{-1}$) than with 1 mM $Na_2S_2O_3$ ($20\,\mu molC \times g_{prot}^{-1} \times min^{-1}$).

That the presence of an electron donor increases the carbon fixation rate indicates that $Na_2S_2O_3$, and Fe^{2+} at least contribute to fuelling *R. exoculata* epibionts, and our autoradiography data suggest that chemosynthesis occurs at least in the large filamentous bacteria (*epsilonproteobacteria* of Marine Group 1), which appeared more intensely labelled than the thin filamentous and rod-shaped ones (*epsilonproteobacteria* of Marine Group 2 and *gammaproteobacteria*). The view that *R. exoculata* epibionts have sulphide-oxidising activity is consistent, moreover, with the fact *epsilon-* and *gammaproteobacteria* are assumed to have such activity, on the basis of the group affiliation of the former (Petersen *et al.*, 2009; Goffredi, 2010; Guri *et al.*, 2012) and because the latter possess functional *SoxB* and *aprA* genes (Hügler *et al.*, 2010, 2011). We cannot say, however, what the epibiotic bacteria of *R. exoculata* use as predominant energy source. Methane and hydrogen, found in hydrothermal fluids from the Rainbow vent field along with sulphide and iron (Charlou *et al.*, 2002; Douville *et al.*, 2002; Schmidt *et al.*, 2008), are also potential drivers of chemoautotrophy. In particular, the type-I methanotrophic *gammaproteobacteria* may use methane as both electron and carbon source (Zbinden *et al.*, 2008; Guri *et al.*, 2012), *deltaproteobacteria* are believed to use H_2 for sulphate reduction (Hügler *et al.*, 2011), and *epsilonproteobacteria* (of Marine Groups I and II) may use H_2 instead of sulphide for chemosynthesis, as proposed for *Bathymodiolus* gill endosymbionts (Petersen *et al.*, 2011). The possibility that *R. exoculata* epibionts might use H_2 is strongly supported by the identification of a *hupL* gene sequence from Group-2 *epsilonproteobacteria* (Hügler *et al.*, 2011) among the *R. exoculata* epibionts and by the metabolic capabilities reported for Campylobacterales, especially of the family Thiovulgaceae (Campbell *et al.*, 2006; Goffredi, 2010). We have also tested methane and hydrogen (see Supplementary Information 1), but we observed rapid death of the incubated shrimps, so they were discarded. Furthermore, whether CH_4- or H_2-metabolic genes are actively expressed or not has not been determined. Biotic iron oxidation by *R. exoculata* epibionts has been proposed (Zbinden *et al.*, 2004, 2008; Corbari *et al.*, 2008a) on the basis of the close association of these bacteria with heavy iron-oxyhydroxide deposits. Our results support this hypothesis, but evidence is lacking as to the ability of the bacterial phylotypes identified so far to oxidise iron. Furthermore, abiotic iron-oxide precipitation can compete strongly with biotic iron oxidation (Schmidt *et al.*, 2009), bacterial cell walls can induce it (Corbari *et al.*, 2008a).

We also show here that *R. exoculata* epibionts can incorporate ^{14}C-acetate and ^{3}H-lysine much faster than they incorporate ^{14}C from bicarbonate. In the branchiostegite bacterial mats, the rate of organic carbon incorporation from acetate ($61.7\,\mu molAc_{inc} \times gC_{sam}^{-1} \times h^{-1}$) was 10–20 times the rate observed with ^{14}C-bicarbonate, depending on whether thiosulphate was present ($5.4\,\mu molC_{inc} \times gC_{sam}^{-1} \times h^{-1}$) or not ($2.8\,\mu molC_{inc} \times gC_{sam}^{-1} \times h^{-1}$). This may be due to the presence of heterotrophic bacteria, but to date, this has not been investigated. Our observation that the thick bacterial filaments were intensely labelled with all three radiotracers, and that the thin ones were also labelled to a lesser extent, suggests that at least the *epsilonproteobacteria* might switch to a mixotrophic metabolism and use small organic molecules, when available, as energy and/or carbon sources. Acetate and amino-acid assimilation is thus unsurprising and might reflect a capacity of certain chemolithoautotrophic bacterial epibionts to adjust their metabolism to changes in their geochemical environment. A versatile (autotrophic/mixotrophic/heterotrophic) energy metabolism using several electron donors (including hydrogen and organic compounds) and acceptors (including oxygen and nitrate) has indeed been reported for free and symbiotic *epsilonproteobacteria* of the Thiovulgaceae family (Campbell *et al.*, 2006; Goffredi, 2010) and suggested for *R. exoculata* ectosymbionts (Hügler *et al.*, 2011). Mixotrophy/heterotrophy is also commonly accepted as a possible feature of *gammaproteobacteria* of the Thiotrichaceae family (Goffredi, 2010), as most *Beggiatoa* species can grow on acetate as sole added carbon source (Larkin and Strohl, 1983). It has been proposed but not investigated for *R. exoculata* epibionts (Hügler *et al.*, 2011). In support of this hypothesis, a metagenomic study has revealed in *Riftia pachyptila* endosymbionts the presence of all genes required for heterotrophic metabolism (Robidart *et al.*, 2008), and a metaproteomic study has pinpointed acetate as a substrate for bacterial endosymbionts of the gutless marine worm *Olavius algarvensis* (Kleiner *et al.*, 2012). Schulz and Jørgensen (2001) interpret the metabolic flexibility of filamentous sulphur-oxidising bacteria, especially those of the *Thiothrix* group, and their ability to grow heterotrophically or autotrophically on different sulphur species, as a need to overcome disadvantages of their sessile life and to adapt their activity to changes in substrate availability (oxygen,

sulphide). In *R. exoculata*, the obvious variability of bacterial assemblages according to the gill chamber area, the individual and the vent site (Zbinden *et al.*, 2008; Petersen *et al.*, 2009; Hügler *et al.*, 2011) suggests a consortium composition plasticity as a response to varying vent fluid composition (Charlou *et al.*, 2002; Schmidt *et al.*, 2008) and to fluctuating geochemical or micro-environmental conditions in the zone of mixing with deep water.

The relatively high carbon fixation rate observed in SW alone suggests that *R. exoculata* epibionts have an internal energy store that supplies autotrophic metabolisms in the absence of an external electron donor, for example, when the shrimps swim from reduced-compound-rich hydrothermal fluid to oxic (reduced-compound-poor) deep water. Such carbon fixation has previously been evidenced in *Bathymodiolus thermophilius* and *R. exoculata* symbionts (Nelson *et al.*, 1995; Polz *et al.*, 1998). Energy could be stored as iron polyphosphate and sulphur globules like those observed ultrastructurally by Wirsen *et al.* (1993) and Zbinden *et al.* (2008) in thin filamentous bacteria. These could be identified as *Leucothrix*-like *gamma-ectosymbionts* because their APS pathway allows production of intermediate sulphur compounds and because the storage role of similar globules is well documented in their shallow-water relatives (Larkin and Strohl, 1983; Schulz and Jørgensen, 2001). Furthermore, these globules were shown to be empty in specimens maintained in a pressurised aquarium without electron donors (Zbinden *et al.*, 2008). This suggests that the enhanced carbon fixation observed in the presence of thiosulphate as compared with pure SW might reflect a switch of *gamma-* and/or *epsilon-epibionts* to an external energy source supporting autotrophic metabolism.

Bacteria–host transfers

Several authors propose that organic nutrients might be transferred from epibionts to *R. exoculata* (Casanova *et al.*, 1993; Zbinden *et al.*, 2004; Corbari *et al.*, 2008b). Others, arguing that the cuticle is impermeable, reject this hypothesis (Segonzac *et al.*, 1993; Gebruk *et al.*, 2000). The latter authors refer to an experiment (Anderson and Stephens, 1969) or to subsequent review papers (Stephens, 1988; Preston, 1993; Gebruk *et al.*, 2000) suggesting that crustaceans, in contrast to many other marine invertebrates, cannot take up dissolved organic matter or dissolved organic carbon. According to Anderson and Stephens (1969), the apparent incorporation of radiotracers by crustaceans was due to uptake by epibionts alone and not by the crustaceans themselves. Yet these authors worked with whole organisms, and never separated the internal tissues from the integument and the epibionts as we have done here.

The present results demonstrate the transfer of carbon fixed by bacteria to the host shrimp tissues and the ability of shrimps to take up dissolved organic molecules such as acetate or lysine across their integument. Together with our autoradiographs, the higher radiotracer concentrations in the shrimp tissues than in the incubation media (Table 2) and the incorporation of ^{3}H-lysine and ^{14}C-acetate into the *Mu* (proteins) and the *HP* (storage lipids) confirm their active uptake and their accumulation in shrimp insoluble organic matter. Our separate analysis of the old and new cuticles of the abdominal integument and the corresponding autoradiographs also suggest that the new cuticle and the secreting epithelium incorporate more labelled molecules, probably because of the intense biosynthetic activity at this level in pre-ecdysial crustaceans.

These results thus constitute *in-vivo* experimental evidence of nutritional transfer of bacteria-fixed

Table 2 Initial and final concentrations (in μM) of labelled compounds (^{13}C, ^{14}C-bicarbonate, ^{14}C-acetate, ^{3}H-lysine) in the incubation media and the shrimp body parts

Labelled compounds in each incubation medium	*Initial concentration (μM) of labelled compounds in the incubation medium*	*Final concentration (μM) obtained after 1 h in bacteria and shrimps tissues*	
$NaH^{13}CO_3$	11 764	MP	157.17 ± 52.92
		DT	49.94 ± 0.29
		BB	42.04 ± 13.84
		Mu	20.42 ± 9.13
		OB	8.30 ± 7.33
$NaH^{14}CO_3$	3000	MP	33.01 ± 16.31
		OB	19.88 ± 15.13
		DT	15.84 ± 16.30
		BB	12.20 ± 4.89
		AC	7.02 ± 2.95
		Gi	5.97 ± 2.04
		HP	2.13 ± 0.55
		Mu	1.75 ± 1.01
^{14}C-acetate	200	**MP**	**524.24 ± 100.53**
		BB	**281.48 ± 47.86**
		Gi	**245.47 ± 66.43**
		OB	111.52 ± 53.91
		AC_n	101.97 ± 80.37
		U	46.19 ± 9.14
		AC	33.01 ± 0.35
		DT	18.79 ± 9.61
		AC_o	14.87 ± 0.91
		Mu	9.01 ± 3.76
		HP	7.84 ± 0.99
^{3}H-lysine	0.2	**MP**	**14.82 ± 7.92**
		BB	**3.02 ± 2.97**
		Gi	**0.54 ± 0.28**
		OB	**0.48 ± 0.22**
		Mu	0.06 ± 0.00
		DT	0.00 ± 0.01
		HP	0.00 ± 0.00

Abbreviations: AC, abdominal cuticle; ACn, new abdominal cuticle; AC_o, old abdominal cuticle; BB, branchiostegite biofilm; DT, digestive tract; Gi, gills; HP, hepatopancreas; MP, mouthpart; Mu, muscles; OB, outer branchiostegite; U, uropods.
In bold are the data for compartments that accumulate the radiotracers (in > out). For the comparative estimation of tissue concentrations, 1 g fresh weight was considered equal to 1 ml liquid. All values are taken from experiments in pure seawater.

carbon to shrimps. They are in good agreement with previous stable isotope studies (Gebruk *et al.*, 1993; Pond *et al.*, 1997a, b, 2000; Rieley *et al.*, 1999; Colaço *et al.*, 2007) and confirm that *R. exoculata* depends on its epibionts for its nutrition. They thus strengthen the view that the relationship between bacteria and shrimp is mutualistic: the epibionts supply carbon compounds to the shrimp and the shrimp, thanks to its gill chamber flow and its swimming behaviour, offers them protection and a supply of chemical compounds, maintaining their position at the oxic/anoxic interface around active chimneys (Casanova *et al.*, 1993; Segonzac *et al.*, 1993). The *R. exoculata* bacterial epibiosis can thus be regarded as a true mutualistic trophic ectosymbiosis, similar to what is known about the chemosynthetic endosymbiosis of organisms such as *R. pachyptila* (Felbeck, 1981; Fisher *et al.*, 1989), *Calyptogena magnifica* (Childress *et al.*, 1991) and *S. velum* (Stewart and Cavanaugh, 2006; Scott and Cavanaugh, 2007).

Finally, the view that bacterial products are assimilated across the shrimp integument rather than *via* the *DT* is strongly supported by: (1) the significant incorporation of both ^{14}C-acetate and ^{3}H-lysine after an incubation time as short as 1 h. This is insufficient for uptake by ingestion assimilation, which commonly takes several hours (ingestion assimilation of carbon from bicarbonate, for example, requires prior incorporation by the bacteria, followed by grazing of bacteria from the *MP*) (Chipps, 1998; Hoyt *et al.*, 2000); (2) the high incorporation levels recorded in the gill chamber integument lining (*OB*, *Gi*), as opposed to (3) the much lower levels recorded in the *DT* (Figure 6). These results are in agreement with the view that the shrimps do not graze on their epibionts (Zbinden *et al.*, 2004; Corbari *et al.*, 2008b), but rather farm them (Segonzac *et al.*, 1993; Polz and Cavanaugh, 1996), although they might also ingest some chimney bacteria along with sulphides (Van Dover *et al.*, 1988; Segonzac, 1992). The low but nevertheless significant incorporation of ^{14}C from bicarbonate in the *DT* corroborates the data of Polz *et al.* (1998), although they found higher rates than ours (upon incubating isolated gut segments). This incorporation might be due to chemosynthetic activity of the midgut microbial community (Polz *et al.*, 1998; Zbinden and Cambon-Bonavita, 2003; Durand *et al.*, 2010), but this community would be less active than the gill chamber community.

The view that soluble carbon-containing compounds are transferred from bacteria to shrimp by crossing the gill chamber integument tallies with the ultrastructural characteristics of this integument, which resemble those of permeable and/or transporting tissues (Martinez *et al.*, 2005): a very thin cuticle (30 μm), reduced blood-water distance, mitochondria-rich cells with apical infolding in the branchiostegite epithelium. In *R. exoculata*, the uptake of bacterial nutrients across the integument

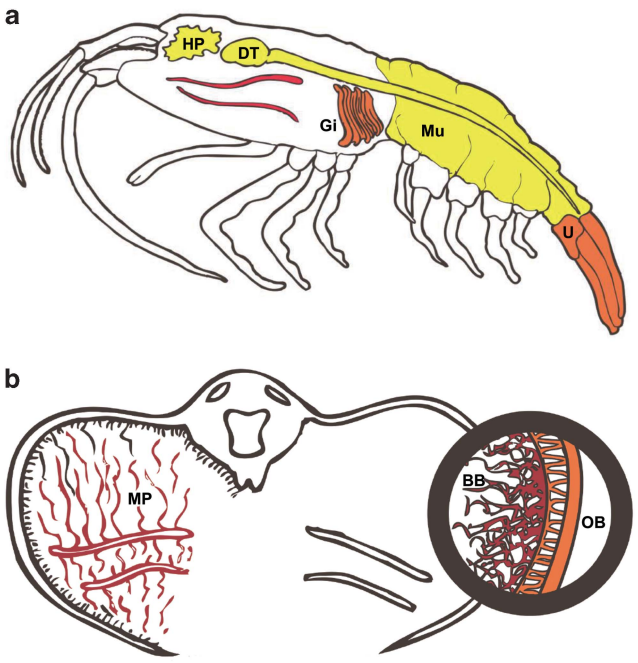

Figure 6 Schematic view of *R. exoculata* (**a**) and its gill chamber—transversal view (**b**) showing the level of ^{14}C-tracers incorporation in the internal organs by colour range from the highest levels in red to the lowest in yellow. *U*, uropods.

could be the major source of nourishment, along with complementary sources such as grazing on chimney minerals (Van Dover *et al.*, 1988; Segonzac *et al.*, 1993), ingestion of bacteria-colonised exuviae, and midgut microflora activities (Zbinden and Cambon-Bonavita, 2003; Zbinden *et al.*, 2004; Corbari *et al.*, 2008b; Durand *et al.*, 2010). It could be regarded as a peculiar adaptation of the shrimp. Although some authors have discarded this hypothesis, the present results may bring it back into favour. By extension, they suggest that this process might exist in many crustacean species, which would derive their nourishment at least partly from dissolved organic matter or dissolved organic carbon, as is commonly accepted for many marine invertebrates: annelids (Richards and Arme, 1982; Ahearn *et al.*, 2000; Peppler and Ahearn, 2003), molluscs (Wright and Secomb, 1986; Wright, 1988; Wright and Pajor, 1989; De Eguileor *et al.*, 2000) and cuticle-lined parasitic organisms such as nematodes (Fleming and Fetterer, 1984; Gordon and Burford, 1984; Masood, 1984). Arbitrarily rejected for crustaceans (Stephens, 1988) and especially decapods, this idea is surprisingly accepted without demonstration for parasitic rhizocephalan barnacles such as *Sacculina carcini* (Bresciani and Høeg, 2001) and for parasitic copepods (Kannupandi, 1976; Poquet *et al.*, 1994) with a modified cuticle. It is well known, furthermore, that in pre-ecdysis, crustaceans (and other arthropods) absorb soluble molecules (for example, sugars and amino acids) from their degrading old cuticle through the new cuticle and re-utilise them for its synthesis (Compère *et al.*,

2004). These conflicting views regarding the capacity of marine crustaceans to assimilate dissolved organic carbon will be tested in further studies.

Acknowledgements

We thank F Gaill, chief scientist of the MoMARDREAM-Naut cruise, the captain and crew of the RV 'Pourquoi Pas?' and the 'Nautile' team. We thank N Decloux for excellent technical assistance, A Saussu for drawing the shrimp diagram, Mrs K Broman (KBrO Science and Communication SPRL, broman.translations@swing.be) for the English revision as well as the reviewers and the editorial board for their constructive comments. This work was funded by the European RTN-MOMARnet program and the Belgian National Fund for Scientific Research (FNRS–FRFC, convention no. 2.4594.07.F). JP is a PhD student supported by an FNRS-FRIA fellowship (Belgium) and GL is associated researcher of the FRS-FNRS (Belgium).

References

Ahearn H, Ahearn G, Gomme J. (2000). Integumentary L-histidine transport in a euryhaline polychaete worm: regulatory roles of calcium and cadmium in the transport event. *J Exp Biol* **203**: 2877–2885.

Anderson JW, Stephens GC. (1969). Uptake of organic material by aquatic invertebrates. VI. Role of epiflora in apparent uptake of glycine by marine crustaceans. *Mar Biol* **4**: 243–249.

Bresciani J, Høeg JT. (2001). Comparative ultrastructure of the root system in Rhizocephalan barnacles (Crustacea: Cirripedia: Rhizocephala). *J Morphol* **249**: 9–42.

Campbell BJ, Engel AS, Porter ML, Takai K. (2006). The versatile ε-proteobacteria: key players in sulphidic habitats. *Nat Rev Microbiol* **4**: 458–468.

CAREX Identification of model organisms in extreme environments. *CAREX - Workshop Report*; 5 November 2010; Sasbachwalden (Black Forest) Germany http://www.carex-eu.org/.

Casanova B, Brunet M, Ségonzac M. (1993). L'impact d'une épibiose bactérienne sur la morphologie fonctionnelle de crevettes associées à l'hydrothermalisme Médio-Atlantique. *Cah Biol Mar* **34**: 573–588.

Cavanaugh C, McKiness Z, Newton I, Stewart F. (2006). Marine Chemosynthetic Symbioses. In: Dworkin M, Falkow S, Rosenberg E, Schleifer K-H, Stackebrandt E (eds). *The Prokaryotes*. Springer Science + Business Media, Inc.: Singapore, pp 475–507.

Charlou J-L, Donval J-P, Fouquet Y, Jean-Baptiste P, Holm N. (2002). Geochemistry of high H_2 and CH_4 vent fluids issuing from ultramafic rocks at the Rainbow hydrothermal field (36°14′N, MAR). *Chem Geol* **191**: 345–359.

Childress JJ, Fisher CR, Favuzzi JA, Sanders NK. (1991). Sulfide and carbon dioxide uptake by the hydrothermal vent clam, *Calyptogena magnifica*, and its chemoautotrophic symbionts. *Physiol Zool* **64**: 1444–1470.

Chipps SR. (1998). Temperature-dependent consumption and gut-residence time in the opossum shrimp *Mysis relicta*. *J Plankton Res* **20**: 2401–2411.

Colaço A, Desbruyères D, Guezennec J. (2007). Polar lipid fatty acids as indicators of trophic associations in a deep-sea vent system community. *Mar Ecol* **28**: 15–24.

Compère P, Jeuniaux C, Goffinet G. (2004). The integument: morphology and biochemistry. In: Forest J, Van Vaupel Klein JC (eds). *Treatise on Zoology, 1. Anatomy, Taxonomy and Biology, The Crustacea. vol. 1:* Brill, Leiden, pp 59–144.

Corbari L, Cambon-Bonavita M-A, Long GJ, Grandjean F, Zbinden M, Gaill F *et al.* (2008a). Iron oxide deposits associated with the ectosymbiotic bacteria in the hydrothermal vent shrimp *Rimicaris exoculata*. *Biogeosciences* **5**: 1295–1310.

Corbari L, Zbinden M, Cambon-Bonavita M-A, Gaill F, Compère P. (2008b). Bacterial symbionts and mineral deposits in the branchial chamber of the hydrothermal vent shrimp *Rimicaris exoculata*: relationship to moult cycle. *Aquat Biol* **1**: 225–238.

Dattagupta S, Schaperdoth I, Montanari A, Mariani S, Kita N, Valley JW *et al.* (2009). A novel symbiosis between chemoautotrophic bacteria and a freshwater cave amphipod. *ISME J* **3**: 935–943.

De Eguileor M, Leonardi MG, Grimaldi A, Tettamanti G, Fiandra L, Giordana B *et al.* (2000). Integumental amino acid uptake in a carnivorous predator mollusc (*Sepia officinalis*, Cephalopoda). *Tissue Cell* **32**: 389–399.

Douville E, Charlou J-L, Oelkers EH, Bienvenu P, Jove Colon CF, Donval J-P *et al.* (2002). The rainbow vent fluids (36°14′N, MAR): the influence of ultramafic rocks and phase separation on trace metal content in Mid-Atlantic Ridge hydrothermal fluids. *Chem Geol* **184**: 37–48.

Dubilier N, Bergin C, Lott C. (2008). Symbiotic diversity in marine animals: the art of harnessing chemosynthesis. *Nat Rev Microbiol* **6**: 725–740.

Dubilier N, Mulders C, Ferdelman T, de Beer D, Pernthaler A, Klein M *et al.* (2001). Endosymbiotic sulphate-reducing and sulphide-oxidizing bacteria in an oligochaete worm. *Nature* **411**: 298–302.

Durand L, Zbinden M, Cueff-Gauchard V, Duperron S, Roussel EG, Shillito B *et al.* (2010). Microbial diversity associated with the hydrothermal shrimp *Rimicaris exoculata* gut and occurrence of a resident microbial community. *FEMS Microbiol Ecol* **71**: 291–303.

Felbeck H. (1981). Chemoautotrophic potential of the hydrothermal vent tube worm, *Riftia pachyptila* jones (Vestimentifera). *Science* **213**: 336–338.

Fisher CR, Childress JJ, Minnich E. (1989). Autotrophic carbon fixation by the chemoautotrophic symbionts of *Riftia pachyptila*. *Biol Bull* **177**: 372–385.

Fleming MW, Fetterer RH. (1984). *Ascaris suum*: continuous perfusion of the pseudocoelom and nutrient absorption. *Exp Parasitol* **57**: 142–148.

Gebruk AV, Pimenov NV, Savvichev AS. (1993). Feeding specialization of bresiliid shrimps in the TAG site hydrothermal community. *Mar Ecol Prog Ser* **98**: 247–253.

Gebruk AV, Southward EC, Kennedy H, Southward AJ. (2000). Food sources, behaviour, and distribution of hydrothermal vent shrimps at the Mid-Atlantic Ridge. *J Mar Biol Assoc UK* **80**: 485–499.

Gillan DC, Dubilier N. (2004). Novel epibiotic *Thiothrix* bacterium on a marine Amphipod. *Appl Environ Microbiol* **70**: 3772–3775.

Gillan DC, Ribesse J, De Ridder C. (2004). The iron-encrusted microbial community of *Urothoe poseidonis* (Crustacea, Amphipoda). *J Sea Res* **52**: 21–32.

Goffredi SK. (2010). Indigenous ectosymbiotic bacteria associated with diverse hydrothermal vent invertebrates. *Environ Microbiol Rep* **2**: 479–488.

Goffredi SK, Jones WJ, Erhlich H, Springer A, Vrijenhoek RC. (2008). Epibiotic bacteria associated with the recently discovered Yeti crab, *Kiwa hirsuta*. *Environ Microbiol* **10**: 2623–2634.

Gordon R, Burford IR. (1984). Transport of palmitic acid across the tegument of the entomophilic nematode *Romanomermis culicivorax*. *J Nematol* **16**: 14–21.

Guri M, Durand L, Cueff-Gauchard V, Zbinden M, Crassous P, Shillito B *et al.* (2012). Acquisition of epibiotic bacteria along the life cycle of the hydrothermal shrimp *Rimicaris exoculata*. *ISME J* **6**: 597–609.

Hoyt M, Fleeger JW, Siebeling R, Feller RJ. (2000). Serological estimation of prey-protein gut-residence time and quantification of meal size for grass shrimp consuming meiofaunal copepods. *J Exp Mar Biol Ecol* **248**: 105–119.

Hügler M, Gärtner A, Imhoff JF. (2010). Functional genes as markers for sulfur cycling and CO_2 fixation in microbial communities of hydrothermal vents of the Logatchev field. *FEMS Microbiol Ecol* **73**: 526–537.

Hügler M, Petersen JM, Dubilier N, Imhoff JF, Sievert SM. (2011). Pathways of carbon and energy metabolism of the epibiotic community associated with the deep-sea hydrothermal vent shrimp *Rimicaris exoculata*. *PLoS ONE* **6**: e16018.

Kannupandi T. (1976). Cuticular adaptations in two parasitic copepods in relation to their modes of life. *J Exp Mar Biol Ecol* **22**: 235–248.

Kleiner M, Wentrup C, Lott C, Teeling H, Wetzel S, Young J *et al.* (2012). Metaproteomics of a gutless marine worm and its symbiotic microbial community reveal unusual pathways for carbon and energy use. *Proc Natl Acad Sci* **109**: E1173–E1182.

Larkin JM, Strohl WR. (1983). *Beggiatoa*, *Thiothrix*, and *Thioploca*. *Annu Rev Microbiol* **37**: 341–367.

Lepoint G, Gobert S, Dauby P, Bouquegneau J-M. (2004). Contributions of benthic and planktonic primary producers to nitrate and ammonium uptake fluxes in a nutrient-poor shallow coastal area (Corsica, NW Mediterranean). *J Exp Mar Biol Ecol* **302**: 107–122.

Macpherson E, Jones WJ, Segonzac M. (2005). A new squat lobster family of Galatheoidea (Crustacea, Decapoda, Anomura) from the hydrothermal vents of the Pacific-Antarctic Ridge. *Zoosystema* **27**: 709–723.

Martinez A-S, Charmantier G, Compère P, Charmantier-Daures M. (2005). Branchial chamber tissues in two caridean shrimps: the epibenthic *Palaemon adspersus* and the deep-sea hydrothermal *Rimicaris exoculata*. *Tissue Cell* **37**: 153–165.

Masood K. (1984). Transcuticular absorption of amino acids by *Ascaridia galli*. *Indian J Parasitol* **7**: 185–188.

Miyake H, Kitada M, Tsuchida S, Okuyama Y, Nakamura K-i. (2007). Ecological aspects of hydrothermal vent animals in captivity at atmospheric pressure. *Mar Ecol* **28**: 86–92.

Nelson DC, Hagen KD, Edwards DB. (1995). The gill symbiont of the hydrothermal vent mussel *Bathymodiolus thermophilus* is a psychrophilic, chemoautotrophic, sulfur bacterium. *Mar Biol* **121**: 487–495.

Peppler JE, Ahearn GA. (2003). Effect of heavy metals on the uptake of [3H]-L-histidine by the polychaete *Nereis succinea*. *Comp Biochem Physiol C Toxicol Pharmacol* **136**: 181–189.

Petersen JM, Ramette A, Lott C, Cambon-Bonavita M-A, Zbinden M, Dubilier N. (2009). Dual symbiosis of the vent shrimp *Rimicaris exoculata* with filamentous gamma- and epsilonproteobacteria at four Mid-Atlantic Ridge hydrothermal vent fields. *Environ Microbiol* **12**: 2204–2218.

Petersen JM, Zielinski FU, Pape T, Seifert R, Moraru C, Amann R *et al.* (2011). Hydrogen is an energy source for hydrothermal vent symbioses. *Nature* **476**: 176–180.

Polz MF, Cavanaugh CM. (1995). Dominance of one bacterial phylotype at a Mid-Atlantic Ridge hydrothermal vent site. *Proc Natl Acad Sci USA* **92**: 7232–7236.

Polz MF, Cavanaugh CM. (1996). The ecology of ectosymbiosis at a Mid-Atlantic Rigde hydrothermal vent site. *Biosyst Ecol Ser* **11**: 337–352.

Polz MF, Robinson JJ, Cavanaugh CM, Van Dover CL. (1998). Trophic ecology of massive shrimp aggregations at a Mid-Atlantic Ridge hydrothermal vent site. *Limnol Oceanogr* **43**: 1631–1638.

Pond DW, Bell MV, Dixon DR, Fallick AE, Sargent JR. (1997a). Occurrence of 16:2(n-4) and 18:2(n-4) fatty acids in the lipids of the hydrothermal vent shrimp *Rimicaris exoculata*: nutritional and trophic implications. *Marine Ecology Progress Series* **156**: 167–174.

Pond DW, Gebruk A, Southward EC, Southward AJ, Fallick AE, Bell MV *et al.* (2000). Unusual fatty acid composition of storage lipids in the bresilioid shrimp *Rimicaris exoculata* couples the photic zone with MAR hydrothermal vent sites. *Mar Ecol Prog Ser* **198**: 171–179.

Pond DW, Segonzac M, Bell MV, Dixon DR, Fallick AE, Sargent JR. (1997b). Lipid and lipid carbon stable isotope composition of the hydrothermal vent shrimp *Mirocaris fortunata*: evidence for nutritional dependence on photosynthetically fixed carbon. *Mar Ecol Prog Ser* **157**: 221–231.

Poquet M, Ribes E, Bozzo MG, Durfort M. (1994). Ultrastructure and cytochemistry of the integument of *Modiolicola gracilis*, parasitic copepod in mussel gills (*Mytilus galloprovincialis* and *Mytilus edulis*). *J Morphol* **221**: 87–99.

Preston RL. (1993). Transport of amino acids by marine invertebrates. *J Exp Zool* **265**: 410–421.

Ravaux J, Gaill F, Le Bris N, Sarradin P-M, Jollivet D, Shillito B. (2003). Heat-shock response and temperature resistance in the deep-sea vent shrimp *Rimicaris exoculata*. *J Exp Biol* **206**: 2345–2354.

Richards KS, Arme C. (1982). Integumentary uptake of dissolved organic materials by earthworms. *Pedobiologia* **23**: 358–366.

Rieley G, Van Dover CL, Hedrick DB, Eglinton G. (1999). Trophic ecology of *Rimicaris exoculata*: a combined lipid abundance/stable isotope approach. *Mar Biol* **133**: 495–499.

Robidart JC, Bench SR, Feldman RA, Novoradovsky A, Podell SB, Gaasterland T *et al.* (2008). Metabolic versatility of the *Riftia pachyptila* endosymbiont revealed through metagenomics. *Environ Microbiol* **10**: 727–737.

Rouwenhorst RJ, Frank Jzn J, Scheffers WA, Van Dijken JP. (1991). Determination of protein concentration by total organic carbon analysis. *J Biochem Biophys Methods* **22**: 119–128.

Schmidt C, Corbari L, Gaill F, Le Bris N. (2009). Biotic and abiotic controls on iron oxyhydroxide formation in the gill chamber of the hydrothermal vent shrimp *Rimicaris exoculata*. *Geobiology* **7**: 454–464.

Schmidt C, Vuillemin R, Le Gall C, Gaill F, Le Bris N. (2008). Geochemical energy sources for microbial primary production in the environment of hydrothermal vent shrimps. *Mar Chem* **108**: 18–31.

Schulz HN, Jørgensen BB. (2001). Big Bacteria. *Annu Rev Microbiol* **55**: 105–137.

Scott KM, Cavanaugh CM. (2007). CO_2 uptake and fixation by endosymbiotic chemoautotrophs from the Bivalve *Solemya velum*. *Appl Environ Microbiol* **73**: 1174–1179.

Segonzac M. (1992). The hydrothermal vent communities of Snake Pit area (Mid-Atlantic Ridge; 23°N, 3480 m): megafaunal composition and microdistribution. *Mar Biol* **314**: 593–600.

Segonzac M, De Saint Laurent M, Casanova B. (1993). L'énigme du comportement trophique des crevettes Alvinocarididae des sites hydrothermaux de la dorsale médio-atlantique. *Cah Biol Mar* **34**: 535–571.

Shillito B, Jollivet D, Sarradin P-M, Rodier P, Lallier F, Desbruyères D *et al.* (2001). Temperature resistance of *Hesiolyra bergi*, a polychaetous annelid living on deep-sea vent smoker walls. *Mar Ecol Prog Ser* **216**: 141–149.

Stams AJM, Plugge CM. (2009). Electron transfer in syntrophic communities of anaerobic bacteria and archaea. *Nat Rev Microbiol* **7**: 568–577.

Stephens GC. (1988). Epidermal amino acid transport in marine invertebrates. *Biochim Biophys Acta* **947**: 113–138.

Stewart FJ, Cavanaugh CM. (2006). Bacterial endosymbioses in *Solemya* (Mollusca: Bivalvia) - model systems for studies of symbiont-host adaptation. *Antonie Van Leeuwenhoek* **90**: 343–360.

Thurber AR, Jones WJ, Schnabel K. (2011). Dancing for food in the Deep Sea: bacterial farming by a new species of yeti crab. *PLoS ONE* **6**: e26243.

Ullberg S, Larsson B, Tjälve H. (1982). Autoradiography. In: Glenn HJ (ed). *Biologic Applications of Radiotracers*. CRC Press: Boca Raton, Florida pp 55–108.

Van Dover CL, Fry B, Grassle JF, Humphris S, Rona PA. (1988). Feeding biology of the shrimp *Rimicaris exoculata* at hydrothermal vents on the Mid-Atlantic Ridge. *Mar Biol* **98**: 209–216.

Williams AB, Rona PA. (1986). Two new caridean shrimps (Bresiliidae) from a hydrothermal field on the Mid-Atlantic Ridge. *J Crust Biol* **6**: 446–462.

Wirsen CO, Jannasch HW, Molyneaux SJ. (1993). Chemosynthetic microbial activity at Mid-Atlantic Ridge hydrothermal vent sites. *J Geophys Res* **98**: 9693–9703.

Wright SH. (1988). Amino acid transport in the gill epithelium of a marine bivalve. *Comp Biochem Physiol A Physiol* **90**: 635–641.

Wright SH, Pajor AM. (1989). Mechanisms of integumental amino acid transport in marine bivalves. *Am J Physiol* **257**: R473–R483.

Wright SH, Secomb TW. (1986). Epithelial amino acid transport in marine mussels: role in net exchange of taurine between gills and sea water. *J Exp Biol* **121**: 251–270.

Zbinden M, Cambon-Bonavita M-A. (2003). Occurrence of *Deferribacterales* and *Entomoplasmatales* in the deep-sea Alvinocarid shrimp *Rimicaris exoculata* gut. *FEMS Microbiol Ecol* **46**: 23–30.

Zbinden M, Le Bris N, Gaill F, Compère P. (2004). Distribution of bacteria and associated minerals in the gill chamber of the vent shrimp *Rimicaris exoculata* and related biogeochemical processes. *Mar Ecol Prog Ser* **284**: 237–251.

Zbinden M, Shillito B, Le Bris N, De Villardi de Montlaur C, Roussel E, Guyot F *et al.* (2008). New insights on the metabolic diversity among the epibiotic microbial communitiy of the hydrothermal shrimp *Rimicaris exoculata*. *J Exp Mar Biol Ecol* **359**: 131–140.

Supplementary Information accompanies the paper on The ISME Journal website (http://www.nature.com/ismej)

Chemical Senses, 2017, Vol 42, 319–331
doi:10.1093/chemse/bjx007
Original Article
Advance Access publication February 22, 2017

Original Article

Comparative Study of Chemosensory Organs of Shrimp From Hydrothermal Vent and Coastal Environments

Magali Zbinden[1], Camille Berthod[1], Nicolas Montagné[2], Julia Machon[1], Nelly Léger[1], Thomas Chertemps[2], Nicolas Rabet[3], Bruce Shillito[1] and Juliette Ravaux[1]

[1]Sorbonne Universités, Univ Paris 06, UMR CNRS MNHN 7208 Biologie des Organismes Aquatiques et Ecosystèmes (BOREA), Equipe Adaptation aux Milieux Extrêmes, Bât. A, 4e étage, 7 Quai St Bernard, 75005 Paris, France, [2]Sorbonne Universités, Univ Paris 06, Institut d'Ecologie et des Sciences de l'Environnement (iEES-Paris), 4 place Jussieu, 75005 Paris, France and [3]Sorbonne Universités, Univ Paris 06, UMR CNRS MNHN 7208 Biologie des Organismes Aquatiques et Ecosystèmes (BOREA), Département des milieux et peuplements aquatiques, CP26, 43 rue Cuvier, 75005 Paris, France

Correspondence to be sent to: Magali Zbinden, Université Pierre et Marie Curie, UMR 7208 BOREA, 7 quai St Bernard - Bat A, 4ème étage, pièce 417 (Boite 5), 75252 Paris Cedex 05, France. e-mail: magali.zbinden@upmc.fr

Editorial Decision 24 January 2017.

Abstract

The detection of chemical signals is involved in a variety of crustacean behaviors, such as social interactions, search and evaluation of food and navigation in the environment. At hydrothermal vents, endemic shrimp may use the chemical signature of vent fluids to locate active edifices, however little is known on their sensory perception in these remote deep-sea habitats. Here, we present the first comparative description of the sensilla on the antennules and antennae of 4 hydrothermal vent shrimp (*Rimicaris exoculata*, *Mirocaris fortunata*, *Chorocaris chacei*, and *Alvinocaris markensis*) and of a closely related coastal shrimp (*Palaemon elegans*). These observations revealed no specific adaptation regarding the size or number of aesthetascs (specialized unimodal olfactory sensilla) between hydrothermal and coastal species. We also identified partial sequences of the ionotropic receptor IR25a, a co-receptor putatively involved in olfaction, in 3 coastal and 4 hydrothermal shrimp species, and showed that it is mainly expressed in the lateral flagella of the antennules that bear the unimodal chemosensilla aesthetascs.

Key words: aesthetascs, decapod, hydrothermal shrimp, IR25a, olfaction

Introduction

Chemical senses are crucial in mediating important behavioral patterns for most animals. In crustaceans, chemical senses have been shown to play a role in various social interactions, search and evaluation of food, as well as in evaluation and navigation in the habitat (Steullet et al. 2001; Derby and Weissburg 2014). Chemoreception in decapod crustaceans is mediated by chemosensory sensilla that are mainly localized on the first antennae (antennules), pereiopod dactyls and mouthparts (Ache 1982; Derby et al. 2016). Chemoreception has been proposed to be differentiated into 2 different modes (Schmidt and Mellon 2011; Mellon 2014; Derby et al. 2016): 1) "olfaction" mediated by olfactory receptor neurons (ORNs) housed in specialized unimodal olfactory sensilla (the aesthetascs), restricted to the lateral flagella of the antennules (Laverack 1964; Grünert and Ache 1988;

Cate and Derby 2001) and projecting to the olfactory lobe of the brain (Schmidt and Ache 1996b) and 2) "distributed chemoreception" mediated by numerous bimodal sensilla (containing mecano- and chemo-receptor neurons) occurring on all appendages, projecting to the second antenna and lateral antennular neuropils and the leg neuromeres (Schmidt and Ache 1996a). Although the molecular mechanisms of olfaction have been well studied in insects, they remain largely unknown in crustaceans, and the existing knowledge is restricted to a few number of model organisms (lobsters, crayfish, and the water flea *Daphnia pulex*; review in Derby et al. 2016). In particular, the nature of crustacean odorant receptors has remained elusive until recently, since searches for the traditional insect olfactory receptors have been unsuccessful. A new family of receptors involved in odorant detection, named the Ionotropic Receptors (IRs), was recently described in *Drosophila melanogaster*, and was subsequently shown to be conserved in Protostomia, including the crustacean *D. pulex* (Benton et al. 2009; review in Croset et al. 2010). Lately, several IRs were identified in other crustaceans, the spiny lobster *Panulirus argus* (Corey et al. 2013), the American lobster *Homarus americanus* (Hollins et al. 2003), the hermit crabs *Pagurus bernhardus* (Groh et al. 2014) and *Coenobita clypeatus* (Groh-Lunow et al. 2015), and were proposed to mediate the odorant detection in the antennules. In the lobster, the authors propose that IRs function as heteromeric receptors, with IR25a and IR93a being common subunits that associate with other IR subunits to determine the odor sensitivity of ORNs.

Chemoreception in crustaceans has been largely studied in large decapods like lobsters (Devine and Atema 1982; Cowan 1991; Moore et al. 1991; Derby et al. 2001; Shabani et al. 2008; and see review in Derby et al. 2016). However, this research theme remains poorly investigated in shrimp, especially in deep-sea species. Deep-sea hydrothermal vent shrimp inhabit patchy and ephemeral environments along the mid-oceanic ridges. Inhabiting such sparsely distributed habitats presents challenges for the detection of active emissions by endemic fauna, especially in the absence of light. In the early developmental stages, after release and dispersal in the water column, sometimes tens or hundreds of kilometers from their starting point, larvae need to locate a vent site to settle and begin their adult life (Pond et al. 1997; Herring and Dixon 1998). Later as adults, mobile vent fauna may need to evaluate their environment, to find hydrothermal fluid either to feed their symbiotic bacteria or just to be able to detect the appropriate habitat, in an environment characterized by steep physicochemical gradients (Sarradin et al. 1999; Sarrazin et al. 1999; Le Bris et al. 2006). Chemical compounds like sulfide, temperature and dim light emitted by vents have been proposed to be potential attractants for detection of hydrothermal emissions (Van Dover et al. 1989; Renninger et al. 1995; Gaten et al. 1998).

Only a few studies on olfaction in the hydrothermal shrimp *Rimicaris exoculata* have been published (Renninger et al. 1995; Chamberlain et al. 1996; Jinks et al. 1998), providing the first, brief, description of the sensilla on the antennules and antennae of this species. These authors also reported preliminary behavioral observations, suggesting an attraction to sulfide, and registered electrophysiological responses to sulfide in antennal filaments (but surprisingly not in the antennular lateral ones bearing aesthetascs).

Here, we present a comparative morphological description of antennae and antennules of 4 hydrothermal vent shrimp (*R. exoculata*, *Mirocaris fortunata*, *Chorocaris chacei*, and *Alvinocaris markensis*). We also identified partial sequences of the candidate co-receptor IR25a and studied its expression pattern in the different species. All the approaches were conducted in parallel on a closely related coastal shrimp (*Palaemon elegans*), to give insights in the potential adaptations of sensory organs in deep-sea species. Comparisons within hydrothermal species were also conducted to examine possible specific adaptations related to their different environments and lifestyles, as previous studies showed that chemical senses of crustaceans rapidly evolve and present specialized adaptations according to phylogeny, lifestyle and habitat, as well as to trophic levels (Beltz et al. 2003; Derby and Weissburg 2014). Knowledge of the sensory capabilities of hydrothermal species is especially relevant with the growing interest of mining companies for extraction of seafloor massive sulfides hydrothermal deposits (Hoagland et al. 2010). Possible impacts of sulfide exploitation on vent species encompass habitat destruction, increase of suspended particles and the presence of higher levels of toxic elements, leading to physiological disturbances and to potential alteration of their ability to perceive their environment (Lahman and Moore 2015) and detect hydrothermal emissions.

Materials and methods

Choice of models

Shrimp are one of the dominant macrofaunal taxa of hydrothermal sites in the Mid-Atlantic Ridge (Desbruyères et al. 2000, 2001). They are highly motile, and according to species, occupy different habitats, exhibit different food diets, and show various degrees of association with bacteria. Therefore they provide good models for studying olfactory capabilities since individuals belonging to different species are potentially not sensitive to the same attractants. *Rimicaris exoculata* lives in dense swarms (up to 2500 ind/m^2, Desbruyères et al. 2001) on the chimney walls, at around 20–30 °C, near the fluid emissions in order to feed their dense symbiotic chemoautotrophic bacterial community (Van Dover et al. 1988; Zbinden et al. 2004, 2008). *Chorocaris chacei* is much less abundant (locally 2–3 ind/dm^2) than *R. exoculata*, but may live close to it. It is also found as on sulfide blocks, in areas of weak fluid emissions (Desbruyères et al. 2006; Husson et al. 2016). *Chorocaris* also harbors a bacterial symbiotic community, though less developed than in *Rimicaris* (Segonzac 1992). *Mirocaris fortunata* lives at lower temperature (4.8–6.1 °C, Husson et al. 2016), in diffuse flow habitats and among *Bathymodiolus* mussel assemblages (Sarrazin et al. 2015). *Mirocaris* is opportunistic and feeds on mussel tissue, shrimp and other invertebrates, being reported as predators and/or scavengers (Gebruk et al. 2000; De Busserolles et al. 2009). *Alvinocaris markensis* occurs as solitary individuals, at the base of and on the walls of active edifices, close to *R. exoculata* aggregates, and also on mussel assemblages. It has been reported as necrophagous (Desbruyères et al. 2006), but also as a predator (Segonzac 1992).

In order to identify potential adaptations of hydrothermal shrimp sensory faculties, comparisons were made with the related shallow-water palaemonid species *P. elegans*. The description of palaemonid antennal structures is also interesting per se since olfaction is poorly analyzed in shrimp in general. Two additional palaemonid species, *Palaemon serratus* and *Palaemonetes varians*, were used for identifying the IR25a sequence.

Animal collection, conditioning, and maintenance

Specimens of Alvinocarididae *M. fortunata*, *R. exoculata*, *C. chacei*, and *A. markensis* were collected during the Momarsat 2011 and 2012, Biobaz 2013, and Bicose 2014 cruises, on the Mid-Atlantic Ridge (see Table 1 for cruises and sites). Shrimp were collected with the suction sampler of the ROV "Victor 6000" operating from the

RV "Pourquoi Pas?". Immediately after retrieval, living specimens were dissected and tissues of interest (see below) were fixed in a 2.5% glutaraldehyde/seawater solution for morphological observations or frozen in liquid nitrogen for molecular biology experiments.

Specimens of Palaemonidae *P. elegans*, *P. serratus*, and *P. varians* were collected from Saint-Malo region (France; 48°64′N, −2°00′W), between October 2011 and January 2015, using a shrimp hand net. They were transported to the laboratory and transferred to aerated aquaria with a 12 h:12 h light:dark cycle, a salinity of 35 g/L, and a water temperature of 18 °C. The shrimp were regularly fed with granules (JBL Novo Prawn). Tissues of interest were also fixed in a 2.5% glutaraldehyde/seawater solution for morphological observations or frozen in liquid nitrogen for molecular biology experiments.

Tissue collection

For morphological observations, antennae and antennules (both medial and lateral flagella) were used. For molecular biology experiments, the following organs were dissected for *P. elegans*: the antennular medial and lateral flagella (internal and external ramus separated), the antennae, the mouthparts (mandibles and 2 pairs of maxillae), the first and second walking legs and the eyestalks. For the hydrothermal shrimp, the dissection included the following organs: the antennular medial and lateral flagella, the antennae, and abdominal muscles.

Scanning electron microscopy

Samples were post-fixed in osmium tetroxide 1% once in the lab and dehydrated through an ethanol series. They were then critical-point-dried (CPD7501, Quorum Technologies) and platinum-coated in a Scancoat six Edwards sputter-unit prior to observation in a scanning electron microscope (Cambridge Stereoscan 260), operating at 20 kV.

RNA extraction and reverse transcription

Frozen shrimp tissues were ground in TRIzol Reagent (Thermo Fisher Scientific) with a Minilys homogenizer (Bertin Corp). Total RNA was isolated according to the manufacturer's protocol, and quantified by spectrophotometry and electrophoresis in a 1.2% agarose gel under denaturing conditions. RNA (500 ng) was DNAse treated to remove contamination using the TURBO DNAse kit (Thermo Fisher Scientific) and then reverse transcribed to cDNA with the Superscript II reverse transcriptase kit (Thermo Fisher Scientific) using a oligo$(dT)_{18}$ primer according to the manufacturer's instructions.

IR25a sequencing and mRNA expression (reverse transcription polymerase chain reaction)

The cDNA fragments encoding IR25a were amplified by 2 rounds of polymerase chain reaction (PCR). Oligonucleotide primers were designed from a multiple-sequence alignment of IR25a sequences of crustaceans (*D. pulex*, Croset et al. 2010; *H. americanus* AY098942, Hollins et al. 2003, *Lepeophtheirus salmonis* PRJNA280127 genome sequencing project), insects (*Acyrthosiphon pisum, Aedes aegypti, Anopheles gambiae*, *Apis mellifera*, *Bombyx mori, Culex quinquefasciatus*, *D. melanogaster*, *Nasonia vitripennis*, *Pediculus humanus*, *Tribolium castaneum*, Croset et al. 2010), gastropod molluscs (*Aplysia californica*, *Lottia gigantea*, Croset et al. 2010), nematods (*Caenorhabditis briggsae* XM_002643827, Stein et al. 2003, *Caenorhabditis elegans* NM_076040, The *C. elegans* Sequencing Consortium) and an annelid (*Capitella capitata*, Croset et al. 2010) (primer sequences are listed in Supplementary Table S1). PCR amplification reactions were performed in a 20 µL volume containing 1 µL of cDNA template, 2 µL of each primer [10 µM], 11.7 µL of H_2O, 2 µL of PCR buffer [10×], 0.8 µL of MgCl2 [50 mM], 0.4 µL of dNTP [10 mM] and 0.1 µL of BIOTAQ polymerase [5 U/µL] (Eurobio AbCys). The thermal profile consisted of an initial denaturation (94 °C, 3 min), followed by 35 cycles of denaturation (94 °C, 30 s), annealing (45 to 55 °C, 45 s) and extension (72 °C, 2 min), and a final extension (72 °C, 10 min) step. The PCR products were separated on a 1.5% agarose gel, purified with the GeneClean kit (MP Biomedicals), and cloned into a pBluescript KS plasmid vector using the T4 DNA ligase (Thermo Fisher Scientific). The ligation product was introduced in competent *Escherichia coli* cells (DH5alpha) that were cultured at 37 °C overnight. The clone screening was performed through PstI/HindIII (Thermo Fisher Scientific) digestion of plasmid DNA after plasmid extraction. Positive clones were sequenced on both strands (GATC Biotech). The resulting nucleotide sequences were deposited in the GenBank database under the accession numbers KU726988 (*M. fortunata* IR25a; consensus sequence from 6 clones), KU726987 (*R. exoculata* IR25a; consensus sequence from 3 clones), KU726989 (*C. chacei* IR25a; consensus sequence from 4 clones), KU726990 (*A. markensis* IR25a; consensus sequence from 4 clones), KU726984 (*P. elegans* IR25a; consensus sequence from 11 clones), KU726985 (*P. varians* IR25a; consensus sequence from 12 clones), and KU726986 (*P. serratus* IR25a; consensus sequence from 3 clones). Specific primers were further designed to amplify IR25a sequences in diverse tissues of the 4 alvinocaridid species and the palaemonid *P. elegans* (Supplementary Table S1). PCR amplifications were performed using BIOTAQ polymerase (Eurobio, AbCys) in a thermocycler (Eppendorf, Hamburg, Germany) with the following program: 94 °C for 3 min, 35 cycles of (94 °C for 30 s, 55 °C for 45 s, 72 °C for 2 min), and 72 °C for 10 min, with minor modifications of annealing temperature for different primer pairs.

Sequence analyses

A dataset of IR amino acid sequences was created, including the IR25a sequences identified in shrimp (present study), in other decapods (*P. argus*, Corey et al. 2013; *C. clypeatus*, Groh-Lunow et al. 2015; *H. americanus* AY098942, Hollins et al. 2003) and

Table 1. Cruises, locations and depths of the different sampling sites of the samples used in this study

Sites	Lat.	Long.	Depth (m)	Cruise, year	Ship/ submersible	Chief scientist
Menez Gwen	37°51′N	31°31′W	840	Biobaz, 2013	Pourquoi Pas? / ROV Victor	F. Lallier
Lucky Strike	37°17′N	32°16′W	1700	Biobaz, 2013	Pourquoi Pas? / ROV Victor	F. Lallier
				Momarsat, 2011	Pourquoi Pas? / ROV Victor	M. Cannat
				Momarsat, 2012	Thalassa / ROV Victor	M. Cannat and P. M. Sarradin
Rainbow	36°13′N	33°54′W	2260	Biobaz, 2013	Pourquoi Pas? / ROV Victor	F. Lallier
TAG	26°08′N	44°49′W	3600	Bicose, 2014	Pourquoi Pas? / ROV Victor	M. A. Cambon-Bonavita
Snake Pit	23°23′N	44°58′W	3480	Bicose, 2014	Pourquoi Pas? / ROV Victor	M. A. Cambon-Bonavita

in other crustaceans (*D. pulex*, Croset et al. 2010; *L. salmonis* PRJNA280127) together with IR sequences from the insects *B. mori*, *D. melanogaster*, *A. mellifera*, and *T. castaneum* (Croset et al. 2010). *Drosophila melanogaster* ionotropic glutamate receptor sequences were also included to serve as an out-group, and the final data set contained 173 sequences. These amino acid sequences were aligned with MAFFT v.6 (Katoh and Toh 2010) using the FFT-NS-2 algorithm and default parameters. The alignment was then manually curated to remove highly divergent regions (500 amino acid positions conserved in the final dataset). The phylogenetic reconstruction was carried out using maximum-likelihood. The LG+I+G+F substitution model (Le and Gascuel 2008) was determined as the best-fit model of protein evolution by ProtTest 1.3 (Abascal et al. 2005) following Akaike information criterion. Rate heterogeneity was set at 4 categories, and the gamma distribution parameter was estimated from the data set. Tree reconstruction was performed using PhyML 3.0 (Guindon et al. 2010), with both Subtree Pruning and Regrafting (SPR) and Nearest Neighbour Interchange (NNI) methods for tree topology improvement. Branch support was estimated by approximate likelihood-ratio test (aLRT) (Anisimova et al. 2006). Images were created using the iTOL web server (Letunic and Bork 2011).

Results

Morphology of the chemosensory organs: description and distribution of setal types on the antennae and antennules

In the 5 shrimp species studied for morphology (*P. elegans*, *M. fortunata*, *R. exoculata*, *C. chacei*, and *A. markensis*), antennae and antennules both consist of a peduncle and segmented flagella (one for the antennae and 2 for the antennules: an outer or lateral, and an inner or medial). In the 3 flagella, the diameter and length of the annuli vary, being large and short at the base and becoming thinner and longer towards the apex. The aesthetasc dimensions vary also along the flagella, being thinner and shorter at the base and growing toward the apex. The set of values (maximum, minimum, mean and standard deviation of diameter and length) for aesthetasc, as well as for non-aesthetasc sensilla, are given in Supplementary Table S2.

Palaemon elegans

The antennules are made of 3 basal annuli and 2 distal flagella. The lateral flagella are divided in 2 rami after a short fused basal part: a long external one and a shorter internal one (1/3 of the long one, n = 12, SD = 0.61) (Figure 1A). The aesthetascs are localized

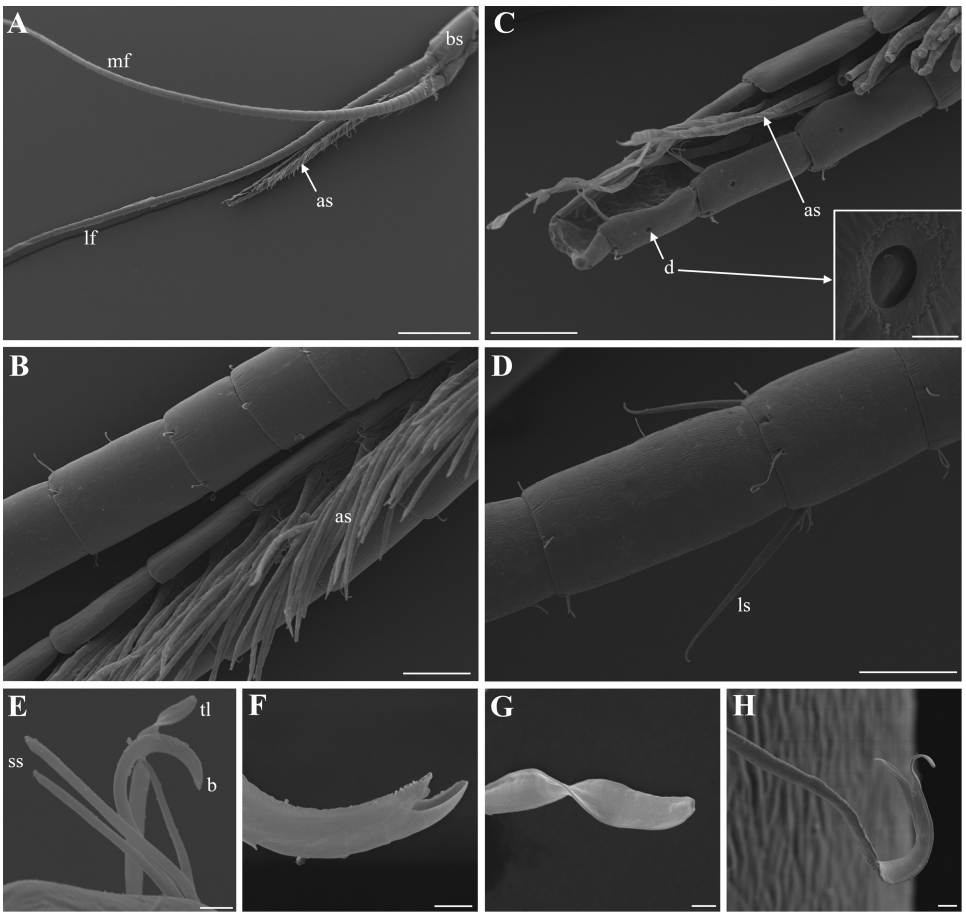

Figure 1. Morphology of antennules and setal types of *Palaemon elegans*. (A) Antennules are made of 3 basal annuli (bs) and 2 flagella: a medial (mf) and a lateral one (lf), which is divided in 2 rami: a long (outer) and a short (inner), bearing the aesthetascs (as). (B) Close-up on the ventral side of the furrow on the shorter ramus of the lateral flagellum bearing the aesthetascs. (C) Apex of the shorter ramus, showing the absence of aesthetascs on the last 2 annuli and the occurrence of small cuticular depressions (d), enlarged in insert. (D) Medial antennular flagellum showing the long simple seta (ls). (E) Tuft of 3 simple short (ss), one twisted flat (tf) and one beaked scaly (b) setae. (F) Beaked scaly seta. (G) Twisted flat seta. (H) Bifid seta. Scale bars: A = 1 mm; B, C, D = 100 µm; E = 10 µm; F, G, H = 2 µm. Scale bar in insert in C = 5 µm.

ventrally, in a furrow on the shorter ramus (Figure 1B). They are present from the basal fused part of the antennules to the apex of the short ramus (except from the last 2 annuli, Figure 1C). Two rows of 5 to 6 aesthetascs occur on each annulus (one row at the distal part of the annulus and the other at the middle part) (Figure 1B). The 2 or 3 basal and apical annuli have a smaller number of aesthetascs, giving a total number of approximately 140 aesthetascs per ramus (Table 2). Aesthetascs are up to 20.3 µm in diameter (n = 14) and 393 µm in length (n = 10) (Supplementary Table S2). They bear annulation throughout their length (short at the base and longer towards the apex), and lack a terminal pore.

Non-aesthetasc setae are also present on all the annuli of the 3 flagella (antennae and antennules), where they are distributed (up to 8) around the distal part of each annulus (Figure 1D). Five setal types are observed on the flagella, named after their morphology (dimensions are given in Table 2): 1) short simple seta (Figure 1E), 2) long simple seta (Figure 1D), 3) beaked scaly seta (Figure 1F), 4) twisted flat seta (Figure 1G), and 5) bifid seta (Figure 1H). All these 5 types appear to have a terminal pore. Short simple, beaked scaly and twisted flat setae are present on the antennae, the medial flagella of the antennules and the long ramus of the lateral flagella of the antennules. They occur as tufts of 5 setae, containing 3 simple short, one twisted flat and one beaked scaly seta (Figure 1E). These tufts are present on each annulus near the base but are spaced further apart towards the apex. The bifid setae are found only on the 2 flagella of the antennules, whereas the long simple are only found on medial flagella of the antennules (2 every 5 annuli, on each side of the flagellum). Small round cuticular depressions (5,5 to 6,7 µm in diameter) are observed on the medial side of the short ramus of the lateral flagella of the antennules, as well as on the antennae (insert in Figure 1C).

Mirocaris fortunata

In *M. fortunata*, as well as in the 3 other hydrothermal species, the antennules are also made of 3 basal annuli and 2 distal flagella (lateral and medial) (Figure 2A). In *M. fortunata*, the aesthetascs are localized latero-ventrally on the inner side of the lateral flagella, from the base to 2/3 of the flagella. One row of 3 to 4 aesthetascs occurs on the distal part of each annulus (Figure 2B), leading to a total number of approximately 60 aesthetascs per ramus (Table 2). Aesthetascs are up to 18.3 µm in diameter (n = 21) and 290.3 µm in length (n = 46) (Supplementary Table S2). They bear annulation on the apical half, and lack a terminal pore.

The rows of aesthetascs are flanked on the inner side by non-aesthetasc setae, organized as follows: one intermediate seta (thinner and shorter than the aesthetascs) and 2 or 3 short thin setae (thinner and shorter than the former) (Figure 2B). The intermediate setae have a peculiar apex shape with no obviously visible pore (Figure 2D), whereas the short setae are simple with a clearly visible pore at the apex (Figure 2E).

Intermediate and short simple setae also occur along with a sparse third type of non-aesthetasc setae (Figure 2F) on the 2 other flagella (medial flagella of the antennules and the antennae), distributed around the distal part of each annulus (about 10 over the entire circumference by extrapolation of what is seen on one face). Small round cuticular depressions (7 to 10 µm in diameter) are observed on the lateral flagella of the antennules, on the medial side of the aesthetascs (Figure 2B). Flagella are often densely covered by a thick bacterial layer of filamentous and rod-shaped bacteria (Figure 2C), which was never observed on *P. elegans*. Rod-shaped bacteria also sometimes covered the entire aesthetasc surface (not shown).

Rimicaris exoculata

The aesthetascs are localized laterally on the medial side of the lateral flagella, from the base (except the 2 or 3 first annuli) up to the apex (except for the 4 last annuli). One row of 3 to 4 aesthetascs occurs on the distal part of each annulus (Figure 3A), leading to a total number of approximately 108 aesthetascs per ramus. Aesthetascs are up to 22 µm in diameter (n = 22) and 191 µm in length (n = 26) (Supplementary Table S2). They bear annulation on the apical half, and lack a terminal pore.

Table 2. Comparative table of aesthetascs setae characteristics in different species of decapods

Species	Total number	Number per row	Dimensions (diameter × length in µm)	Reference
Lobster				
Panulirus argus (20–60 cm)	2000 to 4000	9–10	40 × 1000	Gleeson et al. 1993 Laverack 1964
Homarus americanus (20–60 cm)	2000	10–12	20 × 600	Guenther and Atema 1998
Crayfish				
Orconectes propinquus (4–10 cm)	160	3–6	12 × 150	Tierney et al. 1986
Cherax destructor (10–20 cm)	260[a]	2–5	18 × 100	Sandeman and Sandeman 1996 Beltz et al. 2003
Crab				
Callinectes sapidus (23 cm)	1400	~20	12 × 795	Gleeson et al. 1996
Carcinus maenas (9 cm)	100–300	8–10	13 × 750	Fontaine et al. 1982
Shrimp				
Lysmata[b] (5–7 cm)	210–460	3–5	20 × 800	Zhang et al. 2008
Palaemon elegans (7 cm)	280	5–6	14 × 230	This study
Mirocaris fortunata (3 cm)	120[a]	3–4	16 × 234	This study
Rimicaris exoculata (5.5 cm)	206[a]	3–4	20 × 170	This study
Chorocaris chacei (5.5 cm)	226[a]	2–4	19 × 251	This study
Alvinocaris markensis (8.2 cm)	220[a]	3–4	21 × 531	This study

Rough animal lengths are given for comparison. Total length is given for lobster, crayfish and shrimp, carapace width for crabs.

[a]Species with only one row of aesthetascs per annuli.

[b]Study realized on *Lysmata boggessi, L. wurdemanni, L. amboinensis*, and *L. debelius*.

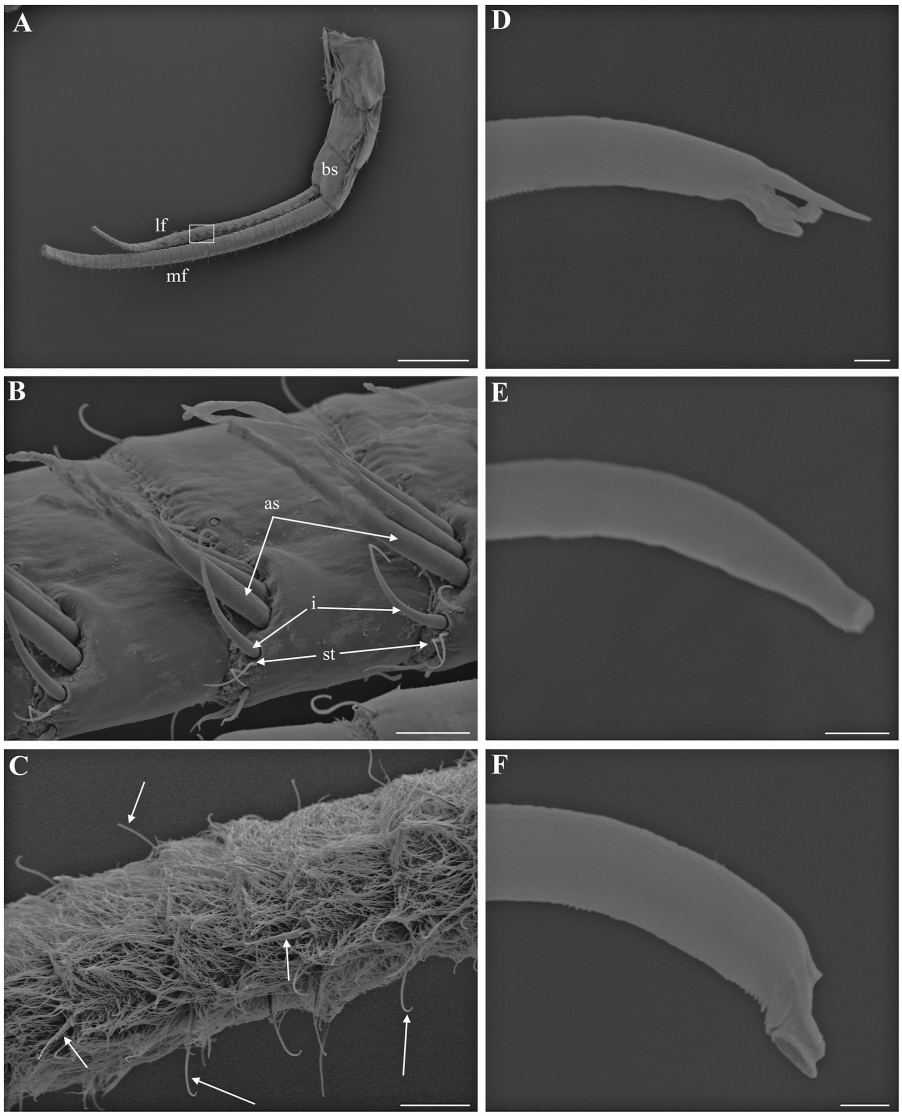

Figure 2. Morphology of antennule and setal types of *Mirocaris fortunata*. (A) Antennules are made of 3 basal annuli (bs) and 2 flagella: a medial (mf) and a lateral one (lf), bearing the aesthetascs (as). Box: area enlarged in B. (B) Close-up on the lateral flagellum bearing the aesthetascs, and intermediate (i) and short thin setae (st). (C) Lateral flagellum covered by dense filamentous and rod-shaped bacteria. Some setae are visible, protruding from the layer of bacteria (arrows). (D) Apex of the intermediate simple setae. (E) Short setae are simple with a clear pore at the apex. (F) Third setal type. Scale bars: A = 1 mm; B = 50 µm; C = 100 µm; D, E, F = 1 µm

The arrangement pattern of the non-aesthetasc setae around the aesthetascs is quite similar to that observed in *M. fortunata*, but with different setal types: 1 long thick beaked seta, 1 intermediate beaked seta and 6 or 7 short thin beaked setae (Figure 3B). All these setae have a pore at the apex (Figure 3C), but they are devoid of scales unlike the beaked setae observed in *P. elegans*.

Long thick, intermediate and short thin beaked setae also occur on the outer side of the lateral flagella, on the medial flagella of the antennules, and on the antennae, distributed over the circumference (20–25 over the entire circumference by extrapolation of setae seen on one face, or counted on the periphery of the apex), with a tight tuft of 6–8 setae on the inner side.

Small round cuticular depressions were (rarely) observed (6 to 8 µm in diameter) in *R. exoculata*, but they are barely observable due to a dense rod-shaped bacterial coverage. Indeed, for this species too, we have observed that the flagella (even the aesthetascs) can be covered by layer of filamentous and rod-shaped bacteria (not shown).

Chorocaris chacei

The aesthetascs are localized laterally on the medial side of the lateral flagella, from the base (except the 4 or 5 first annuli) to 2/3 of the flagella. One row of 2 to 4 aesthetascs occurs on the distal part of each annulus (Figure 3D), leading to a total number of approximately 113 aesthetascs per ramus. Aesthetascs are up to 23.2 µm in diameter (n = 50) and 339.5 µm in length (n = 58) (Supplementary Table S2). They bear annulation on the apical half, and lack a terminal pore.

The arrangement pattern of the non-aesthetasc setae around the aesthetascs is also quite similar to that observed in *M. fortunata* with one intermediate beaked seta, and 1 to 3 short simple or beaked thin setae on both the medial and lateral sides (Figures 3E and F).

Intermediate beaked and short setae (either simple or beaked shaped) also occur on the medial flagella of the antennules, and on the antennae, distributed over the circumference, roughly equidistant (around 15 over the entire circumference by extrapolation of

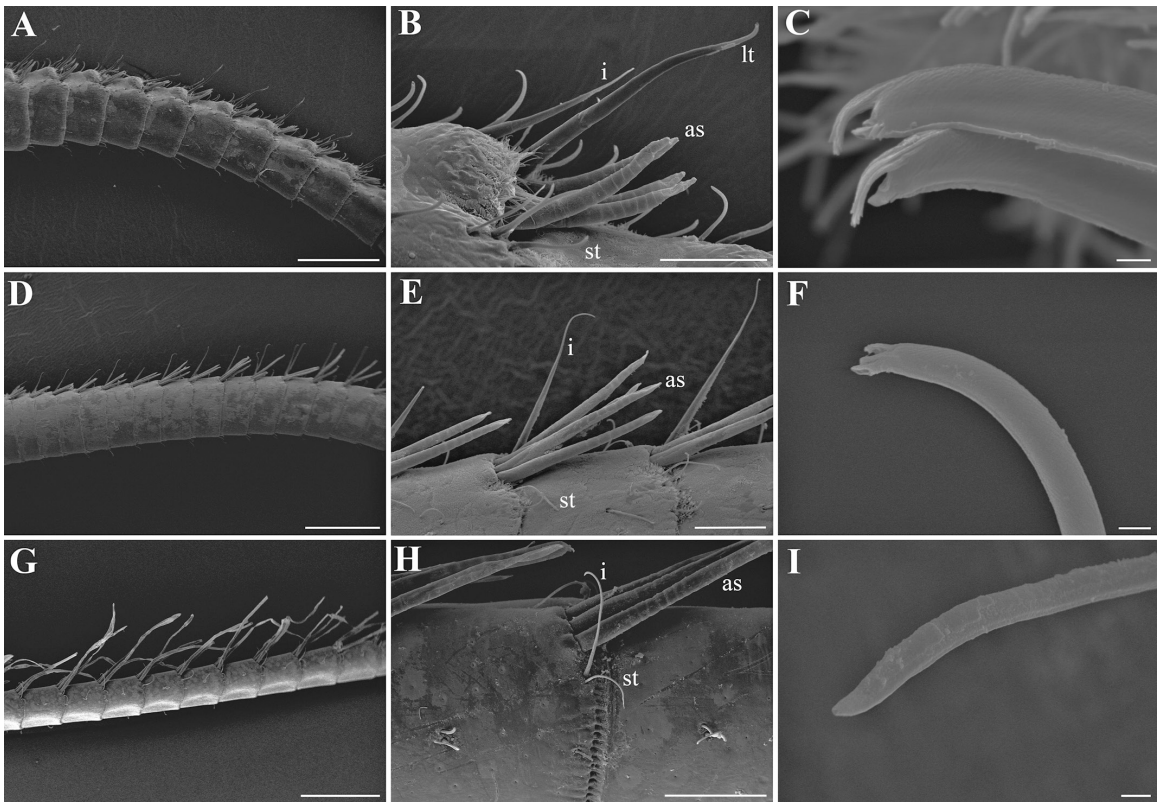

Figure 3. Morphology of lateral flagella and setal types of *Rimicaris exoculata* (A, B, C), *Chorocaris chacei* (D, E, F) and *Alvinocaris markensis* (G, H, I). as: aesthetascs, lt: long thick seta, i: intermediate seta, st: short thin seta, Scale bars: A, D, G = 500 µm; B, E, H = 100 µm; C, F, I = 2 µm.

setae seen on one face, or counted on the periphery of the apex), with a tight tuft of 8 to 10 setae on the inner side.

Small cuticular depressions (5 to 5.5 µm in diameter) are observed on the lateral flagella of the antennules, on the medial side of the aesthetascs but are difficult to observe as they are covered by rod-shaped bacteria. For this species again, the flagella (and even the aesthetascs) can be covered by filamentous and rod-shaped bacteria (not shown).

Alvinocaris markensis

The aesthetascs are localized laterally on the medial side of the lateral flagella, from the base (except the 3 or 4 first annuli) up to half of the flagella. One row of 3 to 4 aesthetascs (rarely 5) occurs on the distal part of each annulus (Figure 3G), leading to a total number of approximately 110 aesthetascs per ramus. Aesthetascs are up to 25.2 µm in diameter (n = 39) and 879.1 µm in length (n = 49) (Supplementary Table S2). They bear annulation almost throughout their length (short at the base and longer towards the apex), and lack a terminal pore.

The arrangement pattern of the non-aesthetasc setae around the aesthetascs is quite similar to that observed in *M. fortunata* with 1 intermediate seta and 1 short thin seta (Figure 3H). Two (sometimes 3 or 4) short setae occur at mid-length of each annulus. Intermediate and short thin setae all seem to all be simple, with a pore (Figure 3I). They also occur on the medial flagella of the antennules and on the antennae, in fewer numbers than observed in the other species (4–6 over the entire circumference, mostly on the medial side). Long simple setae also occur on few basal annuli on the medial flagella of the antennules and of the antennae.

Small cuticular depressions (4.5 to 7.5 µm diameter) were also observed in *A. markensis*, on the lateral flagella of the antennules, on the distal part of the annuli, occurring by one, 2 or sometimes 3, which had not been observed in other species (not shown). They are also observed on the antennae. Only a few rod-shaped bacteria occurred on the 2 specimens observed.

Identification and expression of the putative olfactory co-receptor IR25a in hydrothermal vent and coastal shrimp

In order to identify the regions of antennules and antennae putatively involved in olfaction, we studied the expression pattern of the IR IR25a, which belongs to a conserved family of olfactory receptors amongst Protostomia (review in Croset et al. 2010), involved in olfaction, taste, thermosensation, and hygrosensation. Recently the homologue of IR25a was identified in the lobster, and had been associated with olfactory sensilla (Corey et al. 2013). Using homology-based PCR with primers designed from the alignment of IR25a sequences from diverse organisms, we obtained partial sequences for 7 species of shrimp: 903 bp for *R. exoculata*, *P. elegans*, and *P. varians*, 763 bp for *M. fortunata*, *C. chacei*, and *A. markensis*, and 881 bp for *P. serratus* (Figures 4A and B). A phylogenetic analysis confirmed that these sequences are IR25a orthologs (Figure 5). All shrimp sequences grouped with IR25a sequences from other arthropods, and were closely related to IR25a sequences from the decapod crustaceans *P. argus* (Corey et al. 2013), *H. americanus* (Hollins et al. 2003) and *C. clypeatus* (Groh-Lunow et al. 2015). The Palaemonidae and Alvinocarididae sequences formed distinct clusters within the shrimp sequences, therefore being congruent with the phylogeny of these groups (Figure 6). The IR25a partial amino acid sequences obtained in this study are about 250 to 300 amino acids in length, which represents 25 to 30% of the total length expected for such sequences (Figure 4). They include the ligand-gated ion channel

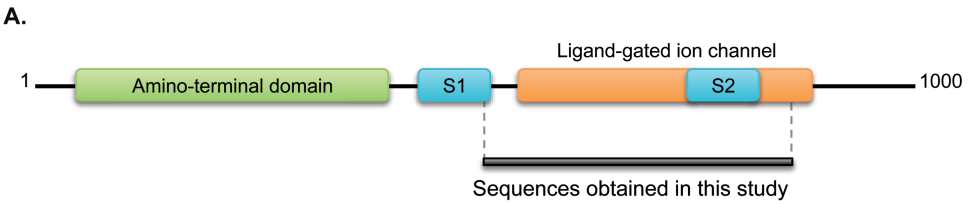

B.

```
R.exoculata      -------DLVGITILMKKPDVPTSLFKFLTVLEPEVWVCILFAYAFTSVLLYIFDRFSPY 53
C.chacei         -------------------------------------VCILFAYAFTSVLLYIFDRFSPY 23
A.markensis      -------------------------------------VCILFAYAFTSVLLYISDRFSPY 23
M.fortunata      -------------------------------------VCILFAYAFTSVLLYIFDRFSPY 23
P.elegans        DFTVPDYDLVGITILMKKPEVPTSLFKFLTVLEPEVWVCILFAYGFTSVLLYIFDRFSPY 60
P.varians        DFTVPYYDLVGITILMKKPEVPTSLFKFLTVLEPEVWVCILFAYGFTSVLLYIFDRFSPY 60
P.serratus       -------DLVGITILMKKPEVPTSLFKFLTVLEPEVWVCILFAYGFTSVLLYIFDRFSPY 53

R.exoculata      SYQNNKERYKDDDEKREFTFKECLWFCMTSLTPQGGGEAPKNLSGRLVAATWWLFGFIII 113
C.chacei         SYQNNKERYKDDDEKREFTFKECLWFCMTSLTPQGGGEAPKNLSGRLVAATWWLFGFIII 83
A.markensis      SYQNNKERYKDDDEKREFTFKECLWFCMTSLTPQGGGEAPKNLSGRLVAATWWLFGFIII 83
M.fortunata      SYQNNKERYKDDDEKREFTFKECLWFCMTSLTPQGGGEAPKNLSGRLVAATWWLFGFIII 83
P.elegans        SYQNNKEKYKDDDEKREFTFKECLWFCMTSLTPQGGGEAPKNLSGRLVAATWWLFGFIII 120
P.varians        SYQNNKEKYKDDDEKREFTFKECLWFCMTSLTPQGGGEAPKNLSGRLVAATWWLFGFIII 120
P.serratus       SYQNNKEKYKDDDEKREFTFKECLWFCMTSLTPQGGGEAPKNLSGRLVAATWWLFGFIII 113

R.exoculata      ASYTANLAAFLTVSRLDTPIESLDDLSNQYKVQYAPMNGTSTMTYFERMAYIEKKFYEIW 173
C.chacei         ASYTANLAAFLTVSRLDTPIESLDDLSNQYKVQYAPMNGTSTMTYFERMAYIEKKFYEIW 143
A.markensis      ASYTANLAAFLTVSRLDTPIESLDDLSNQYKVQYAPMNGTSTMTYFERMAYIEKKFYEIW 143
M.fortunata      ASYTANLAAFLTVSRLDTPIESLDDLSNQYKVQYAPMNGTSTMTYFERMAYIEKKFYEIW 143
P.elegans        ASYTANLAAFLTVSRLDTPIESLDDLSNQYKVQYAPVNGTSTMTYFERMAYIENKFYEIW 180
P.varians        ASYTANLAAFLTVSRLDTPIESLDDLSNQYKVQYAPVNGTSTMTYFERMAYIENKFYEIW 180
P.serratus       ASYTANLAAFLTVSRLDTPIESLDDLSNQYKVQYAPVNGTSTMTYFERMAYIENKFYEIW 173
                                                  ________*_________

R.exoculata      KDMSLNDSMSDVERAKLAVWDYPVSDKYTKMWQSMQEAGLPPDFDKALERVRKSTSSSEG 233
C.chacei         KDMSLNDSMSDVERAKLAVWDYPVSDKYTKMWQSMQEAGLPPDFDKALERVRKSTSSSEG 203
A.markensis      KDMSLNDSMSDVERAKLAVWDYPVSDKYTKMWQSMQEAGLPINFDKALDRVRKSTSSSEG 203
M.fortunata      KDMSLNDSMSDVERAKLAVWDYPVSDKYTKMWQSMQEAGLPNTFEKALERVRKSTSSSEG 203
P.elegans        KDMSLNDSMSEVERAKLAVWDYPVSDKYTKMWQSMQEAGLPRTMESAVERVRKSTSSSEG 240
P.varians        KDMSLNDSMSEVERAKLAVWDYPVSDKYTKMWQSMQEAGLPRTMESAVERVRKSTSSSEG 240
P.serratus       KDMSLNDSMSEVERAKLAVWDYPVSDKYTKMWQSMQEAGLPRTMESAVERVRKSTSSSEG 233
                 ____________________________________________________________

R.exoculata      FAYIGDATDIRYLVLTNCDLQIVGEEFSRKPYAVAVQQGSPLKDQFNDAILKLLNQRKLE 293
C.chacei         FAYIGDATDIRYLVLTNCDLQIVGEEFSRKPYAVAVQQGSPLKDQFNDAIL--------- 254
A.markensis      FAYIGDATDIRYLVLTNCDLQIVGEEFSKKPYAVAVQQGSPLKDQFNDAIL--------- 254
M.fortunata      FAYIGDATDIRYLVLTNCDLQIVGEEFSRKPYAVAVQQGSPLKDQFNDAIL--------- 254
P.elegans        FAFIGDATDI-YLVLTNCDLQMVGEEFSRKPYAVAVQQGSPLKDQFNDAILKLLNQRKLE 299
P.varians        FAFIGDATDIRYLVLTNCDLQMVGEEFSRKPYAVAVQQGSPLK-QFNDAILKLLNQRKLE 299
P.serratus       FAFIGDATDIRYLVLTNCDLQMVGEEFSRKPYAVAVQQGSPLKDQFNDAILKLLNQRKLE 293
                 _____*

R.exoculata      TLKERWWK 301
C.chacei         -------- 
A.markensis      -------- 
M.fortunata      -------- 
P.elegans        T------- 300
P.varians        K------- 300
P.serratus       K------- 294
```

Figure 4. IR25a partial sequences obtained for hydrothermal and coastal shrimp. (A) IR25a protein domain organization (modified from Croset et al. 2010) showing the position of the shrimp partial sequences obtained in the present study. The ligand-binding domains are named S1 and S2. (B) Alignement of shrimp IR25a sequences. The ligand-binding S2 domain is underlined, and putative ligand-binding residues are indicated by an asterisk.

and the ligand-binding S2 domain, localized in the C-terminal part of the protein. When considering the ligand-binding S2 domain, the threonine and aspartate, which are characteristic glutamate binding residues, are conserved among shrimp sequences.

Then, we studied the expression pattern of IR25a in antennules, antennae, mouthparts and walking legs, as well as in non-chemosensory tissues (abdominal muscles, eye), from the 4 hydrothermal vent shrimp and the coastal shrimp *P. elegans* (Figure 7). IR25a was predominantly expressed in the lateral antennular flagella (A1 lateral) for all shrimp. In *P. elegans*, a weaker expression was observed in the external ramus (A1 lateral R2) than in the internal ramus of the lateral antennular flagella (A1 lateral R1), which bear the aesthetascs. A weak expression was also detected in the medial antennular flagella of *R. exoculata* and *C. chacei* (A1 medial), and in the antennae (A2) of *R. exoculata*. IR25a transcripts were undetectable in other tissues.

Discussion

Comparative morphology of sensilla of antennae and antennules among decapods, and in coastal palaemonid versus hydrothermal alvinocarid shrimp

Setae are outgrowths of the arthropod integument presenting a multitude of sizes and shapes. These ubiquitous features of crustacean

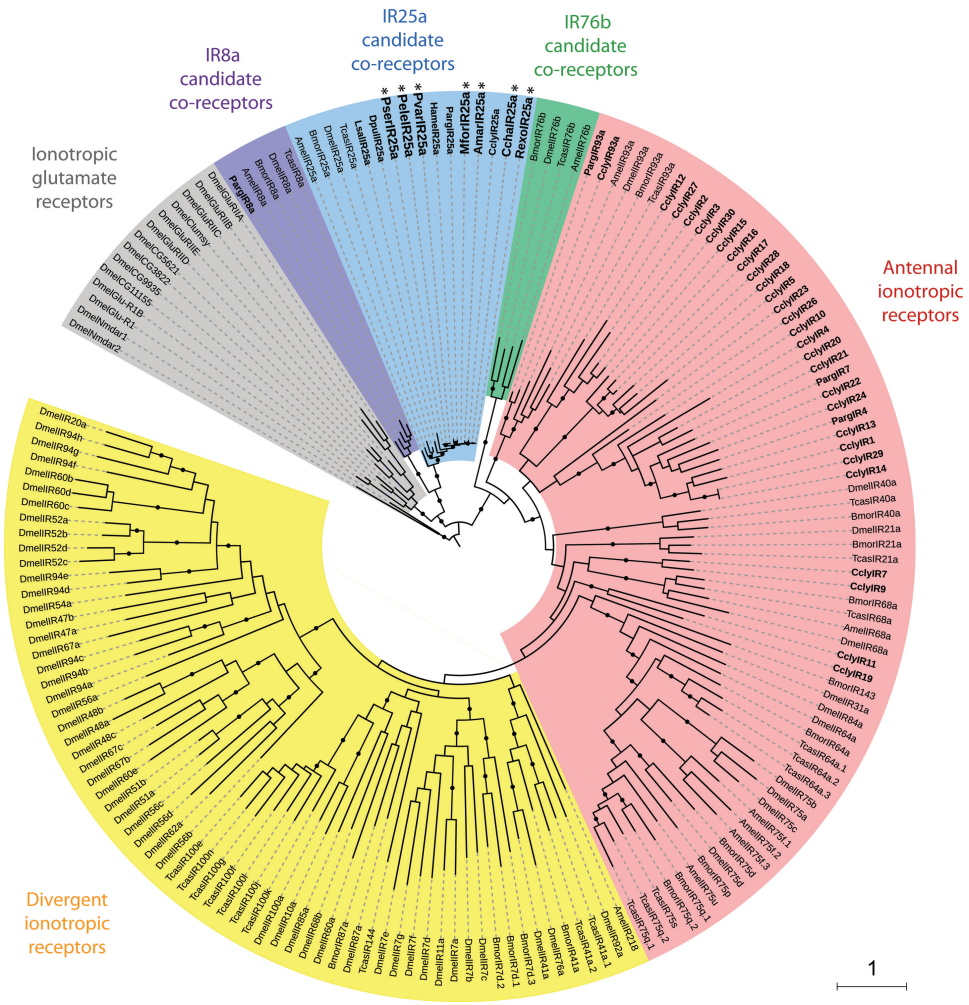

Figure 5. Phylogeny of insect and crustacean ionotropic receptors (IRs). This tree is based on a maximum-likelihood analysis of an amino acid dataset. *Drosophila melanogaster* ionotropic glutamate receptor sequences were used as an out-group. Branch support was estimated by approximate likelihood-ratio test (aLRT) (circles: >0.9). The scale bar corresponds to the expected number of amino acid substitutions per site. Crustacean IRs are in bold and the new IRs identified in this study are in larger font size, and highlighted with an asterisk. Amar, *Alvinocaris markensis*; Amel, *Apis mellifera*; Bmor, *Bombyx mori*; Ccha, *Chorocaris chacei*; Ccly, *Coenobitus clypeatus*; Dmel, *Drosophila melanogaster*; Dpul, *Daphnia pulex*; Hame, *Homarus americanus*; Lsal, *Lepeophtheirus salmonis*; Mfor, *Mirocaris fortunata*; Parg, *Panulirus argus*; Pele, *Palaemon elegans*; Pser, *Palaemon serratus*; Pvari, *Palaemon varians*; Rexo, *Rimicaris exoculata*; Tcas, *Tribolium castaneum*.

integuments are involved in a variety of vital functions including locomotion, feeding, sensory perception and grooming (Felgenhauer 1992). Sensilla (setae innervated by sensory cells) were shown to present a great inter- and intra-specific diversity in crustaceans (see references in the paragraphs below).

In the most studied large decapods like lobsters and crayfish, the aesthetascs are localized in tufts on the distal half or two-thirds of the ventral side of each lateral antennular flagellum (*P. argus*, Cate and Derby 2001; *H. americanus*, Guenther and Atema 1998; *Orconectes sanborni*, McCall and Mead 2008; *O. propinquus*, Tierney et al. 1986; *Procambarus clarkii*, Mellon 2012). The localization at the tip of the antennules may increase the spatial resolution of the chemical environment, but could also increase their chance of damage during encounters with the environment or other animals. On the contrary, in shrimp (the 4 alvinocaridid species and *P. elegans* [this study], as well as other palaemonid species like *P. serratus* and *Macrobrachium rosenbergii* [Hallberg et al. 1992]), the aesthetascs are localized on the basal half or two-thirds of the lateral flagella (for the alvinocaridae) or on the basal part of the short ramus of the lateral flagella (for the palaemonidae). The aesthetascs are thus less likely to be lost or damaged, but this arrangement may decrease spatial resolution.

The aesthetascs are usually organized in 2 successive rows (in the different lobsters and crayfishes cited above and also in *Lysmata* shrimp, Zhang et al. 2008) or in 2 juxtaposed rows in the short antennules of the crab *Carcinus maenas* (Fontaine et al. 1982). Surprisingly, there is only one row of aethetascs on each annulus in the 4 hydrothermal species (an exception also occurs in the crayfish *Cherax destructor*, see Table 2). Nevertheless, comparisons of the total number of aesthetascs in diverse decapod species (Table 2) revealed that this number is relatively similar among shrimp group and other decapods of comparable size (the crayfish *Orconectes propinquus* or the crab *C. maenas*) (Table 2 and see Beltz et al. 2003 for more comprehensive data). Hydrothermal shrimp do not seem to present any specific adaptation regarding this character. The total number, as well as the size of aesthetascs seems related to the size of the animal rather than to its environment. Indeed, based on a study of 17 Reptentia decapods, Beltz et al. (2003) found a strong linear relationship between the number of aesthetascs and carapace

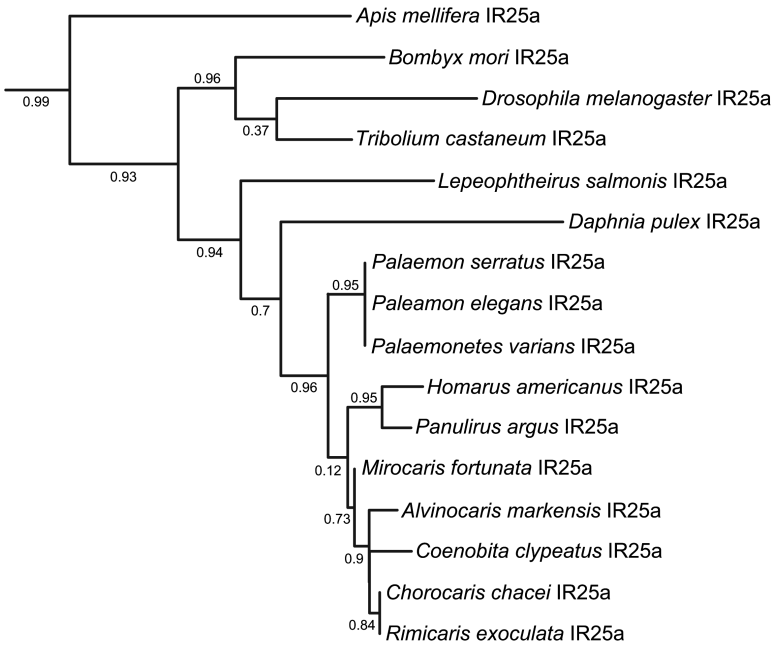

Figure 6. Detail of the IR25a clade of the IR phylogeny. This sub-tree is a zoom of the IR25a clade from the tree depicted in Figure 5.

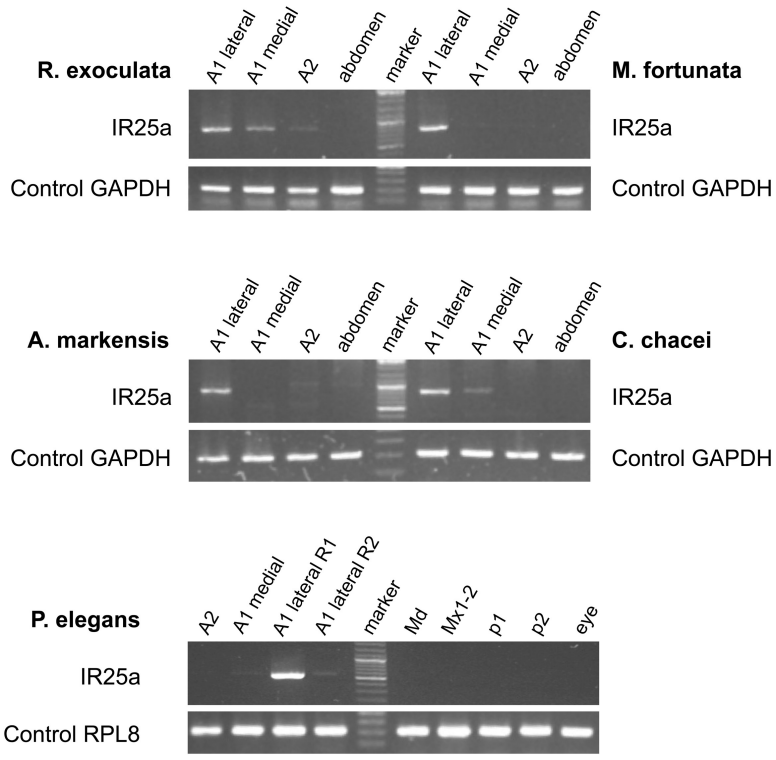

Figure 7. IR25a gene expression in hydrothermal vent shrimp Rimicaris exoculata, Mirocaris fortunata, Alvinocaris markensis, Chorocaris chacei, and in the coastal shrimp *P. elegans*. Control RT-PCR products for comparative analysis of gene expression correspond to the glycolysis enzyme GAPDH for hydrothermal vent shrimp, and to the ribosomal protein gene RPL8 for *P. elegans*. No amplification was detected in the absence of template (data not shown). A1, antennules; R1, internal ramus of the lateral antennular flagella; R2, external ramus of the lateral antennular flagella; A2, second antennae; Md, mandibles; Mx1-2, maxillae; p1 and p2, first and second walking legs.

length, which was also reported earlier for the crayfish *C. destructor* by Sandeman and Sandeman (1996). Among hydrothermal species, it can however be noted that the aesthetascs of *A. markensis* are longer than those of the 3 other species, with the maximum length being 2 to 4 times higher than for the 3 other species (see Supplementary Table S2). The adult hydrothermal shrimp lack the usual externally differentiated eye (eye-stalked), having instead a pair of large, highly reflective, dorsal organs (Van Dover et al. 1989). These modifications

have been reported to be an adaptation for the detection of extremely faint sources of light emitted by the vents (Pelli and Chamberlain 1989). These eyes are unusual in having no image-forming optics, but a solid wall of light-sensitive rhabdom containing rhodopsin, with the exception of *A. markensis*, which also lacks this photoreceptor and is completely blind (Wharton et al. 1997; Gaten et al. 1998). The longer olfactory sensilla observed in this species may possibly be interpreted as a development of the olfactory capacity to compensate for the lack of vision. Zhang et al. (2008) showed for *Lysmata* species that shrimp living in aggregations (*L. boggessi* and *L. wurdemanni*, 460 aesthetascs) possess a significantly higher number of aethetascs than pair-living species (*L. amboinensis* and *L. debelius*, 210 aesthetascs), suggesting a possible correlation between the number of aesthetascs and the social behavior. Our results do not support this hypothesis, since no significant differences were observed between vent species living in dense swarms (*R. exoculata*) and the others.

Most studies on olfaction in crustaceans have focused on aesthetascs. Several lines of evidence however suggest that non-aesthetasc bimodal chemosensilla (innervated by mecano- and chemo-receptive cells, also called distributed chemosensilla [Schmidt and Mellon 2011]) or non-olfactory sensilla (Derby and Weissburg 2014), distributed over both flagella of the antennules, as well as on the antennae, also play a role in the detection of water-borne chemicals (Guenther and Atema 1998; Cate and Derby 2001). Non-aesthetasc setae exhibit a wide variety of sizes and morphologies. These setae are named in the literature according to their morphology, size or location on the flagellum. For example, there are 9 setal types in *P. argus* (hooded, plumose, short setuled, long simple, medium simple, short simple, guard, companion, and asymmetric: Cate and Derby 2001), but only 1 type in the shrimp *Thor manningi* (curved simple: Bauer and Caskey 2006). The role of these setae is still poorly known and whether their diversity corresponds to a multiplicity of perceived stimuli remains an open question (Cate and Derby 2001; Derby and Steullet 2001). Among the shrimp studied here, the coastal shrimp *P. elegans* showed the highest diversity in non-aesthetasc setal types (5 setal types: short simple, long simple, beaked scaly, twisted flat, bifid) when compared with the 4 hydrothermal species (2 or 3 types). Among hydrothermal species, the setal types vary essentially by their size (long, intermediate or short) and less by their morphology (all simple in *Alvinocaris*, all beaked in *Rimicaris*, a mix of the 2 in *Chorocaris*, whereas *Mirocaris* exhibit more original morphologies [see Figures 2D and 2F]). At this point of our knowledge, it is difficult to explain the observed differences and even more to speculate on the functions of these different setae.

Surprisingly, dense bacterial populations were often observed on the antennae and antennules of the 4 hydrothermal shrimp (see e.g., *Mirocaris*, Figure 2C), sometimes even covering the whole surface of aesthetacs (not shown), whereas no bacterial coverage was ever observed in the coastal *P. elegans* specimens. The type of bacteria present on the antennae of hydrothermal shrimp, as well as their potential impact on olfaction or other role for the shrimp should be investigated in future studies.

Comparative expression of the putative olfactory co-receptor IR25a in hydrothermal vent and coastal shrimp

We identified, in the 4 alvinocaridid hydrothermal shrimp and in 3 palaemonid species (*P. elegans*, *P. varians*, and *P. serratus*), a member of the IR family, which was recently proposed to be involved in the odorant detection in crustaceans: the common IR25a subunit (Corey et al. 2013). In the 5 shrimp species tested, IR25a was predominantly expressed in the lateral antennular flagella that bear the aesthetascs olfactory sensilla (Figure 7), consistent with the expression pattern of this IR subunit in *H. americanus* (iGluR1, Stepanyan et al. 2004), *P. argus* (Corey et al. 2013), and *C. clypeatus* (Groh-Lunow et al. 2015). IR25a expression in other chemosensory tissues than the lateral antennular flagella varies amongst decapod crustacean species, with either no detection (for *M. fortunata*, *A. markensis*, *P. elegans*: this study; for *H. americanus*: Stepanyan et al. 2004), or detection in different organs (medial antennular flagella in *R. exoculata* and *C. chacei*: this study; mouth and 2 first walking legs in *P. argus*: Corey et al. 2013). Taken together, these results raise the question of whether IR25a may play a more general role in decapod crustacean chemosensation beyond just mediating odor detection (Corey et al. 2013), or if organs other than the aesthetascs bearing flagella can also have an olfactory role, as Keller et al. (2003) suggested for the antennae and walking legs of the blue crab *Callinectes sapidus*. According to several recent studies and reviews (Schmidt and Mellon 2011, Mellon 2014; Derby and Weissburg 2014; Derby et al. 2016), only the aesthetascs are considered as olfactory sensilla, which rather plead for the first hypothesis.

Among hydrothermal species, the different patterns of IR25a expression obtained for *R. exoculata* and *C. chacei* on one hand and for *M. fortunata* and *A. markensis* on the other hand, would suggest different chemosensory mechanisms in these 2 shrimp groups. This may be related to their diet and thus to their direct dependence to the hydrothermal fluid. Indeed, *Rimicaris* and *Chorocaris* to a lesser extent live in symbiosis with chemoautotrophic bacteria from which they derive all or part of their food (Segonzac et al. 1993; Ponsard et al. 2013), forcing them to stay permanently close to hydrothermal emissions to supply their bacteria in reduced compounds necessary for chemosynthesis. These 2 species are also phylogenetically closely related, which recently led Vereshchaka et al. (2015) to propose to synonymize all the genus *Chorocaris* with *Rimicaris*. On the other hand, *Mirocaris* and *Alvinocaris* are secondary consumers, scavenging on local organic matter and living at greater distances from the vent emissions. Regarding the IR25a expression pattern, the coastal shrimp *P. elegans* has a profile similar to hydrothermal secondary consumers *Mirocaris* and *Alvinocaris*, itself having an opportunistic omnivorous diet of invertebrate tissues.

In future studies, we will attempt to identify, and subsequently localize, other receptors of the IR family that could be involved in olfaction, and in particular the members generally found associated with IR25a (like IR93a and IR8a). We recently developed an electrophysiological method that allows the recording of shrimp ORNs activity (Machon et al. 2016). This method will be used to conduct a comparative study of the global antennule activity upon exposure to environmental stimuli, in the hydrothermal species *M. fortunata* and the coastal species *P. elegans*. An ultrastructural approach could help to refine the morphological comparison between hydrothermal and coastal species, by analyzing other characteristics like the number of ORNs per aesthetascs, the number of outer dendritic segments per ORNs or the aesthetasc cuticle thickness. This combined morphological and functional approach will provide insights into deep-sea vent shrimp olfaction, and ultimately in the potential adaptations of the sensory organs to their peculiar environment.

Supplementary Material

Supplementary data are available at *Chemical Senses* online.

Funding

This work was supported by the European Union Seventh Framework Programme (FP7/2007–2013) under the MIDAS project [grant agreement n° 603418].

Acknowledgments

The authors thank the electronic microscopy platform of the Institute of Biology Paris-Seine (IBPS), and especially V. Bazin and M. Trichet. We also thank the 2 chief scientist of the Momarsat 2011 and 2012 cruise M. Cannat and P. M. Sarradin, the chief scientist of the Biobaz 2013 (F. Lallier) and the Bicose 2014 (MA Cambon-Bonavita) cruises, as well as Jozée Sarrazin for hydrothermal shrimp sampling.

References

Abascal F, Zardoya R, Posada D. 2005. ProtTest: selection of best-fit models of protein evolution. *Bioinformatics*. 21(9):2104–2105.

Ache B. 1982. Chemoreception and thermoreception. In: Bliss D, editor, *The Biology of Crustacea*. Vol 3. New York: Academic Press. p. 369–398.

Anisimova M, Gascuel O. 2006. Approximate likelihood-ratio test for branches: a fast, accurate, and powerful alternative. *Syst Biol*. 55(4):539–552.

Bauer R, Caskey J. 2006. Flagellar setae of the second antennae in decapod shrimps: sexual dimorphism and possible role in detection of contact sex pheromones. *Invertebr Reprod Dev*. 49(1–2):51–60.

Beltz BS, Kordas K, Lee MM, Long JB, Benton JL, Sandeman DC. 2003. Ecological, evolutionary, and functional correlates of sensilla number and glomerular density in the olfactory system of decapod crustaceans. *J Comp Neurol*. 455(2):260–269.

Benton R, Vannice KS, Gomez-Diaz C, Vosshall LB. 2009. Variant ionotropic glutamate receptors as chemosensory receptors in *Drosophila*. *Cell*. 136(1):149–162.

Cate HS, Derby CD. 2001. Morphology and distribution of setae on the antennules of the Caribbean spiny lobster *Panulirus argus* reveal new types of bimodal chemo-mechanosensilla. *Cell Tissue Res*. 304(3):439–454.

Chamberlain S, Battelle B, Herzog E, Jinks R, Kass L, Renninger G. 1996. *Sensory neurobiology of hydrothermal vent shrimp from the Mid-Atlantic Ridge. Abstract*. FARA-IR Mid-Atlantic Ridge Symposium. Reykjavik, Iceland.

Corey EA, Bobkov Y, Ukhanov K, Ache BW. 2013. Ionotropic crustacean olfactory receptors. *PLoS One*. 8(4):e60551.

Cowan D. 1991. The role of olfaction in courtship behavior of the American lobster *Homarus americanus*. *Bio Bull*. 181:402–407.

Croset V, Rytz R, Cummins SF, Budd A, Brawand D, Kaessmann H, Gibson TJ, Benton R. 2010. Ancient protostome origin of chemosensory ionotropic glutamate receptors and the evolution of insect taste and olfaction. *PLoS Genet*. 6(8):e1001064.

De Busserolles F, Sarrazin J, Gauthier O, Gelinas Y, Fabri MC, Sarradin PM, Desbruyeres D. 2009. Are spatial variations in the diets of hydrothermal fauna linked to local environmental conditions? *Deep-Sea Res II*. 56:1649–1664.

Derby CD, Steullet P. 2001. Why do animals have so many receptors? The role of multiple chemosensors in animal perception. *Biol Bull*. 200(2):211–215.

Derby C, Steullet P, Horner A, Cate H. 2001. The sensory basis of feeding behavior in the Caribbean spiny lobster, *Panulirus argus*. *Mar Freshwater Res*. 52:1339–1350.

Derby C, Weissburg M. 2014. The chemical senses and chemosensory ecology of Crustaceans. In: Derby C, Thiel M, editors, *The Natural History of the Crustacea.- Vol. 3: Nervous Systems and Control Behavior*. New York: Oxford Univ. Press. p. 263–292.

Derby CD, Kozma MT, Senatore A, Schmidt M. 2016. Molecular mechanisms of reception and perireception in crustacean chemoreception: a comparative review. *Chem Senses*. 41(5):381–398.

Desbruyères D, Almeida A, Biscoito M, Comtet T, Khripounoff A, Le Bris N, Sarradin PM, Segonzac M. 2000. A review of the distribution of hydrothermal vent communities along the northern Mid-Atlantic Ridge: dispersal vs. environmental controls. *Hydrobiologia*. 440:201–216.

Desbruyères D, Biscoito M, Caprais JC, Colaço A, Comtet T, Crassous P, Fouquet Y, Khripounoff A, Le Bris N, Olu K, *et al*. 2001. Variations in deep-sea hydrothermal vent communities on the Mid-Atlantic Ridge near the Azores plateau. *Deep-Sea Res I*. 48:1325–1346.

Desbruyères D, Segonzac M, Bright M. 2006. Handbook of deep-sea hydrothermal vent fauna. Second completely revised edition. Linz (Austria): Denisia.

Devine D, Atema J. 1982. Function of chemoreceptor organs in spatial orientation of the lobster, *Homarus americanus*: differences and overlap. *Bio Bull*. 163:144–153.

Felgenhauer B. 1992. External anatomy and integumentary structures of the Decapoda. In: Harrison F, Humes A, editors, *Microscopic Anatomy of Invertebrates*. New York: Wiley-Liss. p. 7–43.

Fontaine M, Passelecq-Gerin E, Bauchau A. 1982. Structures chemoreceptrices des antennules du crabe *Carcinus maenas* (L.) (Decapoda Brachyura). *Crustaceana*. 43(3):271–283.

Gaten E, Herring P, Shelton P, Johnson M. 1998. The development and evolution of the eyes of vent shrimps (Decapoda: Bresiliidae). *Cah Biol Mar*. 39:287–290.

Gebruk A, Southward E, Kennedy H, Southward A. 2000. Food sources, behaviour, and distribution of hydrothermal vent shrimp at the Mid-Atlantic Ridge. *J Mar Biol Ass UK*. 80:485–499.

Gleeson R, Carr W, Trapido-Rosenthal H. 1993. Morphological characteristics facilitating stimulus access and removal in the olfactory organ of the spiny lobster, *Panulirus argus*: insight from the design. *Chem Senses*. 18(1):67–75.

Gleeson R, McDowell L, Aldrich H. 1996. Structure of the aesthetasc (olfactory) sensilla of the blue crab, *Callinectes sapidus*: transformations as a function of salinity. *Cell Tissue Res*. 284:279–288.

Groh K, Vogel H, Stensmyr M, Grosse-Wilde E, Hansson B. 2014. The hermit crab's nose—antennal transcriptomics. *Front Neurosci*. 7:Article 266. doi:210.3389/fnins.2013.00266.

Groh-Lunow K, Getahun M, Grosse-Wilde E, Hansson B. 2015. Expression of ionotropic receptors in terrestrial hermit crab's olfactory sensory neurons. *Front. Cell Neurosci*. 8:Article 448. doi:410.3389/fncel.2014.00448.

Grünert U, Ache B. 1988. Ultrastructure of the aesthetasc (olfactory) sensilla of the spiny lobster, *Panulirus argus*. *Cell Tissue Res*. 251:95–103.

Guenther C, Atema J. 1998. Distribution of setae on the *Homarus americanus* lateral antennular flagella. *Biol Bull*. 195:182–183.

Guindon S, Dufayard JF, Lefort V, Anisimova M, Hordijk W, Gascuel O. 2010. New algorithms and methods to estimate maximum-likelihood phylogenies: assessing the performance of PhyML 3.0. *Syst Biol*. 59(3):307–321.

Hallberg E, Johansson KU, Elofsson R. 1992. The aesthetasc concept: structural variations of putative olfactory receptor cell complexes in Crustacea. *Microsc Res Tech*. 22(4):325–335.

Hallberg E, Skog M. 2011. Chemosensory sensilla in Crustaceans. In: Breithaupt T, Thiel M, editors, *Chemical communication in Cristaceans*. New York: Springer Science+ Business Media. p. 103–121.

Herring P, Dixon DR. 1998. Extensive deep-sea dispersal of postlarval shrimp from a hydrothermal vent. *Deep-Sea Res I*. 45:2105–2118.

Hoagland P, Beaulieu S, Tivey M, Eggert R, German C, Glowka L, Lin J. 2010. Deep-sea mining of seafloor massive sulfides. *Marine Policy*. 34(3):728–732.

Hollins B, Hardin D, Gimelbrant AA, McClintock TS. 2003. Olfactory-enriched transcripts are cell-specific markers in the lobster olfactory organ. *J Comp Neurol*. 455(1):125–138.

Husson B, Sarradin P, Zeppilli D, Sarrazin J. 2016. Picturing thermal niches and biomass of hydrothermal vent species. *Deep-sea Res. II*. In press. doi:http://doi.org/10.1016/j.dsr2.2016.05.028

Jinks R, Battelle B, Herzog E, Kass L, Renninger G, Chamberlain S. 1998. Sensory adaptations in hydrothermal vent shrimps from the Mid-Atlantic Ridge. *Cah Biol Mar*. 39:309–312.

Katoh K, Toh H. 2010. Parallelization of the MAFFT multiple sequence alignment program. *Bioinformatics*. 26(15):1899–1900.

Keller T, Powell I, Weissburg M. 2003. Role of olfactory appendages in chemicammy mediated orientation of blue crabs. *Mar Ecol Prog Ser*. 261:217–231.

Lahman SE, Moore PA. 2015. Olfactory sampling recovery following sublethal copper exposure in the rusty crayfish, *Orconectes rusticus*. *Bull Environ Contam Toxicol*. 95(4):441–446.

Laverack MS. 1964. The antennular sense organs of *Panulirus argus*. *Comp Biochem Physiol*. 13:301–321.

Le SQ, Gascuel O. 2008. An improved general amino acid replacement matrix. *Mol Biol Evol*. 25(7):1307–1320.

Le Bris N, Govenar B, Le Gall C, Fisher C. 2006. Variability of physico-chemical conditions in 9 degrees 50' NEPR diffuse flow vent habitats. *Mar Chem*. 98(2–4):167–182.

Letunic I, Bork P. 2011. Interactive Tree Of Life v2: online annotation and display of phylogenetic trees made easy. *Nucleic Acids Res*. 39:W475–W478.

Machon J, Ravaux J, Zbinden M, Lucas P. 2016. New electroantennography method on a marine shrimp in water. *J Exp Biol*. 219(Pt 23):3696–3700.

McCall JR, Mead KS. 2008. Structural and functional changes in regenerating antennules in the crayfish *Orconectes sanborni*. *Biol Bull*. 214(2):99–110.

Mellon D Jr. 2012. Smelling, feeling, tasting and touching: behavioral and neural integration of antennular chemosensory and mechanosensory inputs in the crayfish. *J Exp Biol*. 215(Pt 13):2163–2172.

Mellon D. 2014. Sensory Systems of Crustaceans. In: Derby C, Thiel M, editors, *The Natural History of the Crustacea. Vol. 3: Nervous Systems and Control Behavior*. New York: Oxford Univ. Press.

Moore PA, Scholz N, Atema J. 1991. Chemical orientation of lobsters, *Homarus americanus*, in turbulent odor plumes. *J Chem Ecol*. 17(7):1293–1307.

Pelli DG, Chamberlain SC. 1989. The visibility of 350 degrees C blackbody radiation by the shrimp *Rimicaris exoculata* and man. *Nature*. 337(6206):460–461.

Pond DW, Segonzac M, Bell MV, Dixon DR, Fallick AE, Sargent JR. 1997. Lipid and lipid carbon stable isotope composition of the hydrothermal vent shrimp *Mirocaris fortunata*: evidence for nutritional dependance on photosynthetically fixed carbon. *Mar Ecol Prog Ser*. 157:221–231.

Ponsard J, Cambon-Bonavita MA, Zbinden M, Lepoint G, Joassin A, Corbari L, Shillito B, Durand L, Cueff-Gauchard V, Compère P. 2013. Inorganic carbon fixation by chemosynthetic ectosymbionts and nutritional transfers to the hydrothermal vent host-shrimp *Rimicaris exoculata*. *ISME J*. 7(1):96–109.

Renninger GH, Kass L, Gleeson RA, Van Dover CL, Battelle BA, Jinks RN, Herzog ED, Chamberlain SC. 1995. Sulfide as a chemical stimulus for deep-sea hydrothermal vent shrimp. *Biol Bull*. 189(2):69–76.

Sandeman R, Sandeman D. 1996. Pre- and postembryonic development, growth and turnover of olfactory receptor neurones in crayfish antennules. *J Exp Biol*. 199(Pt 11):2409–2418.

Sarradin P, Caprais J, Riso R, Kerouel R. 1999. Chemical environment of the hydrothermal mussel communities in the LuckyStrike and Menez Gwen vent fields, Mid Atlantic ridge. *Cah Biol Mar*. 40(1):93–104.

Sarrazin J, Juniper K, Massoth G, Lehgendre P. 1999. Physical and chemical factors influencing species distributions on hydrothermal sulfide edifices of the Juan de Fuca Ridge, northeast Pacific. *Mar Ecol Prog Ser*. 190:89–112.

Sarrazin J, Legendre P, De Brusserolles F, Fabri M, Guilini K, Ivanenko V, Morineaux M, Vanreusel A, Sarradin P. 2015. Biodiversity patterns, environmental drivers and indicator species on a High-temperature Hydrothermal edifice, mid-Atlantic ridge. *Deep-sea Res II*. 121:177–192.

Schmidt M, Ache B. 1996a. Processing of antennular input in the brain of the spiny lobster, *Panulirus argus*. I. Non-olfactory chemosensory and mechanosensory pathway of the lateral and median antennular neuropils. *J Comp Physiol A*. 178:579–604.

Schmidt M, Ache B. 1996b. Processing of antennular input in the brain of the spiny lobster, *Panulirus argus*. II. The olfactory pathway. *J Comp Physiol A*. 178:605–628.

Schmidt M, Mellon D. 2011. Neuronal processing of chemical information in crustaceans. In: Breithaupt T, Thiel M, editors, *Chemical communication in Cristaceans*. New York: Springer Science+ Business Media. p. 123–147.

Segonzac M. 1992. Les peuplements associés à l'hydrothermalisme océanique du Snake Pit (dorsale médio-Atlantique, 23°N, 3480m): composition et microdistribution de la mégafaune. *CR Acad Sci*. 314, série III:593–600.

Segonzac M, de Saint-Laurent M, Casanova B. 1993. L'énigme du comportement trophique des crevettes Alvinocarididae des sites hydrothermaux de la dorsale médio-atlantique. *Cah Biol Mar*. 34:535–571.

Shabani S, Kamio M, Derby CD. 2008. Spiny lobsters detect conspecific blood-borne alarm cues exclusively through olfactory sensilla. *J Exp Biol*. 211(Pt 16):2600–2608.

Shillito B, Ravaux J, Sarrazin J, Zbinden M, Barthélémy D, Sarradin P. 2015. Long-term maintenance and public exhibition of deep-sea fauna: the AbyssBox Project. *Deep-Sea Res I*. 121:137–145.

Stein L, Bao Z, Blasiar D, Blumenthal T, Brent M, Chen N, Chinwalla A, Clarke L, Clee C, Coghlan A, *et al*. 2003. The genome sequence of *Caenorhabditis briggsae*: a platform for comparative genomics. *PLoS Biol*. 1(2):e45. doi:10.1371/journal.pbio.0000045.

Stepanyan R, Hollins B, Brock SE, McClintock TS. 2004. Primary culture of lobster (*Homarus americanus*) olfactory sensory neurons. *Chem Senses*. 29(3):179–187.

Steullet P, Dudar O, Flavus T, Zhou M, Derby CD. 2001. Selective ablation of antennular sensilla on the Caribbean spiny lobster Panulirus argus suggests that dual antennular chemosensory pathways mediate odorant activation of searching and localization of food. *J Exp Biol*. 204(Pt 24):4259–4269.

Tierney A, Thompson C, Dunham D. 1986. Fine structure of aethetasc chemoreceptors in the crayfish Oronectes propinquus. *Can J Zool*. 64:392–399.

The C. *elegans* Sequencing Consortium. 1998. Genome sequence of the nematode *C. elegans*: a platform for investigating biology. *Science*. 282(5396):2012–2018.

Van Dover C, Fry B, Grassle J, Humphris S, Rona P. 1988. Feeding biology of the shrimp *Rimicaris exoculata* at hydrothermal vents on the Mid-Atlantic Ridge. *Mar Biol*. 98:209–216.

Van Dover CL, Szuts EZ, Chamberlain SC, Cann JR. 1989. A novel eye in 'eyeless' shrimp from hydrothermal vents of the Mid-Atlantic Ridge. *Nature*. 337(6206):458–460.

Vereshchaka AL, Kulagin DN, Lunina AA. 2015. Phylogeny and new classification of hydrothermal vent and seep shrimps of the family alvinocarididae (decapoda). *PLoS One*. 10(7):e0129975.

Wharton D, Jinks R, Herzog E, Battelle B, Kass L, Renninger G, Chamberlain S. 1997. Morphology of the eye of the hydrothermal vent shrimp *Alvinocaris markensis*. *J Mar Biol Ass UK*. 77:1097–1108.

Zbinden M, Le Bris N, Gaill F, Compère P. 2004. Distribution of bacteria and associated minerals in the gill chamber of the vent shrimp *Rimicaris exoculata* and related biogeochemical processes. *Mar Ecol Prog Ser*. 284:237–251.

Zbinden M, Shillito B, Le Bris N, De Vilardi de Montlaur C, Roussel E, Guyot F, Gaill F, Cambon-Bonavita M-A. 2008. New insights on the metabolic diversity among the epibiotic microbial community of the hydrothermal shrimp *Rimicaris exoculata*. *J Exp Mar Biol Ecol*. 159(2):131–140.

Zhang D, Cai S, Liu H, Lin J. 2008. Antennal sensilla in the genus *Lysmata* (Caridea). *J Crust Biol*. 28(3):433–438.

RESEARCH ARTICLE

Bacterial communities associated with the wood-feeding gastropod *Pectinodonta* sp. (Patellogastropoda, Mollusca)

Magali Zbinden[1], Marie Pailleret[1,2], Juliette Ravaux[1], Sylvie M. Gaudron[1], Caroline Hoyoux[3], Josie Lambourdière[4], Anders Warén[5], Julien Lorion[6], Sébastien Halary[1] & Sébastien Duperron[1]

[1]Systématique, Adaptation, Evolution, AMEX, Université Pierre et Marie Curie, Paris, France; [2]Laboratoire de Paléobotanique, Paléodiversité et Paléoenvironnements, Université Pierre et Marie Curie, Paris, France; [3]Laboratoire de Morphologie fonctionnelle et évolutive, Unité de Morphologie ultrastructurale, Université de Liège, Liège, Belgium; [4]Département Systématique et Evolution, Muséum National d'Histoire Naturelle, CNRS-MNHN, Paris, France; [5]Swedish Museum of Natural History, Stockholm, Sweden; [6]Département Systématique et Evolution, Museum National d'Histoire Naturelle, UMR 7138 UPMC-IRD-MNHN-CNRS, Paris, France

Correspondence: Magali Zbinden, Université Pierre et Marie Curie – Paris VI, CNRS, UMR7138, Systématique, Adaptation, Evolution, AMEX, 7 Quai St Bernard, case courrier 5, F-72252 Paris cedex 05, France. Tel.: +33 144 273 502; fax: +33 144 275 801; e-mail: magali.zbinden@snv.jussieu.fr

Received 23 December 2009; revised 16 July 2010; accepted 28 July 2010.
Final version published online 10 September 2010.

DOI:10.1111/j.1574-6941.2010.00959.x

Editor: Michael Wagner

Keywords
sunken woods; wood-feeding gastropod; symbiosis; cellulolytic activity.

Abstract

Even though their occurrence was reported a long time ago, sunken wood ecosystems at the deep-sea floor have only recently received specific attention. Accumulations of wood fragments in the deep sea create niches for a diverse fauna, but the significance of the wood itself as a food source remains to be evaluated. *Pectinodonta* sp. is a patellogastropod that exclusively occurs on woody substrates, where individuals excavate deep depressions, and is thus a potential candidate for a wood-eating lifestyle. Several approaches were used on *Pectinodonta* sampled close to Tongoa island (Vanuatu) to investigate its dietary habits. Host carbon is most likely derived from the wood material based on stable isotopes analyses, and high cellulase activity was measured in the digestive mass. Electron microscopy and FISH revealed the occurrence of two distinct and dense bacterial communities, in the digestive gland and on the gill. Gland-associated 16S rRNA gene bacterial phylotypes, confirmed by *in situ* hybridization, included members of three divisions (*Alpha-* and *Gammaproteobacteria*, *Bacteroidetes*), and were moderately related (90–96% sequence identity) to polymer-degrading and denitrifying bacteria. Gill-associated phylotypes included representatives of the *Delta-* and *Epsilonproteobacteria*. The possible involvement of these two bacterial communities in wood utilization by *Pectinodonta* sp. is discussed.

Introduction

Although their abundance on the sea floor had been established since the end of the 19th century (Agassiz, 1892; Murray, 1895; Bruun, 1959), it is only one century later that large organic falls such as whale falls or sunken drift woods have received specific attention (Turner, 1973, 1977; Smith, 1992; Smith & Baco, 2003). Plant debris of various sizes (leaves, nuts, wood branches or trunks) can reach the oceans through rivers and sink to abyssal depths. Locally, these terrestrial inputs occur in large amounts and attract dense micro- and macrofauna exploiting this resource (Wolff, 1979; Palacios *et al.*, 2006, 2009). Wood-feeders and metazoans grazing bacterial mats on wood surface use these organic matters as a food source. These organisms are then themselves a food source for predators or scavengers (Turner, 1977). Chemoautotrophy is also probably significant. Indeed, sulfate reduction, mediated by heterotrophic bacteria deriving their carbon from the wood, produces sulfide (Leschine, 1995; Laurent *et al.*, 2009; Gaudron *et al.*, 2010). Sulfide then sustains chemoautotrophic bacteria occurring free-living or as symbionts for example in *Idas* and *Adipicola* mytilids (Duperron *et al.*, 2008). Wood remains thus allow the development of long-lasting ecosystems, relying on both wood degradation and chemosynthesis. Their role in deep-sea ecology, although not yet understood, could be significant (Cayré & Richer de Forges, 2002). Fauna colonizing wood deposits at the deep-sea floor is diverse. It comprises gastropod, polyplacophoran and bivalve molluscs, decapod and peracarid crustaceans, polychaetes and echinoderms

(Turner, 1973, 1977; Wolff, 1979; Cayré & Richer de Forges, 2002). Macrofaunal species documented to degrade wood in marine environments include wood-boring molluscs (bivalve families *Teredinidae* and *Xylophagainae*) and crustaceans (isopod families *Limnoridae* and *Sphaeromatidae*) (Gareth Jones *et al.*, 2001).

Cellulose, the main component of the wood, is hydrolyzed into glucose by the action of a group of enzymes known as cellulases. These enzymes have been shown to exist since a long time in plant, fungi and bacteria. In the last few years, recent evidence has revealed the occurrence of endogenous cellulases in a wide range of metazoans, such as arthropods (termites and other wood-boring insects, Watanabe & Tokuda, 2010) and crustaceans (Crawford *et al.*, 2004), nematods (Smant *et al.*, 1998), various molluscs (Watanabe & Tokuda, 2001), echinoderms (sea urchins, Nishida *et al.*, 2007) and sea squirts (Lo *et al.*, 2003). However, the symbiotic cellulase production is still the favored explanation for cellulose digestion in most metazoans (Watanabe & Tokuda, 2001). The best-documented examples of xylophagy are terrestrial and typically involve complex microbial symbiotic communities. For example, lower termites harbor numerous flagellates within their enlarged hindgut paunch, and flagellates themselves harbor both extra- and intracellular symbioses involving multiple *Bacteria* and *Archaea* (Brune & Stingl, 2005). In marine environments, the most documented examples are the wood-boring bivalves of the family *Teredinidae* that benefit from cellulolytic and nitrogen-fixing gammaproteobacterial symbionts (Waterbury *et al.*, 1983; Distel *et al.*, 2002; Luyten *et al.*, 2006).

During several cruises dedicated to the sampling of naturally sunken woods around Vanuatu islands (*BOA0* 2004, *BOA1* 2005, *SantoBOA* 2006), we collected other mollusc species, in particular chitons and limpets, obviously able to degrade wood. Animals were indeed attached or clinging to the surface of dredged pieces of wood, where they sometimes had excavated deep depressions. The most abundant were true limpets (Patellogastropoda) of the genus *Pectinodonta* (family *Acmaeidae*). In this study, we address whether *Pectinodonta* specimens, collected during the *SANTOBOA* 2006 cruise at two different stations of similar depths, are real wood-feeders. A multidisciplinary approach was conducted to investigate potential bacterial partners of *Pectinodonta*, including morphological and ultrastructural observations, localization and molecular characterization of associated bacteria, cellulase activity assays and stable isotope analyses.

Materials and methods

Samples

Pectinodonta sp. specimens were recovered during the *SANTOBOA* 2006 cruise aboard the *RV Alis*, in the Vanuatu archipelago. Samples were trawled at two stations close to Tongoa island: AT120 (latitude 15°41215′N, longitude 167°01701′E, between 431 and 445 m depth) and AT121 (latitude 15°39778′N, longitude 167°01639′E, between 275 and 290 m depth). Specimens from this cruise are named *Pectinodonta*-2006. A second set of specimens, used only for isotopic analyses, were collected with their host wood during the *BOA0* 2004 cruise aboard the *RV Alis*, in the Vanuatu archipelago. Samples were trawled between the Malekula and the Epi islands (station CP2304: latitude 16°37.4′N, longitude 167°59.8′E between 564 and 582 m depth). These specimens, labelled *Pectinodonta*-2004, have a morphology very similar to *Pectinodonta*-2006 specimens and were stored with the wood in ethanol 80%.

Upon recovery from trawl bags, *Pectinodonta* specimens were either fixed directly, or dissected in body parts: the gill, digestive mass (which comprises both the digestive tract and the digestive gland) and foot.

Samples for electron microscopy were fixed in a 2.5% glutaraldehyde–seawater solution and later postfixed in 1% osmium tetroxide. Samples for DNA extraction were either frozen or fixed in 95% ethanol. Samples for FISH were fixed in 4% formaldehyde in filtered seawater at 4 °C for 2 h, rinsed twice in filtered seawater and once in seawater/ethanol (1 : 1), and stored at 4 °C in ethanol 95%. Samples for enzymatic activity measurements were frozen in liquid nitrogen. Samples for isotopic analyses were either frozen in liquid nitrogen (*Pectinodonta*-2006) or stored in ethanol 80% (*Pectinodonta*-2004).

Light microscopy and transmission electron microscopy (TEM)

The gills, digestive tracts and digestive glands of two *Pectinodonta*-2006 specimens were prepared, using classical techniques, as described in Duperron *et al.* (2009).

Scanning electron microscopy (SEM)

The gills, digestive tracts, radulas and shells of two specimens, as well as wood pieces collected under (rasped) and away (nonrasped) from *Pectinodonta* specimens, were observed. Samples were prepared, using a classical protocol, as described in Duperron *et al.* (2009).

Amplification, cloning and sequencing of host and bacterial genes

DNA was extracted from the foot tissue of 11 *Pectinodonta*-2006 specimens using the QIAamp® DNA Micro Kit (Qiagen). The 5′-end of the host cytochrome *c* oxidase subunit I (COI) mtDNA-encoding gene was amplified using universal primers LCO 1490/HCO 2198 (Folmer *et al.*, 1994) and a standard PCR protocol described elsewhere (Samadi *et al.*, 2007). DNA was also extracted from dissected

gill tissue and digestive mass of two *Pectinodonta*-2006 specimens, and bacterial 16S rRNA-encoding genes were amplified during 35 cycles from each sample using universal primers 27F (5′-AGAGTTTGATCATGGCTCAG-3′) and 1492R (5′-GTTACCTTGTTACGACTT-3′) as described by Duperron *et al.* (2005). The PCR products obtained for host COI were sequenced directly. PCR products obtained for bacterial 16S rRNA genes were purified and cloned using the TOPO™ cloning kit (Invitrogen, Carlsbad, CA). Inserts from positive clones were sequenced after plasmid extraction. Sequencing was performed by Genoscreen (Lille, France).

Amplifications of fragments of genes linked to certain bacterial metabolisms were attempted, but failed to yield PCR products. The metabolisms tested were autotrophy (ribulose 1,5-bisphosphate carboxylase/oxygenase), sulfur metabolism (adenosine 5′-phosphosulfate reductase) and methane oxidation (particulate methane monooxygenase α subunit). Tissues of dual symbiotic *Bathymodiolus* mytilids, and of two thiotroph-associated *Myrtea* (Bivalvia: Lucinidae) and *Lamellibrachia* (Annelida: Siboglinidae), were used as controls.

Sequences were deposited at the EMBL database under accession numbers FN421451–FN421461 (host COI sequences from 11 specimens), FM994656–FM994674 (16S rRNA gene sequences from the gill) and FM994675–FM994682 (16S rRNA gene sequences from the digestive mass).

Gene sequence analysis

Bacterial 16S rRNA gene sequences were compared with the GenBank database. New sequences of this study, their best BLAST hits and a dataset containing representative sequences of all bacterial divisions recovered were aligned, representing a sum of 288 sequences. Alignments were performed using SINA webaligner (http://www.arb-silva.de/aligner/) and manually checked. Neighbor-joining methods were used to assess the preliminary phylogenetic relationships among these 288 bacterial 16S rRNA gene sequences. A final data set of 70 sequences was selected from these and analyzed using a Maximum Likelihood (ML) algorithm with a randomized input order of sequences using PHYLIP (Felsenstein, 2002). Bootstrap values were calculated based on 1000 ML replicates.

FISH

Four *Pectinodonta*-2006 specimens were used for FISH. Gill tissue and visceral mass were dissected and embedded separately in wax (90% poly-ethylene-glycol, 10% 1-hexadecanol). Sections, 10 μm thick, were cut using a microtome (JUNG, Heidelberg, Germany) and collected on Superfrost® Plus slides (Roth, Germany). After wax removal in ethanol and rehydration, each section was hybridized following the protocol described in Duperron *et al.* (2005), air dried and mounted using a SlowFade medium (Invitrogen).

FISH probes, summarized in Table 1, were labelled with Cy3, Cy5 or fluorescein isothiocyanate. Observations were performed on a fluorescence microscope (Olympus BX61, Tokyo, Japan) equipped with Optigrid™ (QiOptic, Rochester, NY). Image stacks were obtained by acquiring images on consecutive focal planes separated by 0.3 μm over the entire thickness of the sections. Stacks obtained for each fluorochrome were then merged to create an RGB image displaying the localization of each type of bacteria in the host tissue.

Cellulase activity assays

Two feet, two digestive masses and six gills (pooled in two samples) were homogenized separately on ice in 50 mM NaAc buffer (1 vol sample/1 vol buffer). Homogenates were centrifuged at 10 000 ***g*** (10 min) at 4 °C and the extracted proteins were quantified in the supernatant with the Bio-Rad protein assay using bovine serum albumin (Sigma) as the standard. Cellulase activity was measured using the microplate-based filter paper assay described by Xiao *et al.* (2004). Briefly, 20 μL aliquots of extracts were added to wells of a 96-well PCR plate containing 40 μL of 50 mM NaAc buffer, and a filter paper disk (Whatman No. 1 filters cut into 7-mm-diameter circles). After 60 min of incubation at 50 °C, 120 μL of dinitrosalicylic acid was added to each reaction and incubated at 95 °C for 5 min. Finally, a 36-μL aliquot of each sample was transferred to the wells of a flat-bottom plate containing 160 μL H_2O, and the absorbance was measured at 540 nm using a Microplate reader

Table 1. Oligonucleotide probes used in this study, position in the 16S rRNA gene of *Escherichia coli* and percentage of formamide used

Probe	Sequence (5′–3′)	Position	% Formamide	Target	Reference
EUB338	GCTGCCTCCCGTAGGAGT	338	20–40	Most eubacteria, positive control	Amann *et al.* (1990)
DEL495a	AGTTAGCCGGTGCTTSTT	495	30	Some *Delta Beta* and *Gammaproteobacteria*, some *Actinobacteria*	Loy *et al.* (2002)
GAM42	GCCTTCCCACATCGTTT	42	30	*Gammaproteobacteria*	Manz *et al.* (1992)
ARC94	TGCGCCACTTAGCTGACA	94		*Arcobacter*	Snaidr *et al.* (1997)
EPSY549	CAGTGATTCCGAGTAACG	549	20	*Epsilonproteobacteria*	Manz *et al.* (1992)
ALF968b	GGTAAGGTTCTKCGCGTT	968	20	Various bacteria (not highly specific)	Neef (1997)
CF319	TGGTCCGTGTCTCAGTAC	319	35	*Bacteroides*	Manz *et al.* (1996)

Target refers to the main groups targeted by probes as obtained from a 'probe match' search in ribosomal database project.

(Bio-Rad, France). Standard curves were obtained using glucose solutions (Sigma-Aldrich). A positive control for the reaction was also performed using Cellulase C-2605 from *Aspergillus* sp. (Sigma-Aldrich). Results are expressed as micromole glucose produced per minute per milligram protein.

Stable isotope analyses and sample preparation

Tissues from six *Pectinodonta*-2006 specimens were analyzed (six gills pooled in one sample due to the low amounts of dry material, foot tissue from six specimens, five digestive tracts and six digestive glands).

Pectinodonta-2004 specimens available in the lab were also investigated because the wood piece to which they were attached was also available (wood and animals were fixed and stored in ethanol 80%). Five whole specimens (without their shell), and dissected organs from five other specimens (five foot samples pooled in three samples, five digestive tracts pooled in two samples, five gills pooled in one sample, five digestive glands pooled in one sample) were analyzed. Three samples of the wood, identified to belong to the genus *Leucaena* sp. (Pailleret *et al.*, 2007), were also analyzed. All these samples were rinsed, dried at 60 °C for 30 h, ground to a powder and weighed (about 1 mg) before stable isotopes analyses.

The C/N atomic ratios of all samples were measured using a CHN elemental analyzer (EuroVector, Milan, Italy). The resultant gas was introduced into an isotope ratio mass spectrometer (IRMS) (GV IsoPrime, UK) to determine carbon and nitrogen isotopes. Stable isotopic data are expressed as the relative per mil (‰) differences between the samples and the conventional standard Pee Dee Belemnite for carbon and air N_2 for nitrogen.

Because ethanol fixation may induce a bias in the analyses of the isotopic ratio, in the form of increased $\delta^{13}C$ (Kaehler & Pakhomov, 2001), isotopic signatures of the foot of *Pectinodonta*-2004 and *Pectinodonta*-2006 were compared with test the effect of ethanol fixation using unbalanced one-way ANOVA (MINITAB 15).

Results and discussion

Characterization of *Pectinodonta* specimens

Among the plant remains collected from the Caribbean area (at depths below 1200 m), Wolff (1979) reported significant diversity and abundance of cocculinid gastropods, with at least seven species occurring in and on wood. All specimens recovered for the present study were assigned to the genus *Pectinodonta*, based on some group characteristics such as shell morphology (Fig. 1b) and the radula (Fig. 1e and f). Shells were between 0.9 and 1.8 cm in length. The radula, similar to a carpenter's saw, is characteristic of the genus *Pectinodonta*, as described by Marshall (1998). To test whether all the specimens represented a single species, mitochondrial COI mtDNA sequences were obtained from 11 *Pectinodonta*-2006 specimens from two trawls (AT120 and AT121) performed during the *SANTOBOA* cruise. The mean Kimura 2 Parameter (K2P) genetic distance measured among specimens, using the MEGA 4.0 software (Tamura *et al.*, 2007), was 0.1% (maximum value measured between two sequences: 0.3%). Such a low level of divergence is a strong indication that all specimens represented a single species, because COI displays a significant variation among species in Patellogastropoda (Nakano & Ozawa, 2007). Hence, the most similar COI sequences available in the GenBank database belong to *Pectinodonta rhyssa* and *Bathyacmaea nipponica*, and differ by mean K2P genetic distances of 19.0% and 18.4%, respectively. Given the fact that *Pectinodonta*-2006 specimens all come from the same location and similar depth, and that they are morphologically and genetically homogeneous, it is reasonable to assume that *Pectinodonta*-2006 specimens belong to a single species (Meier *et al.*, 2008). However, they cannot be assigned to any described species because sequences from very few species are available in databases.

Evidence for wood-feeding

Activities of marine wood-boring organisms (mainly bivalves of the *Teredinidae* and *Pholadidae* families, and crustaceans of the *Limnoridae* and *Sphaeromatidae* families) in shallow waters have been intensively studied because of their impact on human activities (wooden fishing boats, harbors, wharfs, piers, aquaculture facilities, etc.). Nevertheless, their deep-sea counterparts are much less known. A common question discussed about wood gribbles is whether animals bore into the wood for protection or to utilize the wood, or bacterial mats on its surface, as a food source. In the case of *Pectinodonta*, individuals do not bore inside the wood for protection as they are protected by their strong shell when firmly attached to the wood surface. Hence, they most probably ingest the wood for food, either to acquire nutrition from microorganisms on the wood, or from the wood itself. Wolff (1979) assumed that all cocculinids occurring on organic remains utilized them as food, grazing the microbial cover rather than the substrate. Considering the observations and analyses detailed below, we rather assume that the *Pectinodonta* specimens from this study are real wood-feeders.

Indeed, all our specimens were recovered from wood trunks, where they can be found at high densities (see Fig. 1a; from this wood piece, Pailleret *et al.* (2007) counted 248 individuals, corresponding to a density of 0.25 individuals cm^{-3}). The genus *Pectinodonta* seems to be present only on large trunks of hardwood, and was not seen on leaves, *Pandanus* stems or other soft wood (A. Warèn, pers. commun.; Marshall, 1985). They occur at the bottom of small

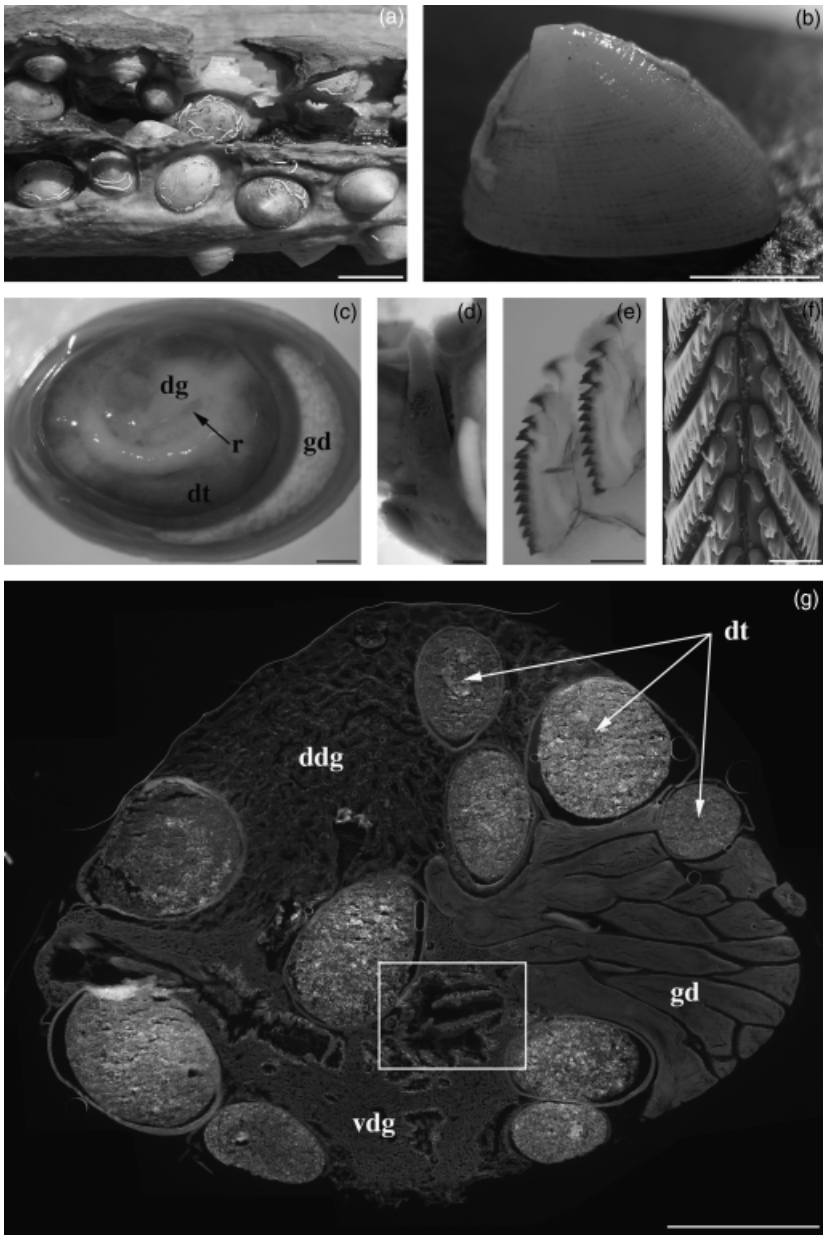

Fig. 1. *Pectinodonta* morphology and anatomy. (a) A densely colonized wood recovered during *BOA0*, showing *Pectinodonta* specimens located in the hollows. (b) *Pectinodonta* shell. (c) Dorsal view of a specimen without the shell, showing the digestive tract (dt), the radular ribbon (r), the dorsal part of the digestive gland (dg) and ventro-laterally the gonad (gd). (d) The gill extending anteriorly from the left to the right. (e–f), radula, photonic (e) and SEM (f) views. (g) Overview of a transversal section of a specimen (mosaic of 25 pictures of a specimen prepared for FISH), showing several sections of the digestive tract (dt), the dorsal (ddg) and ventral (vdg) digestive gland and the gonad (gd). White squares indicate the location of Fig. 6f and g. Scale bars: a = 1 cm, b = 0.5 cm, c = 1 mm, d = 0.5 mm, e, f = 50 μm, g = 1 mm.

depressions (see Fig. 1a) that they very likely dig beneath themselves, if we consider the shape concordance of the hollows and the shells. Microscopic observations indicate that the wood under the specimens is devoid of bacteria (data not shown). The occurrence of *Pectinodonta* in these depressions suggests that individuals always rasp the wood at the same place, which would preclude a regular recolonization by bacteria, making the bacterial biofilm grazing hypothesis (Wolff, 1979) unlikely.

Macroscopic, light and electron microscopic observations show that the gut is filled with tightly packed wood chips (Figs 1g and 2). Careful examination failed to reveal any conspicuous bacterial community associated with the wood fragments (Fig. 2c, d), free in the digestive tract or even attached to the epithelium. Very few prokaryotes were observed, sparsely distributed in the gut lumen (not shown).

Cellulase activity was assayed in the gill, foot and digestive mass of *Pectinodonta*. The activities, measured per milligram protein against filter paper in the different tissues, are summarized in Fig. 3. The highest activity was measured in the digestive mass. The value (48×10^{-3} μmol glucose min^{-1} mg^{-1} protein) is more than fourfold higher than that measured in the foot (10.7×10^{-3} μmol glucose min^{-1} mg^{-1} protein), and about sixfold higher than that in the gill (8.2×10^{-3} μmol

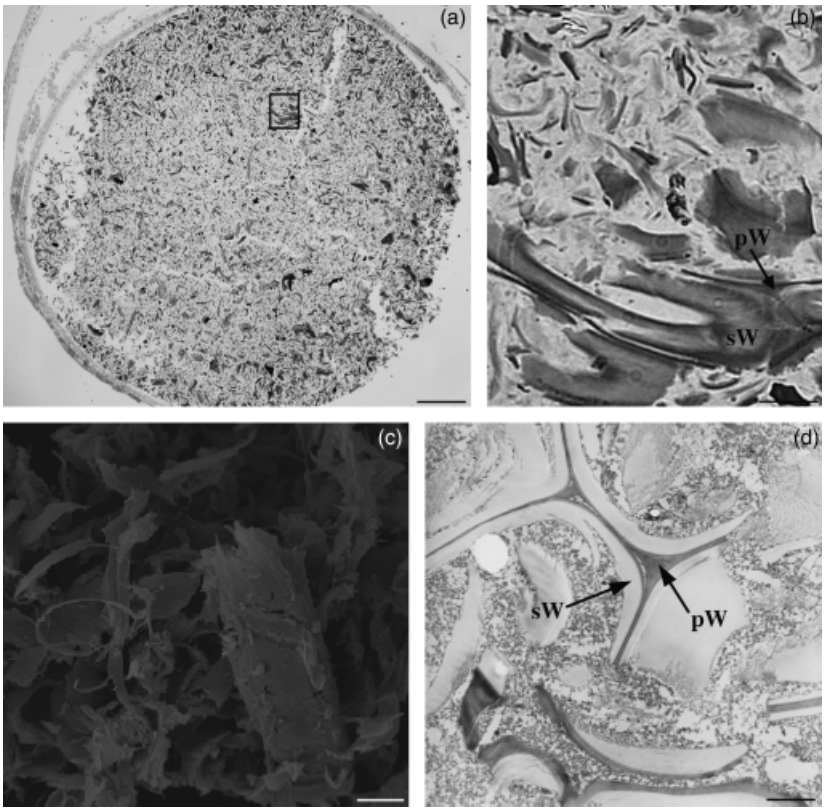

Fig. 2. *Pectinodonta* digestive tract. (a–b) Semi-thin section of the gut, full of wood fragments [square in (a) is enlarged in (b)]. (c–d) SEM and TEM views, respectively, of the gut content, full of wood fragments. Wood cell walls can be seen on the semi-thin and thin sections (sW, secondary wall; pW, primary wall). Note the absence of associated microorganisms. Scale bars: a = 100 μm, b = 10 μm, c = 5 μm, d = 2 μm.

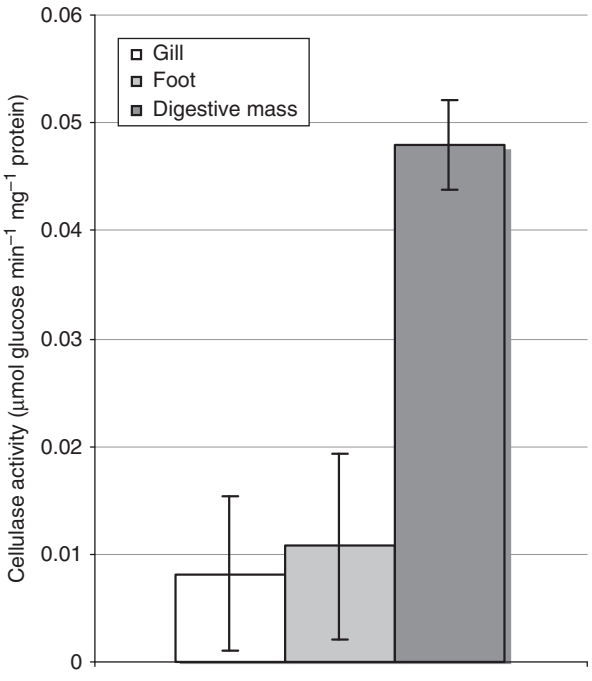

Fig. 3. Cellulase activity in *Pectinodonta* sp. tissues. Values are expressed as means ± SD.

glucose min^{-1} mg^{-1} protein). In comparison, the cellulase activity measured for the digestive mass is higher than that of a commercially available cellulase preparation from the cellulolytic fungi *Aspergillus* sp. (11.6×10^{-3} μmol glucose min^{-1} mg^{-1} protein). *Pectinodonta* are thus apparently able to degrade cellulose either with the help of symbiotic partners or using their own enzymes, as it occurs, respectively, in lower and higher wood-boring termites (Ohkuma, 2003).

The contribution of the wood to the carbon pool of *Pectinodonta* was supported by stable isotope analyses (Fig. 4). The $\delta^{13}C$ signature of *Pectinodonta*-2004 (-24.3 ± 0.3‰) was close to the $\delta^{13}C$ isotopic values of the wood (-27.0 ± 0.3‰) on which it was sampled (see Fig. 1a). These ^{13}C isotopic ratios are very similar to those published by Nishimoto *et al.* (2009) for the wood-boring bivalve *Xylophaga* sp. (-24.1 ± 0.4‰) and its host wood (-26.9 ± 1.1‰). Another potential carbon source in the ocean may be phytoplankton, but $\delta^{13}C$ isotopic ratios are less negative (-19‰ to -22‰, Fontugne & Duplessy, 1981; Rau *et al.*, 1982), suggesting that the wood is a better candidate as the main source of *Pectinodonta* diet. Among tissues of both *Pectinodonta*-2004 and *Pectinodonta*-2006, the most depleted values were consistently recorded for the digestive tract (-26.0 ± 0.1‰ and -25.4 ± 0.7‰, respectively) and the most enriched values were obtained for the

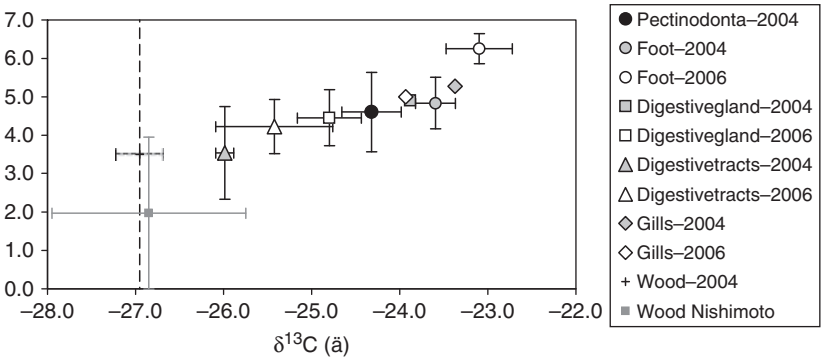

Fig. 4. Stable isotope signatures ($\delta^{15}N$ vs. $\delta^{13}C$) of isolated tissues (foot, digestive gland, digestive tract, gill), whole animal from *Pectinodonta*-2004 and its food source (wood). White symbols show the isolated tissues of *Pectinodonta*-2006 specimens, and the gray show those for *Pectinodonta*-2004 specimens. Black symbols are for the entire animal. As the nitrogen content of our wood sample was negligible, we only present the $\delta^{13}C$ value (-27‰) with its SD (± 0.3). For comparison, wood isotopic values from the Nishimoto *et al.*'s (2009) study are included in the figure.

gill (-23.4‰ and -24.0‰, respectively) and the foot (-23.6 ± 0.2‰ and -23.1 ± 0.4‰, respectively) (Fig. 4). Tissues such as muscles (foot) have a slow turnover, reflecting the food source integration of a long period of time, whereas tissues such as the digestive gland have a faster turnover, reflecting the diet of a shorter period of time (Lorrain *et al.*, 2002). This may explain the different ^{13}C isotopic ratios measured among the different organs for both *Pectinodonta* specimens (Fig. 4). No statistical difference was observed on the $\delta^{13}C$ isotopic signatures of the foot tissue between *Pectinodonta*-2006 (stored frozen) and *Pectinodonta*-2004 (stored in ethanol) specimens (ANOVA: $F_{(1,1)} = 4.33$; $P = 0.08$). The $\delta^{15}N$ signatures of the 2004 and 2006 specimens were between 3.5‰ and 6.3‰, the lowest value being measured from the digestive tract and the highest value being measured from the foot and the gill (Fig. 4). The nitrogen content within the wood was negligible (C/N ratio was very low; data not shown) and organisms that feed on wood in marine habitats, as seen in *Teredinidae*, obtain their nitrogen thanks to symbionts (Lechene *et al.*, 2007; Nishimoto *et al.*, 2009). Therefore, the missing data on the $\delta^{15}N$ signature of the wood in this study would not provide more insight into the fractionation of 3–4‰ usually observed between the primary producer and the primary consumer (De Niro & Epstein, 1978; Minagawa & Wada, 1984).

Considering only the *Pectinodonta*-2004 specimens, for which the $\delta^{13}C$ of the wood substrate was measured, a 3.5‰ shift was observed between the wood and the different tissues, well above the typical 1‰ difference documented for a single trophic level (De Niro & Epstein, 1978) (Fig. 4). This suggests that the wood is not directly, or not only, used by the limpet. Possible explanations are as follows: (1) an additional trophic intermediate may exist between the host and the wood that fractionates carbon and leads to a ^{13}C enrichment, as seen for some termites (Tayasu, 1998) and wood-borers (Nishimoto *et al.*, 2009); (2) the limpet also receives a second source of food in its diet besides the wood that is more enriched in ^{13}C (such as phytoplankton), yielding a $\delta^{13}C$ value that is a mean of $\delta^{13}C$ values from these two different food sources. In this second case, the animal could digest the wood using either its own cellulases or cellulases provided by symbiotic bacteria. Considering the absence of anything except for wood in the gut, and the occurrence of bacteria combined with the high cellulolytic activity measured in the digestive mass, the first hypothesis seems to be more likely.

Associated bacterial communities and their potential role

TEM and FISH (the FISH probes used are summarized in Table 1) revealed two distinct bacterial communities occurring in high densities in the ventral part of the digestive gland and on the gill surface (Figs 5–7).

A total of 40 and 38 partial 16S rRNA-encoding gene sequences (from the digestive mass and gill, respectively) were obtained from two specimens. Full sequences representative of the different phylotypes were obtained and used for phylogenetic reconstruction (Fig. 8). Three phylotypes were recovered from the digestive mass, affiliated with *Alphaproteobacteria* (phylotype B-DT-1, 36 clones), *Bacteroidetes* (phylotype A-DT-19, three clones) and *Gammaproteobacteria* (phylotype A-DT-24, one clone). The digestive gland is well developed and surrounds the intestine in the visceral mass (see Fig. 1g). The dorsal and ventral lobes displayed different structures. The dorsal part consisted of large flattened lobes (roughly 500×200 μm) (Fig. 5a and inset) surrounded by a thick epithelium constituted of secretory cells. Neither FISH nor TEM observations revealed the occurrence of bacteria in these structures. The ventral part of the gland consisted of smaller rounded lobes (25–50 μm diameter) (Fig. 5b). Strong, unambiguous, bacteria-specific FISH signals were seen associated with these sections using probe EUB338 (Fig. 5c; see Table 1 for probes' description). TEM observations showed that rounded lobes consisted of structures with a central lumen surrounded by abundant rod-shaped, gram-negative bacteria, roughly 0.5×2 μm in size, located extracellularly among folds of the gland wall (Fig. 5d, e). These bacteria only hybridized with probes EUB338 and ALF968b (Fig. 6a, c), indicating that they likely correspond to phylotype B-DT-1, the dominant

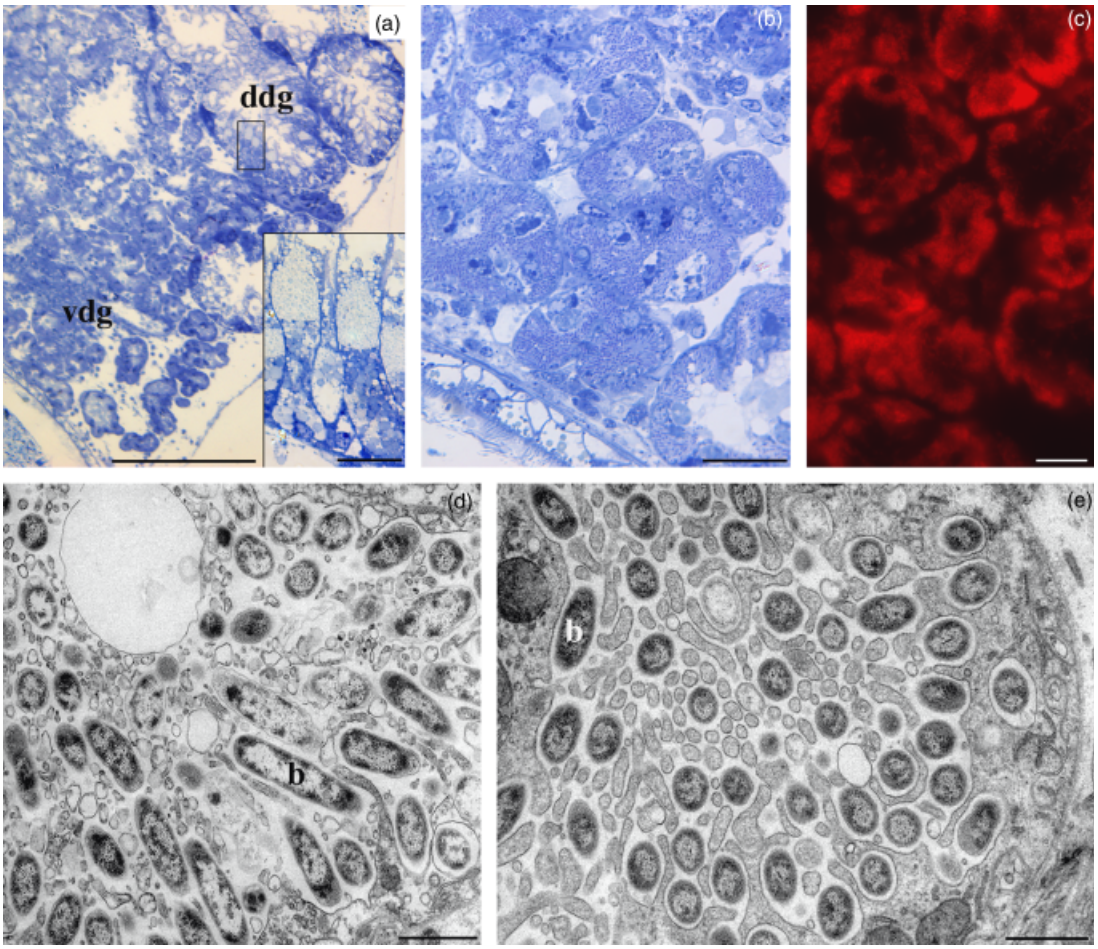

Fig. 5. *Pectinodonta* digestive gland. (a) Semi-thin section of the digestive gland, showing both large lobe sections of the dorsal digestive gland (ddg) and small lobe sections of the ventral digestive gland (vdg). Square in 'a' showing the secretory cells of the large lobes is enlarged in the inset. (b–c) Enlarged view of the ventral digestive lobe sections, (b, semi-thin section; c, FISH with EUB338). (d–e) TEM view of the ventral digestive gland, showing bacteria (b) in folds of the gland wall. Scale bars: a = 200 μm (inset: 20 μm), b = 20 μm, c = 10 μm, d and e = 1 μm.

phylotype recovered from the digestive mass. This alphaproteobacterial phylotype is moderately related (90% sequence identity) to several strains from seawater, a strain from the toxic dinoflagellate *Alexandrium tamarense*, several strains within genera *Ochrobactrum*, *Ahrensia* and *Labrenzia*, and to the heterotrophic denitrifying bacterium *Pseudovibrio denitrificans* (Shieh *et al.*, 2004).

The two other bacterial phylotypes, A-DT-19 and A-DT-24, cluster within the *Bacteroidetes* and *Gammaproteobacteria*, respectively. FISH using group-specific probes GAM42 and CF319 indicated that *Gammaproteobacteria* and *Bacteroidetes* were present within the gland, but only in restricted areas (Fig. 6b, e). They occurred in the ventral part of the gland, restricted to a thin layer delimiting large cavities (Fig. 6d, and see Fig. 1g for localization). Both types of bacteria were mixed, but no cohybridization was observed, indicating that the cooccurrence of the two bacterial types was real, and suggesting that they could function as a consortium. The closest relatives of A-DT-24 (95–96% sequence identity), *Psychromonas* sp., are obligate to facultative anaerobic psychrophilic heterotrophs, able to hydrolyze polymers such as starch (Auman *et al.*, 2006). Phylotype A-DT-19 is moderately related (92–93% sequence identity) to several *Bacteroidetes*, including uncultivated clones, as well as strains within the genera *Zobellia*, *Flexibacter*, *Arenibacter* and *Cellulophaga*, which are reported to be chemoorganotrophs and to be proficient in degrading various biopolymers such as cellulose, chitin and pectin (Kirchman, 2002). Such properties would make sense in bacteria associated with a digestive gland, and support the potential role of the bacterial community in wood digestion and measured cellulolytic activity. Because wood debris were not observed within the gland, the action of bacteria on wood is indirect, probably via extracellular enzymes transferred to the gut lumen through ducts. This has been suggested previously for *Teredinidae*, which harbor symbionts in their gill tissues. It is still unclear how the cellulolytic

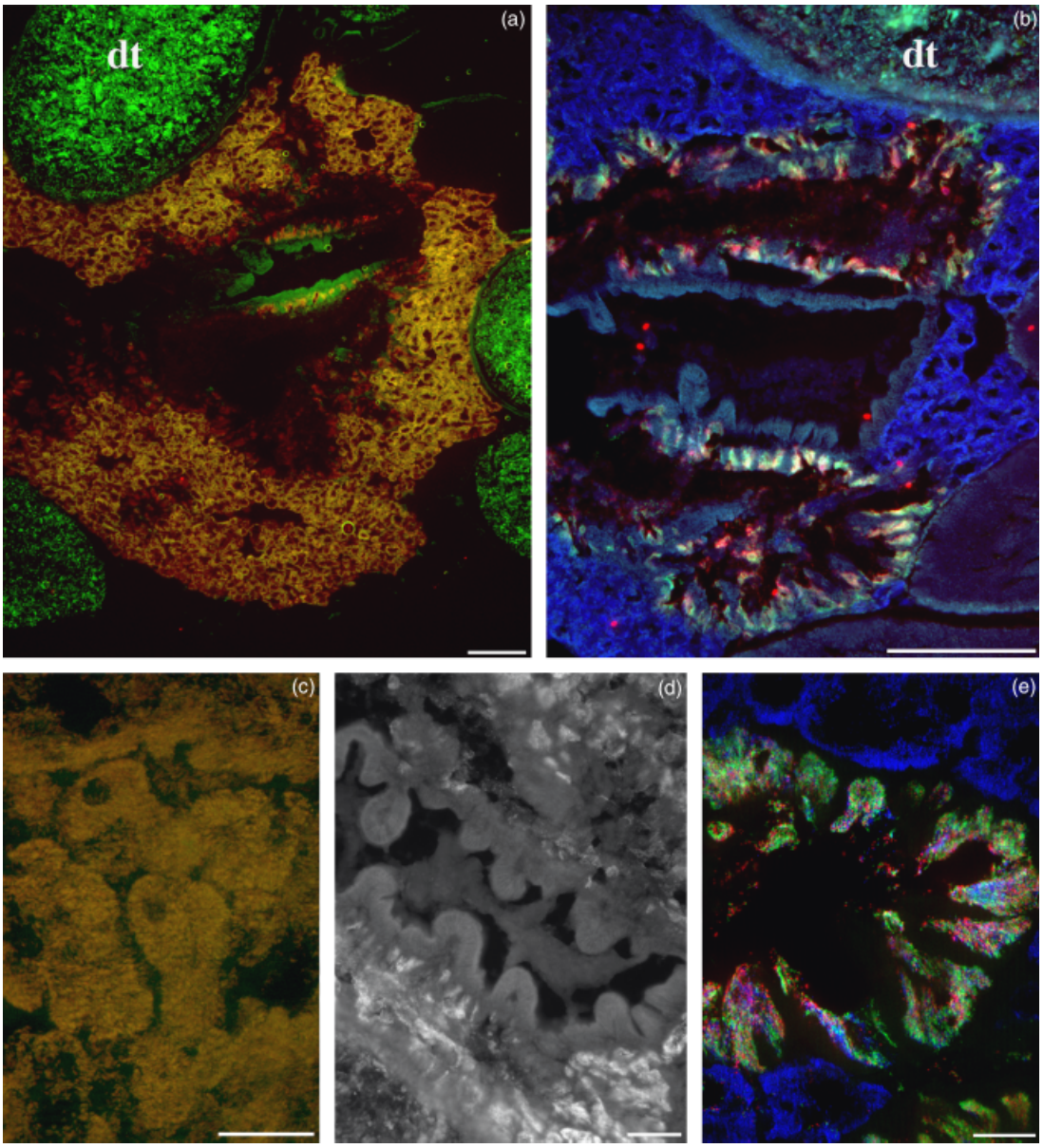

Fig. 6. *Pectinodonta* digestive gland: FISH observations of the ventral digestive gland (see localization on Fig. 1). (a) [enlarged in (c)], *Alphaproteobacteria* appear in yellow (composite view of a double hydridization: ALF968b signal in green, EUB338 signal in red). Wood in the digestive tract (dt) section appears green due to autofluorescence. (b) [enlarged in (e)], *Alphaproteobacteria* appear in blue (targeted only by the EUB338 probe), *Bacteroides* appear in cyan/green (CF319 probe signal in green) and *Gammaproteobacteria* appear in magenta/red (GAM42 probe signal in red). (d) View of the epithelium containing the *Bacteroides* and *Gammaproteobacteria* of a specimen prepared for FISH. Scale bars: a, b = 200 μm; c, d, e = 20 μm.

enzymes produced in the shipworm gills can be transported to the gut where the wood is degraded. Saraswathy (1971) suggested that a duct in the afferent branchial vein could connect the gills to the esophagus, but it has never been observed. The 'scaly-foot snail' (family *Peltospiridae*, gen. nov., sp. nov., Warén *et al.*, 2003) also houses a dense bacterial endosymbiotic population of thiotrophic *Gammaproteobacteria*, located in its esophageal gland. In this species, a hypertrophied circulatory system was highlighted between the gland and the foot, which seems to be the path for metabolic exchange between the bacteria and their host (Goffredi *et al.*, 2004). Apart from cellulose digestion, another possible role that deserves further attention is nitrogen fixation. Indeed, nitrogen-fixing bacteria are reported to be associated with many animals with a nitrogen-deficient diet, such as termites and *Teredinidae* bivalves (Waterbury *et al.*, 1983; Lechene *et al.*, 2007).

A second bacterial community, distinct from that of the digestive gland, was observed on the gill. Abundant

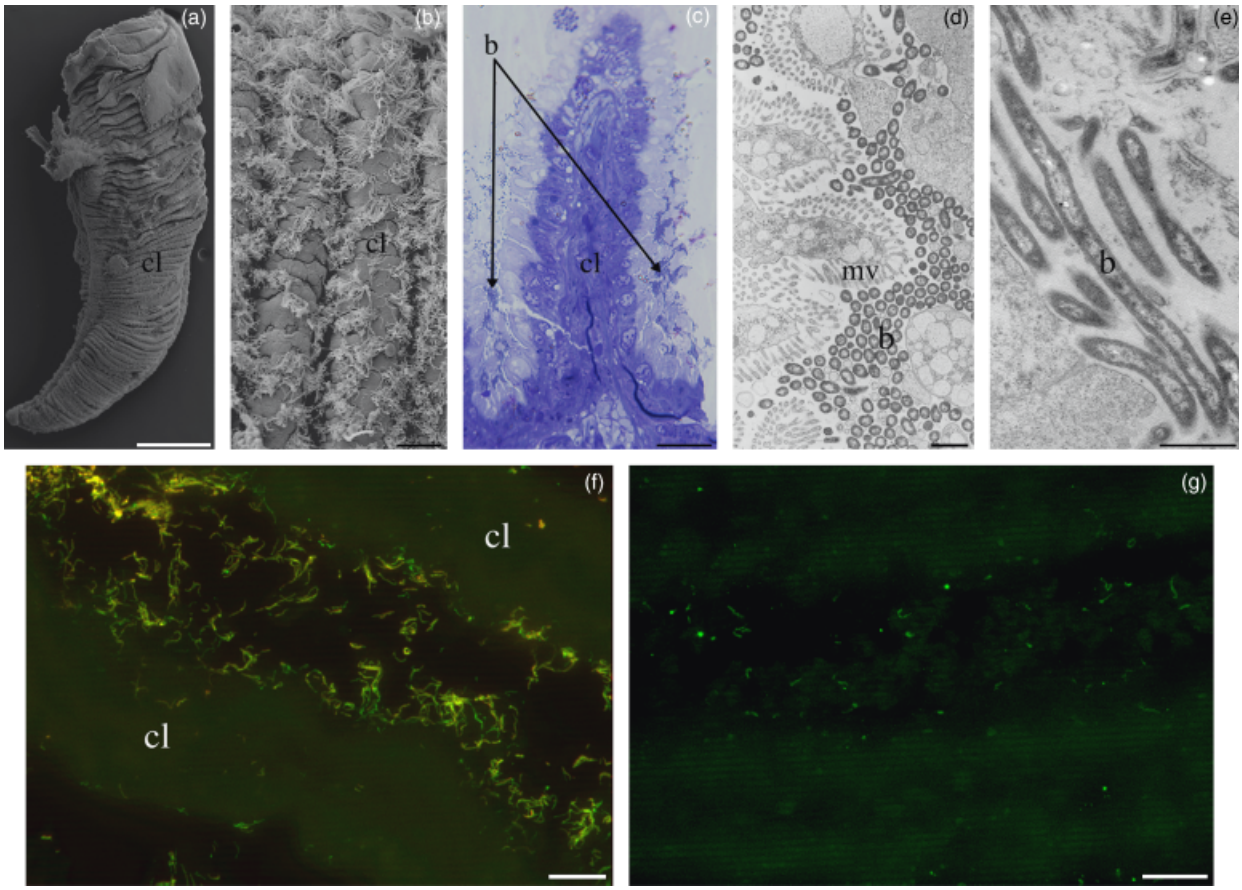

Fig. 7. *Pectinodonta* ctenidium. (a, b), SEM view of the whole gill (a) and a closer view on the lamella (b) showing the cilia. (c) Semithin sections of a ctenidial lamella, showing the bacteria (b) between the lamella. (d, e), TEM views of the gill, showing the bacteria (b) located close to microvilli (mv) of the lamella. (f, g) FISH observations of the gill showing numerous *Deltaproteobacteria* (f) [dual hybridization with probes EUB338 (green) and DEL495a (red), resulting in a yellow color], and only a few *Arcobacter* (g) (ARC94 probe signal in green). cl, ctenidial lamella. Scale bars: a = 500 μm; b, c = 20 μm; d, e = 1 μm; f, g = 10 μm.

filamentous bacteria were attached to the surface of host gill epithelial cells. The gill, a true ctenidium, located over the head and oriented from the left to the right (Figs 1d and 7a), is typical of the *Acmaeidae* family (Sasaki, 1998). The surface of the ctenidial lamellae is ciliated and bacterial filaments were located among the cilia, at the surface of animal cells (Fig. 7b–d). They seemed to be anchored on the cell surface (not shown). Each filament is a single, long and thin bacterium (0.3 μm in diameter and up to 5.5 μm in length, Fig. 7e) with a typical gram-negative membrane. All filaments hybridized with the Bacteria-specific probe EUB338.

Gill-associated phylotypes included *Epsilon-*, *Delta-* and *Gammaproteobacteria*, and *Bacteroidetes*. Based on FISH results (Fig. 7f and g), most of the gill bacteria hybridized with the *Deltaproteobacteria*-specific probe DEL495a. Two closely related deltaproteobacterial phylotypes were identified. B-G-64 and A-G-4 (0.2% divergence, 18 out of 36 clones) are not closely related to any known bacterium. Their closest relative, clone zEL76, a sequence obtained from a biofilm collected at a sulfidic cave, displayed only 87% sequence similarity. Because many *Deltaproteobacteria*, such as clone zEL76, live in sulfur-rich environments, it can be hypothesized that a metabolism involving sulfur compounds is likely. Many *Deltaproteobacteria* involved in sulfur metabolism are anaerobic and produce sulfide; hence, their occurrence in the gill appears to be a paradox. However, a different metabolism cannot be ruled out because of the low similarity to known bacteria. *Epsilonproteobacteria* were also present in the gill (phylotype B-G-52, 18 clones, Fig. 7g), related to a *Helicobacter* clone identified in the gorgonian *Muricea elongate* (91% sequence identity), whose role is unknown. Phylotypes B-G-4 and B-G-14, related to *Gammaproteobacteria* and *Bacteroidetes*, respectively, were detected in clone libraries (one clone each), but FISH did not confirm the occurrence of these groups (not shown).

Epi- or endosymbiotic associations were previously reported to be associated with the gills of several gastropod

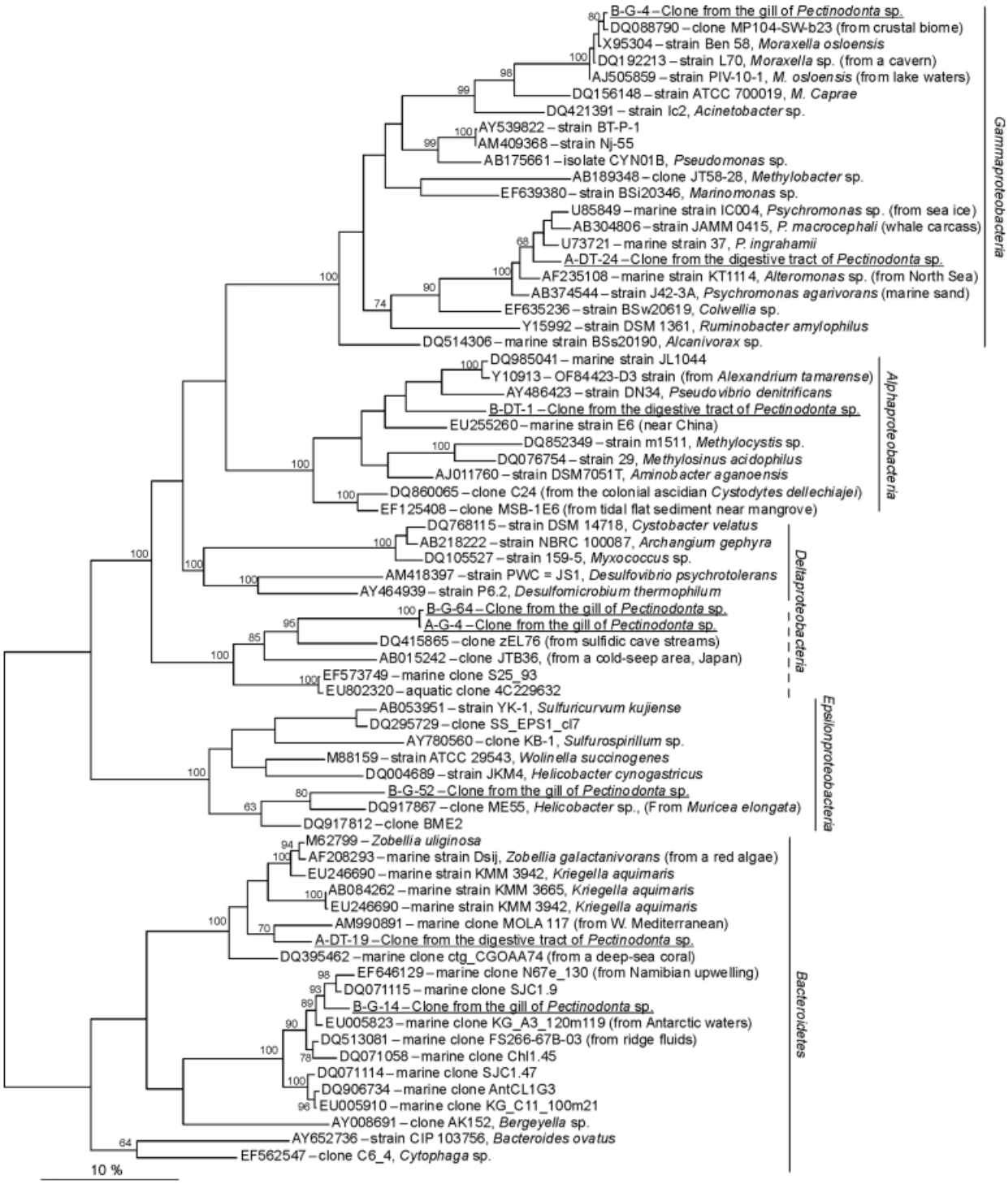

Fig. 8. Tree displaying the phylogenetic position of 16S rRNA-encoding gene sequences recovered from the gill and digestive tract of *Pectinodonta* (underlined). The tree was obtained using a ML algorithm. The value at the nodes represents percentage bootstrap support (1000 replicates, > 60% shown). *Bacteroidetes* are used as an outgroup. Scale bar corresponds to estimated 10% sequence divergence.

species, although not involving *Deltaproteobacteria* (*Lepetodrilus fucensis*, de Burgh & Singla, 1984; Bates, 2007a, b; several species of the genus *Alviniconcha*, Suzuki *et al.*, 2006; *Ifremeria nautilei*, Borowski *et al.*, 2002). These bacteria, with sulfur- or methane-linked metabolisms, are thought to contribute to host nutrition and also to protect the host

from the toxicity of sulfide. In the case of *Pectinodonta* however, the nutritional role of gill-associated bacteria is supported neither by stable isotope analyses nor by the low cellulolytic activity measured in that tissue.

Overall, bacteria identified in the digestive gland and on the gill are only distantly related to known bacteria. The closest documented relatives of *Pectinodonta* in terms of both the host phylogeny and the food source would be the shipworms, but limpet symbionts are not closely related to shipworm's symbiotic bacteria. Physiological assumptions based only on the phylogenetic position of *Pectinodonta*-associated sequence must be made with caution, and thus the exact role and contribution of each bacterial partner cannot be addressed as yet. In particular, the metazoan or the bacterial origin of cellulolytic activity measured in the digestive mass needs to be ascertained. The detailed study of sunken wood-associated organisms is an emerging field of deep-sea research and, except for shipworms, little information is available. *Pectinodonta*, with its bacterial populations associated with two organs, appears to be an interesting new model of interaction between metazoans and bacteria.

Acknowledgements

We thank the captain and crew of the *RV Alis*, and B. Richer de Forges, Sarah Samadi and Françoise Gaill, chief scientists and principal investigators of the *BOA0* and *SANTOBOA* cruises. We thank S. Lefebvre (U. Lille, France) for his expertise in stable isotopes analyses and M.-P. Bataillé (U. Caen, France) for her technical support in IRMS. We also thank P. Compère and G. Lepoint (U. Liège, Belgium) for their help with isotope analyses. TEM and SEM were performed at the Service de Microscopie Electronique, IFR 83 de Biologie Integrative-CNRS/UPMC. This work is part of a project included in the European research group DiWood supported by the CNRS (France), and received funding from ANR Deep Oases (M.P., PhD grant). The Santo expedition was partially funded by the Total Foundation.

References

Agassiz A (1892) Reports on the dredging operations off the west coast of Central America. *Bull Mus Comp Zool* **23**: 1–89.

Amann R, Binder B, Olson R, Chisholm S, Devereux R & Stahl D (1990) Combination of 16S rRNA-targeted oligonucleotide probes with flow cytometry for analysing mixed microbial populations. *Appl Environ Microb* **56**: 1919–1925.

Auman A, Breezee JL, Gosink JJ, Kämpfer P & Staley JT (2006) *Psychromonas ingrahamii* sp. nov., a novel gas vacuolate, psychrophilic bacterium isolated from Arctic polar sea ice. *Int J Syst Evol Bacteriol* **56**: 1001–1007.

Bates A (2007a) Persistence, morphology, and nutritional state of a gastropod hosted bacterial symbiosis in different levels of hydrothermal vent flux. *Mar Biol* **152**: 557–568.

Bates A (2007b) Feeding strategy, morphological specialisation and presence of bacterial episymbionts in lepetodrilid gastropods from hydrothermal vents. *Mar Ecol-Prog Ser* **347**: 87–99.

Borowski C, Giere O, Krieger J, Amann R & Dubilier N (2002) New aspects of the symbiosis in the provannid snail *Ifremeria nautilei* from the north Fidji back arce bassin. *Cah Biol Mar* **43**: 321–324.

Brune A & Stingl U (2005) Prokaryotic symbionts of termite gut flagellates: phylogenetic and metabolic implications of a tripartite symbiosis. *Progress in Molecular and Subcellular Biology. Molecular Basis in Symbiosis*, *Vol. 41* (Müller W, Jeanteur P, Kuchino Y, Macieira-Coelho A, Rhoads R & Overmann J, eds), pp. 39–60. Springer-Verlag, Berlin.

Bruun A (1959) General introduction to the reports and list of deep-sea stations. *Galathea Rep* **1**: 7–28.

Cayré P & Richer de Forges B (2002) Faune mystérieuse des océans profonds. *La Recherche* **355**: 59–62.

Crawford AC, Kricker JA, Anderson AJ, Richardson NR & Mather PB (2004) Structure and function of a cellulase gene in redclaw crayfish, *Cherax quadricarinatus*. *Gene* **340**: 267–274.

de Burgh M & Singla C (1984) Bacterial colonization and endocytosis on the gill of a new limpet species from a hydrothermal vent. *Mar Biol* **84**: 1–6.

De Niro M & Epstein S (1978) Influence of diet on the distribution of carbon isotopes in animals. *Geochim Cosmochim Ac* **42**: 495–506.

Distel D, Morrill W, MacLaren-Toussaint N, Franks D & Waterbury J (2002) *Teredinibacter turnerae* gen. nov., sp. nov., a dinitrogen-fixing, cellulolytic, endosymbiotic γ-proteobacterium isolated from the gills of wood-boring molluscs (Bivalvia: Teredinidae). *Int J Syst Evol Micr* **52**: 2261–2269.

Duperron S, Nadalig T, Caprais JC, Sibuet M, Fiala-Médioni A, Amann R & Dubilier N (2005) Dual symbiosis in a *Bathymodiolus* sp. mussel from a methane seep on the Gabon continental margin (southeast Atlantic): 16S rRNA phylogeny of the symbionts in gills. *Appl Environ Microb* **71**: 1694–1700.

Duperron S, Laurent M, Gaill F & Gros O (2008) Sulphur-oxidizing extracellular bacteria in the gills of *Mytilidae* associated with wood falls. *FEMS Microbiol Ecol* **63**: 338–349.

Duperron S, De Beer D, Zbinden M, Boetius A, Schipani V, Kahil N & Gaill F (2009) Molecular characterization of bacteria associated with the trophosome and the tube of *Lamellibrachia* sp., a siboglinid annelid from cold seeps in the eastern Mediterranean. *FEMS Microbiol Ecol* **69**: 395–409.

Felsenstein J (2002) *PHYLIP: Phylogeny Inference Package, Version 3.69*. University of Washinton, Seattle.

Folmer O, Black M, Hoeh W, Lutz R & Vriejenhoek R (1994) DNA primers for amplification of mitochondrial cytochrome *c* oxidase subunit I from diverse metazoan invertebrates. *Mol Mar Biol Biotech* **3**: 294–299.

Fontugne M & Duplessy J (1981) Organic carbon isotopic fractionation by marine plankton in the temperature range −1 to −31 °C. *Oceanol Acta* **4**: 85–90.

Gareth Jones E, Turner R, Furtado S & Kühne H (2001) Marine biodeteriogenic organisms. I. Lignicolous fungi and bacteria and the wood boring mollusca and crustacea. *Int Biodeter Biodegr* **48**: 112–126.

Gaudron SM, Pradillon F, Pailleret M, Duperron S, Le Bris N & Gaill F (2010) Colonization of organic substrates deployed in deep-sea reducing habitats by symbiotic species and associated fauna. *Mar Environ Res* **70**: 1–12.

Goffredi S, Warén A, Orphan V, Van Dover C & Vriejenhoek R (2004) Novel forms of structural integration between microbes and a hydrothermal vent gastropod from the Indian Ocean. *Appl Environ Microb* **70**: 3082–3090.

Kaehler S & Pakhomov E (2001) Effects of storage and preservation on the ä13C and ä15N signatures of selected marine organisms. *Mar Ecol-Prog Ser* **219**: 299–304.

Kirchman D (2002) The ecology of Cytophaga–Flavobacteria in aquatic environments. *FEMS Microbiol Ecol* **39**: 91–100.

Laurent M, Gros O, Brulport J-P, Gaill F & Le Bris N (2009) Sunken wood habitat for thiotrophic symbiosis in mangrove swamps. *Mar Environ Res* **67**: 83–88.

Lechene C, Luyten Y, McMahon G & Distel D (2007) Quantitative imaging of nitrogen fixation by individual bacteria within animal cells. *Science* **317**: 1563–1566.

Leschine S (1995) Cellulose degradation in anaerobic environments. *Annu Rev Microbiol* **49**: 399–426.

Lo N, Watanabe H & Sugimura M (2003) Evidence for the presence of a cellulase gene in the last common ancestor of bilaterian animals. *P Roy Soc Lond B Bio* **270**: 69–72.

Lorrain A, Paulet Y-M, Chauvaud L, Savoye N, Donval A & Saout C (2002) Differential d13C and d15N signatures among scallop tissues: implications for ecology and physiology. *J Exp Mar Biol Ecol* **275**: 47–61.

Loy A, Lehner A, Lee N *et al.* (2002) Oligonucleotide microarray for 16S rRNA gene-based detection of all recognized lineages of sulfate-reducing prokaryotes in the environment. *Appl Environ Microb* **68**: 5064–5081.

Luyten Y, Thompson J, Morrill W, Polz M & Distel D (2006) Extensive variation in intracellular symbiont community composition among members of a single population of the wood-boring bivalve *Lyrodus pedicellatus* (Bivalvia: Teredinidae). *Appl Environ Microb* **72**: 412–417.

Manz W, Amann R, Ludwig W, Wagner M & Schleifer KH (1992) Phylogenetic oligodeoxynucleotide probes for the major subclasses of *Proteobacteria*: problems and solutions. *Syst Appl Microbiol* **15**: 593–600.

Manz W, Amann R, Ludwig W, Vancanneyt M & Schleifer KH (1996) Application of a suite of 16S rRNA-specific oligonucleotide probes designed to investigate bacteria of the phylum Cytophaga–Flavobacter–Bacteroides in the natural environment. *Microbiology* **142**: 1097–1106.

Marshall B (1985) Recent and tertiary deep-sea limpets of the genus *Pectinodonta* Dall (Mollusca: Gastropoda) from New Zealand and New South Wales. *New Zeal J Zool* **12**: 273–282.

Marshall B (1998) A new deep-sea limpet of the genus *Pectinodonta* Dall, 1882 from New Zealand and new distribution records for *P. aupouria* and *P. morioria* Marshall, 1985. *The Nautilus* **112**: 52–57.

Meier R, Zhang G & Ali F (2008) The use of mean instead of smallest interspecific distances exaggerates the size of the 'barcoding gap' and leads to misidentification. *Syst Biol* **57**: 809–813.

Minagawa M & Wada E (1984) Stepwise enrichment of 15N along food chains: further evidence and the relation between δ15N and animal age. *Geochim Cosmochim Ac* **48**: 1135–1140.

Murray J (1895) A summary of the scientific results obtained at the sounding, dredging and trawling stations of the HMS Challenger. *Rep Sci Results Voyage HMS Challenger* **2**: 817–822.

Nakano T & Ozawa T (2007) Worldwide phylogeography of limpets of the order *Patellogastropoda*: molecular, morphological and palaeontological evidence. *J Mollus Stud* **73**: 79–99.

Neef A (1997) Anwendung der *in situ* Einzelzell-Identifizierung von Bakterien zur Populationsanalyse in komplexen mikrobiellen Biozönosen. PhD Thesis, Technische Universität München

Nishida Y, Suzuki K, Kumagai Y, Tanaka H, Inoue A & Ojima T (2007) Isolation and primary structure of a cellulase from the Japanese sea urchin *Strongylocentrotus nudus*. *Biochimie* **89**: 1002–1011.

Nishimoto A, Mito S & Shirayama Y (2009) Organic carbon and nitrogen source of sunken wood communities on continental shelves around Japan inferred from stable isotope ratios. *Deep-Sea Res II* **56**: 1683–1688.

Ohkuma M (2003) Termite symbiotic systems: efficient bio-recycling of lignocellulose. *Appl Microbiol Biot* **61**: 1–9.

Pailleret M, Petit P, Privé-Gill C, Saedlou N, Gaill F & Zbinden M (2007) Sunken woods from the Vanuatu Islands: identification of wood substrates and preliminary description of associated fauna. *Mar Ecol* **28**: 233–241.

Palacios C, Zbinden M, Baco A *et al.* (2006) Microbial ecology of deep-sea sunken wood: quantitative measurements of bacterial biomass and cellulolytic activities. *Cah Biol Mar* **41**: 415–420.

Palacios C, Zbinden M, Pailleret M, Gaill F & Lebaron P (2009) Highly similar prokaryotic communities of sunken wood at shallow and deep-sea sites across the oceans. *Environ Microbiol* **58**: 737–752.

Rau G, Sweeney R & Kaplan I (1982) Plankton $^{13}C/^{12}C$ ration changes in latitude: differences between northern and southern oceans. *Deep-Sea Res A* **29**: 1035–1039.

Samadi S, Quéméré E, Lorion J *et al.* (2007) Molecular phylogeny in mytilids supports the wooden steps to deep-sea vents hypothesis. *C R Biol* **330**: 446–456.

Saraswathy M (1971) Observations on the structure of the shipworms, *Nausitora hedleyi*, *Teredo furcifera* and *Teredora*

pricesae (Bivalvia: Teredinidae). *Trans Roy Soc Edinb* **68**: 508–562.

Sasaki T (1998) Comparative anatomy and phylogeny of the recent *Archaeogastropda* (Mollusca: Gastropoda). *The University of Tokyo, Bull* **38**: 1–223.

Shieh W, Lin Y & Jean W (2004) *Pseudovibrio denitrificans* gen. nov., sp. nov., a marine, facultatively anaerobic, fermentative bacterium capable of denitrification. *Int J Syst Evol Bacteriol* **54**: 2307–2312.

Smant G, Stokkermans J, Yan Y *et al.* (1998) Endogenous cellulases in animals: isolation of β-1,4-endoglucanase genes from two species of plant-parasitic cyst nematodes. *P Natl Acad Sci USA* **95**: 4906–4911.

Smith C (1992) Whale falls. Chemosynthesis on the deep seafloor. *Oceanus* **35**: 74–78.

Smith C & Baco A (2003) The ecology of whale falls at the deep-sea floor. *Oceanogr Mar Biol Annu Rev* **41**: 311–354.

Snaidr J, Amann R, Huber I, Ludwig W & Schleifer KH (1997) Phylogenetic analysis and *in situ* identification of bacteria in activated sludge. *Appl Environ Microb* **63**: 2884–2896.

Suzuki Y, Kojima S, Sasaki T *et al.* (2006) Host–symbiont relationships in hydrothermal vent gastropods of the genus *Alviniconcha* from the southwest Pacific. *Appl Environ Microb* **72**: 1388–1393.

Tamura K, Dudley J, Nei M & Kumar S (2007) MEGA4: Molecular evolutionary genetics analysis (MEGA) software version 4.0. *Mol Biol Evol* **24**: 1596–1599.

Tayasu I (1998) Use of carbon and nitrogen isotope ratios in termite research. *Ecol Res* **13**: 377–387.

Turner R (1973) Wood-boring bivalves, opportunistic species in the deep sea. *Science* **180**: 1377–1379.

Turner R (1977) Woods, mollusks, and deep-sea food chains. *Bull Am Malacol Union* **213**: 13–19.

Warén A, Bengtson S, Goffredi S & Van Dover C (2003) A hot-vent gastropod with iron sulfide dermal sclerites. *Science* **302**: 1007.

Watanabe H & Tokuda G (2001) Animal cellulases. *Cell Mol Life Sci* **58**: 1167–1178.

Watanabe H & Tokuda G (2010) Cellulolytic systems in insects. *Annu Rev Entomol* **55**: 609–632.

Waterbury J, Calloway C & Turner R (1983) A cellulolytic nitrogen-fixing bacterium cultured from the gland of Deshayes in shipworms (Bivalvia: Teredinidae). *Science* **221**: 1401–1403.

Wolff T (1979) Macrofaunal utilization of plant remains in the deep sea. *Sarsia* **64**: 117–136.

Xiao Z, Storms R & Tsang A (2004) Microplate-based filter paper assay to measure total cellulase activity. *Biotechnol Bioeng* **88**: 832–837.

Mar Biol (2015) 162:435–448
DOI 10.1007/s00227-014-2591-7

ORIGINAL PAPER

Epsilonproteobacteria as gill epibionts of the hydrothermal vent gastropod *Cyathermia naticoides* (North East-Pacific Rise)

Magali Zbinden · Lise Marqué · Sylvie Marylène Gaudron · Juliette Ravaux · Nelly Léger · Sébastien Duperron

Received: 22 July 2014 / Accepted: 22 November 2014 / Published online: 11 December 2014

Abstract Mollusks, and particularly gastropods, are one of the major taxonomic groups at vents. In these ecosystems, devoid of light, chemoautotrophic bacteria are at the base of the food web and symbiotic association between metazoa and these bacteria is numerous. Nevertheless, apart few "large-size" well-known species, the "small-size" gastropods (shell <5 mm), although very abundant, remain poorly studied regarding symbioses. We investigated here *Cyathermia naticoides* (Warén and Bouchet in Zool Scr 18(1), 1989), a small coiled gastropod found in abundance on the East Pacific Rise among *Riftia pachyptila* tubes, and usually inferred to graze on tubeworm bacterial cover, and/or filter feeding. Among mollusks, symbioses are well known in large species and almost exclusively rely on sulfide or methane-oxidizing proteobacterial endosymbionts, occurring within the host tissues in gill epithelial bacteriocytes. Combining several approaches (molecular biology, microscopy, stable isotopes analyses), we described here an unusual symbiosis, where autotrophic filamentous Epsilonproteobacteria are located extracellularly, at the base of host gill filaments. Numerous endocytotic lysosome-like structures were observed in the gill epithelium of the animal suggesting bacteria may contribute to its nutrition through intracellular digestion by gill cells. Additional food source by non-symbiotic proteobacteria grazed on *R. pachyptila* tubes could complete the diet. The possible role of temperature in the selection of Epsilon- *vs* Gammaproteobacterial partners is discussed.

Communicated by M.Kühl.

Electronic supplementary material The online version of this article (doi:10.1007/s00227-014-2591-7) contains supplementary material, which is available to authorized users.

M. Zbinden (✉) · L. Marqué · S. M. Gaudron · J. Ravaux · N. Léger · S. Duperron
Sorbonne Universités, UMR7208 MNHN CNRS UPMC IRD Biologie des Organismes Aquatiques et Ecosystèmes, Equipe Adaptation aux Milieux Extrêmes, Université Pierre et Marie Curie Paris 06, 7 Quai St Bernard, 75252 Paris Cedex 05, France
e-mail: magali.zbinden@snv.jussieu.fr

Present Address:
S. M. Gaudron
UMR8187 Laboratoire d'Océanologie et de Géosciences (UL1 CNRS ULCO), Station marine de Wimereux, 28 Avenue Foch, 62930 Wimereux, France

Introduction

To date, about 600 metazoan species have been reported at hydrothermal vents, belonging to 12 phyla. Among those, 150 species of molluska and more than 100 species of Gastropoda have been described (Desbruyères et al. 2006), making them one of the major taxonomic groups at vents. Gastropod feeding habits are extremely diverse, although most species make use of a radula in some aspect of their feeding behavior (see review in Kohn 1983). Grazers can be herbivorous, rasping either micro- or macroalgae, or predators, rasping on encrusting invertebrates such as hydroids, sponges, cnidarians or ascidians. Herbivorous may also swallow sand containing algae. And carnivores may also hunt their prey and use their radula to drill mollusk shells or calcareous echinoids test, or perforate prey soft tissues (polychaetes, fishes, etc.). Some predators have lost the radula and engulf animal prey whole. Various feeding modes, using no radula, are also encountered in gastropods. In filter feeders, hypertrophy of the ctenidium as a ciliary-mucous food collecting device is used as a trap to capture and sort particles suspended in seawater. Other feeding strategies include parasitic species, devoid

of radula, that feed on body fluids thank to a sucker, and establishment of nutritional symbioses. Some herbivorous species can suck algal cell content and establish symbioses with chloroplastes (family Elysiidae) or zooxanthellae (family Aeolidae). Chemoautotrophic symbioses also occur in a wide range of habitats, including cold seeps, whale and wood falls, shallow-water coastal sediments and continental margins (Dubilier et al. 2008).

In the hydrothermal vent environment, chemosynthetic production by bacteria is the main food source of primary consumers (Felbeck and Somero 1982). The majority of hydrothermal gastropods are thus grazers or filter feeders that appear to feed on free-living bacteria (Bates 2007a). Another widespread strategy at vents is symbiotic association with chemoautotrophic bacteria. Up to now, such symbioses have been demonstrated in at least 7 different phyla (Dubilier et al. 2008), including mollusks, the most famous examples being described in gills of bivalves (Bathymodiolinae and Vesicomyidae) and involve sulfur-oxidizing Gammaproteobacteria endosymbionts. But it also exists among gastropods. The best known examples are *Alviniconcha hessleri* and *Ifremeria nautilei*, found in the western Pacific (Windoffer and Giere 1997; Borowski et al. 2002; Suzuki et al. 2005a, b, 2006; Urakawa et al. 2005; Saito and Hashimoto 2010). Most of the examples described for these two species also rely on sulfur-oxidizing Gammaproteobacteria gill endosymbionts. But recently, Epsilonproteobacteria were described as gill endosymbionts in some species of Provannidae (Urakawa et al. 2005; Suzuki et al. 2006, Beinart et al. 2013). Symbioses in smaller gastropod species remain poorly studied, and the presence of bacteria as symbionts has only been documented in *Lepetodrilus fucensis* from the Juan de Fuca Ridge (Bates 2007a), in which a nutritional role has been suggested.

In this study, we investigate a coiled gastropod, the Neomphalina *Cyathermia naticoides* (Warén and Bouchet 1989). Not much is known about it, despite it is a common species, found in abundance among *Riftia pachyptila* clumps (Mills et al. 2007) and in lower abundances among *Alvinella pompejana* and *Bathymodiolus thermophilus* (Warén et al. 2006). Up to now, *C. naticoides* was inferred to graze on tubeworm bacterial cover, but also to use filter feeding, based on its very large bipectinate gill (Warén and Bouchet 1989). A distinct labial notch described by Warén and Bouchet (1989) in the shell morphology is interpreted as an adaptation to allow the gill to be extended outside the shell even when the snail is resting on the substrate, partially retracted into the shell (Warén and Bouchet 1989; Sasaki et al. 2010). Here, we investigate an additional hypothesis as feeding strategy in *C. naticoides*. Our study describes an unusual symbiosis, where epibiotic autotrophic Epsilonproteobacteria are endocytosed within the gill filaments of the animal. The large size of the gill, the recurrent observation of endocytosis and lysis of bacteria, and the stable isotope results advocate for a nutritional symbiosis.

Materials and methods

Animal collection and conditioning

Cyathermia naticoides specimens were collected, among *R. pachyptila* tubes, using the DSV Nautile during the Mescal 2010 cruise (East Pacific Rise, 2,500 m depth), on two different sites: 9°50′N (Bio9 site) and 12°50′N (Genesis site). Once on board, the entire specimens were fixed (operculum removed) in: (1) 2.5 % glutaraldehyde (for light and electron microscopies), (2) ethanol (for DNA extraction), (3) 2–4 % formaldehyde (for fluorescent in situ hybridization, FISH) and (4) liquid nitrogen (for stable isotope analyses and chitinase activity assays).

Light and electron microscopies

Gut and gill tissues of three specimens of *C. naticoides* from 9°50′N were dissected. Two other specimens were embedded whole. Samples were postfixed in osmium tetroxide 1 %, dehydrated in increasing ethanol series (50, 70, 95 and 100 %) and embedded in Epon resin (48 h, 60 °C). Sections were cut using a Reichert–Jung ultramicrotome. Semi-thin (600 nm) sections were stained with toluidine blue and observed with an Olympus BX 61. Thin (60 nm) sections were mounted on copper grids, contrasted using uranyl acetate and observed using a HITACHI H-7100 transmission electron microscope, operated at 80 kV.

Fluorescence in situ hybridization (FISH)

Four specimens from 9°50′N and 2 from 12°50′N were used. Specimens were pulled out of their shells and, after 2–4 h in 4 % formaldehyde, were rinsed and dehydrated in 50, 70 and 96 % ethanol. They were then embedded whole in polyethylene glycol (PEG) distearate: 1-hexadecanol (9:1). Sections of 7–10 µm were cut using a Jung microtome and deposited on Superfrost Plus slides. Wax was removed, and tissue rehydrated in decreasing ethanol series. Sections were hybridized as described in Zbinden et al. (2010), using 30 % formamide for 3 h at 46 °C, rinsed (15 min, 48 °C), covered with SlowFade containing DAPI, and examined under an Olympus BX-61 epifluorescence microscope (Olympus, Japan). Following probes, labeled with Cy-3 and Cy-5, were used: Eub-338 (5′-GCTGCCTCCCGTAGGAGT-3′, Amann et al. 1990), Gam-42 (5′-GCCTTCCCACATCGTTT-3′, Manz et al.

Table 1 Number of sequences representing each identified OTU in each sample investigated in this study

OTU ID	**3**	**1**	**8**	**11**	**5**	**2-p**	**16-p**	**12**	**13**	**4-p**	**15**	Sum
Accession	KM213004	KM213002	KM213007	KM213008	KM213006	KM213003	KM213012	KM213009	KM213010	KM213005	KM213011	
Affiliation	E	E	E	E	E	E	E	D	M	M	B	
9-1-Gi	7	7			1	4				1		30
9-1-VM	3	20	3		1	3				1		32
9-2-Gi	14	7	3	1	5							32
9-2-VM	7	7	3		5			4	1		1	32
9-2-Sh		9	14	2				1			1	31
9-3	15	6	2		1		1	1	2	1		32
12-1-Gi	11											11
12-1-VM			11	7								19
12-2-Gi	5		5	2								17
12-2-VM		2	3	3								13
12-3-Gi	6		2	1			3					17
12-3-VM		1	11	5			1					29
Sum per OTU	68	59	57	21	13	7	5	6	3	3	2	244
Percentage	23.05	20	19.32	7.12	4.41	2.37	1.69	2.03	1.02	1.02	0.68	82.71
Arc-94	+	−	+	+	−	1 mis	+	−	−	−	−	
Epsy-549	+	1 mis	+	+	−	+	+	−	−	−	−	

OTU names in bold correspond to full-length sequences included in the phylogeny, and the suffix '-p' indicates a partial sequence. Affiliation based on best BLAST hits: Epsilonproteobacteria (E), Deltaproteobacteria (D), Mollicutes (M) and Bacteroides (B). Names of samples are indicated by site (9 or 12), specimen ID (1 to 3) and tissue type (Gi-gill, VM-visceral mass, Sh-shell) as follows: site-specimen-tissue. Sum of sequences per OTU and percentage of total sequence counts are indicated. Finally, the two bottom rows indicate whether the OTU has no mismatch (+), a single mismatch (1mis) or more (−) to FISH probes Arc-94 and Epsy-549

Table 2 Analysis of fragments of functional genes encoding APS reductase (aprA) and ATP citrate Lyase (aclB), their length, the identity of the representative sequence, GENBANK accession number, percentage out of 70 (aprA) and 35 sequences (aclB), number of specimens in which the sequence occurred out of 3 (aprA) and 2 (aclB), tissue occurrence (G: gill, R: visceral mass), and best hit according to BLASTX-translated nucleotide sequence analysis

Fragment	Approx length	Clone ID	Accession number	%/total	Specimen occurrence	Tissue occurrence	Best BLAST hit (BlastX)
aprA	365 nt	761	KP115589	40.0	3	R	96 % EU265804 Epibiont of the vent crab *Kiwa hirsuta* (Gammaproteobacteria)
		843	KP115590	24.3	2	R	91 % GU197406 bacterium associated with the oligochete *Tubificoides benedii* (Gammaproteobacteria)
		144	KP115591	10.0	2	R	90 % GU197406 bacterium associated with the oligochete *Tubificoides benedii* (Gammaproteobacteria)
		820	KP115592	18.6	2	R	100 % FM165456 bacterium associated with the tube of *Lamellibrachia anaximandri* (Gammaproteobacteria)
		786	KP115593	4.3	1	R	96 % EF633097 bacterium associated with *Echinocardium cordatum* (Deltaproteobacteria)
		827	KP115594	1.4	1	R	97 % AM234053 *Olavius algarvensis* Delta-4 endosymbiont (Deltaproteobacteria)
aclB	305nt	765	KP115581	54.3	2	G	98 % FN659794 bacterium from branchial chamber of *Rimicaris exoculata* (Epsilonproteobacteria)
		782	KP115582	11.4		G, R	98 % FN908920 bacterium from hydrothermal fluid, Clueless (Epsilonproteobacteria)
		847	KP115583	2.9	1	R	99 % FR670537 bacterium from Lucky Strike (Epsilonproteobacteria)
		766	KP115584	2.9	1	R	98 % FN659786 branchial chamber of *Rimicaris exoculata* (Epsilonproteobacteria)
		805	KP115585	2.9	1	R	98 % FN908920 bacterium from hydrothermal fluid, Clueless (Epsilonproteobacteria)
		808	KP115586	17.1		R, G	99 % FN562694 bacterium from the Irina II vent, Logatchev (Epsilonproteobacteria)
		840	KP115587	2.9	1	R	99 % FN908925 Bacterium from the Logatchev vent field (Epsilonproteobacteria)
		163	KP115588	5.8	1	R	97 % FN562694 bacterium from the Irina II vent, Logatchev (Epsilonproteobacteria)

1992), Del-495a (5′-AGTTAGCCGGTGCTTST-3′, Loy et al. 2002), Epsy-549 (5′-CAGTGATTCCGAGTAACG-3′, Manz et al. 1992) and Arc-94 (5′-TGCGCCACTTAGCTGACA-3′, Moreno et al. 2003). Phylotypes targeted by the different probes are indicated in Table 1.

DNA extraction and 16S rRNA amplification

DNA was extracted from three specimens from 9°50′N and three from 12°50′N. Specimens were dissected as follows: At 9°50′N, gill was extracted from two of the specimens

(9-1-Gi and 9-2-Gi), while the visceral mass (i.e., the rest of the animal containing the digestive tract and the heart, gonad, digestive gland, liver and excretory organs) was treated separately (9-1-VM and 9-2-VM). A third specimen (9-3) was treated as a whole. DNA was also extracted from the empty shell of specimen 2 (9-2-Sh). At 12°50′ N, DNA was extracted separately from the gill and visceral mass of three specimens (12-1, 12-2, 12-3). Extractions were performed using the DNA Tissue Kit (Qiagen). A 1500-bp fragment of the 16S rRNA-encoding gene was amplified by PCR using primers 27F and 1492R, over 32 cycles. Three PCR products were pooled together for each sample, to reduce PCR bias. Fragments were cloned using a TOPO TA Kit (Invitrogen, CA). About 11–32 clones were successfully sequenced from each sample by GATC Biotech (Table 1).

Genes encoding for key enzymes of sulfur oxidation (*aprA*) and autotrophic carbon fixation (*aclB*) were sought. Fragments of the *aprA* gene encoding APS (adenosine 5′-phosphosulfate) reductase and the *aclB* gene encoding ATP Citrate Lyase (the key enzyme in reverse tricarboxylic acid (rTCA) cycle) were amplified using primer sets aps1F/aps4R and 892F/1204R, respectively, as described previously and using 32–35 PCR cycles (Campbell et al. 2003; Meyer and Kuever 2007). Obtained PCR products were cloned, and inserts were sequenced (Table 2).

Gene sequence analyses

Chromatograms were checked for quality. For each sample, sequences were aligned and grouped in Operational Taxonomic Units (OTUs) when >97 % of the nucleotide positions were identical. For the 16S rRNA-encoding genes, overall 11 OTUs were present in more than a single sample. Sequences were compared with databases using BLAST (Altschul et al. 1990; Cole et al. 2009), and the 8 OTUs for which full sequences were available were included in a dataset with their best hits and reference sequences and aligned using SINA Web Aligner (Pruesse et al. 2007). Alignment was manually checked, and phylogenetic relationships were inferred by using the maximum-likelihood (ML) method. For the reconstruction, a general time-reversible model, with a Gamma distribution of evolutionary rates among sites, was used (five categories and invariant sites). For *aprA* and *aclB* genes, recovered sequences were compared to the database using BlastX (Table 2). For *aclB*, best hits and representative sequences were included in a dataset, and phylogenetic reconstruction was based on a 100-aa-long fragment using a ML approach, a JTT model of amino acid substitution and a Gamma distribution of evolutionary rates among sites (tree in Fig. S1). All analyses were conducted using MEGA6 (Tamura et al. 2013).

Stable isotope analysis

Frozen *C. naticoides* ($n = 4$ for $\delta^{13}C$ and $\delta^{15}N$, $n = 10$ for $\delta^{34}S$ for 9°50′N and $n = 5$, only $\delta^{13}C$ and $\delta^{15}N$, for 12°50′N) were dissected under a dissecting microscope to remove the shell. Specimen tissues were rinsed in distilled water, dried (3 days, 60 °C) and then reduced into powder. To avoid significant changes in $\delta^{15}N$ isotopic composition, no HCl was used to remove carbonates (Kaehler and Pakhomov 2001). About 1 mg (± 0.1 mg) of dried tissues (except 8 mg for sulfur stable isotopes; pool of 10 specimens) were analyzed by a GV IsoPrime (UK) stable isotope mass spectrometer (Iso-Analytical, Crewe, UK). Values of $\delta^{13}C$, $\delta^{15}N$ and $\delta^{34}S$ were determined and expressed as relative per mil (‰) differences between samples and Pee Dee Belemnite (PDB) for carbon, air N_2 for nitrogen and Canyon Diablo Troilite for sulfur according to the following equation:

$$\delta(X) = \left[\left(\frac{R_{\text{sample}}}{R_{\text{standard}}}\right) - 1\right] * 1000$$

where X (‰) is ^{13}C, ^{15}N or ^{34}S abundance and R is the $^{13}C/^{12}C$, $^{15}N/^{14}N$ or $^{34}S/^{32}S$ ratios.

Chitinolytic activity assays

Chitinolytic activity was determined using a modification by Gutowska et al. (2004) of the standard procedure of Jeuniaux (1966), which measures the production of *N*-Acetyl glucosamine (NAG). Five specimens from 12°50′N were removed from their shell and ground together in liquid nitrogen. The powder was homogenized in 0.15 M citric acid and 0.3 M Na_2HPO_4 buffer (pH = 5 and pH = 7). The homogenates were then centrifuged at 2,000 g for 10 min at 4 °C, and the supernatants were recovered and assayed for their chitinolytic activity. The standard mixture consisted of 2 vol of tissues extract, 1 vol of chitobiase and 1 vol of chitin suspension (5 mg ml^{-1}). Two control assays were added, with either the tissues extract or the chitin solution replaced by distilled water. For comparison, assays with commercial *Streptomyces griseus* chitinase (Sigma C6137) were also conducted in parallel. They were all incubated at 37 °C, and aliquots were taken after $t = 0$ min, $t = 90$ min and $t = 180$ min. Chitinolytic reaction was stopped by mixing 1 vol of the reaction medium with 1 vol of boiling water. The mix was placed 10 min at 100° C, then centrifuged at 2,000 g for 10 min. The supernatants were used for NAG measurements by adding $K_2B_4O_7$ 0.8 M, and further incubating for 3 min at 100 °C. *p*-dimethylaminobenzaldehyde (DMAB) was added, and after 20 min at 37 °C, the concentration of NAG released was determined by comparing each sample's absorbance at 585 nm to NAG standard curves. The activity was expressed as µg of NAG released per gram protein per hour.

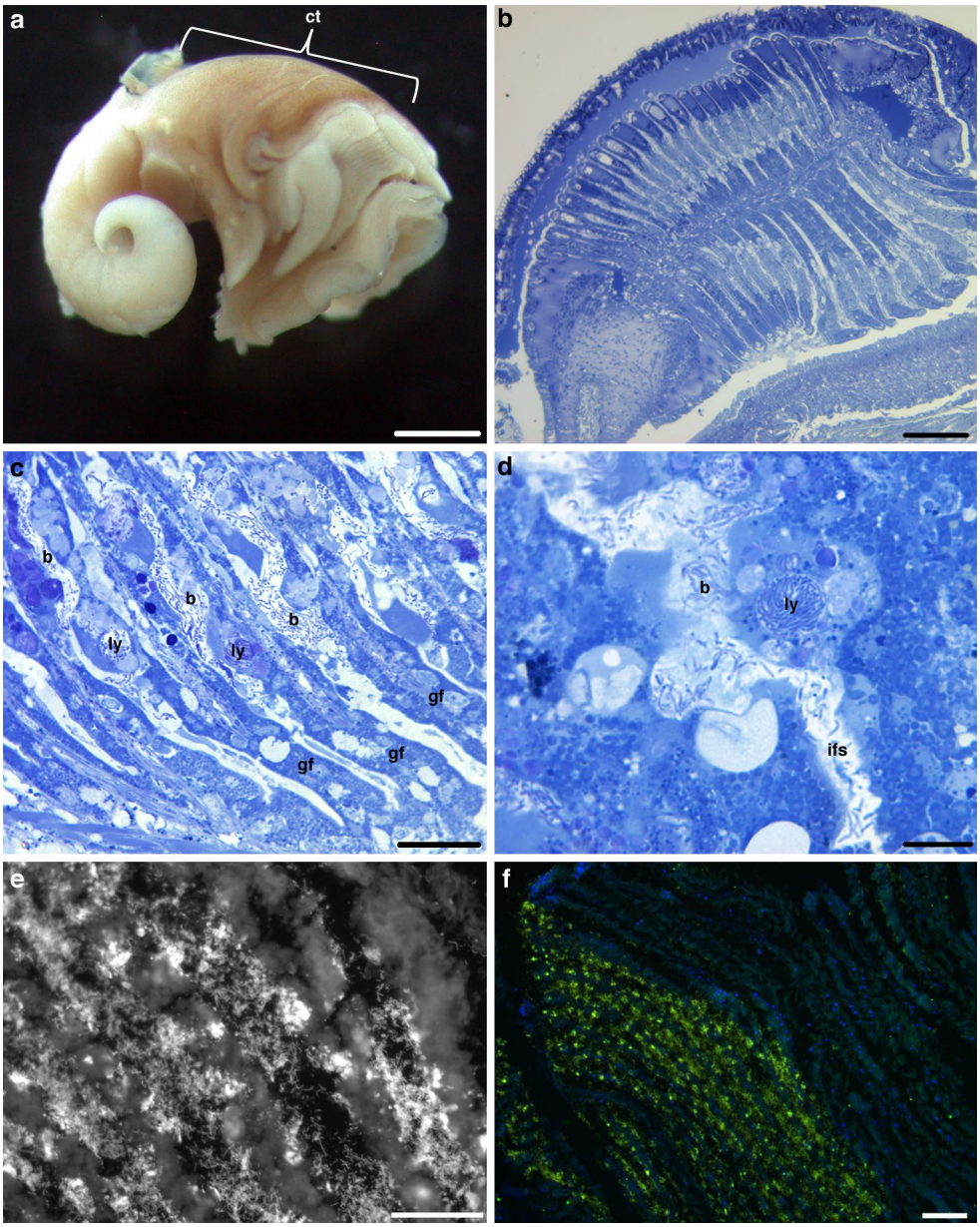

Fig. 1 *Cyathermia naticoides* ctenidium. **a** Specimen outside its shell showing the extension of the ctenidium (*ct*). **b** Semi-thin section of the ctenidium. **c** Basal part of the gill filaments showing the accumulation of bacteria (*b*) between the gill filaments (*gf*) and in lysosome-like structure (*ly*). **d** Close-up of bacteria in the inter-filament space (*ifs*) and in lysosome-like structure (*ly*). **e** Transverse section through the gill, displaying bacterial filaments in white, hybridized with the FISH probe Arc-94. **f** Transverse section through the gill displaying animal cells (DAPI-labeled nuclei in *blue*) and bacteria labeled with probes Eub-338 (Cy3, *red*) and Arc-94 (Cy5, *green*), overlaying signals resulting in a yellow color. *Scale bars* **a** = 1 mm, **b** = 100 µm, **c** = 20 µm, **d** = 10 µm, **e** = 50 µm, **f** = 100 µm

Results

Morphology and ultrastructure of gut and gill

Cyathermia naticoides is a gastropod with a regularly coiled shell (diameter up to 7 mm), with a deep notch at basal side of the outer lip. This gastropod possesses a very large bipectinate gill, which occupies most of the anterior part of the animal (Fig. 1a, b). Semi-thin sections revealed an abundant bacterial community associated with the gill (Fig. 1c, d). These gram-negative filamentous bacteria (0.5–0.6 µm in diameter and up to 5.8 µm in length, Fig. 2a, b) were located extracellularly, between the gill filaments, mainly at their base. Some of the bacteria were free in the inter-lamellar space, but many have also been observed trapped in lysosome-like structures in the gill epithelium

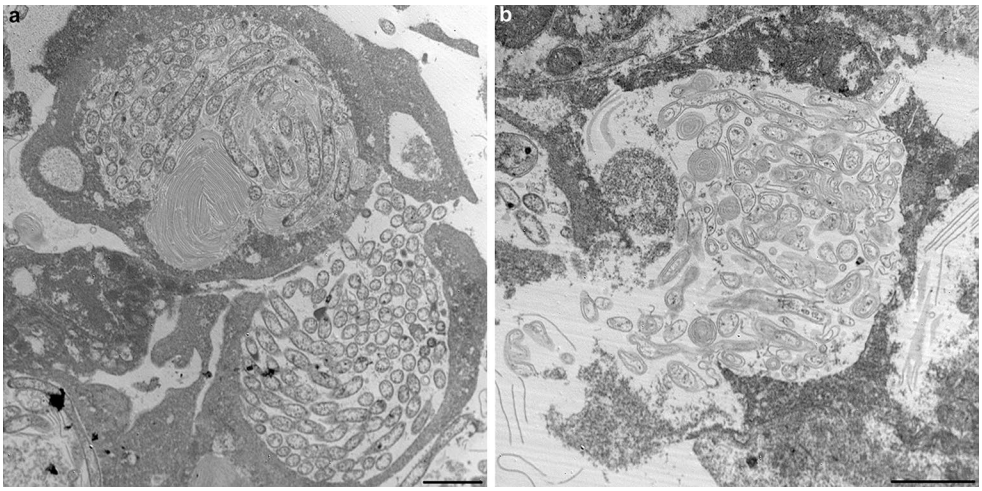

Fig. 2 Transmission electron micrographs of the gill (**a**, **b**) of *C. naticoides*. **a** Bacteria are endocyted in the gill epithelium and **b** progressively degraded. *Scale bars* **a**, **b** = 2.5 µm

(see Figs. 1d and 2a) and appeared to undergo different stages of degradation (Fig. 2b). Bacterial colonization and endocytosis occurred on each animal and all sections observed.

The digestive tract contained pieces of *R. pachyptila* tubes (not shown), recognizable by chitin microfibrils organized in parallel bundles with various orientations (Gaill and Shillito 1995). No bacteria similar to those present on the gill were observed in the gut contents.

Fluorescence microscopy observations

Probes Eub-338 and Arc-94 yielded strong signals in regions of the gill filaments of *C. naticoides* from both 9°50′N and 12°50′N (Fig. 1e, f). Cy-3-labeled probe Epsy-549 yielded weaker signal, but signal-to-noise ratio was greatly improved when letting tissue autofluorescence decrease under the laser for 30 s. Signals from the three probes fully overlapped in gills (not shown). Hybridized objects corresponded to thin filamentous bacteria. Parts of the gill filaments were free of bacteria and did not display any signal, suggesting that the distribution of bacteria was not homogeneous (Fig. 1f). Probes Gam-42 and Del-495a did not display any signal in the gills. No FISH signal was observed from the gut epithelium or content.

Chitinolytic activity

Chitinase activity was assayed on crude extracts from whole specimens. The measured activity (20 µg NAG released g^{-1} protein h^{-1}) was very weak when compared to the reference sample (*Streptomyces griseus* chitinase, 6,500 µg NAG released g^{-1} protein h^{-1}). Another gastropod (*L. elevatus*) found on *R. pachyptila* tubes was also analyzed for comparison and showed a twofold higher activity (42 µg NAG released g^{-1} protein h^{-1}), which was still very weak when compared to *S. griseus*.

Bacterial communities associated with digestive tract and gill

Out of 295 sequences obtained, 244 (83 %) belonged to one of the 11 OTUs (defined as groups of sequences displaying above 97 % identical positions) that were present in more than a single sample (see Table 1). The remaining sequences corresponded to single reads occurring in a single sample. Above 78.0 % of total sequences and seven of the 11 OTUs (94.3 % of the OTUs-assigned sequences) were assigned to the Epsilonproteobacteria. Five of the OTUs (1, 3, 8, 11, 16-p), including the 4 most abundant and representing 90 % of the OTU-assigned sequences, were present at both sampling sites 9°50′N and 12°50′N.

OTUs 3, 1 and 8 dominated clone libraries, representing 23.1, 20.0 and 19.3 % of the total sequences, respectively (Table 1). OTU 3 was present in gills and visceral mass at 9°50′N and gill at 12°50′N. This sequence displayed above 98 % identity and was most closely related to sequences from an epibiont of the gastropod *L. fucensis*, and to various *Arcobacter* from the EPR (Fig. 3). OTU 1 was present in all samples from 9°50′N and in visceral mass samples from two specimens at 12°50′N. The sequence was closely related and highly similar (>98 %) to sequences from bacteria associated with the tube of *Ridgeia piscesae* on the EPR. The third, OTU 8, was present in gill, visceral mass and shell at all sites and displayed above 98 % identity with several sequences related to the sulfur-oxidizing chemolithotroph *Sulfurovum* from the Brothers Seamount (Kermadec Arc) and vents.

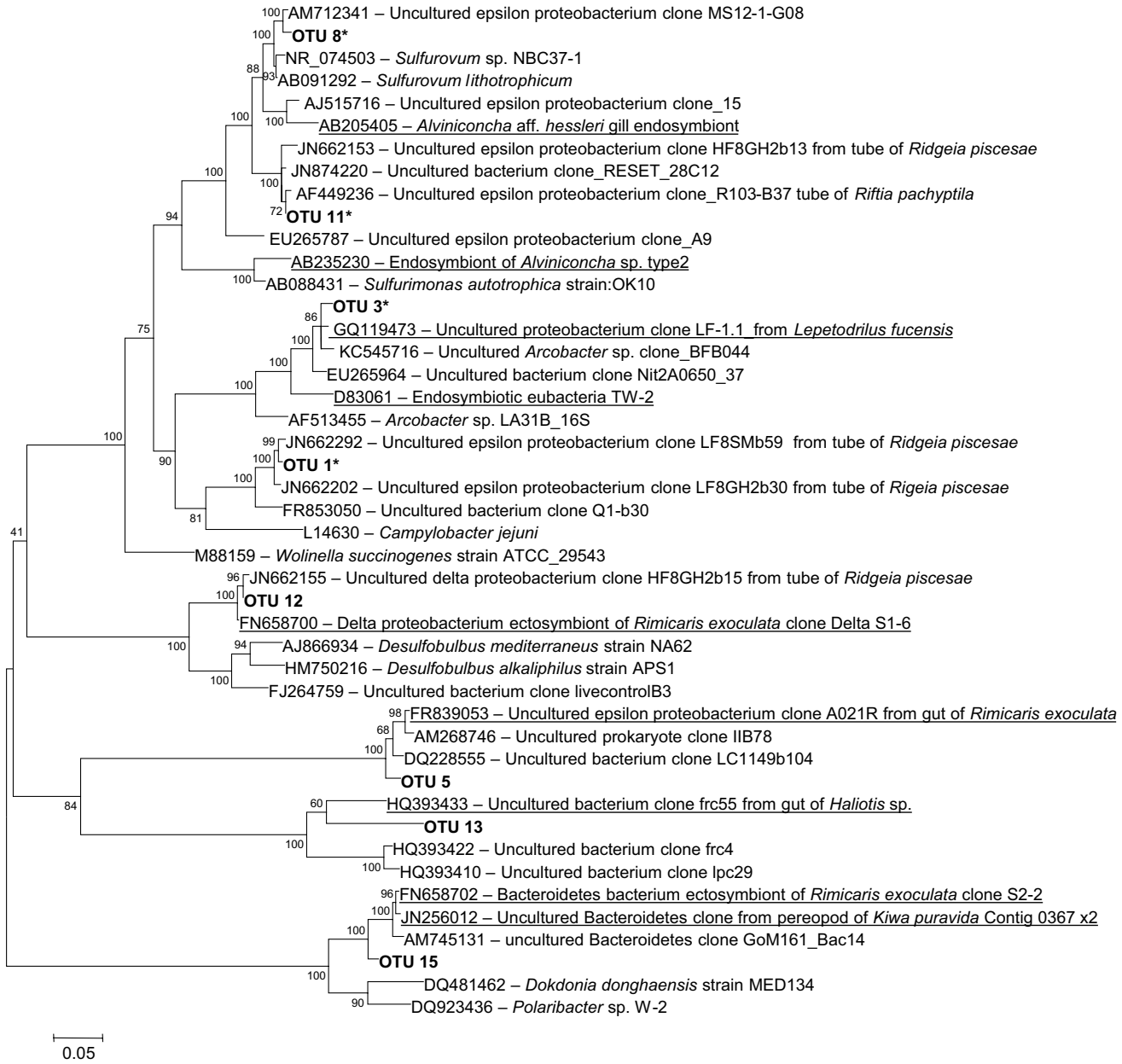

Fig. 3 Phylogenetic tree based on the analysis of 16S rRNA-encoding gene sequences. The tree with the highest log likelihood (-13800) is shown. The percentage of trees in which the associated taxa clustered together is shown next to the branches. *Scale bar* represents the number of substitutions per site. Full (>1,400 bp) sequences from this study appear in *bold,* and an *asterisk* indicates an OTU that is present at both 9°50'N and 12°50'N. Sequences corresponding to confirmed metazoan symbionts or epibionts are underlined. All positions with less than 95 % site coverage were eliminated. There were a total of 1,302 positions in the final dataset, and partial sequences were excluded

Functional gene analysis

Overall, 70 *aprA* sequences were obtained from the visceral mass of three specimens, and none from the gill tissue. Six distinct nucleotide sequences were obtained, 4 of which were related to Gammaproteobacteria and represented above 94 % of total sequences (Table 2). The dominant sequence, clone 761, was 96 % similar (amino acids) to a sequence from an epibiont of the Yeti crab *Kiwa hirsuta*. Other sequences were similar to a sequence from a bacterium associated with the oligochete *Tubificoides benedii* and from the tube of the siboglinid annelid *Lamellibrachia anaximandri* (Table 2).

PCRs on the *aclB* gene yielded faint bands from the visceral mass of specimen 9-1 and 9-2 and from the gills of specimen 9-2. Out of 28 sequenced clones from each

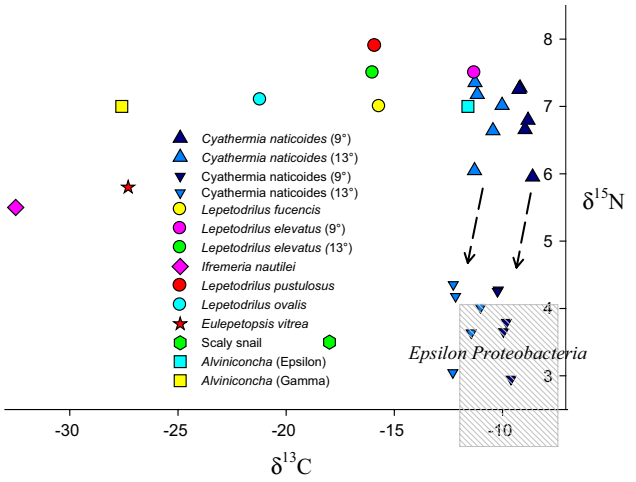

Fig. 4 $\delta^{13}C$ and $\delta^{15}N$ values of *C. naticoides* and other heterotrophic and symbiotic vent gastropods. *Triangle up* are isotopic ratios of *C. naticoides*, with *dark blue symbols*, those sampled at EPR 9°50'N (9°), and *light blue symbols*, those sampled at EPR 12°50′N (13°). *Triangle down* displayed previous isotopic values, respectively, after correction using trophic step fraction of 1.0 ‰ for $\delta^{13}C$ and 3.3 ‰ for $\delta^{15}N$. The *rectangle with dashed lines* represents the stable isotopes ratios of ε-proteobacteria from Campbell et al. (2003). $\delta^{13}C$ and $\delta^{15}N$ values of other gastropods are from: Levesque et al. (2006) for *L. fucencis*; Gaudron et al. (in revision) for *L. elevatus* (9° and 13°), *L. pustulosus*, *L. ovalis* and *Eulepetopsis vitrea*; Henry et al. (2008) for *I. nautilei*; Goffredi et al. (2004) for the Scaly snail; Beinart et al. (2013) for $\delta^{13}C$ for *A. hessleri* dominated by ε-proteobacteria [*Alviniconcha* (Epsilon)] and for *A. hessleri* dominated by γ-proteobacteria [*Alviniconcha* (Gamma)]. $\delta^{15}N$ of *A. hessleri* is not documented, except for *Alviniconcha* sp. from Henry et al. (2008), which was used in this study

of these 3 samples, only 35 good quality sequences were obtained. The majority (24) were from the gill, of which 19 corresponded to a single sequence, clone 765, and were related to various sequences of Epsilonproteobacteria from hydrothermal vents and to epibionts from the gill chamber of the vent shrimp *Rimicaris exoculata* (around 98 % amino acid similarity, Table 2 and Fig S1).

Stable isotope composition

The $\delta^{13}C$ values of *C. naticoides* varied following vent sites, with −9.0 ‰ (±0.3 ‰) for 9°50′N and −0.8 ‰ (±0.4 ‰) for 12°50′N (Fig. 4). These stable isotopic ratios of carbon fall after correction of fractionation (1 ‰ for $\delta^{13}C$ and 3.3 ‰ for $\delta^{15}N$) into the range of stable isotopic ratios of carbon of Epsilonproteobacteria (range between −8 and −12 ‰; Campbell et al. 2003; Fig. 4). Regarding $\delta^{15}N$, value of both sites was 6.8 ‰ (±0.5 ‰). This nitrogen stable isotopic ratio is typical of a primary consumer at vents (between 4 and 8 ‰). Isotopic signatures of $\delta^{34}S$ measured in a pool of *C. naticoides* ($n = 10$) was 5.5 ‰.

Discussion

Grazing vs. filter feeding

Gastropods have two main feeding strategies, i.e., grazing, using their radula to rasp various kinds of substrates, or filter feeding, using their gills as a trap to capture and sort particles suspended in seawater. At hydrothermal vents, where the organic matter synthesis relies on chemoautotrophic bacteria, most gastropods appear to feed on free-living bacteria (Bates 2007b). Up to now, *C. naticoides* was inferred to graze on tubeworm bacterial cover, but also to use filter feeding, based on its very large bipectinate gill (Warén and Bouchet 1989). Grazing on tubeworm bacterial cover is congruent with our observations, as we noted the occurrence of *R. pachyptila* tube pieces in the gut content. Conversely, filter feeding on bacteria is not well supported by our data. The position of the filamentous bacteria, deep between the filaments, and the large number of endocytosed and lysed bacteria advocates for a stronger association than a classic trapping through filter-feeding mechanism for transport to the gut. Nevertheless, filter feeding on particulate organic matter cannot be discarded.

A diet based on bacteria

Despite that *R. pachyptila* tube pieces, which contain up to 25 % of chitin (Ravaux et al. 1998), are rasped and ingested by *C. naticoides*, a weak chitinolytic activity was measured for this species, when compared to the reference chitinase of *Streptomyces griseus*, or to values obtained for chitin-degrading animals, such as fishes feeding on crustaceans (Gutowska et al. 2004). This suggests a minor nutritional input of chitin and that *C. naticoides* rather grazes on *R. pachyptila* tubes for feeding either on proteins contained therein (representing 37–41 % of the tube, Ravaux et al. 1998) or on the bacterial biofilm. López-García et al. (2002) observed dense microbial populations on *R. pachyptila* tubes, with very diverse 16S rRNA phylotypes, belonging mostly to Epsilon-, but also to Delta-, Alpha- and Gammaproteobacteria. Interestingly, among our recovered bacterial phylotypes, OTUs 1 and 11 are closely related to several sequences from the tubes of *R. piscesae* and *R. pachyptila* (Fig. 3; Forget and Juniper 2013; López-García et al. 2002). These could be bacteria ingested alongside with tube fragments. Indeed, of the 59 sequences of OTU 1, for example, 36 were from the visceral mass of *C. naticoides* (3.4–63 % of the sequences depending on the sample). This sequence displays 5 and 1 mismatches with FISH probes Arc94 and Epsy549 and thus does not hybridize with them. It is thus surely not the sequence from the bacteria located in the gills, which respond to both probes. Sequences encoding APS reductase were successfully

amplified from the visceral mass of all tested specimens. Related sequences were typically associated with the tube or cuticle of protostomes. These might again correspond to sequences of bacteria ingested with scrapings of tubes. The dense colonies of filamentous Epsilonproteobacteria observed on *C. naticoides* gill surface could be another nutritional pathway. Many are indeed endocytosed within lysosomes, arguing for an internal digestion of bacteria in the gill epithelium.

Vent gastropods at hydrothermal vents are considered as primary consumers feeding both on free-living bacteria of different origins but also on particulate organic matter (Limén et al. 2007), resulting in a range of stable isotope nitrogen ratio between 4 and 8 ‰ (Bergquist et al. 2007; Limén et al. 2007; Gaudron et al. 2012), which includes our values for *C. naticoides*. Several species of *Lepetodrilus* are known to be also primary consumers (heterotrophic) such as *L. elevatus*, *L. pustulosus* and *L. ovalis*, displaying the same range of stable isotopic nitrogen values (Fig. 4). However, *L. fucencis* known to harbor symbiotic bacteria within its gills also has a similar stable isotopic nitrogen value (7 ‰, Bates et al. 2011), as well as other larger symbiotic gastropods (*Alviniconcha* spp) harboring Epsilonproteobacteria (Fig. 4), meaning that heterotrophic and symbiotic diet may co-occur in *C. naticoides* and cannot be easily distinguished based on nitrogen isotopes.

In the previously studied symbioses involving Epsilonproteobacteria, a trophic role has been suggested based on carbon stable isotope signatures of hosts ($\delta^{13}C$ values between −11 and −10.7 ‰ for *A.* aff *hessleri*; −12.8 and −11.2 ‰ for *A. pompejana* and −12 to −10 ‰ for *R. exoculata*, Suzuki et al. 2005b; Desbruyères et al. 1998; Polz et al. 1998). These values indeed fall within the range of typical values measured in Epsilonproteobacteria which use the reverse TCA cycle for autotrophic carbon fixation (−12 to −8 ‰, Campbell et al. 2006; Sievert and Vetriani 2012). Similar values are measured in *C. naticoides* (−10.84 ± 0.58 ‰; Fig. 4), suggesting that similar bacteria may significantly contribute to the host diet, either those grazed on tubes or those endocyted in the gill. López-García et al. (2002) identified that most bacteria (68 %) present on *R. pachyptila* tube surface belonged to the Epsilonproteobacteria ($\delta^{13}C$ value for scrappings from *R. pachyptila* tubes is -12.5 ‰). In *Cyathermia*, this is further supported by the identification of ATP Citrate Lyase-encoding genes from the visceral mass of specimens, which confirm the presence of rTCA. On the other hand, a single dominant ATP Citrate Lyase sequence is also identified from gill-associated bacteria, which supports the hypothesis of a significant contribution of the gill bacteria to the host carbon nutrition. The next step will be to quantify the respective roles of gill-associated versus ingested bacteria.

The vast majority of symbiotic bacteria described at present in mollusks are chemoautotrophic sulfur-oxidizing bacteria. The $\delta^{34}S$ value of an animal indicates the origin of the assimilated sulfur. Marine invertebrates for which the sulfur source comes from chemosynthetic sulfur oxidation have values lower than 5 ‰. $\delta^{34}S$ of *C. naticoides* (5 ‰) is at the upper end normally measured into thiotrophic metazoans, which is between −25 and 5 ‰ (Vetter and Fry 1998), allowing to suppose that some sulfur absorbed by the animal comes from chemosynthetic sulfur oxidizers. If evidence for thiotrophic metabolism has been shown through sequencing of APS reductase in the visceral mass (possibly coming from the bacteria in the gut, rasped on *R. pachyptila* tubes), no positive PCR result was obtained from gills. We cannot thus confirm the thiotrophic metabolism of gill-associated bacteria.

Symbiosis

A widespread feeding strategy at hydrothermal vents is to obtain organic carbon through symbiotic associations. Among mollusks, symbioses are well known and described in large species, such as the mussels and clams (Mytilidae and Vesicomyidea, Dubilier et al. 2008) or the large gastropods *I. nautilei* and *A. hessleri* (Provannidae, Borowski et al. 2002; Suzuki et al. 2005a, b). In all these symbioses, sulfide-oxidizing Gammaproteobacterial symbionts are endosymbionts, occurring within the host tissues in gill epithelial bacteriocytes. The hosts are fueled by by-products of bacterial metabolism (ultimately relying on sulfide oxidation) or intracellular bacterial digestion (Bates 2007b).

Here, we described the occurrence of a dense population of filamentous bacterial located extracellularly at the base of the gill filaments. Some are free in the inter-lamellar space, but many have also been observed trapped in lysosome-like structures, in the gill epithelium. At hydrothermal vents, epibiotic symbioses have been described in only a few groups: Ciliophora (Kouris et al. 2007), annelids (*A. pompejana*, Haddad et al. 1995; Cary et al. 1997; Bright and Giere 2005) and crustaceans (*R. exoculata* (Segonzac et al. 1993; Zbinden et al. 2008; Petersen et al. 2010), the galatheid crabs *Kiwa hirsuta* (Macpherson et al. 2005; Goffredi et al. 2008), *Kiwa puravida* (Thurber et al. 2011) and *Shinkaia crosnieri* (Miyake et al. 2007). In Mollusks, only very few examples are known: in Aplacophora (Katz et al. 2006) and in Gastropoda (*L. fucensis*, Bates 2007a, b). The kind of symbiosis described in *L. fucensis* is the closest to what we observed in *C. naticoides*, with a few exceptions. *L. fucensis* hosts dense colonies of filamentous bacteria on its gill surface, where bacteria are found partially embedded in the host's gill epithelium and extend into the fluid circulating between the lamellae (de Burgh and Singla 1984; Bates 2007a, b). Frequent

endocytosis was observed in the epithelium (de Burgh and Singla 1984). Observed residual bodies of lysosome-like organelles, with concentric membrane stacks, mirror our observations. The main difference between *L. fucensis* and *C. naticoides* is that most abundant *L. fucensis* epibionts are Gammaproteobacteria (Bates et al. 2011) and those of *C. naticoides* belong to Epsilonproteobacteria. Furthermore, stables isotope analyses ($\delta^{13}C = -19.5$ to -14.8 ‰ and $\delta^{15}N = 2.5$ to 5 ‰) situate *L. fucensis* within a group of known deposit feeding invertebrates at the Juan de Fuca Ridge vents (Fox et al. 2002), whereas *Cyathermia* values fall within the range of typical values measured in Epsilonproteobacteria and in organisms living in symbiosis with these bacteria (−12 to −8 ‰, Campbell et al. 2006; Sievert and Vetriani 2012).

As suggested by de Burgh and Singla (1984) and Bates (2007a), there are three ways in which the gill bacteria may contribute to the organic carbon of the host: (1) The bacteria may be farmed and ingested; (2) dissolved organic molecules, by-product of the bacterial metabolism, may pass from the bacteria to the host through the epithelium, as it was suggested for *A. pompejana* and evidenced for the shrimp *R. exoculata* and its epibionts (Ponsard et al. 2013); (3) bacteria may be endocytosed in the gill epithelium and digested within lysosomes.

For *L. fucensis*, Bates (2007b) argues that endocytosis of bacteria by the gill epithelium followed by lysosomal digestion (de Burgh and Singla 1984) may not be an important feeding mechanism. In our case, the huge number of lysosome-like structures observed, with bacteria at different stages of degradation conversely rather advocates for the third hypothesis. Nevertheless, additional contribution by the two other ways cannot be discarded.

These gill bacteria likely correspond to our OTU 3, which is the predominantly associated with gill samples. Indeed, 43 of the 68 sequences were from gill samples, representing between 22 and 100 % of sequences in the various gill samples. Besides, OTU 3 was present in gills of all specimens at both sites, and far less abundant in visceral mass samples, representing only from 0 to 22 % of the sequences. Furthermore, it responds to both Arc-94 and Epsy-549 probes, as do gill bacteria observed using FISH. Finally, it is closely related to one of the documented gill epibionts of *L. fucensis*. OTU 3 might be a widespread epibiont of gastropod gills.

The third most abundant OTU identified in our clone libraries, namely OTU 8, related to *Sulfurovum* also responds to both FISH probes. However, only 10 of the 57 recovered sequences were from gill tissue, representing 0–29 % of sequences depending on gill sample, while 14 were found on the shell analyzed (45 %) and 33 in the visceral mass. Closest relatives do not include any reported symbiont. This bacterium is thus most probably an environmental bacterium, although this cannot be ascertained using FISH probes from this study.

As seen above, the large majority of the mollusk-associated symbionts from chemosynthetic environments are Gammaproteobacteria (in the Thyasiridae, Lucinidae, Solemyidae, Vesicomyidae, Mytilidae and some Provannidae). But recently (Suzuki et al. 2005a, b), Epsilonproteobacteria were described as symbionts (and as endosymbionts) in some species of Provannidae (*Alviniconcha* sp.). *A. hessleri* from the Mariana Trough, *Alviniconcha* sp. type 1 from Manus Basin and Fiji, and *Alviniconcha* sp. from Lau Basin harbor sulfur-oxidizing chemoautotrophic Gammaproteobacterial endosymbionts that mediate the Calvin-Benson cycle to fix CO_2, whereas *Alviniconcha aff. hessleri* from the Central Indian Ridge and *Alviniconcha* sp. type 2 from Manus Basin and Fiji harbor chemoautotrophic Epsilonproteobacterial endosymbionts that mediate the reductive tricarboxylic acid (rTCA) cycle for CO_2 fixation (Urakawa et al. 2005; Suzuki et al. 2006). A fragment of the gene encoding ATP Citrate Lyase was identified in the gill and visceral mass of *C. naticoides*. In particular, the most abundant sequence in the gills was related to sequences from various vent bacteria including gill epibionts of the vent shrimp *R. exoculata*. This advocates for the presence of this pathway in gills of *C. naticoides*. This finding is congruent with the dominance of Epsilonproteobacteria in the gill, and it is possible that the dominant *aclB* sequence (clone 765) is indeed associated with the dominant 16S rRNA OTU 3, or one of the other dominant gill-associated phylotypes.

Symbiotic association with filamentous Epsilonproteobacteria has been described, but mostly as ectosymbioses, as in the crustaceans *R. exoculata*, *K. hirsuta*, *K. puravida* or *S. crosnieri* and in the annelid *A. pompejana* (see references above). The *C. naticoides* symbiosis described here thus represents an unusual type of association in the long list of symbiosis within Mollusks, with Epsilonproteobacteria as ectosymbionts being the first example of this combination in mollusks, to our knowledge.

Epsilon- versus Gammaproteobacteria: an issue with temperature?

Urakawa et al. (2005) suggest that thermal gradient may affect the acquisition and evolutionary selection of either Epsilon- or Gammaproteobacterial symbionts. Vent hosts harboring Epsilonproteobacterial symbionts such as shrimps or polychetes usually live at higher temperatures than those harboring Gammaproteobacteria, such as clams or vestimentiferans. Indeed, the two Provannidae gastropods, *Alviniconcha* spp. and *I. nautilei*, studied by Urakawa, co-occur at the same sites in the Manus Basin, the former harboring Epsilonproteobacterial symbionts living at higher temperatures than *I. nautilei,* which harbors Gammaproteobacteria.

This could be congruent with our example, as *C. naticoides* that lives on tubes of *R. pachyptila* may in fact live in a warmer microhabitat that the tubeworm itself and its Gammaproteobacterial endosymbionts, the latter being protected by the chitinous tube. *C. naticoides* lives in sympatry with another small gastropod, *L. elevatus* on the tube of *R. pachyptila*, where a vertical microzonation has been observed. Individuals of *C. naticoides* cluster at the base of the tubes, where temperatures up to 25 °C were measured (Sarradin et al. 1998), whereas *L. elevatus* rather graze higher up the tubes (P. Tyler, pers. obs. cited in Mills et al. 2007), where temperatures ranged between 1.6 and 10 °C (Sarradin et al. 1998). So *C. naticoides* is associated with the warmer part of *R. pachyptila* tube and is also sometimes found among *A. pompejana* tubes (Desbruyères et al. 2006; Mills et al. 2007), which live on the chimney walls at even higher temperatures (up to 50 °C was measured at 2–5 cm within the tube assemblages, Le Bris et al. 2005). Temperature can also be put forward to explain the different bacterial partners in *C. naticoides* (Epsilonproteobacteria) et *L. fucensis* (Gammaproteobacteria) ectosymbioses. Indeed, *L. fucensis* was reported (Bates et al. 2005) to be abundant in fluids with temperature between 4 and 10 °C and to be absent where maximum fluid temperature reached 18 °C. Although precise temperatures have not been reported in the literature, *C. naticoides* is probably exposed to temperatures exceeding 20 °C in the habitats it occupies (base of *R. pachyptila* tubes or *A. pompejana* clumps).

This selection of either Epsilon- or Gammaproteobacterial symbionts, which seem to be affected by temperature, could also be linked to oxygen availability (both being negatively correlated). Sulfur metabolism pathways are indeed not the same in Epsilon- and Gammaproteobacteria. Both of the pathways used by deep-sea hydrothermal Gammaproteobacteria (the reverse sulfate reduction and the Sox multienzyme system) require O_2 as a terminal electron acceptor in most cases. This indicates that a relatively O_2-depleted environment is less suitable for their growth (Yamamoto and Takai, 2011). Thus, it is predicted that the metabolically habitable niches for deep-sea chemoautotrophic Gammaproteobacteria strictly require co-existence of reduced sulfur compounds and O_2. Besides oxygen, some Epsilonproteobacteria are also able to use sulfur compounds as electron acceptors (Yamamoto and Takai, 2011), which may allow them to tolerate and colonize O_2-depleted and warmer niches within the mixing zone, closer to the reducing hydrothermal fluid.

Conclusion

Cyathermia naticoides harbors dense populations of filamentous Epsilonproteobacteria in its gill, which may contribute to their nutrition through intracellular digestion by gill cells. OTU 3 was identified as a probable candidate dominant gill bacterium. Yet, the diet could be mixotrophic, an additional food source being the bacteria grazed on *R. pachyptila* tubes. OTUs 1 and 11 identified here are likely siboglinid tube-associated Epsilonproteobacteria that may be significant food sources on this route. Novel for mollusks by the combination of the location (ectosymbionts) and bacterial phylotype (Epsilonproteobacteria) encountered and the feeding mechanism, the symbiosis of *C. naticoides,* represents an unusual type of association in the already long list of molluskan symbioses, of which more await characterization in particular in smaller-sized species.

Acknowledgments We thank the chief scientists, N. Le Bris and F. Lallier, as well as the captain and crew of the RV Atalante and the 'Nautile' team for their help during the Mescal 2010 cruise. We thank E. Thiébaut and Marjolaine Matabos for their help in sorting an identifying the various gastropods sampled. TEM was performed at the 'Plateforme de Microscopie Electronique' (MNHN) with the help of C. Djediat. Work was funded through UPMC and CNRS.

Conflict of interest The authors declare that they have no conflict of interest.

Ethical standard The authors declare that the experiments comply with the current laws of the country they were performed (France).

References

Altschul S, Gish W, Miller W, Myers E, Lipman D (1990) Basic local alignment search tool. J Mol Biol 215:403–410

Amann R, Binder B, Olson R, Chisholm S, Devereux R, Stahl D (1990) Combination of 16S rRNA-targeted oligonucleotide probes with flow cytometry for analysing mixed microbial populations. Appl Environ Microbiol 56:1919–1925

Bates A (2007a) Feeding strategy, morphological specialisation and presence of bacterial episymbionts in lepetodrilid gastropods from hydrothermal vents. Mar Ecol Prog Ser 347:87–99

Bates A (2007b) Persistence, morphology, and nutritional state of a gastropod hosted bacterial symbiosis in different levels of hydrothermal vent flux. Mar Biol 152:557–568

Bates A, Tunnicliffe V, Lee R (2005) Role of thermal conditions in habitat selection by hydrothermal vent gastropods. Mar Ecol Prog Ser 305:1–15

Bates A, Harmer T, Roeselers G, Cavanaugh C (2011) Phylogenetic characterization of episymbiotic bacteria hosted by a hydrothermal vent limpet (Lepetodrilidae, Vetigastropoda). Biol Bull 220:118–127

Beinart R, Sanders J, Faure B, Sylva S, Lee R, Becker E, Gartman A, Luther III G, Seewald J, Fisher C, Girguis P (2013) Evidence for the role of endosymbionts in regional-scale habitat partitioning by hydrothermal vent symbioses. Proc Natl Acad Sci 109(47): doi:10.1073/pnas.1202690109

Bergquist D, Eckner J, Urcuyo I, Cordes E, Hourdez S, Macko S, Fisher C (2007) Using stable isotopes and quantitative community characteristics to determine a local hydrothermal vent food web. Mar Ecol Prog Ser 330:49–65

Borowski C, Giere O, Krieger J, Amann R, Dubilier N (2002) New aspects of the symbiosis in the provannid snail *Ifremeria nautilei* from the north Fiji back arc basin. Cah Biol Mar 43:321–324

Bright M, Giere O (2005) Microbial symbiosis in Annelida. Symbiosis 38:1–45

Campbell B, Stein J, Cary S (2003) Evidence of chemolithoautotrophy in the bacterial community associated with *Alvinella pompejana*, a hydrothermal vent polychaete. Appl Environ Microbiol 69(9):5070–5078

Campbell B, Engel A, Porter M, Takai K (2006) The versatile ε-proteobacteria: key players in sulphidic habitats. Nat Rev Microbiol 4:458–468

Cary S, Cottrell M, Stein J, Camacho F, Desbruyères D (1997) Molecular identification and localization of filamentous symbiotic bacteria associated with the hydrothermal vent Annelid *Alvinella pompejana*. Appl Environ Microbiol 63:1124–1130

Cole J, Wang Q, Cardenas E, Fish J, Chai B, Farris R, Kulam-Mohideen A, McGarrell D, Marsh T, Garrity G, Tiedje J (2009) The ribosomal database project: improved alignments and new toolds for rRNA analysis. Nucleic Acids Res 37:141–145

de Burgh M, Singla C (1984) Bacterial colonization and endocytosis on the gill of a new limpet species from a hydrothermal vent. Mar Biol 84:1–6

Desbruyères D, Chevaldonné P, Alayse A, Jollivet D, Lallier F, Jouin-Toulmond C, Zal F, Sarradin P, Cosson R, Caprais J, Arndt C, O'Brien J, Guezennec J, Hourdez S, Riso R, Gaill F, Laubier L, Toulmond A (1998) Biology and ecology of the "Pompeii worm" (*Alvinella pompejana* Desbruyères and Laubier), a normal dweller of an extreme deep-sea environment: a synthesis of current knowledge and recent developments. Deep Sea Res Part II 45:383–422

Desbruyères D, Segonzac M, Bright M (2006) Handbook of deep-sea hydrothermal vent fauna. Second completely revised edition. Biologiezentrum der Oberösterreichischen Landesmuseen, Austria

Dubilier N, Bergin C, Lott C (2008) Symbiotic diversity in marine animals: the art of harnessing chemosynthesis. Nat Rev Microbiol 6:725–740

Felbeck H, Somero G (1982) Primary production in deep-sea hydrothermal vent organisms: roles of sulfide-oxidizing bacteria. Trends Biochem Sci 7(6):201–204

Forget N, Juniper K (2013) Free-living bacterial communities associated with tubeworm (*Ridgeia piscesae*) aggregations in contrasting diffuse flow hydrothermal vent habitats at the Main Endeavour Field, Juan de Fuca Ridge. MicrobiologyOpen 2(2):259–275

Fox M, Juniper S, Vali H (2002) Chemoautotrophy as a possible nutritional source in the hydrothermal vent limpet *Lepetodrilus fucensis*. Cah Biol Mar 43:371–376

Gaill F, Shillito B (1995) Chitin from deep sea hydrothermal vent organisms. In: André J (ed) Giraud-Guille M. Chitin in Life Science, Lyon, pp 88–96

Gaudron SM, Lefebvre S, Nunes Jorge A, Gaill F, Pradillon F (2012) Spatial and temporal variations in food web structure from newly-opened habitat at hydrothermal vents. Mar Environ Res 77:129–140

Goffredi S, Waren A, Orphan V, Van Dover C, Vriejenhoek R (2004) Novel forms of structural integration between microbes and a hydrothermal vent gastropod from the Indian Ocean. Appl Environ Microbiol 70(5):3082–3090

Goffredi S, Jones W, Ehrlich H, Springer A, Vriejenhoek C (2008) Epibiotic bacteria associated with the recently discovered Yeti crab, Kiwa hirsuta. Environ Microbiol 10(10):2623–2634

Gutowska M, Drazen J, Robison B (2004) Digestive chitinolytic activity in marine fishes of Monterey Bay, California. Comp Biochem Physiol Part A 139:351–358

Haddad A, Camacho F, Durand P, Cary S (1995) Phylogenetic characterization of the epibiotic bacteria associated with the hydrothermal vent polychaete *Alvinella pompejana*. Appl Environ Microbiol 61(5):1679–1687

Henry M, Childress J, Figueroa D (2008) Metabolic rates and thermal tolerances of chemoautotrophic symbioses from Lau Basin hydrothermal vents and their implications for species distributions. Deep Sea Res Part I 55:679–695

Jeuniaux C (1966) Chitinases. Methods Enzymol 8:644–650

Kaehler S, Pakhomov E (2001) Effects of storage and preservation on the delta C-13 and delta N-15 signatures of selected marine organisms. Mar Ecol Prog Ser 219:299–304

Katz S, Cavanaugh C, Bright M (2006) Symbiosis of epi- and endocuticular bacteria with *Helicoradomenia* spp. (Mollusca, Aplacophora, Solenogastres) from deep-sea hydrothermal vents. Mar Ecol Prog Ser 320:89–99

Kohn A (1983) Feeding biology of Gastropods. In: Wilbur KM (ed) The Mollusca. Academic Press, New York, pp 1–63

Kouris A, Juniper K, Frebourg G, Gaill F (2007) Protozoan–bacterial symbiosis in a deep-sea hydrothermal vent folliculinid ciliate (Folliculinopsis sp.) from the Juan de Fuca Ridge. Mar Ecol 28:63–71

Le Bris N, Zbinden M, Gaill F (2005) Processes controlling the physico-chemical micro-environments associated with Pompeii worms. Deep sea Res Part I 52:1071–1083

Levesque C, Juniper K, Limén H (2006) Spatial organization of food webs along habitat gradients at deep-sea hydrothermal vents on Axial Volcano, Northeast Pacific. Deep Sea Res Part I 53:726–739

Limén H, Levesque C, Juniper K (2007) POM in macro-/meiofaunal food webs associated with three flow regimes at deep-sea hydrothermal vents on Axial Volcano, Juan de Fuca Ridge. Mar Biol 153:129–139

López-García P, Gaill F, Moreira D (2002) Wide bacterial diversity associated with tubes of the vent worm *Riftia pachyptila*. Environ Microbiol 4(4):204–215

Loy A, Lehner A, Lee N, Adamczyk J, Meier H, Ernst J, Schleifer K, Wagner M (2002) Oligonucleotide microarray for 16S rRNA gene-based detection of all recognized lineages of sulfate-reducing prokaryotes in the environment. Appl Environ Microbiol 68:5064–5081

MacPherson E, Jones W, Segonzac M (2005) A new lobster family of Galatheoidea (Crustacea, Decapoda, Anomura) from the hydrothermal vents of the Pacific-Antarctic Ridge. Zoosystema 27(4):709–722

Manz W, Amann R, Wagner M, Schleifer K (1992) Phylogenetic oligodeoxynucleotide probes for the major subclasses of Proteobacteria: problems and solutions. Syst Appl Microbiol 15:593–600

Meyer B, Kuever J (2007) Phylogeny of the alpha and beta subunits of the dissimilatory adenosine-5'-phosphosulfate (APS) reductase from sulfate-reducing prokaryotes—origin and evolution of the dissimilatory sulfate-reduction pathway. Microbiology 153:2026–2044

Mills S, Mullineaux L, Tyler P (2007) Habitat associations in gastropod species at East Pacific Rise hydrothermal vents (9 50'N). Biol Bull 212:185–194

Miyake H, Kitada M, Tsuchida S, Okuyama Y, Nakamura K (2007) Ecological aspects of hydrothermal vent animals in captivity at atmospheric pressure. Mar Ecol 28:86–92

Moreno Y, Botella S, Alonso J, Ferrús M, Hernández M, Hernández J (2003) Specific detection of arcobacter and campylobacter strains in water and sewage by PCR and fluorescent in situ hybridization. Appl Environ Microbiol 69:1181–1186

Petersen J, Ramette A, Lott C, Cambon-Bonavita M-A, Zbinden M, Dubilier N (2010) Dual symbiosis of the vent shrimp *Rimicaris exoculata* with filamentous gamma- and epsilonproteobacteria

at four Mid-Atlantic Ridge hydrothermal vent fields. Environ Microbiol 12(8):2204–2218

Polz M, Robinson J, Cavanaugh C, Van Dover C (1998) Trophic ecology of massive shrimp aggregations at a mid-Atlantic Ridge hydrothermal vent site. Limnol Oceanogr 43(7):1631–1638

Ponsard J, Cambon-Bonavita M-A, Zbinden M, Lepoint G, Joassin A, Corbari L, Shillito B, Durand L, Cueff-Gauchard V, Compère P (2013) Inorganic carbon fixation by chemosynthetic ectosymbionts and nutritional transfers to the hydrothermal vent host-shrimp, *Rimicaris exoculata*. ISME J 7:96–109

Pruesse E, Quast C, Knittel K, Fuchs B, Ludwig W, Peplies J, Glöckner F (2007) SILVA: a comprehensive online resource for quality checked and aligned ribosomal RNA sequence data compatible with ARB. Nucleic Acids Res 35:7188–7196

Ravaux J, Shillito B, Gaill F, Gay L, Voss-Foucart M-F, Childress J (1998) Tubes synthesis and growth process in the hydrothermal vent tube-worm *Riftia pachyptila*. Cah Biol Mar 39:325–326

Saito H, Hashimoto J (2010) Characteristics of the fatty acid composition of a deep-sea vent gastropod, *Ifremeria nautilei*. Lipids 45:537–548

Sarradin P, Caprais J, Briand P, Gaill F, Shillito B, Desbruyères D (1998) Chemical and thermal description of the environment of the Genesis hydrothermal vent community (13°N, EPR). Cah Biol Mar 39:159–167

Sasaki T, Warén A, Kano Y, Okutani T, Fujikura K (2010) Gastropods from recent hot vents and cold seeps: systematics, diversity and life strategies. In: Kiel S (ed) The vent and seep biota. Springer Science, New York

Segonzac M, de Saint-Laurent M, Casanova B (1993) L'énigme du comportement trophique des crevettes Alvinocarididae des sites hydrothermaux de la dorsale médio-atlantique. Cah Biol Mar 34:535–571

Sievert S, Vetriani C (2012) Chemoautotrophy at deep-sea vents: past, present, and future. Oceanography 25(1):218–233

Suzuki Y, Sasaki T, Suzuki M, Tsuchida S, Nealson K, Horikoshi K (2005a) Molecular phylogenetic and isotopic evidence of two lineages of chemoautotrophic endosymbionts distinct at the subdivision level harbored in one host-animal type: the genus *Alviniconcha* (Gastropoda: Provannidae). FEMS Microbiol Ecol 249:105–112

Suzuki Y, Sasaki T, Suzuki M, Nogi Y, Miwa T, Takai K, Nealson K, Horikoshi K (2005b) Novel chemoautotrophic endosymbiosis between a member of the epsilon-proteobacteria and the hydrothermal-vent gastropod *Alviniconcha aff. hessleri* (Gastropoda: Provannidae) from the Indian Ocean. Appl Environ Microbiol 71(9):5440–5450

Suzuki Y, Kojima S, Sasaki T, Suzuki M, Utsumi T, Watanabe H, Urakawa H, Tsuchida S, Nunoura T, Hirayama H, Takai K, Nealson K, Horikoshi K (2006) Host-symbiont relationships in hydrothermal vent gastropods of the genus *Alviniconcha* from the southwest Pacific. Appl Environ Microbiol 72(2):1388–1393

Tamura K, Stecher G, Peterson D, Filipski A, Kumar S (2013) MEGA6: molecular evolutionary genetics analysis version 6.0. Mol Biol Evol 30:2725–2729

Thurber A, Jones W, Schnabel K (2011) Dancing for Food in the deep sea: bacterial farming by a new species of yeti crab. PLoS One 6(11):e26243. doi:10.1371/journal.pone.0026243

Urakawa H, Dubilier N, Fujiwara Y, Cunningham D, Kojima S, Stahl D (2005) Hydrothermal vent gastropods from the same family (Provannidae) harbour epsilon- and gamma -proteobacterial endosymbionts. Environ Microbiol 7(5):750–754

Vetter R, Fry B (1998) Sulfur contents and sulfur-isotope compositions of thiotrophic symbioses in bivalve molluscs and vestimentiferan worms. Mar Biol 132:453–460

Warén A, Bouchet P (1989) New gastropods from East Pacific hydrothermal vents. Zool Scr 18(1):67–102

Waren A, Bouchet P, von Cosel R (2006) *Cyathermia naticoides* Warèn & Bouchet, 1989. In: Desbruyères D, Segonzac M, Bright M (eds) Handbook of deep-sea hydrothermal vent fauna. Denisia 18, Biologiezentrum Linz, Austria, pp 104

Windoffer R, Giere O (1997) Symbiosis of the hydrothermal vent gastropod *Ifremeria nautilei* (Provannidae) with endobacteria—structural analyses and ecological considerations. Biol Bull 193:381–392

Yamamoto M, Takai K (2011) Sulfur metabolisms in epsilon- and gamma-proteobacteria in deep-sea hydrothermal fields. Front Microbiol 2: doi: 10.3389/fmicb.2011.00192

Zbinden M, Shillito B, Le Bris N, de De Vilardi Montlaur C, Roussel E, Guyot F, Gaill F, Cambon-Bonavita M-A (2008) New insights on the metabolic diversity among the epibiotic microbial community of the hydrothermal shrimp *Rimicaris exoculata*. J Exp Mar Biol Ecol 159(2):131–140

Zbinden M, Pailleret M, Ravaux J, Gaudron S, Hoyoux C, Lorion J, Halary S, Warén A, Duperron S (2010) Bacterial communities associated with the wood-feeding gastropod *Pectinodonta* sp. (Patellogastropoda, Mollusca). FEMS Microbiol Ecol 74:450–463